University of Sheffield

Techno-Economic and Life Cycle Assessment of Power-to-X Systems for the Defossilisation of the Chemical Industry

By:

Gabriela Alejandra Cuevas Castillo

A thesis submitted in fulfilment of the requirements for the degree of:

Doctor of Philosophy

The University of Sheffield

Faculty of Engineering

Department School of Mechanical Engineering

November 2024

Declaration

The candidate confirms that the work submitted is her own and that appropriate credit has been given where reference has been made to the work of others.

Research outputs

Publications

1. Cuevas-Castillo, G. A., Michailos, S., Akram, M., Hughes, K., Ingham, D., & Pourkashanian, M. (2024). Techno economic and life cycle assessment of olefin production through CO_2 hydrogenation within the power-to-X concept. *Journal of Cleaner Production*, *469*, 143143.
2. Cuevas-Castillo, G. A., Michailos, S., Hughes, K., Ingham, D., & Pourkashanian, M. (2025). A comprehensive process modelling, techno-economic and life cycle assessment of a power to ammonia process. *Sustainable Energy Technologies and Assessments*, 76, 104278.
3. Cuevas-Castillo, G. A., Michailos, S., Hughes, K., Ingham, D., Navarro-Pineda, F., & Pourkashanian, M. (2025). Techno-economic and life cycle assessment of power-to-formic acid production using direct air capture and green hydrogen. *Cleaner Engineering and Technology*, 26, 100929.

Poster/presentations in academic events:

1. Cuevas-Castillo, G. A., Michailos, S., Hughes, K., Ingham, D., & Pourkashanian, M. Student poster presentation. University of Sheffield, United Kingdom.
2. Cuevas-Castillo, G. A., Michailos, S., Hughes, K., Ingham, D., & Pourkashanian, M. Oral presentation. Techno economic analysis and Life cycle assessment of a power to olefins case study using CCU and renewable sources. XX International Conference on Carbon Dioxide Utilization. Bari, Italy, 25-29 June 2023.
3. Cuevas-Castillo, G. A., Michailos, S., Hughes, K., Ingham, D., & Pourkashanian, M. Oral presentation. Techno economic and life cycle assessment of olefins production through CO_2 hydrogenation within the Power-to-X concept. The 2nd FERIA Conference, the European Conference on Fuel and Energy Research and Its Applications, University of Sheffield, Sheffield, 4th to 6th September 2023.

Acknowledgements

I thank God for His guidance, strength, and unwavering support throughout this journey. All praise and glory belong to Him.

I wish to express my sincere gratitude to my supervisors, Dr. Kevin Hughes, Dr. Stavros Michailos, Prof. Derek Ingham, Prof. Mohamed Pourkashanian, for their invaluable guidance, support, and expertise throughout this research. Their insights and encouragement have been essential to the successful completion of this thesis.

My thanks extend to the Energy 2050 Research Group and external colleagues for fostering a collaborative and intellectually stimulating environment. I am especially grateful for the support of Dr. Freddy Navarro, whose ideas and discussions have had a significant impact on this research.

I would like to acknowledge the financial support provided by the Mexican Council for Science and Technology (CONACYT) for the PhD scholarship (cvu 703759) which enabled the completion of this work.

I am deeply grateful to my family for their unconditional support, and to my partner, for their patience and encouragement throughout this journey. Their love and belief in me have been a constant source of strength.

Abstract

The chemical industry is a significant contributor to global greenhouse gas (GHG) emissions, making it a critical sector for decarbonization. This research investigates the potential of Power-to-X (PtX) systems as a pathway to produce essential chemicals with reduced environmental impact. PtX involves the conversion of renewable electricity into chemical products via integration with carbon capture and utilization (CCU) technologies. This thesis focuses on the development and assessment of three key PtX applications: olefins, ammonia, and formic acid. Each process is analysed through a combined techno-economic assessment (TEA) and life cycle assessment (LCA), providing a holistic evaluation of their feasibility and sustainability performance. The Power-to-Olefins (PtO) process integrates direct air capture (DAC) of CO_2, electrolytic hydrogen production, methanol synthesis, and methanol-to-olefins conversion, using offshore wind power. Despite its high energy intensity, the PtO system achieves a 49% reduction in global warming potential (GWP) compared to conventional fossil-based routes. The Power-to-Ammonia (PtA) process combines green hydrogen, cryogenic air separation for nitrogen, and the Haber-Bosch synthesis. A detailed model featuring kinetic reactor design and heat integration reveals a 94% reduction in GWP, though the levelized cost remains higher than traditional production. The results underscore the importance of low-cost renewable electricity in achieving economic viability. Finally, the Power-to-Formic Acid (PtFA) route, modelled via a thermocatalytic process, is the first of its kind to integrate TEA and LCA. The system demonstrates up to 90% reductions in CO_2 emissions, water consumption, and fossil resource use. Overall, this thesis provides a novel and comprehensive evaluation of PtX systems for low-carbon chemical production. The findings contribute valuable insights for policymakers and industry stakeholders aiming to defossilising the chemical sector and align with global climate targets.

Glossary of Terms

ADP	Abiotic Depletion Potential
AE	Alkaline Electrolyser
AEA	Aspen Energy Analyzer
AEO	Air Separation Unit
ALO	Agricultural Land Occupation
ASU	Air Separation Unit
ATR	Auto Thermal Reformer
CAPEX	Capital Expenditures
CC	Climate Change
CCU	Carbon Capture and Utilisation
CEPCI	Chemical Engineering Plant Cost Index
CI	Carbon Intensity
CO_2eq	Carbon Dioxide Equivalent
COM	Cost of Operating and Maintenance
CRF	Capital Recovery Factor
CSTR	Continuous Stirred Tank Reactor
CW	Cooling Water / Working Capital (context-specific)
DAC	Direct Air Capture
DME	Dimethyl Ether
DO	Direct Overhead
EP	Eutrophication Potential
FA	Formic Acid
FD	Fossil Depletion
FEWP	Freshwater Ecotoxicity Water Potential

FEP Freshwater Eutrophication Potential

FCI Fixed Capital Investment

FU Functional Unit

GHG Greenhouse Gas

GWP Global Warming Potential

H-B Haber Bosch

HEX Heat Exchanger

HHV High Heating Value

HPC High Pressure Column

HTP Human Toxicity Potential

IC Indirect Cost

ICS Intercooling Compression System

IDC Installed Direct Costs

IEA International Energy Agency

IR Ionising Radiation

IRR Internal Rate of Return

ISO International Organization for Standardization

KPI Key Performance Indicator

LCA Life Cycle Assessment

$LCCO_2$ Levelised Cost of CO_2

LCI Life Cycle Inventory

LCOA Levelised Cost of Ammonia

LCOE Levelised Cost of Electricity

LEAP Livestock Environmental Assessment and Performance

LHV Low Heating Value

LOHC Liquid Organic Hydrogen Carrier

LPC Low Pressure Column

MD Metal Depletion

MEA Methyl Ethyl Amine

MEP Marine Ecotoxicity Potential

MM Millions

MTO Methanol to Olefins

MSP Minimum Selling Price

NIDC Non-Installed Direct Costs

NLT Natural Land Transformation

NPV Net Present Value

NREL National Renewable Energy Laboratory

O&M Operating and Maintenance

ODP Ozone Depletion Potential

OL Operating Labour

OPEX Operating Expenses

ORC Organic Rankine Cycle

OS Operating Supervision

PEC Purchased Equipment Cost

PEM Proton Exchange Membrane

PM Particle Matter

POP Photochemical Oxidation Potential

PP Polypropylene

PPM Parts Per Million

PtA Power to Ammonia

PtFA Power to Formic Acid

PtG Power to Gas

PtH Power to Hydrogen

PtL Power to Liquids

PtM Power to Methanol

PtO Power to Olefins

PtX Power to Any Chemical Compound

PFD Process Flow Diagram

RPlug Reactor Plug Flow

RSTOIC Reactor Stoichiometric

SAM System Advisor Model

SEC Specific Energy Consumption

SOEL Solid Oxide Electrolyser

SPL Splitter

TAP Terrestrial Acidification Potential

TDC Total Direct Cost

TEA Techno-Economic Assessment

TEP Terrestrial Ecotoxicity Potential

TRL Technology Readiness Level

ULO Urban Land Occupation

VLL Vapor Liquid-Liquid

WC Water Consumption

List of Contents

List of Figures

List of Tables

Chapter I

1. Introduction

In this section, an overview of the importance and main strategies for mitigating CO_2 and its utilization in the Power to X (PtX) approach are presented. Additionally, a brief description of the economic and environmental performance of various technologies is discussed. This overview highlights the potential of various CO_2 utilization methods to contribute to sustainable development by reducing greenhouse gas emissions and promoting efficient resource use.

1.1. Climate change

The significant increase in anthropogenic emissions, particularly greenhouse gases (GHGs) from human activities, has heightened concerns about climate change. The extensive use of fossil resources has led to a substantial accumulation of carbon dioxide in the atmosphere, which is a primary driver of global warming. This pollutant is responsible for rising temperatures on Earth, leading to significant changes in average weather patterns. An increase in temperature above 2 °C could cause irreversible damage to the planet's ecosystems and biodiversity. Consequently, many countries have committed to limiting the global temperature rise to 1.5 °C above pre-industrial levels by 2050 [1]. Addressing this challenge requires focused research on energy efficiency and CO_2 reduction strategies to mitigate climate change impacts effectively.

The chemical industry sector is responsible for approximately 23% of energy-related CO_2 emissions globally (Figure 1-1). These emissions are expected to increase by 2050 [2]. In response, countries worldwide have set ambitious targets to reduce greenhouse gas emissions [3]. Strategies to achieve these targets include the adoption of renewable energy sources and the utilization of carbon dioxide as a feedstock for producing hydrogen, carbon monoxide, methanol, and other energy carriers. These approaches aim to reduce dependence on fossil fuels for energy and chemical production and the shift to renewables that offers multiple benefits, such as more secure energy supplies, increased diversity of energy sources, and enhanced process efficiency.

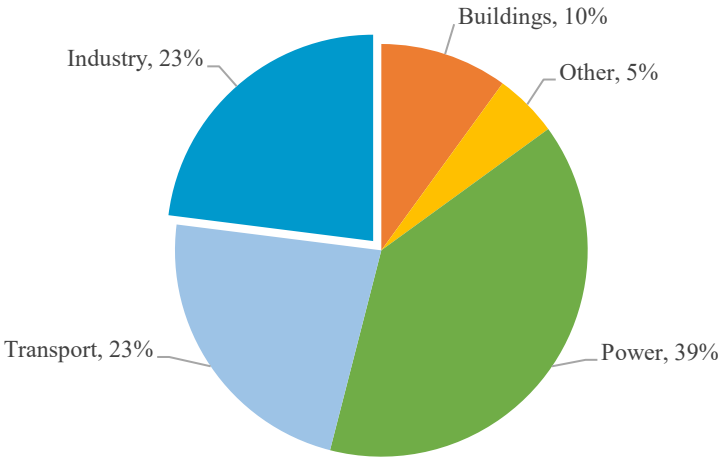

Figure 1-1 Direct CO_2 emissions by sector, 2017 (Source IEA, 2019 [4]).

1.2. Decarbonisation of chemical industry

By 2022, direct CO_2 emissions from primary chemical production remained steady at approximately 935 Mt due to stationary production levels (Figure 1-2). The CO_2 intensity of primary chemicals such as ethylene, propylene, benzene, toluene, mixed xylenes, ammonia, and methanol has also been stable, averaging around 1.3 t CO_2 per tonne of production and it is expected it is reduced to 0.9 by 2030 (red dots).

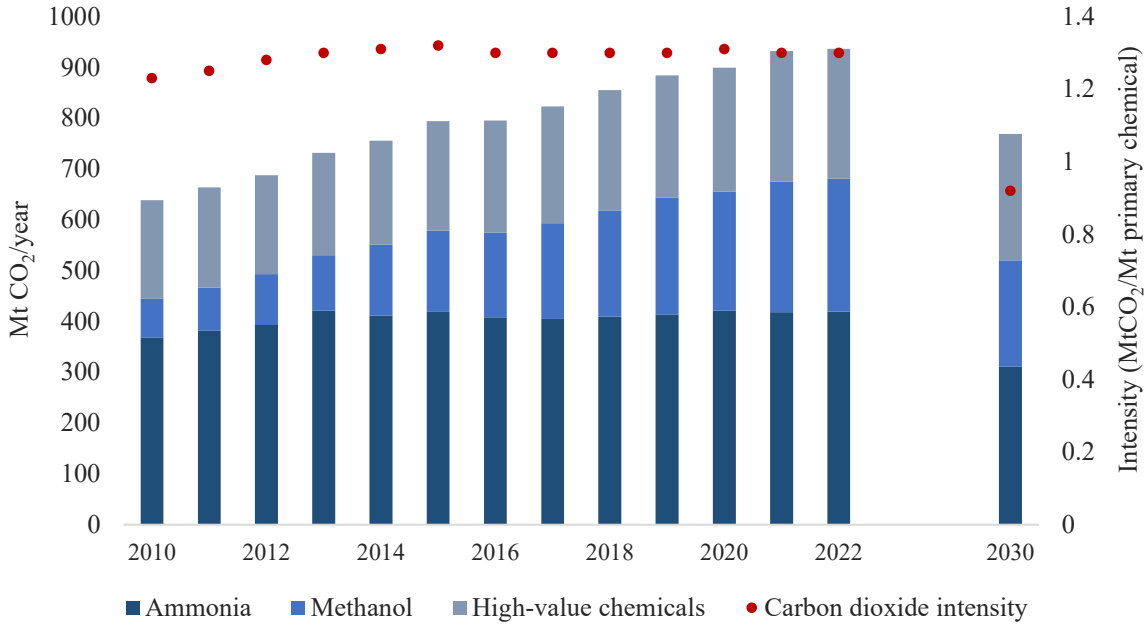

Figure 1-2 . Direct CO_2 emissions from primary chemicals production [5].

Ammonia production is the largest emitter, responsible for 45% of emissions from primary chemical production, followed by methanol (28%) and high-value chemicals (27%). The sector primarily uses oil and gas as feedstock, providing hydrogen and carbon necessary for producing basic chemicals such as ethylene, propylene, and ammonia. As demand for these materials grows, so does the use of oil and gas. Energy consumption in the sector is not just for production but also for process energy, separate from feedstock use.

The primary decarbonisation strategies for the chemical sector include carbon capture, utilization, and the use of electrolytic hydrogen [6]. One effective method for reducing carbon emissions is the replacement of fossil fuels and materials with renewable substitutes, which entails significant advancements in chemical processing methods. Transitioning from fossil fuel-based feedstock to renewable alternatives presents both technical and economic challenges and requires a comprehensive life cycle approach to ensure effectiveness and suitability, preventing double counting and carbon leakage [7].

1.3. Power to X concept (PtX)

The power to X concept involves the use of electrical power, particularly from renewable sources in the conversion of other energy carriers or high value products [8]. The key to this concept is the production of hydrogen by splitting water in an electrolyser. Further, this hydrogen can be converted into other valuable products such as methane [9]. Another important key is carbon dioxide, which is needed to process hydrogen into other energy carriers or chemical products [10]. The X in the name indicates the versatility of the outputs such as liquids (PtL), gas (PtG), chemicals or heat (PtX).

This concept can significantly reduce greenhouse gas emissions by replacing fossil-based chemicals with those derived from renewable electricity and captured CO_2. In addition, by converting electricity into storable forms like hydrogen or synthetic fuels. PtX provides a solution for the intermittency of renewable energy sources, ensuring a reliable energy supply [11]. Many studies have been review and discussed this topic [10–12] and some of the challenges are the economic viability where the price of electricity play a significant role in the feasibility of these processes. Reducing costs through technological advancements and economies of scale is crucial. Another challenge is the efficiency and durability of the electrolysis, the catalyst performance and process integration. In addition, a comprehensive life cycle assessment is needed to evaluate the environmental impact of PtX technologies. This includes considering the energy and materials used in the production and operation stages of these systems [13].

Moreover, PtX offers a versatile and promising pathway for achieving a sustainable and resilient energy system. By converting renewable electricity into various forms of energy carriers and chemicals, this

approach can help decarbonize chemical sector, enhance energy storage capabilities, and improve the overall efficiency of the energy system. However, realizing the full potential of PtX requires overcoming technical, economic, and regulatory challenges through coordinated efforts in research, development, and policymaking.

1.4. Carbon capture utilization (CCU)

The concept of Carbon Capture Utilization (CCU) as an important key of PtX, involves capturing carbon dioxide emissions from power plants, cement plants or directly from the atmosphere and transforming it into high value chemicals, fuel or energy [14]. The aim is to prevent CO_2 from being released into the atmosphere and represents a viable strategy to reduce emissions from the industrial sector. It can be applied to large power plants and includes the processes of CO_2 compression, transportation, and conversion [15].

Direct Air Capture (DAC) enhances CCU by enabling the removal of CO_2 directly from the ambient air, providing a means to offset emissions from diffuse sources and achieve negative emissions. DAC technologies capture CO_2 at a lower concentration than point-source capture, making them a critical tool for addressing emissions that are otherwise challenging to mitigate [16].

CCU is recognized as a crucial technology for achieving net-zero emissions because it assists in the reducing of emissions across various sectors, including power generation, chemical industry, and transportation [17]. As economies grow, the need for more sustainable products intensifies. The significant impact of CCU on climate change mitigation lies in its ability to create renewable substitutes of fossil chemicals and fuels, which can significantly reduce CO_2 emissions currently associated with fossil fuel extraction and use [18]. By targeting these major sources of CO_2, the strategy aims to significantly reduce the carbon footprint and promote the transition to a more sustainable economy.

1.5. Conversion technologies and products

The chemical industry is one of the largest sectors that contributes global CO_2 emissions, for that reason, the need to develop and study a technology that implies use of carbon dioxide as a raw material for chemical products is very important. There are various PtX technologies applied in multiple sectors, methanol production from CO_2 in one of the most prominent pathways since it is an energy carrier with multiple options of conversion as an intermediate for fuels or chemicals, as illustrated in Figure 1-3.

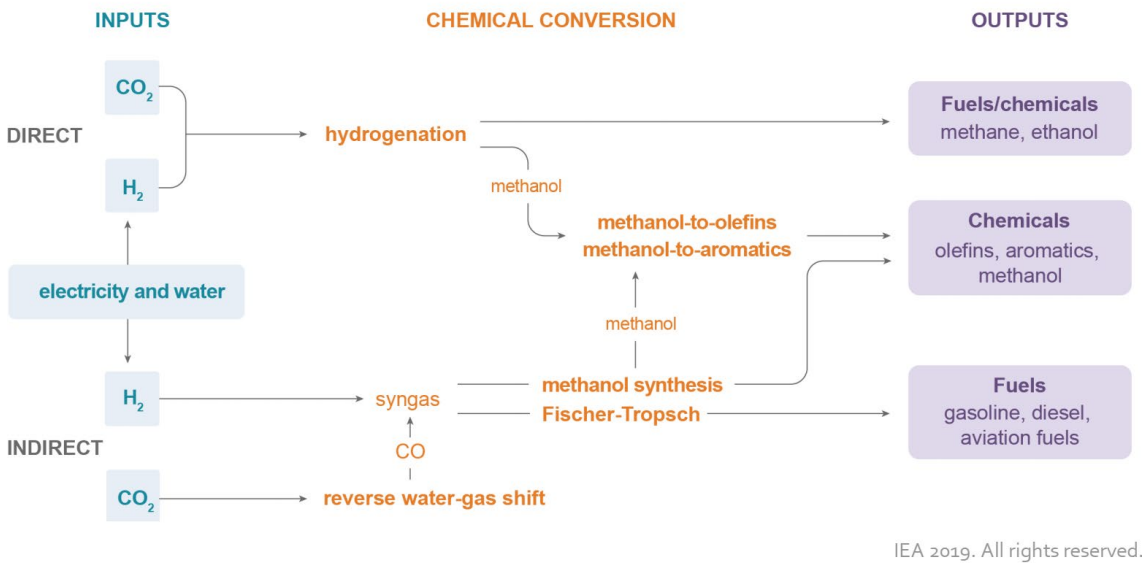

Figure 1-3 Mature conversion routes for CO_2 derived fuels and chemical intermediates (Source IEA. [19]).

Direct chemical conversions include hydrogenation of CO_2 with H_2 to produce various fuels and chemicals such as methane, ethanol, formic acid, among other valuable chemicals. Methanol can be synthesized by CO_2 hydrogenation that serves as an intermediate for other chemical products such as olefins and aromatics. The indirect conversion involves the reverse water gas shift reaction where CO_2 and H_2 are converted to syngas (a mixture of CO and H_2) through the RWGS reaction and it is then used for producing fuels through Fischer-Tropsch synthesis or methanol synthesis.

1.5.1. Methanol and olefins

Hydrogenation is an important technology that provides chemicals and fuels from CO_2. In both categories, methanol (CH_3OH) is a common product termed a "hydrogen carrier" because it can be stored and converted into fuels or electricity. In addition, methanol is a primary product of several chemicals including solvents and Intermediates [20]. It is widely used as a feedstock to produce formaldehyde, olefins, dimethyl ether (DME), formic acid and synthetic fuels and is applied also as an additive in the synthetic gasoline, aviation fuel and other hydrocarbons [21,22]. CO_2 is attractive to produce methanol since it has advantages, such as being a mitigation strategy of greenhouse gases. The most common way to obtain methanol from CO_2 is by the catalytic hydrogenation process [20]. Currently, the commercial production of methanol is based on the syngas production from fossil resources that implies large carbon emissions. Therefore, the conversion of methanol through CO_2 is a high potential pathway because of its environmental and economic benefits regarding the mitigation systems.

Methanol from CO_2 is a potential raw material for chemical industries and for olefins. Light olefins, such as ethylene and propylene, are important building blocks of the chemical industry such as plastics, industrial fibres and rubber [23]. They are the starting material of the polyethylene and polypropylene packaging which has a 36% global demand [24] and it is predicted to grow by 4% per year by 2025 [25]. This highlights the urgent need to explore sustainable chemical pathways to meet the growing demand for olefins. Fossil - based olefin production entails the use of high carbon intensive materials such as natural gas, coal and petroleum naphtha that results in increased GHG emissions [26]. In recent years, research has been focused on developing and evaluating innovative process for a sustainable olefin production. The technique with special interest is the methanol to olefins process (MTO), where propylene and ethylene are the main products as well as heavy hydrocarbons. The advantage of this process compared to the steam cracking process consists in the higher olefin selectivity and its low production of light gases such as CH_4, H_2 and CO [27].

1.5.2. Ammonia

Ammonia production is another interesting route. It is one of the most synthetized chemicals worldwide [28]. About 70% of ammonia is used for fertilizers while the rest is used for industrial applications such as plastics, explosives and synthetic fibres [29,30]. Nowadays, it is gaining much interest as a promising fuel with the potential to contribute to the decarbonisation due to its carbon-free composition, and hence no direct greenhouse gas effects [30]. According to the type of energy source used, the produced ammonia can be labelled as grey, blue or green. Grey ammonia is the conventional production system, which uses natural gas as feedstock for hydrogen and typically grid electricity to run the separation of nitrogen and the Haber – Bosch process [31–33]. It accounts for around 2% of the worldwide energy use [34] and represents 1.2% of the global anthropogenic CO_2 emissions [35]. Thus, fossil-based ammonia is one of the most emissions intensive commodities produced by heavy industry. Green ammonia involves the use of renewable sources for the feedstock production and synthesis of ammonia. This concept, known as power to ammonia (PtA) [36,37] has been proposed as a means of effectively utilizing renewable energy and storing it as ammonia and it has emerged as a near zero emission method. Wind, solar, nuclear and hydropower have been proposed as the most prominent sources of power to ammonia with promising results from the economic and environmental point of view. The United Kingdom (UK) in particular, has raised the importance of wind energy as a potential source for green ammonia [38].

The process is carried out using the water electrolysis concept to supply hydrogen for power and the air separation unit (ASU) to supply nitrogen needed in the ammonia synthesis [39]. Cryogenic distillation is used in the ASU unit because of its commercial application. Ammonia is a good candidate for being an

energy carrier since it has the advantages of being available and a "green" behaviour. Many of these processes involve chemical reactions that include emissions of CO_2 since the chemical industry is still based on hydrocarbons where the emissions are hard to avoid with the switching from fossil to alternative fuels. This is the reason why some companies are adopting decarbonisation pathways such as improving resources and energy efficiency using predictive analytic tools or energy management applications [4]. In the United Kingdom there are projects related to Green ammonia production in order to show the potential of wind energy to be transformed into energy [40]. Other countries such as Australia, Japan and the United States have projects in progress to develop and implement carbon-neutral or free energy from green ammonia.

1.5.3. Formic acid

Among the various chemicals that can be produced using captured CO_2, formic acid (FA) stands out due to its wide range of industrial applications, including its use as a preservative, antibacterial agent, and in fuel cells [41,42]. Formic acid (HCOOH, FA) is the simplest carboxylic acid, a colourless liquid miscible with polar solvents. FA is widely used as a food additive, preservative in silage and animal feed, and as a bactericide. It also finds applications in the dyes, rubber, textile, and leather industries [43]. In the fuel industry, FA is considered a promising candidate for hydrogen storage due to its high volumetric capacity and low toxicity [43–46]. The global market for formic acid reached approximately 750 thousand tonnes in 2022 and is expected to grow at a rate of 4.48% during the forecast period up to 2035, with China being the largest producer [47]. Formic acid has been the focus of several projects in Europe that apply the power-to-chemicals concept [48]. For example, the Norwegian company DNV has developed a pilot plant for the electrochemical conversion of CO_2 into formic acid. Additionally, the European Horizon 2020-funded C2Fuel project aims to produce dimethyl ether (DME) and formic acid from renewable hydrogen (H_2) and captured CO_2 from industrial sources [49].

The conventional production process of formic acid involves two steps: the carbonylation of methanol in the presence of a base catalyst such as sodium or potassium, followed by the hydrolysis of methyl formate to formic acid and methanol [18]. This process has several drawbacks, including an unfavourable hydrolysis equilibrium, which results in a large water requirement and, consequently, high-energy consumption for water removal. Additionally, the carbon monoxide used in the reaction is obtained from fossil resources [18,50]. Alternative technological routes for formic acid production, such as electrolytic CO_2 conversion, have been explored. Various studies have evaluated the feasibility of electrolytic formic acid production, but the main challenges include high electricity consumption and the use of expensive cell materials [44,51–57].

The development of a PtX plays an important role in the decarbonisation of the chemical sector. The transition to renewable alternatives in the chemical industry requires a multifaceted approach that includes advancements in technology, in addition to economic and environmental assessments to ensure these strategies are sustainable and contribute to the overall reduction of the industry carbon footprint.

1.6. Economic and environmental assessment.

The life cycle assessment (LCA) emerges as a suitable tool for the assessment of CO_2 capture and conversion technologies. It evaluates the environmental impacts associated with a product or process during its entire life by accounting for material resources, energy inputs and environmental issues such as emissions to the air, water, and soil. The environmental impacts are mainly fossil resource depletion, water use, abiotic depletion, global warming, acidification potential, eutrophication, human toxicity, etc. [58]. In the CO_2 conversion pathways, LCA is important since utilization of CO_2 does not necessarily reduce climate change impacts. In fact, the emissions may be higher than conventional process of fuels because of the extra processes required to capture systems and the conversion technologies and these are not yet in the maturity stage [59,60]. The techno economic analysis is an approach focused on evaluating the feasibility of the project. This methodology focuses on the quantification of the capital investment, operational costs and gross profit and revenues [61]. The first step in the economic and environmental analysis is the process modelling which consists of all the calculations related with each step of the production process, the model generates a table of results that are used in the equipment sizing to calculate the parameters that are necessary for estimating the capital and operating costs. To develop the system, parameters such as temperatures, pressures, thermodynamics, other operation conditions, kinetics of reactions, unit operations, etc. need to be established. The software used for this purpose is usually a chemical engineering simulation software such as Aspen Plus [15]. In the economic assessments, some additional information is required in addition to the mass and energy balances. Equipment cost estimation, economic assumptions about the plant life, interest rate, and the prices or costs of raw materials, utilities, and products are used to calculate the capital and operational expenditures indicators [62].

1.7. Aim and objectives of the thesis

The inherent increasing of the world population requires unavoidable use of energy in different ways. In emerging economies, the chemical industry significantly relies on fossil fuels, leading to substantial greenhouse gas emissions from the extraction and utilization of these resources. This challenge underscores the critical need to develop efficient technologies and alternative approaches for producing chemicals with minimal environmental impact. Therefore, this study aims to explore various pathways for chemical production within the Power-to-X framework, supporting the decarbonisation of the current industry while

contributing to the reduction of key pollutants, such as carbon dioxide. To achieve this, the following specific objectives have been outlined.

- To evaluate a process model for olefin production via CO_2 hydrogenation, incorporating both techno-economic analysis and life cycle assessment to determine its feasibility, cost-effectiveness, and environmental impact.
- To analyse the environmental and economic performance of a power-to-ammonia plant, specifically utilizing offshore wind as a renewable energy source, by integrating techno-economic analysis and life cycle assessment to assess its potential for sustainable ammonia production.
- To develop and assess a model for power-to-formic acid production, utilizing direct air capture (DAC) of CO_2 and electrolytic hydrogen, with a focus on applying techno-economic analysis and life cycle assessment to evaluate its viability and sustainability.

1.8. Thesis structure

CHAPTER I: Introduction

This chapter provides an overview of the primary research focus and relevant technologies, setting the stage for the thesis. It outlines the aim and objectives of the study, offering a clear roadmap for the subsequent chapters.

CHAPTER II: Literature review

This chapter explores into the current state of the art in technologies related to the production of chemicals through PtX concept. It examines the technical, environmental, and economic aspects of these technologies. Additionally, it provides a brief overview of key indicators used to evaluate process performance. The chapter concludes by identifying the main challenges and research gaps, and proposes approaches to address these gaps.

CHAPTER III: Methodology

This chapter details the methodologies and pathways proposed for producing high value chemicals from renewable sources. It explains the use of specific software tools and methodologies, such as techno-economic analysis and life cycle assessment, to evaluate the sustainability and performance of the system. The aim is to identify areas for improvement and evidence challenges for future research.

CHAPTER IV: Techno economic and life cycle assessment of olefin production through co_2 hydrogenation within the power-to-x concept.

This chapter explores the concept of Power to olefins (PtO) and provides a simulation model for producing olefins via CO_2 hydrogenation pathway. The technical, economic, and environmental performance of this process are analysed and discussed in detail.

CHAPTER V: A comprehensive process modelling, techno-economic and life cycle assessment of a power to ammonia (PtA) process.

This chapter explores a scenario for producing ammonia using renewable offshore wind energy. It discusses the simulation model results, along with the potential and challenges of this process, providing a comprehensive evaluation.

CHAPTER VI: Techno-economic and life cycle assessment of power-to-formic acid (PtFA) production using direct air capture and green hydrogen.

In this chapter, a proposed scenario for producing formic acid using DAC and electrolytic H_2 is presented. The technical, economic, and environmental outcomes are analysed, with discussions focusing on the implications and potential of this approach.

CHAPTER 7: Conclusions and recommendations

As last chapter, a summary of the critical outcomes from each of the previous chapters is discussed, highlighting the main technical, economic and environmental insights from the study. It emphasizes the relevance of the PtX to global efforts to decarbonise the chemical industry. Additionally, this chapter explores the challenges encountered in the technical and simulation modelling process as well as the potential advancements that could enhance the performance of these technologies

Chapter II

2. Literature review

In this chapter, the state of the art in Power-to-X (PtX) technologies is explored. The concept of PtX is defined, along with a comprehensive overview of its various routes and associated technologies. The chapter provides detailed description of the key technologies such as power-to-hydrogen (PtH), power-to-methanol (PtM), power-to-ammonia (PtA), and power-to-liquids (PtL), examining their processes, technological challenges, and potential applications.

2.1. Power to X concept and approach

Power-to-X (PtX) is a concept that involves converting renewable electricity into chemical products, fuels, or other high valuable materials. It utilises renewable energy, typically from wind, solar, or hydropower, to produce "X," which can be a variety of products such as hydrogen, synthetic fuels, or chemicals [9,63]. In the chemical industry, PtX represents an important strategy to shift towards more sustainable and carbon-neutral production processes, enabling the sector to reduce its dependence on fossil fuels and significantly lower its carbon footprint. There are three key elements in the PtX approach as illustrated in Figure 2-1: 1) electrolysis of water where electricity is used to split water into hydrogen and oxygen; 2) CO_2 capture and utilisation, either from industrial emissions or directly from the atmosphere that along with the H_2 is utilised to synthesize a wide range of valuable chemicals and fuels. 3) Integration of renewable energy, PtX relies heavily on the availability and incorporation of renewable sources such as wind, solar, hydropower, nuclear in each stage of the process towards decarbonisation goals.

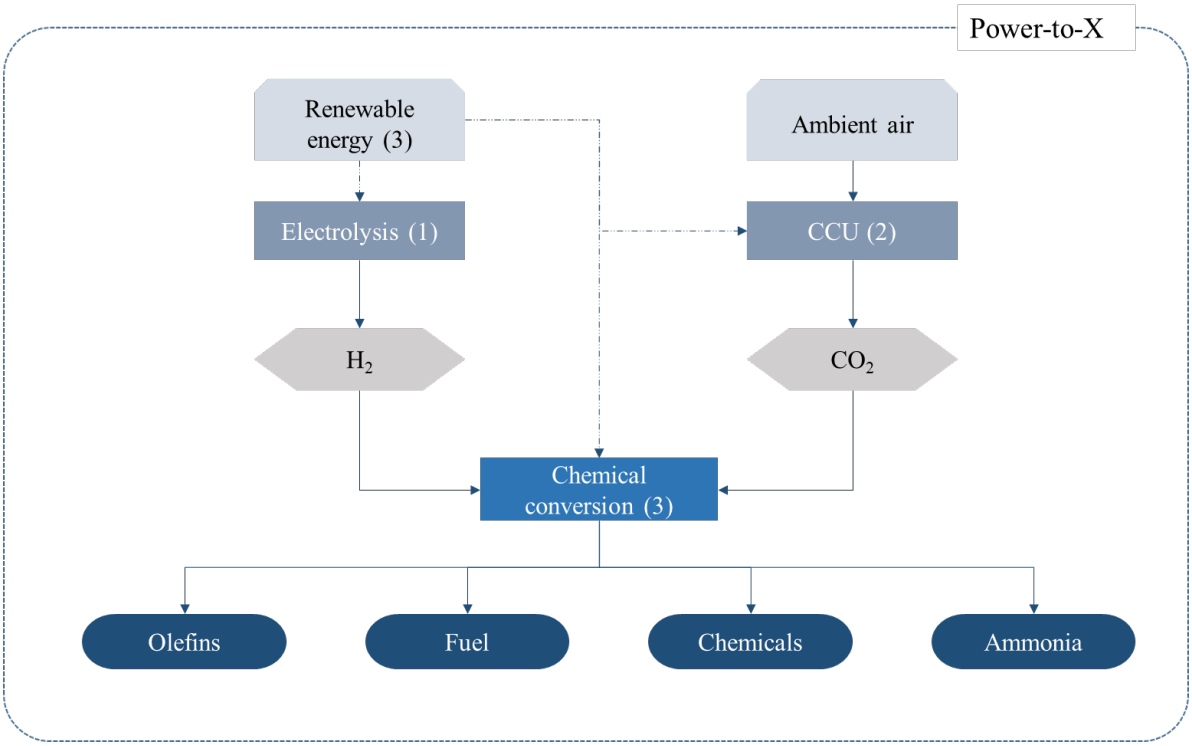

Figure 2-1 Power-to-X framework

In the following sections, a detailed exploration of recent advancements in several key areas will be presented. First, the latest technologies for electrolytic hydrogen production will be investigated. This includes an examination of various electrolysis methods, such as alkaline electrolysis, proton exchange membrane (PEM) electrolysis, and solid oxide electrolysis, all of which are essential for producing hydrogen using renewable energy sources. Then, the carbon dioxide utilization technologies, which are gaining significant attention as part of global efforts to reduce greenhouse gas emissions, are explored. Finally, the concept of integrated PtX systems will be discussed. These systems combine CO_2 hydrogenation with other processes to produce a wide range of high-value chemicals and fuels, such as methanol, olefins, ammonia, and synthetic hydrocarbons. The integration of these systems not only enhances the efficiency and economic viability of PtX technologies but also represents a significant step toward achieving a circular carbon economy. By turning CO_2 and H_2 into useful products, these systems help in decarbonizing the chemical industry, reducing the consumption and use of their counterpart chemicals sourced by fossil fuels, and contributing to global sustainability targets.

2.1. Electrolysis technologies

There are many ways to obtain hydrogen from fossil sources and renewable sources. Among the fossil sources are steam reforming, partial oxidation and autothermal reforming. Those technologies have been

extensively studied and are available in the literature [13,64,65]. In the renewable sources the most common method is water splitting through thermolysis, photolysis and electrolysis [66], with the latter being the focus of this study. Water electrolysis consists in water splitting reaction that is driven by an external electric energy using an electrolyser device including two electrodes and an ionic conductor. In the electrolyser, the electrical work split water molecule into gaseous hydrogen and oxygen according to the reactions 2-1, 2-2 and 2-3[67]:

$$2H^+ + 2e^- \rightarrow H_2 \ (Cathode) \qquad 2\text{-}1$$

$$H_2O \rightarrow \frac{1}{2}O_2 + 2H^+ + 2e^- \ (Anode) \qquad 2\text{-}2$$

$$H_2O \rightarrow H_2 + \frac{1}{2}O_2 \qquad 2\text{-}3$$

The electrolysis is conducted at temperatures lower than 100 °C limited by thermal stability of membrane materials [68]. There are three well-understood technologies for H_2 generation through water electrolysis: alkaline electrolysis (AEL), polymer electrolysis (PEM) and solid oxide electrolysis (SOE).

2.1.1. Alkaline Electrolysis (AEL)

This is the most mature and commercially developed system, and almost 67% of the realized projects in pilot plants from Germany use the AEL [69]. Alkaline solutions, such as KOH or NaOH, are used as electrolytes in atmospheric conditions or at temperatures of 70 °C and 140 °C with pressures from 1 bar to 200 bar producing compressed hydrogen. The mechanism starts with the constituents of alkaline solutions (KOH/NaOH) in the cathode where they are reduced to H_2, and hydroxyl ions are produced. Then, the H_2 is released from the cathode to recombine in gaseous form and the OH^- ions are transferred to the anode by the electrical force where it arrives as O_2 and water. Similar to the H_2 in the cathode, the O_2 in the anode is released and recombined into a gaseous form [66]. The drawback of this electrolysis is the low efficiency, namely between 60% and 71% and this is because of the corrosive solutions and the cost of maintenance [69,70].

The main parameter of importance is the cell voltage since it determines the energy consumption and electricity efficiency. Another parameter is the operating current density, conventional systems have between 1000 and 3000 A/m^2, and this parameter determines the rate of H_2 production and the higher production with higher current densities. However, high densities promote bubble formation that generates resistance and then low efficiencies. The water quality is essential for the correct operation of electrolysers since impurities could cause side reactions or deposition of salts. For example, chloride ions are highly corrosive for the metal components of the electrolysers [71].

2.1.2. Proton Exchange Membrane (PEM)

The PEM system is a new technology based on solid membranes, and it has high purity of products, and more flexibility compared to the AEL. In contrast, they are expensive due to the recent applications and its availability. Finally, solid oxide employs zirconium as the electrolyte that can reach electrical efficiencies of about 100% because of the low costs. Despite of this advantage, this technology is currently employed in laboratory scale and it needs much more research to be performed at the large scales [70]. In this approach, as in the previous electrolyser, water is split into H_2 and O_2 in the same way. Oxygen is released in the anode and the proton H^+ passes through the membrane to the cathode side where it is recombined into H_2. The polymer electrolyse membrane provides high proton conductivity, compact design, and high-pressure operation. It can operate at higher current densities ($2A/cm^2$) which reduces the operational costs. The high-pressure advantage allows less energy in compression for hydrogen for the end use. In addition, increasing the pressure minimizes the expansion and dehydration of the membranes, thus extending their life [72]. A comparison of the specification of previous two electrolysis systems is listed in Table 2-1, data taken from Carmo et al. [72] . As it may be observed, the PEM runs under higher densities than the AEL, however, in the main constraints of this technology involves the high cost of materials in the separator plates and collectors because the acidic environment of the proton flowrates.

Table 2-1. Specification of the AEL and PEM systems.

Specifications	*Alkaline electrolysis*	*PEM electrolysis*
Cell temperature (°C)	60–80	50–80
Cell pressure (bar)	<30	<30
Current density (mA cm^{-2})	0.2–0.4	0.6–2.0
Cell voltage (V)	1.8–2.4	1.8–2.2
Power density (mW cm^{-2})	<1	<4.4
Voltage efficiency HHV (%)	62–82	67–82
Specif. energy consumption: Stack (kW h Nm^{-3})	4.2–5.9	4.2–5.6
Specif. energy consumption: System (kW h Nm^{-3})	4.5–7.0	4.5–7.5
Lower partial load range (%)	20–40	0–10
Cell area (m^2)	>4	<0.03
H_2 production rate: Stack-system (Nm^3 h^{-1})	<760	<10
Lifetime stack (h)	<90,000	<20,000
Lifetime system (y)	20–30	10–20
Degradation rate (μV h^{-1})	<3	<14

2.1.3. Solid Oxide Electrolysis (SOE)

In solid oxide electrolysis, water is fed in the form of steam at the cathode side where it is reduced to H_2 while the oxide ions travel through the electrolyte from the cathode to the anode to be recombined into the oxygen molecules. The electrolyte materials are conventionally oxide ion conductors mostly from zirconia-based materials [73]. This approach operates at high pressures and high temperatures between 500–850 °C and it can achieve efficiencies of 90 – 100% as their main advantages. However, SOE has a lack of stability and degradation as the main concerns [66]. For these reasons, its application is still under development, and it needs more research before commercialization.

2.2. Carbon capture technologies

In addition to hydrogen, carbon dioxide is obtained as a feedstock through several technological routes. It can be captured from anthropogenic activities such as from flue gases of steel or cement plants, post combustion systems or direct from atmospheric air. The latter has been considered one of the most promising routes and it has boosted the research on this topic in the last few years [74]. The most important technologies for carbon capture are described in the subsequent section.

2.2.1. Post combustion CO_2 capture

The post combustion CO_2 capture is the most recognised technology of carbon capture systems. It involves separating CO_2 from the flue gases produced after fossil fuel combustion in industries such as cement, power, and Industrial furnaces [75]. This technology has the potential for reducing greenhouse gases emissions directly from the source. The absorption process with amines is the most common process in power plants where the flue gases have a concentration of CO_2 in the range of 5%-25% [76]. It also has been used in the removal of sulphuric acid from natural gas. A typical absorption process of post combustion capture is shown in Figure 2-2.

Initially, the hot gas is cooled down to a temperature between 40 °C - 60 °C. Then, the flue gases are passed through the absorber column where the amine solvent as monoethanolamine (MEA) bonds the CO_2 and releases the exhaust gas as cleaned gas. The CO_2 leaves the column attached to the solvent in higher concentration, after that, it is sent to a desorber column where amine solvent is recovered by heating to temperatures of 100 °C – 140 °C while the CO_2 gas flows to the compression stage [77]. Post-combustion is the most used commercial CO_2 capture process, suitable for high CO_2 concentrations. Its advantages include energy savings because of the low heat of reaction, high applicability to existing plants, the use of different solvents with low degradation such as ammonia with tolerance to oxygen, among others [76].

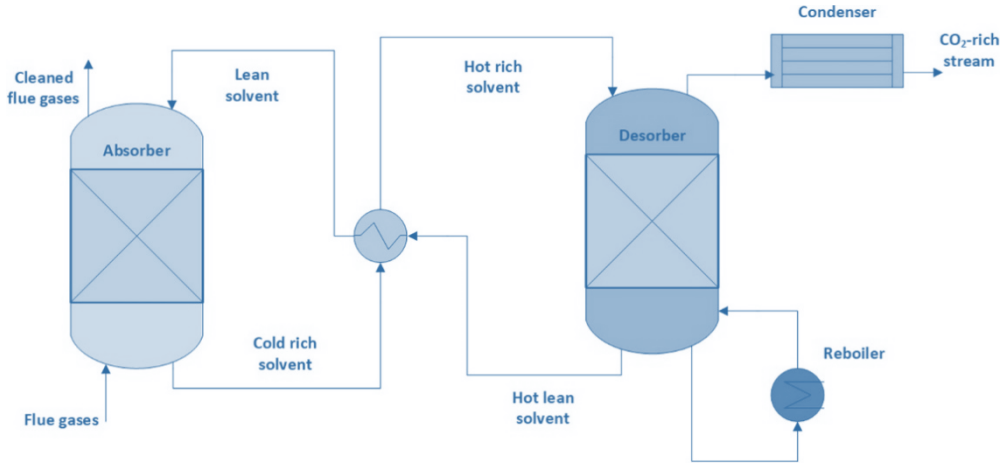

Figure 2-2. Schematic of the amine absorption technology of CO_2 capturing (Taken from Al-Hamed et al. [78]).

This system is able to recover 80-90% of the carbon dioxide and it is applicable to most of the existing coal-fired power plants [76]. In contrast, the large amount of energy required to regenerate the solvent has a major impact on the technical performance and costs [79]. Moreover, acid gases such as sulphur and nitrous oxides react with the solvent to form stable salts that reduce the absorption of CO_2. Thus, lower concentrations of these gases is desirable to avoid the loss of costs [79,80].

2.2.2. Pre-combustion carbon capture

The pre-combustion system refers to removing CO_2 from fossil source before combustion is completed. It includes a fuel-reforming step before the CO_2 separation. In the pre-reforming, the fuel is converted into syngas, which is a mixture of hydrogen (H_2) and carbon monoxide (CO). The mixture is sent to the shift reactor to transform water and CO into CO_2 and H_2 where CO_2 is captured.

Research on pre combustion systems is turning to advances in capture by liquid solvents, solid sorbents, and membranes to improve the separation of CO_2 at the final stage. The liquid solvent employs a liquid solution to absorb the CO_2. Its advantages include less energy to regenerate the material by increasing the temperature or increase pressure. Examples of physical solvents are *Selexol, Rectisol* and propylene carbonate. The main challenge is that its performance is better at low temperatures that involves the use of cooling systems and therefore additional energy requirements. The benefits of the process include 90 – 95% of CO_2 emissions capture, it is applicable to natural gas and coal plants and produces an enriched hydrogen fuel that can be further utilized [81]. The recovered heat is used to produce steam that also drives a turbine generator designed to generate electricity. Solid sorbent materials are also developing to remove CO_2 at higher temperatures. Lithium-silicate sorbents have been tested at temperatures of 250 – 550 °C, showing a removal of 90% of CO_2 from simulated syngas and it has contaminants tolerance in addition to a good

regeneration and resistance to high temperatures. It is stated that lithium silicate sorbent can separate CO_2 from syngas and promote the water gas shift reaction and thus increasing the efficiency of the process [76]. The process is known as the integrated gasification combine cycle and it is still being developed as a promising configuration for H_2 production [76]. Pre-combustion systems are more efficient than post combustion capture with around 90% capture efficiency. However, this system is not applicable to certain existing systems such as ships [82].

2.2.3. Oxy-combustion capture

This technology is applied to the flue gases as an alternative to increasing the amount of CO_2 in the stream and this then increase the efficiency. To attain higher concentrations, the fuel is burned with pure oxygen provided by an air cryogenic separation unit. After that, the flue gas comprises water vapour and CO_2 and the former is recovered through condensation [77]. The cost of the oxy-combustion is not as low as that of the conventional capture systems because the air separation unit and the flue gas recirculation imply additional cost of energy and maintenance [76]

2.2.4. Direct air capture of CO_2 (DAC)

Direct air capture (DAC) is the process that separates the carbon dioxide directly from the atmospheric air with a concentration of about four hundred parts per million, and the captured CO_2 can be stored in geological formations, or it can be used to produce chemicals and fuels [83,84]. The benefits of direct air capture as a carbon removal option include its ability to remove CO_2 directly from air and permanently storing it. Moreover, it can be used as a climate neutral feedstock speeding the efforts towards net zero goals [85]. Further, DAC is a technology that can capture more CO_2 without producing more emissions [86]. This means that the process can address larger amounts of air to capture more while the process is energy and cost efficient [86]. However, there are some concerns that academics recommend evaluating from an economic and environmental point of view such as a cleaner and affordable source of electricity [83,87]. At present, the direct air capture is not a long-term option, most large-scale opportunities to use the captured CO_2 are the subsequent conversion into synthetic fuels, but this would result in its re-release into the atmosphere, such as when the fuel is burned [16]. This would not create negative emissions but could still generate climate benefits, for example if synthetic fuels replace conventional fossil fuels [88]. The principle of the air capture from the atmosphere is based on the adsorption/absorption of CO_2, the two main technologies in research are solid and liquid DAC [89].

2.2.4.1. Solid - DAC

In the solid system, a solid adsorbent operates through an adsorption/desorption cycling loop [83]. The adsorption occurs when atmospheric air flows through the collector at normal temperature and pressure. Here a filter captures the carbon dioxide, once the filter is saturated, desorption takes place at vacuum pressure and moderate temperatures between 80-100 °C where concentrated CO_2 is released at purities of 99.9%. [90]. A single unit can capture several tens of tonnes of CO_2 annually (i.e. 50 tonnes of CO_2) and can extract water from the atmosphere approximately 1 tonne of water per tonne of CO_2. The solid DAC plant is designed to be modular, allowing for the inclusion of multiple units as needed. For example, the largest operational plant currently captures 4,000 tonnes of CO_2 annually [85]. Among solid DAC advantages include net water production, less capital intensive, it is a modular system, and the operation can rely on low carbon energy source. In contrast, main trade-offs include the energy intensive process, and the manual maintenance required for adsorbent replacement. The thermal advantages of this process include the low energy consumption and its integration with other units and the capability of generating water from the air moisture. This process has been scaled for the *Climeworks* Company that offers a standard unit of 0.14 t CO_2 per day [91].The energy consumption of this technology ranges from thermal between 1500 and 2000 kWh/ton CO_2 while electrical is in a range of 200 – 300 kWh/ton CO_2 [88,92].

2.2.4.2. Liquid - DAC

The second technology utilizes an aqueous solution of NaOH or KOH where the CO_2 is absorbed to form a carbonate compound. This carbonate is reacted with calcium hydroxide to regenerate the sodium hydroxide and produce calcium carbonate. The latter is calcined at high temperature (i.e. 900 °C) to release the CO_2 and regenerate the calcium hydroxide for the next cycle [93,94]. Four major steps take place in the liquid sorbent DAC: air contactor, pellet reactor, slaker reactor and calciner. The advantages of liquid sorbent in DAC include less energy intensity; it employs commercial solvents; the technology can be adapted from existing commercial units. In turn, the drawbacks are its capital-intensive cost and its reliability on the fossil fuel for the regeneration of the solvent. The thermal energy consumption of liquid DAC ranges between 1420-2250 kWh/ton CO_2 and electrical between 366 and 764 kWh/ton CO_2 captured [86]. In this regard, the present thesis proposes a complete heat integration of the PtX plant where DAC energy needs is covered internally or using renewable sources. The company Carbon engineering has developed a pilot plant using liquid DAC technology with an annual capture capacity of one $MtCO_2$ [89] and it is the world's largest DAC facility.

In the economic performance, in general, the estimated cost of DAC is higher than the traditional flue gases capture, where the cost is from $30 to $100 dollars per ton of CO_2 while the DAC systems are of the

order of $1000 per tonne of CO_2 captured [83,89]. The cost of capture could reach up to $200 per ton only if energy is supplied by wind or solar sources in which the costs of electricity is a parameter of sensitivity in both technologies [83,95]. As mentioned before, the energy consumption is a critical parameter since in both technologies it represents around 43% percent of the total, being the driver of the process within the cost of the plant [88]. For that reason, it is the prime importance for both DAC systems to find a very low-cost renewable energy to reduce the final CO_2 production cost. A comparison of both technologies specifications is shown in Table 2-2.

Table 2-2. Specification comparison of the main two DAC technologies.

Specification	*Units*	*Solid – DAC*	*Liquid - DAC*
CO_2 separation		Solid adsorbent	Liquid sorbent
Specific energy consumption	MWh/tCO_2	2-2.6	1.5-2.4
Share as a heat consumption	%	75-80	80-100
Share as electricity consumption	%	20-25	0-20
Regeneration temperature	°C	80-100	Around 900
Regeneration pressure	-	Vacuum	Ambient
Capture capacity	-	Modular (50 tCO_2/year per unit)	Large scale (0.5-1$MtCO_2$/year)
Life cycle emissions	tCO_2e/tCO_2 captured	0.03-0.91	0.1-0.4
Levelized cost of capture	USD/tCO_2	Up to 540	Up to 340

2.3. Integration of electrolytic H_2 and CCU into PtX concept

In the Power-to-X (PtX) concept, the use of CO_2 and H_2 plays a crucial role in converting renewable energy into chemical products, fuels, or energy carriers, thereby enabling a sustainable energy system. By integrating CO_2 into the production cycle, the PtX concept supports carbon recycling, reducing the overall carbon footprint and contributing to the mitigation of climate change. H_2 use in PtX processes allows for the storage and transport of renewable energy in chemical form, addressing the intermittency of renewable power sources like wind and solar. The integration of CO_2 and H_2 in the PtX concepts provides a pathway for converting renewable electricity into valuable, storable, and transportable products. This approach not only helps in decarbonizing sectors that are difficult to electrify directly but also in closing the carbon loop, making it a vital strategy for achieving global sustainability and energy transition goals. Therefore, the main power to X technological pathways that integrate CO_2 and H_2 are reviewed in the next sections.

2.3.1. Power-to-Methanol

The use of fossil resources results in an intensive accumulation of greenhouse gases (GHG) that are responsible for the temperature increase of the planet and an increase in temperature above 2 °C will cause an irreversible damage to the planet. In view of this, many have agreed to limit the global temperature

increase to 1.5 °C above pre-industrial levels by 2050 according to the Paris Agreement in 2015 [1]. This action incorporates decarbonisation strategies and actions for the chemicals, power and fuels industries in the public and the private sectors [6]. Currently, according to the International Energy Agency (IEA). [24], the chemical sector globally generates about 1.5 gigaton of CO_2 annually, 27% of which comes from high value chemicals including light olefins and aromatics. The consumption trends in high-income regions are closely related to the rising demand for chemicals; the average amount of plastics consumption in the European Union is between 55 – 80 kg per capita and it is anticipated that the global primary chemicals demand will have increased around 30% by 2030 and up to 60% by 2050 [24].

Methanol derived from CO_2 serves as a promising raw material for the chemical industry, particularly to produce olefins. Producing methanol from CO_2 is one of the most established pathways PtX approach. It has garnered recent interest due to the advantages, including well-established technology and existing commercial applications [96]. The catalytic hydrogenation of CO_2 into methanol is typically achieved through a single-step reaction according to reaction 2-4 [21].

$$CO_2 + 3H_2 \leftrightarrow CH_3OH + H_2O \qquad 2\text{-}4$$

The methanol production process from CO_2 occurs within a temperature range of 200 °C to 300 °C and under pressures of 50 to 100 bar, facilitated by a copper-based catalyst supported on metal oxides [61]. A significant challenge in this pathway is the substantial energy requirement for hydrogen production, typically achieved through the electrolysis of water [21], [97]. In the process, both CO_2 and H_2 are initially compressed and then heated before entering the methanol reactor. Post-reaction, unreacted CO_2 is separated and recycled back into the compression system. The resulting methanol-water mixture is directed to a distillation column under atmospheric conditions, where methanol is purified, followed by a final flash separation at 20 °C [61].

An alternative pathway for methanol production is the two-step process, which involves the initial generation of syngas through steam reforming, dry reforming, or the reverse water-gas shift (RWGS) reaction before proceeding to methanol synthesis [98–100]. In this approach, CO_2 is first converted into syngas via dry reforming or RWGS. Subsequently, carbon monoxide reacts with hydrogen to form methanol, as represented in reaction 2-5 and reaction 2-6. To enhance the yield of CO and methanol, the reverse water-gas shift reaction is carried out concurrently [100].

$$CO_2 + 2H_2 \leftrightarrow CO + H_2O \quad \textit{2-5}$$

$$CO + 2H_2 \leftrightarrow CH_3OH \quad \textit{2-6}$$

The source of CO_2 is often from the flue gases of the power plant, direct capture from the air or the cement industry while hydrogen is a key element of the process, commonly obtained from water electrolysis because its environmental advantages.

The two-step pathway has been studies to have a higher methanol yield, lower catalyst cost and smaller reactor size. Previous studies have revealed the minimum selling price of methanol as being \$1-\$1.5 per kg, and this range is above of the market price of \$0.45/kg [101]. The benefit of this approach relies on its reduction of GHG since its main feedstock comes from air or fixed sources such as flue gases and the use of renewable electricity is applied to produce the hydrogen. The emissions of GHG of a methanol production plant from a CO_2 source are 13.6 gCO_2-eq per MJ compared to the conventional process with 91.5 g CO_2-eq per MJ in a study performed by Zhang et al. [101]. As it has been seen, methanol production from CO_2 has potential environmental advantages. The main constraint of their future application is still the economic performance. Indeed, there are some policies applied to the carbon capture and use, however, the research on the optimization routes is already in progress and its of prime importance is to have a better comprehensive analysis of the techno economic behaviour of different routes, including the upgrading of methanol into high value products. Nyari et al. [102] have evaluated the feasibility of the MeOH−CCU plant. They simulated a 5 ktonne of methanol production. The study concludes that under current market conditions, the production of methanol is not feasible; the main costs are related with the H_2 production through electrolysis. It highlights the importance of selling other products such as the oxygen produced and the lowering the hydrogen cost price to have a significant change in the levelized cost of methanol.

2.3.2. Power-to-Olefins

Olefins are important building blocks of chemicals and hydrocarbons with an increasing market over the recent years [23]. The technique with special interest is the methanol to olefins process through power-to-olefins (PtO), where propylene and ethylene are the main products as well as heavy hydrocarbons [27].

After the methanol synthesis, the reaction of methanol into olefins (MTO) can be described in two steps. The first step is the conversion of methanol to dimethyl ether (DME) and water as in reaction 2-7. Next, DME is converted to ethylene and propylene through reactions 2-8 and 2-9. The product selectivity is about 55% towards hydrocarbons and 44% to water [96].

$$2CH_3OH \rightarrow CH_3OCH_3 + H_2O \quad \textit{2-7}$$

$$CH_3OCH_3 \rightarrow C_2H_4 + H_2O \quad \textit{2-8}$$

$$3CH_3OCH_3 \rightarrow 2C_3H_6 + 3H_2O \quad \textit{2-9}$$

During the process, reactions of methanol take place in a fluidized bed reactor, where a portion of the catalyst is periodically removed to prevent coke deposition. The reactor operates within a temperature range of 340 to 540 °C and at pressures between 0.1 and 0.3 MPa [103]. After reaction, the dimethyl ether (DME), water, and olefins products are directed to a separation unit, where water is removed and unreacted DME is recovered. The olefin-rich stream is then processed through a fractionation column, where ethylene and propylene are separated from medium boiling hydrocarbons. The heavier olefins are subsequently sent to a cracking unit, where additional propylene and ethylene are recovered [96].

Fossil - based olefin production entails the use of high carbon intensive materials such as natural gas, coal and petroleum naphtha that results in augmented GHG emissions [26]. In recent years, research has been focused on developing and evaluating innovative process for a sustainable olefin production. For instance, bio-ethylene is produced from sugarcane bioethanol dehydration and other crops and it has been implemented at an industrial scale [24,104]. Mohsenzadeh et al. [105] investigated the techno-economic performance of bio - ethylene production using bioethanol as feedstock. They concluded that the cost of the feedstock has a significant impact on the profitability. Therefore, this approach is only applied in regions with feedstock availability at competitive prices [106]. Alternatively, olefins can be produced using direct CO_2 hydrogenation in one step or via a two-step process with methanol as intermediate in a power to X concept (PtX) coupled with the carbon capture utilisation (CCU) [107]. The purpose of the strategy is to utilise CO_2 as a carbon source to produce clean high value-added chemicals such as olefins utilizing renewable H_2 [108]. This concept has also been the subject of several studies. Zhao et al. [107], explored the economic viability of twenty different olefins manufacturing processes. They compared fossil and renewable processes including the CO_2 to olefin conversion route. They concluded that fossil pathways are more competitive than the renewables routes because of the price of H_2; if the H_2 cost drops by 55% and the plant scale is expanded from 100 to 1000 ktonne per year then costs savings of around 4% - 23% can be achieved. Further, Do and Kim. [109] developed a techno economic analysis of green C_2-C_4 hydrocarbon production through CO_2 hydrogenation and renewable H_2. By using solar or wind electricity for hydrogen production, results revealed low net CO_2 emissions but higher hydrocarbon prices ($2.8 - 5.5 USD/kg C_2-C_4). Nevertheless, when using fossil-based options SMR and coal-based hydrogen, results denoted higher emissions (13.6 kg CO_{2e}/kg C_2-C_4) and a cost of $2.6 USD/kg C_2-C_4 product, making the H_2 price the most

sensitive factor. Similarly, Savaete [110] analysed the techno-economic performance of a catalytic CO_2 conversion into olefins using conventional and renewable methanol as an input. The findings revealed that the MTO process using renewable methanol as an input resulted in an ethylene production cost of 3700 €/ton which is higher than the ethylene from conventional methanol, 935 €/ton. It was suggested carbon taxes would need to be high for the MTO feasibility. Pappijn et al. [111] assessed the economic feasibility and the CO_2 avoidance potential of the electrochemical reduction of CO_2 to ethylene based on a conceptual design excluding the separation and purification stages in the emission counting. They determined that ethylene from electrolytic CO_2 conversion is not feasible under current market conditions and current catalyst performance. They advised the process needs to be powered by green electricity to obtain a net CO_2 balance overall.

Regarding environmental analysis, Keller et al. [112], examined in a cradle to gate evaluation, the environmental impacts of the olefin production-using fossil - based and an alternative feedstock in Germany. Although it was shown that production using renewable resources reduced GHG emissions, other environmental categories were adversely impacted. Rosental et al. [113] provided a life cycle assessment of large volume organic chemicals including olefins from CO_2 capture and renewable H_2. Results revealed that the usage of power generated by offshore wind turbines for CCU methanol, olefins and aromatics synthesis reduces GHG emissions between 88 and 97%. It is important to mention that those reductions included the CO_2 uptake in the capture system. Kuusela et al. [108] evaluated the greenhouse gas emissions of CO_2 based polypropylene (PP) by applying the power to X concept. While using renewable energy for H_2 production, natural gas and electricity from the grid were consumed in the olefins synthesis, resulting in an estimated gross emission factor of 2.79 kg CO_2e/kg PP. The literature review indicated that some studies have assessed the economic impact of olefin production, but they have mostly focused on the olefins synthesis and have not included the process modelling of the CO_2 and H_2 feedstock and potential heat integration opportunities between different components. This work includes the simulation of each step in the chain, identifies, and applies heat integration. Overall, a holistic LCA and TEA of the whole CCU assembly of a power to the olefins (PtO) pathway is currently missing from the literature and the goal of the present study is to fill this gap.

2.3.3. Power to ammonia

The concept of power to ammonia (PtA) is an emerging technological approach that involves producing ammonia using renewable sources. This method offers a sustainable alternative to traditional ammonia production that typically is based on fossil sources through the Haber – Bosch process [32]. The main feedstock of fossil-based process is the hydrogen supplied by syngas (CO + H_2) which conventionally is produced by technologies such as steam methane reforming, RWGS reaction, and dry reforming process.

The carbon footprint of this pathway ranges from 2.3 to 5.2 tonne CO_{2e}/tonne NH_3 produced [114], nearly twice as emissions intensive as crude steel and four times as cement [115,116]. To tackle these emissions, PtA has been proposed as a means of effectively utilizing renewable energy and storing it as ammonia and it has emerged as a near zero emission method. A "green" process is used as the surplus energy from renewable sources to convert the electrical input and water into hydrogen through the electrolysis of water and the air separation unit to supply nitrogen (Figure 2-3) [36,37]. Wind, solar, nuclear and hydropower are proposed as the most prominent sources of power to ammonia with promising results from the economic and environmentally point of view. The United Kingdom (UK) in particular, has raised the importance of wind energy as a potential source for green ammonia [38].

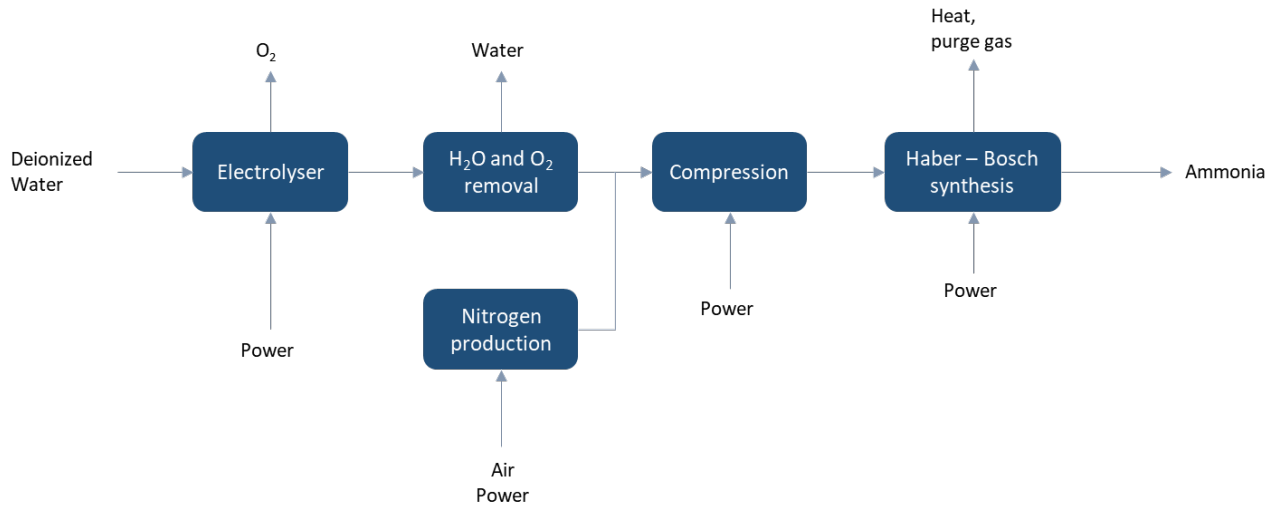

Figure 2-3 Process flow diagram of the power to ammonia concept.

Initially, deionised water is fed to the electrolyser where it is split into H_2 and O_2, after the removal of the water, the gas mixture is sent to a compression unit along with the nitrogen from the air separation unit at pressures between 100 – 450 bar [32]. In the ammonia synthesis, the compressed gas within the reactor reacts at 300 – 350 °C in a multiple bed reactor where 15 – 20 mol % of feed is converted to ammonia according to reaction 2-10*:*

$$3H_2 + N_2 \rightarrow 2NH_3 \qquad 2\text{-}10$$

The iron catalysts are mostly used with promoters such as Al_2O_3, CaO, MgO and SiO_2 because of their thermal stability [65]. The reaction mixture leaves the reactor at 450 – 500 °C and it is cooled down so that ammonia liquefies and can be removed by condensation at -20 to 30 °C [117].

The economic assessment of power to ammonia have been investigated before for small and medium scale plants [4,15–20], while large-scale have received less attention [118–120]. The reported cost of green

ammonia ranges from £400 to £1200/tonne NH_3, depending on the source of energy, technology, efficiencies and scale. Electrolysers, such as the polymer membrane electrolyser (PEM), solid oxide electrolyser (SOEL) and alkaline electrolyser (AEL) are the common technologies applied. Some models use general assumptions such as average price of the electricity cost to estimate the levelized cost of ammonia (LCOA) [119]. Since the electricity consumption is recognized as the main cost driver, the levelized cost of electricity (LCOE) plays an important role on the economic feasibility of ammonia and extensive research is required to better understand the potential improvements.

The environmental aspect of green ammonia has also been assessed [28,114,121–124]. The carbon footprint of green ammonia ranges from 0.149 to 0.8 kg CO_2e/kg NH_3. The range of emissions is due to the different assumptions made in the models, especially in the hydrogen production; the latter is often overlooked within the assessment boundaries and assumptions are employed to account for its emission impact. One of these assumptions is that renewable energy comes with zero carbon emissions and hence excludes upstream emissions such as infrastructure and logistics [125,126]. These assumptions are essential in the sustainability of PtX projects because a large part of the emissions comes from the energy source [127].

Further, the integrated economic and environmental performance of green ammonia have been only addressed in few studies [126,128–130]. These are based on comparisons with blue and green ammonia or utilising electrochemical synthesis. For instance, Lee et al. [126] assessed the techno-economic and the life cycle greenhouse gas emissions of various ammonia production pathways, including green ammonia. The study does not include the hydrogen production as part of the modelling; however, they remark that the hydrogen cost is the major contributor to the LCOA and a lower production cost is required for green ammonia to be cost competitive. Moreover, the study determines that no emissions are derived from renewable sources and suggested a more detailed environmental assessment. On the other hand, Mayer et al. [129] presented a techno-economic and LCA comparison of blue and green ammonia. According to the authors, at current ammonia prices, green ammonia is not profitable, and they show that green ammonia has the lowest emissions with the electricity consumption as the main driver due to the grid connection. The limitations of the studies are that many techno-economic and environmental variables are adopted from the literature and are not derived from comprehensive process modelling, TEA and LCA, and hence their results come with higher uncertainty and certain limitations.

Therefore, this thesis provides a comprehensive analysis of the PtA process, evaluating its technical, economic, and environmental performance. It explores the potential benefits of shifting from conventional ammonia production methods to a renewable energy-based approach, identifying the key drivers, challenges, and opportunities for implementing this innovative process on a large scale.

2.3.4. Power-to-formic acid

The chemical industry is responsible for the production of a wide array of products derived from natural and mineral raw materials, playing a critical role in various sectors. However, this industry is also a significant contributor to global carbon emissions, which has driven research and development efforts aimed at reducing pollution and mitigating environmental impacts. Decarbonisation of the chemical industry is essential to achieving global sustainability and climate targets.

One promising strategy to achieve this goal is the utilization of captured carbon dioxide (CO_2) from air as a feedstock for chemical production through PtX [9,11,131]. This approach not only offers a pathway to reduce carbon emissions but also aligns with circular economy principles by converting waste CO_2 into valuable products [49,132]. Among the various chemicals that can be produced using captured CO_2, formic acid (FA) stands out due to its wide range of industrial applications, including its use as a preservative, antibacterial agent, and in fuel cells [41,42]. Formic acid (HCOOH, FA) is the simplest carboxylic acid, a colourless liquid miscible with polar solvents. FA is widely used as a food additive, preservative in silage and animal feed, and as a bactericide. It also finds applications in the dyes, rubber, textile, and leather industries [43]. In the fuel industry, FA is considered a promising candidate for hydrogen storage due to its high volumetric capacity and low toxicity [43–46].

The global market for formic acid reached approximately 750 thousand tonnes in 2022 and is expected to grow at a rate of 4.48% during the forecast period up to 2035, with China being the largest producer [47]. Formic acid has been the focus of several projects in Europe that apply the power-to-chemicals concept [48]. For example, the Norwegian company DNV has developed a pilot plant for the electrochemical conversion of CO_2 into formic acid. Additionally, the European Horizon 2020-funded C2Fuel project aims to produce dimethyl ether (DME) and formic acid from renewable hydrogen (H_2) and captured CO_2 from industrial sources [49].

The conventional production process of formic acid involves two steps: the carbonylation of methanol in the presence of a base catalyst (such as sodium or potassium), followed by the hydrolysis of methyl formate to formic acid and methanol according to 2-11 and 2-12 [18]. This process has several drawbacks, including an unfavourable hydrolysis equilibrium, which results in a large water requirement and, consequently, high-energy consumption for water removal. Furthermore, the carbon monoxide used in the reaction is obtained from fossil resources [18,50].

$$CH_3OH + CO \rightarrow HCO_2CH_3 \qquad 2\text{-}11$$

$$HCO_2CH_3 + H_2O \rightarrow HCOOH + CH_3OH \qquad 2\text{-}12$$

Alternative technological routes for formic acid production, such as electrolytic CO_2 conversion, have been explored. Various studies have evaluated the feasibility of electrolytic formic acid production, but the main challenges include high electricity consumption and the use of expensive cell materials [44,51–57].

The thermochemical catalytic route of CO_2 conversion is the most advanced and closest to industrial implementation [133]. Advantages of CO_2 transformation into formic acid include the substitution of fossil-based chemicals with renewable feedstock in several commercially important processes, and a good level of technology readiness (TRL 4-6) [51,134]. Several studies have investigated the catalyst performance of CO_2 hydrogenation into formic acid using both heterogeneous and homogeneous catalysts [135]. Heterogeneous catalysts, such as Ru polymeric catalysts, have shown excellent selectivity and stability [135–137]. These catalysts offer the advantages of recyclability and efficient separation from products. Metal catalysts like Au, Si, Pd, Ir, and Ru, along with various support materials, have been tested with promising results [138–142]. For example, Ru catalysts have demonstrated CO_2 conversion efficiencies of around 44%, with favourable turnover frequencies achieved using additives such as ethanol and trimethylamine [142,143].

Homogeneous catalysts also show potential for FA synthesis, particularly due to their reversibility towards H_2 production at high rates and room temperature [42]. High CO_2 conversion rates (greater than 95%) can be achieved under mild conditions, with Ru-phosphine catalysts being the most commonly used due to their high turnover frequencies and selectivity [48,134,135,144]. However, homogeneous catalysts require additional steps for recovery and purification due to decomposition during the FA recovery process.

To achieve sustainability of power to formic acid, it is crucial to evaluate the energy intensity, economic viability, and environmental impact of the carbon utilization technologies for producing FA. Although numerous studies have performed economic and environmental assessments for FA production via the catalytic and electrolytic route, there is a scarcity of research addressing both economic and environmental aspects that integrate a complete process modelling and heat integration.

Kim and Han. [144] presented two commercial-scale processes for catalytic production of formic acid (FA) from CO_2, analysing economic, energy, and environmental indicators. The results showed that the minimum selling price (MSP) of formic acid using a Ru-Ph catalyst (process A) reached US $1029 per tonne of FA, with the primary cost drivers being hydrogen production and the catalyst consumption. They also reported net CO_2 emissions of 0.36 tonnes per tonne FA, accounting for CO_2 uptake and excluding the production of H_2 in the model. In a separate study, Perez-Fortes et al. [48] conducted process modelling to evaluate the techno-economic and environmental aspects of thermocatalytic production process of formic acid from captured CO_2 and renewable H_2. They found that hydrogen capital costs and the catalyst were

the main contributors to an MSP of €1656 per tonne, which is not competitive with the market price. Their environmental assessment allocated zero emissions to renewables, resulting in an underestimation of CO_2 emissions (0.166 tonnes per tonne FA). Gokberk and Wiebren. [145] studied a large-scale CO_2 and biomass-based formic acid production system. He concluded that the biomass route exhibited higher energy efficiency than the CO_2-based route (37% vs. 31%, respectively). However, the CO_2 hydrogenation route involved higher capital expenditures due to reactor costs, while the biomass route had a significantly higher breakeven selling price of US $22,060 compared to US $2363 per tonne FA for the CO_2 route. This discrepancy was attributed to the higher material costs in the biomass case. A recent study by Kang et al. [54] quantified the climate change and fossil depletion impacts of formic acid production through catalytic hydrogenation. They reported that GHG emissions could be reduced by 97%-132% and fossil resource consumption by 69%-94% compared to conventional production. The major contributor to these reductions was the CO_2 capture included in the net emission calculations. Kim and Park. [134] presented a pilot-scale process for formic acid production via CO_2 hydrogenation through the catalytic route, including techno-economic and life cycle assessments. They reported CO_2 conversion rate of 82% and a formic acid purity of over 92%. They reported that their proposed process reduced production costs by 37% and global warming impact by 42% compared to the conventional process. Barbera et al., [146] performed a simulation model incorporating kinetics to convert CO_2 into C1 chemicals through hydrogenation. They assumed H_2 availability from renewable sources obtaining a carbon conversion rate of 88%, an energy ratio of 0.229, and carbon emissions of 0.366 tonnes CO_2 per tonne FA.

Separately, Artz et al., [50] reviewed various published studies on CO_2 conversion through life cycle assessment. They reported that the global warming emissions of formic acid range between 0.54 and 1.58 tonnes CO_{2e} per tonne of FA for scenarios projected for 2020, with CO_2 capture included as part of the net emissions. Kim et al., [44] explored the potential of using formic acid as a liquid organic hydrogen carrier (LOHC). They assessed both heterogeneous catalytic and electrochemical routes. The techno-economic results indicated that the thermocatalytic route requires extensive amounts of steam, leading to high production costs for FA. From an LCA perspective, the production of FA was found to be the primary contributor to the GWP of the LOHC system due to the significant energy consumption needed for H_2 production.

The previous studies have evaluated the potential of producing formic acid (FA) through thermocatalytic routes using renewable sources such as green H_2 and captured CO_2; however, these studies often have limitations. Many of them include fossil resources as fuels or electricity in their processes, which detracts from the overall sustainability. Additionally, these studies often rely on black-box models or simple simulations of FA reactors that do not incorporate detailed reaction kinetics. This lack of detailed modelling

limits the accuracy and applicability of the findings. Moreover, these studies generally do not conduct a comprehensive techno-economic and life cycle assessment (LCA) of the entire power-to-formic-acid (PtFA) process. They typically dismiss the full accounting of the environmental and economic impacts of the feedstock H_2 and CO, as well as the electricity supply used in the process. A common practice in LCA is the inclusion of the carbon uptake in the capture model, but this approach can underestimate the carbon footprint in a cradle-to-gate analysis since the carbon is eventually released back into the atmosphere at the end of the product life cycle.

This study aims to bridge these gaps by evaluating the environmental and economic performance of producing FA through PtFA process. This process incorporates green H_2 and CO_2 captured directly from the air, utilizing renewable offshore wind energy as the primary electricity source. A cradle-to-gate life cycle assessment (LCA) encompassing 18 impact categories under the ReCiPe Midpoint (H) method and an economic analysis using the minimum selling price (MSP) as a feasibility indicator are conducted. The study provides a more detailed and comprehensive evaluation of the PtFA process, including the full integration of renewable energy sources and a thorough assessment of both economic and environmental impacts. This approach will offer a more accurate representation of the potential of PtFA in significantly reducing greenhouse gas emissions, water consumption, and fossil resource use compared to traditional production methods, contributing valuable insights towards the sustainable transformation of the chemical industry

2.4. Research gaps

Identifying research gaps in the fields of Power-to-X (PtX) is crucial for advancing these technologies and making them viable for widespread industrial application. The following are the key research gaps in each of these areas:

2.4.1. Carbon capture

Current carbon capture technologies, while crucial for mitigating CO_2 emissions, face significant challenges due to their high-energy demands. Carbon capture, utilization technologies often require substantial amounts of energy. These processes typically involve energy-intensive operations, such as the regeneration of solvents in chemical absorption systems or the high-pressure compression of CO_2 for further use or storage. A critical aspect of improving the efficiency of carbon capture systems involves comprehensive heat integration within the overall process. In particular, the integration of DAC systems with PtX technologies offers a promising pathway for creating a more energy-efficient and synergistic operation. DAC systems typically require high temperatures for the regeneration of sorbents, often achieved

through energy-intensive processes like calcination. Currently, they rely on external energy sources, such as natural gas, to achieve the necessary temperatures in the calciner, which not only increases costs but also introduces additional carbon emissions into the system. A complete heat integration in addition to the use of renewable energy sources such as wind could significantly reduce the reliance on fossil fuels and lower the overall carbon footprint of the process. Developing such integrated systems could lead to breakthroughs in reducing the energy costs associated with carbon capture, making it a more attractive and feasible option for large-scale deployment.

2.4.2. Olefins

The conversion of CO_2 and H_2 into olefins is a highly energy-intensive process, primarily due to the nature of the feedstock involved. The production of hydrogen through electrolysis and the subsequent hydrogenation of CO_2 requires significant amounts of energy, which poses a challenge for the overall efficiency and sustainability of the process. To address these challenges, advanced process integration strategies are essential to maximize the yield of olefins while minimizing the energy consumption throughout the production chain.

The literature review reveals that while some studies have assessed the economic impact of olefin production from CO_2 and H_2, they have predominantly focused on the olefin synthesis stage itself. These studies often overlook the upstream processes, such as the generation and conditioning of the CO_2 and H_2 feedstock, and do not fully explore the potential for heat integration between different process components. Effective heat integration is crucial for reducing energy consumption and enhancing the overall sustainability of the PtO pathway, yet it remains inadequately addressed in existing research.

This investigation seeks to address these gaps by simulating each step in the PtO production chain, including the renewable offshore wind power generation, production of CO_2 and H_2 feedstock, their conversion into olefins, and the associated heat integration opportunities. By doing so, the study aims to optimize the entire process, improving energy efficiency and reducing costs. Furthermore, this research will undertake a comprehensive Life Cycle Assessment and Techno-Economic Analysis of the entire Carbon Capture and Utilization assembly within the PtO pathway. Such a holistic approach is currently absent from the literature, and this study aims to fill this critical gap by providing a detailed assessment of the environmental and economic performance of the olefins pathway. This comprehensive evaluation will offer valuable insights into the potential of PtO as a sustainable solution for olefin production, contributing to the broader goal of industrial decarbonisation.

2.4.3. Ammonia

Research into green ammonia production methods is critical to advancing the chemical industry's sustainability efforts, particularly in reducing its reliance on fossil fuels. Green ammonia is produced using renewable energy sources, such as hydrogen generated through electrolysis and nitrogen extracted from the air. However, several challenges need to be addressed to make these processes viable on a large scale.

Green ammonia production requires technological advancements that can enhance the efficiency of synthesis production and nitrogen separation, while simultaneously reducing the energy demands and costs associated with these processes. In addition to technological improvements, a comprehensive understanding of the environmental impacts of green ammonia production is essential. This understanding can be achieved through detailed life cycle analyses that compare green ammonia with conventional ammonia production methods. Such analyses are crucial for identifying potential environmental benefits, as well as areas where the green ammonia production process could be further enhanced. However, many existing techno-economic analyses and LCAs rely on assumptions and data extrapolated from literature rather than being supported in detailed process modelling. The few studies that have carried out simulation models tend to shorten the reactor synthesis by using simple reaction models instead of more detailed kinetic reactions. This can result in higher levels of uncertainty and limitations in the conclusions drawn from these studies.

To address these gaps, the current study aims to provide a more robust and comprehensive assessment of green ammonia production. By employing exhaustive process modelling that includes detailed reaction kinetics and energy integration strategies, the study seeks to deliver a more accurate and reliable TEA and LCA. This approach involves simulating each step of the production process, from hydrogen production via low-temperature PEM electrolysis to nitrogen generation through cryogenic distillation, all powered by renewable energy sources like offshore wind. The inclusion of energy integration across the entire production chain ensures that the process is not only environmentally friendly but also economically viable. This comprehensive analysis will contribute significantly to the field by providing a clearer understanding of the potential for green ammonia.

2.4.4. Formic acid

The current processes for converting CO_2 and hydrogen into formic acid are not fully optimized for industrial-scale production. Research is needed to improve reaction kinetics, catalyst efficiency, and overall system integration. Techniques that minimize energy use and improve product purity are needed. A thorough understanding of the lifecycle environmental impacts of PtFA processes is necessary to ensure

they offer genuine sustainability benefits. Research should focus on comparing these processes to conventional formic acid production in terms of carbon footprint and resource use.

Some studies have evaluated the potential of producing formic acid (FA) through thermocatalytic routes using renewable sources such as green H_2 and captured CO_2; however, these studies often have limitations. Many of them include fossil resources as fuels or electricity in their processes, which detracts from the overall sustainability. Additionally, these studies often rely on black-box models or simple simulations of FA reactors that do not incorporate detailed reaction kinetics. This lack of detailed modelling limits the accuracy and applicability of the findings. Moreover, these studies generally do not conduct a comprehensive techno-economic and life cycle assessment of the entire power-to-formic-acid process. They typically dismiss the full accounting of the environmental and economic impacts of the feedstock H_2 and CO, as well as the electricity supply used in the process. A common practice in LCA is the inclusion of the carbon uptake in the capture model, but this approach can underestimate the carbon footprint in a cradle-to-gate analysis since the carbon is eventually released back into the atmosphere at the end of the product lifecycle.

This study aims to bridge these gaps by evaluating the environmental and economic performance of producing FA through PtFA process. This process incorporates green H_2 and CO_2 captured directly from the air, utilizing renewable offshore wind energy as the primary electricity source. The study provides a more detailed and comprehensive evaluation of the PtFA process, including the full integration of renewable energy sources and a thorough assessment of both economic and environmental impacts. This approach will offer a more accurate representation of the potential of PtFA in significantly reducing greenhouse gas emissions, water consumption, and fossil resource use compared to traditional production methods, contributing valuable insights towards the sustainable transformation of the chemical industry

Chapter III

3. Methodology

The following sections offer a comprehensive overview of the methodology employed in developing the process modelling, as well as the economic and environmental assessments. The operational specifications and key assumptions related to each individual PtX process are outlined in the respective chapters.

3.1. Process modelling

The design of all case studies will be performed according to the process design simulation model approach. This methodology consists of a representation of the chemical processes by a mathematical, thermodynamic, and or physics models through a chemical simulation software such as Aspen Plus.

Process simulation models are used to predict the behaviour of a specific process under given operating conditions. Aspen Plus, is a commercial process simulation software to perform steady state heat and mass balancing, sizing, and costing calculations. The main structure of the software contains a database, thermodynamic model database, flowsheet builder, a unit operation model database and the flowsheet solver. The following are the primary steps involved in the process design simulation:

- The first step to simulate a chemical process involves introducing the basic information of the components and the selection of appropriate thermodynamic method which is crucial for accurately predicting the behaviour of mixtures, phase equilibria, and reaction kinetics.
- The second step consists of the creation of the flowsheet using different modules available for equipment and streams. A detail process flow diagram, (PFD) that outlines the sequence of operations, process units, and the flow of materials and energy through the system is developed in which all the unit operations involved in the PtX scenarios pathway, such as compression, heating, catalytic reactors, separation columns, and recycling systems are identified and included in the model. Each unit is represented in the PFD with associated input and output streams.
- Perform heat and mass balance calculations is another important step to ensure all energy and material flows are accounted for. This ensures the conservation of energy and mass throughout the process. In this regard, a heat integration is always performed within all scenarios to minimize energy consumption. This includes recovering waste heat from exothermic reactions or using it to preheat incoming streams.

- Finally, specification should be provided for unit models and streams to execute the simulation. Display of results are given for mass, and energy balances.

When the process is unknown, the process synthesis is applied according to an onion model as illustrated in Figure 3-1. This model is structured in concentric layers, where each layer represents a critical component or system within an industrial process. The design begins from the core of the process and moves outward.

At the core of the model is the reactor, where the main chemical reactions occur. This is the heart of the process where raw materials are transformed into desired products. Close the reactor is the separation and recycle system. This system is responsible for separating the products from unreacted feedstock and by-products. The unreacted materials are typically recycled back into the reactor to enhance efficiency and reduce waste. The next layer is the heat recovery system, which captures and reuses heat generated in the process. This system is crucial for improving the energy efficiency of the process, minimizing the need for external heating or cooling. Enclosing the heat recovery system is the energy utility system. This system provides the necessary utilities such as electricity, steam, and cooling water required to run the process efficiently. The outermost layer is the waste treatment system. This system handles the treatment and disposal of any waste materials generated during the process, ensuring that the process complies with environmental regulations and minimizes its impact on the environment.

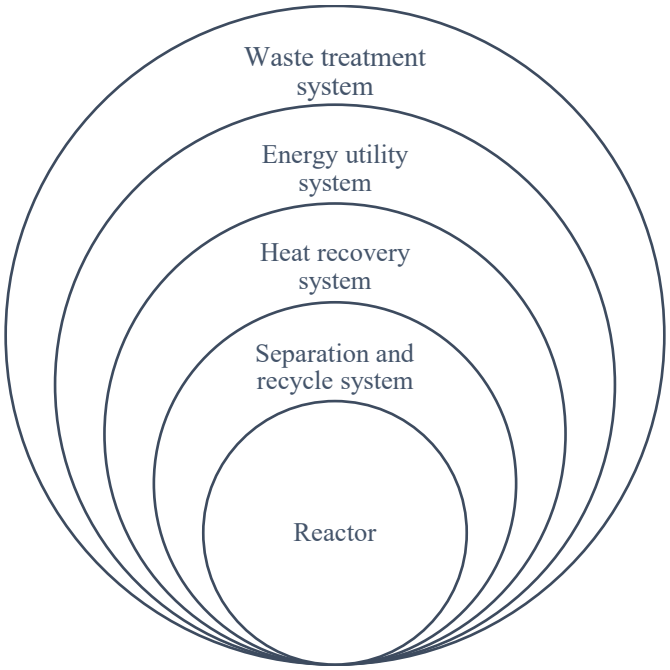

Figure 3-1. The onion model of process modelling.

This onion model emphasizes the connexion of different process components, highlighting the importance of optimizing each layer to achieve an efficient, sustainable, and economically viable industrial process.

In this thesis, the process design simulation model for three case studies have been developed using the aforementioned methodology. The software Aspen Plus V12 has been employed for the mass and energy balances as well as the plant cost equipment and sizing.

3.1.1. Direct air capture model

For those PtX scenarios that employ direct air capture (PtO and PtFA), the general parameters for the simulation reaction have been set in Aspen Plus. The direct air capture system was modelled using the conditions provided by Keith et al. [89] and Bianchi [147]. The following reactions in Table 3-1 include equilibrium, formation and dissociation reactions between the ionic solution and the CO_2. They were defined in the properties, section of chemistry in Aspen Plus. Listed reactions were taken from Bianchi [147]. Each stage of the DAC was modelled as separated Hierarchy in Aspen Plus and described in the subsequent chapters.

Table 3-1. Chemical reactions involved in the DAC system.

Reaction	*Type*	*No.*
$CO_2 + 2\,H_2O \leftrightarrow HCO_3^- + H_3O^+$	Equilibrium A = 231.465; B = -12092.1; C = -36.7816; D = 0	1
$HCO_3\text{-} + H_2O \leftrightarrow CO_3^{-2} + H_3O^+$	Equilibrium A = 216.05; B = -12431.7; C = -35.4819; D = 0	2
$2\,H_2O \leftrightarrow H_3O+ + OH^-$	Equilibrium A = 132.899; B = -13445.9; C = -22.4773; D = 0	3
$CaOH^+ \leftrightarrow Ca^{++} + OH^-$	Equilibrium	4
$CaCO_3 \leftrightarrow CO_3^{-2} + CA^{++}$	Salt	5
$K_2CO_3^{-2} \leftrightarrow CO_3^{-2} + 2\,K^+$	Salt A = -175.998; B = 17765.2; C = 21.6865; D = 0	6
$KOH \rightarrow K^+ + OH^-$	Dissociation	7
$K_2CO_3 \rightarrow 2\,K^+ + CO_3^{-2}$	Dissociation	8
$Ca(OH)_2 \rightarrow CaOH^+ + OH^-$	Dissociation	9

3.2. Electricity supply

The electricity supply model is crucial to the success of Power-to-X technologies, influencing their economic, environmental, and technical performance. The environmental benefits of this approach are directly tied to the carbon intensity of the electricity used. A green electricity supply model ensures that PtX processes significantly contribute to decarbonisation by reducing reliance on fossil fuels. Therefore, in this study, a dedicated offshore wind farm located in Teesside UK was considered to provide the electricity to the plant in all PtX scenarios. The modelling of the wind turbines has required the use of the software

System Advisor Model (SAM) which employs the wind profile of the specific location to estimate the power generation. To perform this, the software Meteonorm v7.2 is used. Using the coordinates of the Teesside location, the software can provide the hourly temperature, pressure, wind speed and direction as main outputs for the year of analysis. Thus, the wind profile is used as an input of the SAM software. An adjustment is made to the wind speed using the equations 3-1 and 3-2 in order to provide the wind speed at the turbine height (80 m) instead of the default measurement at 10 m [148].

$$\alpha = \frac{0.37 - 0.088\ ln\ (U_{ref})}{1 - 0.088\ ln\left(\frac{z_{ref}}{10}\right)} \qquad 3\text{-}1$$

$$\frac{U(z)}{U(z_{ref})} = \left(\frac{z}{z_{ref}}\right)^{\alpha} \qquad 3\text{-}2$$

Where:

α is the power law exponent

U_{ref} is the wind speed at the reference height

$U(z)$ is the wind speed at the current height

z is the actual height

Z_{ref} is the reference height

SAM software uses a commercial turbine model *Senvion 6.2M126 offshore* and the nameplate capacity of the farm to estimate the hourly power output and the number of turbines required in the specific scenario. The software gives an estimation of the real power output provided by the wind farm; however, for all scenarios, the plant requires energy continuously without any fluctuations. For that reason, a backup energy strategy is proposed to have a constant power supply. This strategy consists of utilising the grid network as a storage system when excess of electricity is produced while retrieving electricity from the grid when there is insufficient power generation. The wind farm has been sized in such a way that the electricity sent to and retrieved from the grid is in balance. In addition, the network cost of using the grid is added to the economic analysis.

3.3. Renewable hydrogen production

In this study, a PEM electrolyser is adopted for the H_2 production in all scenarios. According to Hank et al. [149], large scales of PEMs with production capacities > 10 Nm^3 H_2/h do offer efficiencies similar to the alkaline electrolysers in addition to the high purity of the product at temperatures between 50 – 100 °C. The electrolyser unit has been modelled in Aspen Plus as a stoichiometric reactor operated at 80 °C and 35 bar [66]. Deionized water is supplied at a flowrate about of 0.01 m^3/kg H_2 [150]. The lifetime of the equipment is 80,000 h [66]. Product H_2 is purified by a phase separation unit that removes O_2 from the products stream. Unreacted water and H_2 are cooled down up to 25 °C to facilitate a flash separation of them, and this increases the H_2 purity to 99.99%. The O_2 is split into two streams, one is sent to the oxy-combustion in the DAC-calciner where it will be burnt. The other stream of oxygen is liquefied to produce commercial O_2. Liquefaction is configured in a flash separation and a cryogenic cooling as presented in Johnson et al. [151]. The compression reaches 51 bar and cooling temperature of -123 °C followed by expansion to 1.2 bar.

The electricity consumption of the unit is estimated based on the equation 3-3 that involves H_2 high heating value (HHV) and a 75% electrolyser efficiency according to [152] plus an additional 10% of electricity supplied to cover the demand of the auxiliary equipment. The electricity requirements for water purification has a minor contribution to the overall energy requirement and it is included in the balance of the plant (BoP) [153].

$$Electrical\ Efficiency = \frac{Electricty\ produced}{HHV\ of\ Hydrogen} \qquad 3\text{-}3$$

The PEM simulation uses a not rigorous reactor model; however, it is used to obtain the mass and energy balances. The deionisation of water is considered into the economic assessment whereas the infrastructure of the system has been neglected due to their low contribution to the overall carbon footprint [150]. For the PtX scenarios, it is assumed that hydrogen is produced using the same model but adjusting the size of the system according to the amount of hydrogen required.

3.4. Economic assessment

The economic assessment of the PtO, PtA and PtFA have been completed by applying a typical discounted cash flow analysis to estimate the product minimum selling price (MSP) in £/kg. This method requires the calculation of the total capital and operating expenditures (CAPEX/OPEX). The lifetime of the three scenarios is 20 years and the plant operates 8,000 hours per year (Table 3-2).

Table 3-2.Main assumptions for the economic evaluation.

Parameter	*Units*	*Value*
Plant location	-	United Kingdom
Base year	-	2021, 2022 and 2023
Annual production	ktonne/y	103
Lifetime of the project	years	20
Discount rate	%	10
Depreciation method	-	straight line
Operating hours	h/y	8,000

Estimation of CAPEX requires the purchased equipment cost (PEC) calculation. The equipment costs have been taken from simulation results and relevant literature and adjusted to the current size using the scaling factor method, equation 3-4.

$$C = C_0 \left(\frac{S}{S_0}\right)^f \qquad 3\text{-}4$$

Where f is the scaling factor, C and S are the actual equipment cost and size, respectively and C_0 and S_0 are the base cost and size of the unit in the reference. Equipment cost data are detailed in each specific chapter for olefins, ammonia y formic acid respectively. For the DAC equipment, there is no agreement of the scaling factor used since the technology is under current research. However, according to Keith et al. [89], the air contactor and pellet reactor are modular units and their capital cost per unit capacity is almost constant down to 100 ktonne CO_2/year, therefore, a factor of 1 is used in the equation 3-4. On the other hand, calciner and slaker costs strongly depend on size and several studies [86,92,154–157] suggest an exponent of 0.7 as a conservative value.

The Chemical Engineering Plant Cost Index (CEPCI) was utilised to convert the cost plant equipment from the reference base year to the current year. When the cost of the equipment is reported in a different currency than GBP, the value is converted to the current GBP by the exchange rate for the year of reference and then updated to the actual year. In the electrolyser, an extra 28% cost for auxiliaries has been accounted for the PEC as suggested by Buttler and Spliethoff [158].

The Lang factor methodology is applied to the PEC to determine fixed capital investment (FCI), total direct cost (TDC) and indirect costs (IDC). The factors for installation, instrumentation and controls, piping, electrical systems, buildings, yard improvements, and land are given in Table 3-3. These factors have been applied for olefins and ammonia case studies. Formic acid has its own factors described in the respective chapter.

Table 3-3. CAPEX estimation methodology [159,160].

Component	*Lang factor*
Purchased Equipment Cost (PEC)	1
Installed direct costs (IDC)	PEC + (1) + (2) + (3) + (4)
(1) Purchased equipment installation	0.39×PEC
(2) Instrumentation and controls	0.26×PEC
(3) Piping	0.31×PEC
(4) Electrical systems	0.1×PEC
Non-installed direct costs (NIDC)	(5) + (6) + (7)
(5) Buildings	0.29×PEC
(6) Yard improvements	0.12×PEC
(7) Land	0.06×PEC
Total direct costs (TDC)	(ICD) + (NIDC)
Indirect costs (IDC)	0.255×PEC
Fixed Capital Investment (FCI)	TDC + IDC
Start-up costs	0.05×FCI
Interest during construction	Estimated
Working Capital (WC)	0.05×FCI
CAPEX	FCI + Start-up costs + interest during construction

Operational costs have been estimated using specific variable cost for each PtX scenario. Labour is estimated using the empirical equation 3-5 proposed by Peters and Timmerhaus. [161].

$$h_{labour}\left[\frac{h}{year}\right] = 2.13 \times plant\_capacity\left[\frac{kg_{output}}{h}\right]^{0.242} \times n_{process\_steps} \times \frac{h_{plant\_operation}}{24} \qquad 3\text{-}5$$

Plant capacity refers to the hourly production of main product olefins, ammonia or formic acid in kg/h, *n process steps* is the number of subsections that significant physical or chemical changes are carried out and the *h plant hours* represents the total working hours per year. The labour rate is taken at £15/h according to the Office for National employment statistics [162]. The minimum olefin price is the break-even point at which NPV is equal to zero, equation 3-6.

$$NPV = \sum_{n=1}^{20}\left(\frac{Cash\ flow}{(1+i)^n}\right) = 0 \qquad 3\text{-}6$$

Where cash flow is considered after taxes and internal rate i = 10%, n is the years considered in the evaluation.

3.5. Life cycle assessment

Life Cycle Assessment (LCA) has been applied to determine the environmental impacts of the proposed PtX scenarios. The environmental impacts have been assessed over the ten baseline impact categories employing CML 2 baseline 2000 impact method for PtO and PtA while ReCiPe method has been applied to PtFA to be consistent with literature. A *cradle to the gate* approach has been utilised and hence the distribution, use and final disposal are not included [106,113,163,164]. This approach has been adopted as products properties, utilisation and disposal are (or can be) identical for the CCU-based and fossil - based products. The framework of this analysis follows the standardized methodology of ISO 14040/44 in which four steps are involved: goal and scope, inventory data collection, impact categories, and interpretation of results [164]. The model was developed in the SimaPro software v9.4.0.2.

The allocation factors for hydrogen and oxygen in the water electrolysis unit have been estimated by using the exergy of each component in Table 3-4:

Table 3-4. Standard molar chemical exergy

Component	*Value*	*Unit*	*Reference*
Hydrogen	236.12	kJ/mol	[165]
Oxygen	3.97	kJ/mol	[165]

The allocation factors have been calculated using the equation 3-7:

$$AF_{H2} = \frac{\dot{m}_i * ex_i}{\sum_1^n (\dot{m}_i * ex_i)} \qquad 3\text{-}7$$

Where: $\dot{m}_i$ indicates the mass flow of each component, i.e. hydrogen and oxygen in mol/h and ex_i denotes molar exergy value taken from Table 3-4.

Chapter IV

4. Techno economic and life cycle assessment of olefin production through CO_2 hydrogenation within the Power-to-X concept

The chapter deals with exhaustive process modelling, techno-economic and life cycle assessment (TEA/LCA) of olefin (ethylene and propylene) production through captured CO_2 and electrolytic hydrogen. Olefins are important building block chemicals with several applications and carbon capture and utilisation (CCU) can provide a sustainable production route. The proposed system involves direct air capture (DAC) of CO_2; proton exchange membrane (PEM) water electrolysis for hydrogen production, methanol synthesis, methanol to olefins (MTO) upgrade, and power generation from offshore wind turbines. This study proposes a new integrated process as the first attempt to holistically assess a whole CCU assembly aiming at olefins production. Processing modelling has been implemented using the Aspen plus V12.1 and MATLAB R2022a software to solve the mass and energy balances of each unit operation. The modelling results showed a carbon efficiency of 72.3% to ethylene and propylene. In addition, the process is designed and integrated in such a way that no external heat supply is required. A specific energy consumption (SEC) of 150 MJ/kg olefins (41 kWh/kg) has been estimated. A minimum selling price of £3.67 per kg of olefins is required for the proposed process to break even. The sensitivity analysis has revealed that the major cost driver is the cost of electricity. In addition, the life cycle assessment (LCA) has exposed that the proposed synthesis route of olefins has the potential to reduce the global warming potential (GWP) by 47% compared to fossil - based production. The outcomes of this study can be beneficial to engineering conceptual studies, policy makers and contribute new information to the CCU academic community.

4.1. Introduction

Olefins are important building blocks for chemical industry [166]. They are use in a numerous of products including plastics, synthetic fibres, solvents and chemicals used in various industrial processes. The main products from olefins production are ethylene and propylene, which are the most widely used in the plastic industry. These materials are essential in packaging, construction, and consumed goods [167].

Nowadays conventional olefins are produced from fossil sources such as gas natural and coal though the process of steam naphtha [168]. This traditional production process is energy intensive and generates a significant amount of greenhouse gas emissions. While demand of olefins is growing, there is an urgent need to develop a more sustainable production method. The PtO approach offers a potential solution to decarbonise olefins industry through the utilisation of renewable energy such as offshore wind to convert

CO_2 and H_2 into ethylene and propylene. This approach provides a pathway to obtain olefins with a lower carbon footprint, and, at the same time, it integrates the CO_2 capture concept, helping to mitigate industrial emissions. The challenges faced by the PtO include the high energy requirements for hydrogen production which results in high cost of production that are still higher than the market prices [26]. Additionally, using DAC system deals with higher fuel consumption in the CO_2 recovery entailing fossil emissions.

In this chapter, a techno economic and a life cycle assessment of olefins production through CO_2 hydrogenation applying PtX concept has been assessed. Electrolytic hydrogen from a PEM electrolyser powered by offshore wind along with CO_2 capture by DAC system are converted into olefins (mainly ethylene and propylene) though catalytic reaction.

4.2. Methodology

The plant is located in North Yorkshire, United Kingdom where the Teesside offshore wind farm supplied 546 MW of electricity. The installed capacity (1,163 MW) of the wind farm has been calculated by dividing the power consumed (546 MW) in the PtO system with the capacity factor (47%) and then the number of turbines needed for this capacity have been calculated in the System Model Advisor software. Figure 4-1 depicts the schematic diagram of the power to olefins process. The PtO produces around 103 ktonne of olefins per year and consists of CO_2 direct air capture (DAC), electrolytic hydrogen production, methanol and olefin synthesis and purification stages in addition to the power generation modelling. Mass and energy balances have been obtained in the Aspen Plus V12.1 and MATLAB R2022a software.

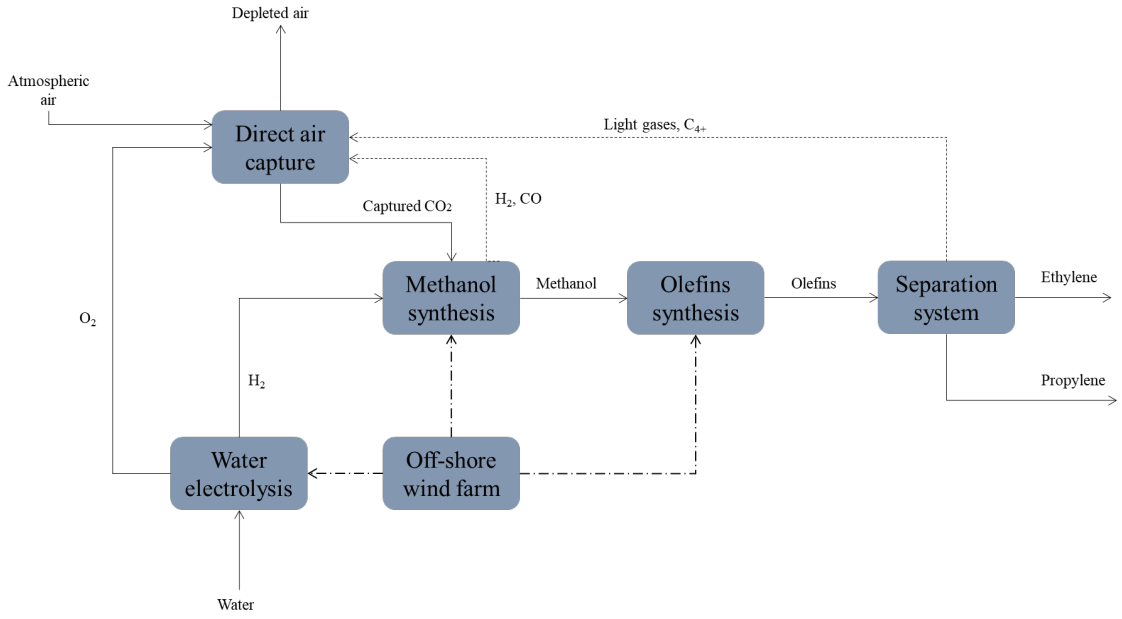

Figure 4-1. Schematic diagram of the power to olefin process based on CCU and water electrolysis.

4.2.1. Direct air capture (DAC)

The Carbon Engineering liquid DAC technology has been considered herein and simulations have been conducted based on the data provided in Keith et al. [89] in which the authors have detailed a description of a direct air capture plant using an aqueous KOH sorbent coupled with a caustic recovery loop to capture almost 1 Mt CO_2/year. This design has been taken as a reference to model the CO_2 capture using the conditions and assumptions of Bianchi [147] in the Aspen Plus v12.1 software.

Two chemical loops are involved in the atmospheric CO_2 capture. First, an ionic KOH solution with concentrations of 1.0 M OH^-, 0.5 M CO_3^{2-} , and 2.0 M K^+ is used to capture CO_2 forming carbonates. Second, carbonates are precipitated through the reaction of Ca^{2+} to form $CaCO_3$ while Ca^{2+} is replaced by the dissolution of Ca $(OH)_2$. The $CaCO_3$ is calcined to release the CO_2 producing CaO, which is hydrated to regenerate Ca $(OH)_2$. Four major operation units are included and discussed in the following sections as shown in Figure 4-2: air contactor, pellet reactor, calciner and slaker [86,89].

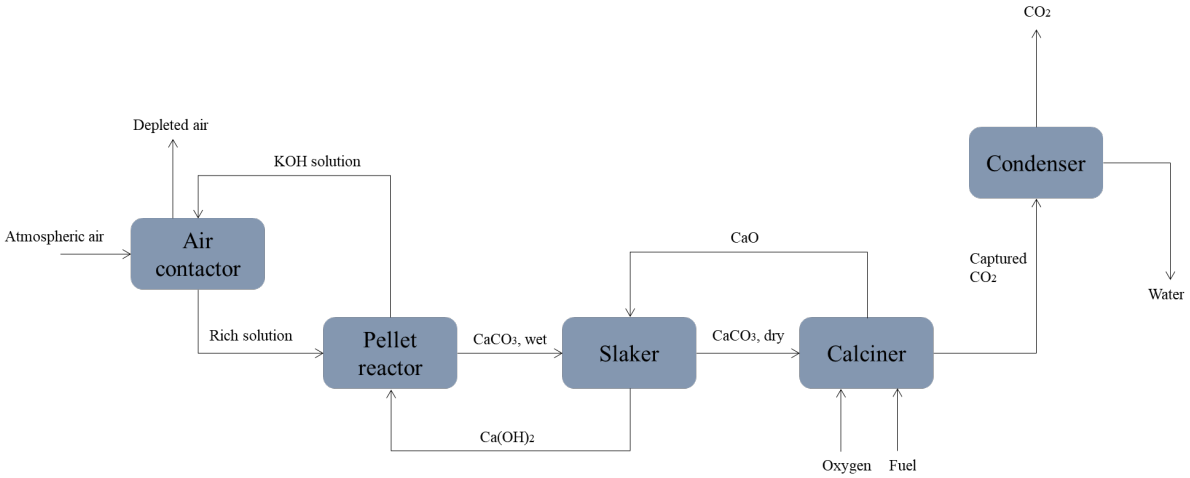

Figure 4-2. . Block flow diagram of the direct air capture system.

Air contactor

The air contactor is simulated in the Aspen Plus software as a separator unit in which the CO_2 capture efficiency is fixed to 75% according to the model performed by Keith et al. [89]. Initially, ambient air is injected to a series of air contactor structures with plastic packaging where an alkali solution of KOH flows in a crossflow configuration. The CO_2 is transferred to the liquid capture solution by a reaction-diffusion process, reaction 4-1 to form an aqueous potassium carbonate precipitate. Here, a pressure drop of 0.005 bar occurs [89,147]. Depleted air with low CO_2 concentration is released to the atmosphere while precipitated solution is pumped at 0.005 bar to restore initial pressure for the subsequent steps [83,147].

$$CO_{2(g)} + 2KOH_{(aq)} \rightarrow K_2CO_{3_{(aq)}} + H_2O_{(l)} \quad 4\text{-}1$$

To simulate the CO_2 capture in Aspen Plus, conditions of Bianchi [147] have been taken into account. An Electrolyte-NRTL thermodynamic model is chosen to represent the Gibbs free energy and the activity coefficients of an electrolyte system based on the alkali ionic mixture. The initial composition of the air and the ionic KOH solution are provided in Table 4-1.

Table 4-1. Operating parameters of the air contactor and pellet reactor.

Parameter	*Value*
Air composition (mol)	N_2 = 0.777
	O_2 = 0.206
	CO_2 = 0.0004
	H_2O = 0.0156
KOH solution	OH^- = 1.0 M
	CO_3^2 = 0.5 M
	K^+ = 2.0 M
Air contactor	75% capture efficiency
Pump	P = 0.005 bar
Pellet reactor	
Temperature	25 °C
Pressure	1 bar
Saturation calculation method	Chemistry
Separator	80% $CaCO_3$
Filter 1	90% solids retention
Filter 2	90% solids retention
Filter 3	90% solids retention

The CO_2-rich solution is then pumped to the pellet reactor section. Figure 4-3 displays the simulation flowsheet of the air contactor and pellet reactor system. The pellet reactor was simulated as a crystallizer block unit available in Aspen Plus [147]. The aim of the pellet reactor was to remove the carbonate ion from the enriched solution according to the causticization reaction in 4-2 .

$$K_2CO_3 + Ca(OH)_2 \rightarrow 2KOH + CaCO_3 \quad 4\text{-}2$$

The crystallizer unit operates at of 25°C and 1 bar. The saturation calculation method option has been selected where the equilibrium and dissociation reactions were previously introduced in the Aspen properties section.

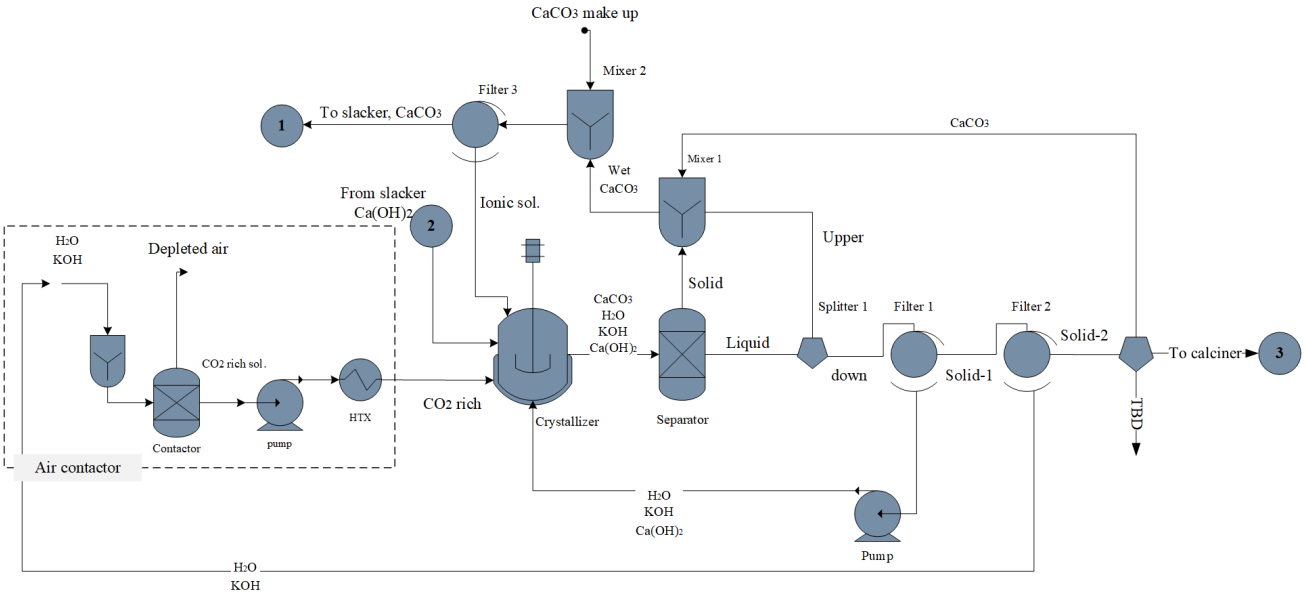

Figure 4-3. Process flows diagram of the air contactor and pellet reactor systems.

In the simulation model, the recycled ionic solution in addition to the $Ca(OH)_2$ stream coming from the slaker loop simulated as an open stream (2) and the CO_2 rich stream are fed to the crystallizer. The causticization reaction is carried out when Ca^{2+} ions reacts with the carbonate ions (CO_3^{2-}) formed in the air contactor rich solution, dissolving the $Ca(OH)_2$ and precipitating $CaCO_3$ into pellets [89]. The products stream is split into two flows to represent the physical solid-liquid separation in the pellet reactor. One of the streams contains manly the $CaCO_3$ solids that are filtrated to increase the calcium retention and recirculate the remaining liquid to the pellet reactor. The second stream (liquid stream) is sent to filters 1 and 2 to enhance $CaCO_3$ solids recovery and obtain a KOH rich solution that is returned to the air contactor [147]. The permeate liquid in the filter 1 is pumped back to the reactor while the liquid from filter 2 is recycled to the air contactor as KOH solution. The $CaCO_3$ solids previously separated in the separator are mixed with the retained solids of the filters 1 and 2 and lastly filtered in filter 3, to remove remaining liquid. Then, the solids are sent to the slaker for a final drying before calcination (1). A stream of make-up $CaCO_3$ is added to account for the lost carbonate in the process

Steam slaker

The slaker is modelled for the hydration of quicklime (CaO) and the drying of the $CaCO_3$ pellets. The reactor runs at 85% conversion, 300 °C and atmospheric pressure. Pellets of $CaCO_3$ flows through the reactor to take advantage of the heating provided by the CaO hydration in reaction 4-3. At the same time, the water vapour removed from the pellets is used in the hydration as reactant. The operations are simulated as separated units but in a real plant those take place in the same unit. Dried $CaCO_3$ is sent to the calciner

for decomposition and the produced Ca $(OH)_2$ is recycled to the pellet reactor. Make up water vapour is injected using steam at 42 bar and 253 °C in a closed loop [89,147].

$$CaO_{(s)} + H_2O_{(l)} \rightarrow Ca(OH)_{2(s)} \qquad 4\text{-}3$$

The next step is the slaking, a flowsheet of the slaker reactor is presented in Figure 4-4 The calcium carbonate coming from the pellet reactor (S1), is passed through a washer tower to separate the liquid hydroxide solution from the solid $CaCO_3$. Liquids are sent back to a mixer (S14) while the solids are heated up to 300 °C to remove the remaining water before passing through the calciner (S5). Two heat exchangers were used to heat up $CaCO_3$ to 300 °C, then, a separator is employed to remove vapour phase and send it to the slaker (S7).

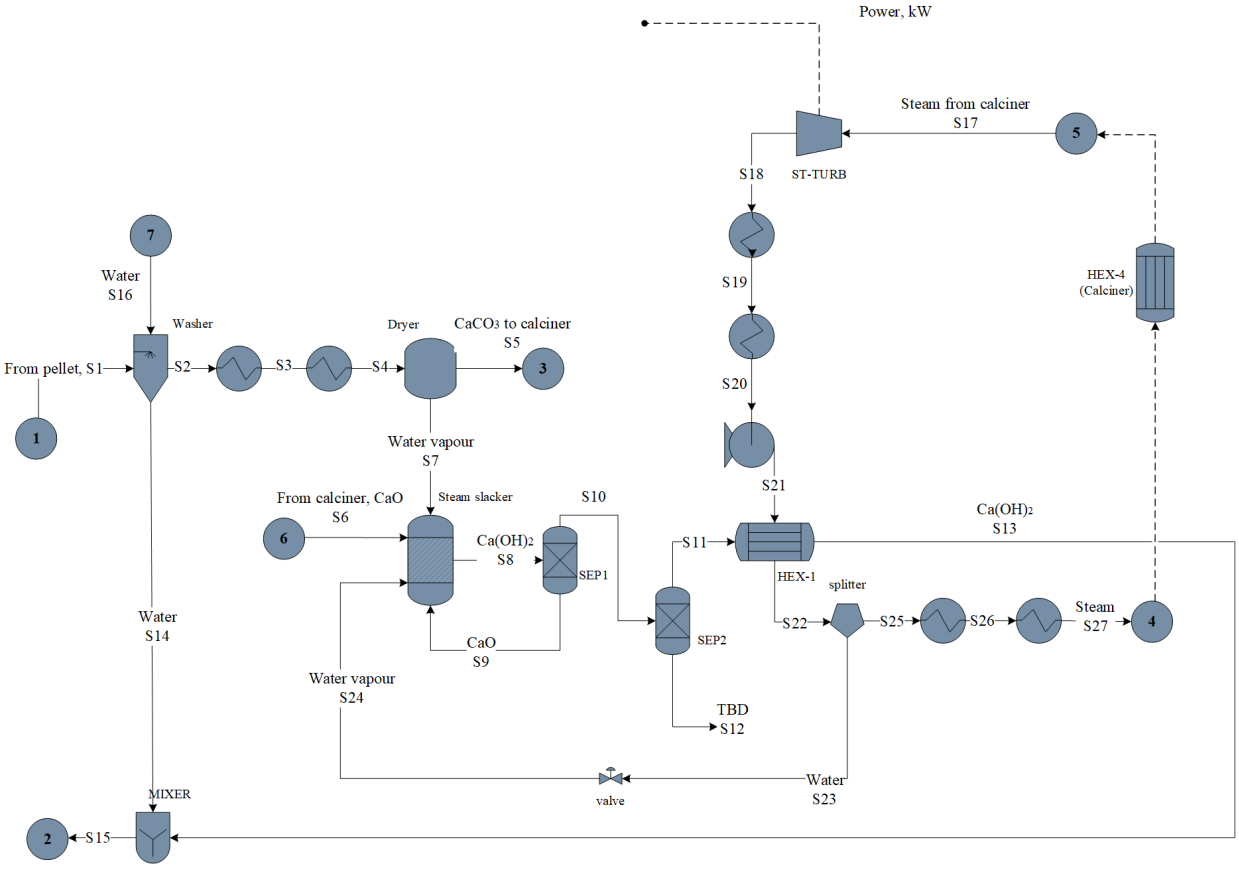

Figure 4-4. Flowsheet diagram of slaker section in DAC system

The stream S6 is the CaO coming from the calciner simulated as an open stream for simplicity. It is hydrated with the steam to form $Ca(OH)_2$ in the slaker reactor. The products (S8) are filtered to recycle most of the unreacted CaO (S9), however, the amount that by passed the first separator (S10), is finally removed in a second separator, and disposed (S12). The $Ca(OH)_2$ stream S11 is cooled down using a water/steam

loop (4 and 5), mixed with stream S14 and finally sent back to the pellet reactor (S15). Operating conditions of the slaker section are shown in Table 4-2**.**

Table 4-2. Operating conditions of slaker subsystem.

Parameter/equipment	*Value*
Slaker reactor	RSTOIC; Conversion = 0.85 $CaO + H_2O \rightarrow Ca(OH)_2$ T = 300 °C; P = 1 bar
Dryer	300 °C
Washer liquid to solid ratio	0.8
Steam turbine	1.0 bar
Pump	42 bar
HTX	Hot stream outlet temperature = 90 °C

The water /steam loop consist of an isentropic turbine which expands the vapour (S17) coming from the calciner heat exchanger (HEX-4) from 42 to 1 bar to provide the electricity for the DAC equipment. Steam is then condensed in the heat exchangers at temperature of 80 °C (S20) and it is pumped at 42 bar to the HEX-1 where it removes heat from the products. The stream S22 is split into two streams, S23 is sent to the slaker after passing through an expander valve while the S25 is vaporized and is sent back to the water/steam loop (4).

Calciner

The calcination of $CaCO_3$ occurs through reaction 4-4. This is the key step to recover the CO_2 captured by the thermal decomposition of the carbonates which requires a high amount of energy. The calciner is simulated as a conversion reactor working at 900 °C and atmospheric pressure. The conversion efficiency of 98% is set according to Bianchi [147] and Keith et al. [89].

$$CaCO_{3(s)} \rightarrow CaO_{(s)} + CO_{2(g)} \qquad 4\text{-}4$$

In the reference of Keith et al. [89], natural gas is utilised to provide the heat for carbonate decomposition (~ 5.25 GJ/tonne CO_2). However, in this proposed design, the heat for the calciner is provided by the combustion of the gas streams from the MTO synthesis such as H_2, CO, CH_4, and the heavier olefins C_{4+} (see Figure 4-1). Thus, no external fossil resource is employed. Cyclones are added to cool down the products and separate the solid CaO and the CO_2. Finally, water is knocked out and clean CO_2 is sent to a four-stage compressor with intercooling to reach the desired pressure for the methanol synthesis, i.e., 78 bar.

The DAC model utilised herein is based on a pilot plant that captures 1 tonne CO_2/day. Hence a limitation of the study is that we have assumed similar behaviour of the system for a capture of 0.5 million tonnes per year; nevertheless, some of the DAC components such as the air contactor and the pellet reactor

are modular and their performance is expected to vary little form the pilot plant. Similar scaling limitations exist with the electrolysis and olefin production sections. To account for these uncertainties we have carried out thorough sensitivity analysis but we acknowledge that a more reliable data can be derived from larger scale operations, but such data is missing now.

A flowsheet diagram of the calcination section is presented in Figure 4-5. The dry $CaCO_3$ pellets coming from slaker (S1) are heated up to the reaction temperature (i.e., 900 °C) using the heat exchangers HEX-2 and HEX-3 before entering the calciner (S3). Calcination occurs at 1 bar and 900 °C with oxygen coming from the electrolyser (S15) along with the gases that come from the MTO stage (S16). The oxy-combustion provides the necessary heat for the decomposition and releases CO_2, water vapour and CaO (as solid).

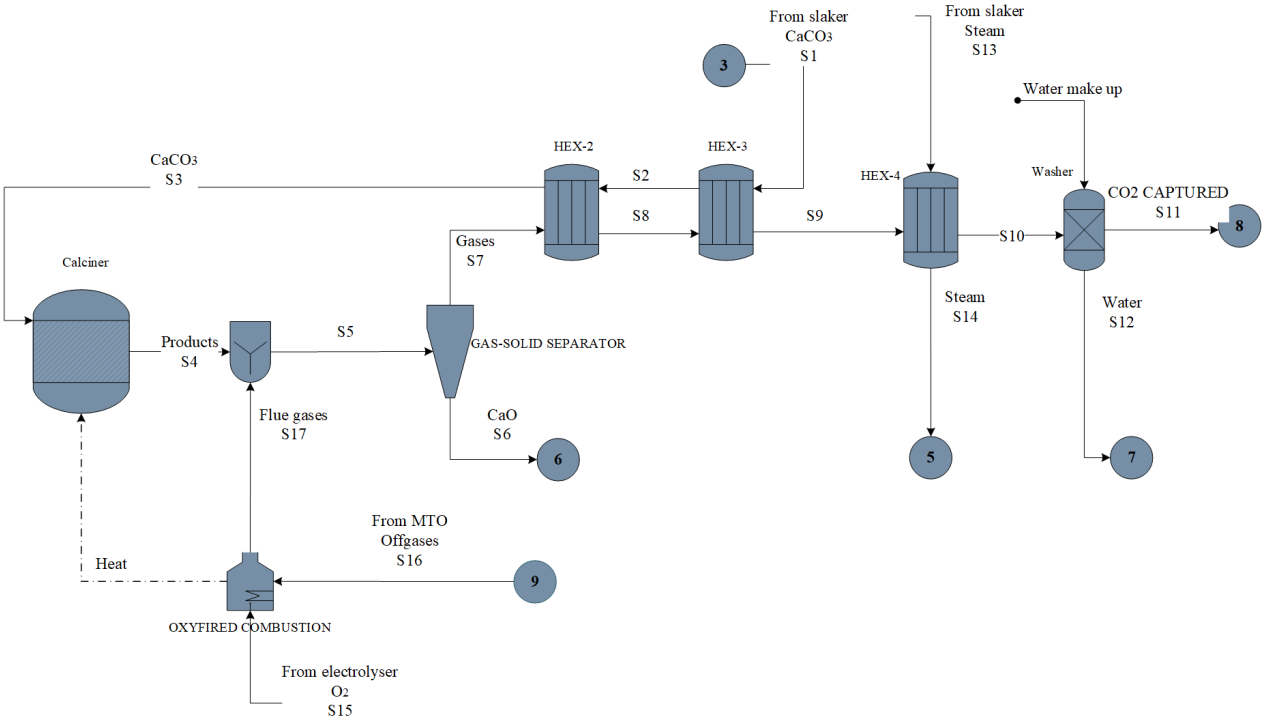

Figure 4-5. Flowsheet diagram of calciner section in DAC system

Once calcined, CaO solids (S6) are removed in a gas-solid separator unit while gases (S7) are cooled down up to 55 °C liberating enough heat for $CaCO_3$ heating (HEX-2 and HEX-3) and steam overheating (HEX-4). Finally, water is removed in the washer (S12) and the CO_2 (S11) with a purity of 96.4% is sent to the compression system (8). Table 4-3 indicates the operating conditions of the calciner reactor and the oxy-combustion units.

Table 4-3. Operating conditions of calciner reactor and the oxy-fired combustion.

Equipment	*Parameters*
Calciner (RSTOIC)	T = 900 °C; P = 1 bar
	$CACO_3$ → CAO + CO_2
	Conversion = 0.98
	Q = 58,522 kW
Boiler (Steam make up)	Q = 8,759
Oxy-fired (RGibbs)	T = 1100 °C; P = 1 bar
	Calculate phase equilibrium and chemical equilibrium
	Considers all components as products
	Q = 73,344 kW

4.2.2. Methanol synthesis

The following step in the PtO is the catalytic hydrogenation of CO_2 into methanol that acts as the intermediate. The reaction in 4-5 takes place at 210 °C and 78 bar in the presence of a commercial catalyst $Cu/ZnO/Al_2O_3$ according to the conditions of Van-Dal and Bouallou [100].

$$CO_2 + 3H_2 \leftrightarrow CH_3OH + H_2O \qquad 4\text{-}5$$

Both CO_2 and H_2 should be compressed before entering the reactor. The CO_2 passes through 4 stages compressors to achieve the desired operating pressure (78 bar) and H_2 was compressed from 30 bar to the operating pressure in a one stage compressor. They are heated up to the operation temperature and injected into the fixed bed adiabatic reactor. The device is packed with 44,500 kg of catalyst, assuming CO_2 is the leading source of carbon for the synthesis [100]. The kinetic model used in this scenario is taken from Vanden Bussche and Froment [169] with the adjusted parameters of Mignard and Pritchard [170]. The conditions for the methanol synthesis are presented in Table 4-4.

Table 4-4. Specification for the methanol synthesis[100].

Parameter	*Value*	*Unit*
Reactor type	Fixed bed adiabatic	-
Operating temperature	210	°C
Operating pressure	78	bar
Catalyst density	1775	kg/m^3
Catalyst bed porosity	0.4	-

After the reaction, the products stream is divided into two different streams in order to use one of them to heat the feed gases. Then, they are mixed again and flashed to separate gases and liquids. The gases are recycled to the compression stage [61] whereas the aqueous methanol is sent to the olefins synthesis. Since the olefin reactor performs with a methanol – water mixture, further methanol purification is not required.

In Figure 4-6 the simulation flowsheet of the methanol synthesis is illustrated. CO_2 and H_2 from the previous stages are compressed in a multi compressor system employing intercooling (S2 and S4). Once compressed, they are mixed with the recycling stream S20 and heated up in HEX-5 using the products stream (S8) and fed into the reactor (S6) that operates at 210 °C and 78 bar.

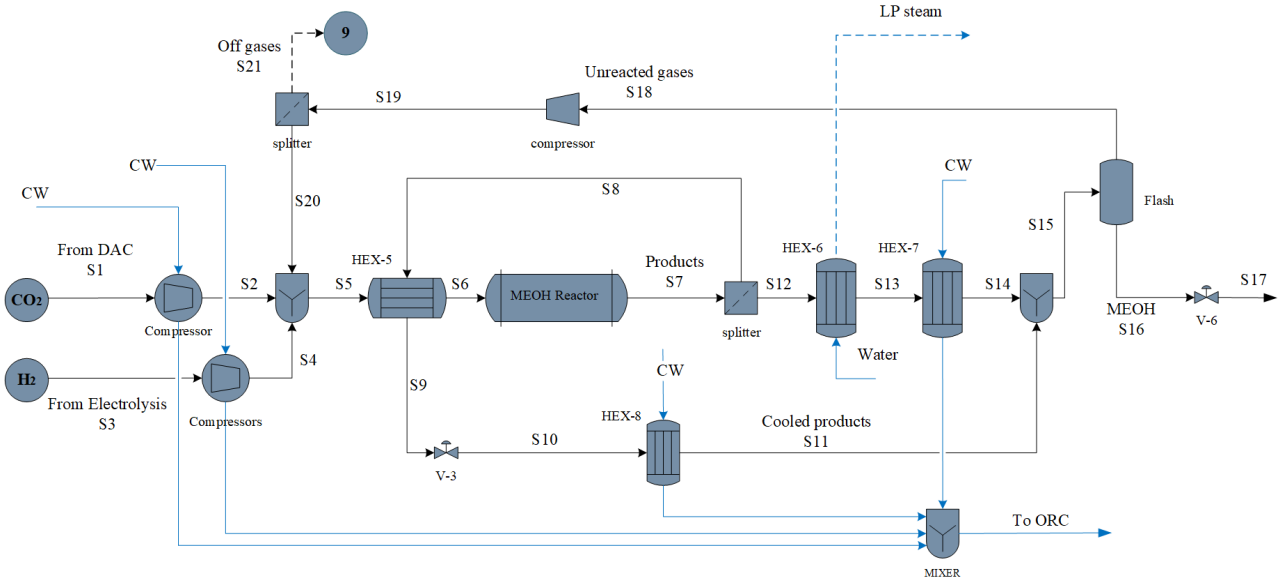

Figure 4-6. Flowsheet diagram of Methanol synthesis.

The reaction is carried out in an Rplug module in which kinetic expressions, provided in Table 4-5, according to the LHHV structure [100]. After reaction, products are divided in two streams, stream S8 is used to heat the inputs while S12 is cooled down to 35 °C through HEX-6 and HEX-7. Further, cooled products S14 and S11 are mixed and flashed to separate unreacted gases (S18) from methanol (S16). Unreacted gases are compressed and split into the recycled stream (S20) and the purge off gases (S21). The next step is the conditioning of the methanol and water mixture for the olefin synthesis. Since the synthesis requires methanol/water ratio of 1, no further methanol purification was applied (S17). The cooling water used in the heat exchangers and intercooling is collected and sent it to an Organic Rankine Cycle (ORC) for power generation.

Table 4-5. Input parameters of the MEOH synthesis.

Equipment	*Parameters*
CO_2 compression	
COMP1	Isentropic; P = 3 bar; intercooling 38 °C
COMP2	Isentropic; P = 9 bar; intercooling 38 °C
COMP3	Isentropic; P = 26 bar; intercooling 38 °C
COMP4	Isentropic; P = 78 bar; intercooling 38 °C
H_2 compressor	Isentropic; P = 78 bar
MEOHSYNT (RPLUG)	Adiabatic
	Length = 10 m
	Diameter = 0.08 m
Kinetic reactions [100]	
R_1	$CO_2 + 3\ H_2 \rightarrow CH_3OH + H_2O$
	$r_{CH3OH} = \frac{k_1 P_{CO2} P_{H2} - k_6 P_{H2O} P_{CH3OH} P_{H2}^{-2}}{(1 + k_2 P_{H2O} P_{H2}^{-1} + k_3 P_{H2}^{0.5} + k_4 P_{H2O})^3}$
R_2	$CO_2 + H_2 \rightarrow CO + H_2O$
	$r_{RWGS} = \frac{k_5 P_{CO2} - k_7 P_{H2O} P_{CO} P_{H2}^{-1}}{(1 + k_2 P_{H2O} P_{H2}^{-1} + k_3 P_{H2}^{0.5} + k_4 P_{H2O})}$
k_1	A1 = -29.87
	B1 = 4811.2
k_2	A2 = 8.147
	B2 = 0
k_3	A3 = -6.452
	B3 = 2068.4
k_4	A4 = -34.95
	B4 = 14928.9
k_5	A5 = 4.804
	B5 = -11797.5
k_6	A6 = 17.55
	B6 = -2249.8
k_7	A7 = 0.1310
	B7 = -7023.5

4.2.3. Olefin synthesis and separation

The olefin synthesis is modelled as a set of parallel reactions (Figure 4-7) based on the work conducted by Lu et al. (2016). The products of the olefins reactor are CH_4 (methane), C_2H_4 (ethylene), C_3H_6 (propylene), C_3H_8 (propane), C_4 (butene) and C_5 (pentene). Also coke formation is taken into account as part of the reaction set. The reactor is simulated as a continuous stirred tank reactor (CSTR) using a commercial SAPO-34 catalyst at a temperature of 465 °C and at atmospheric pressure as proposed in Lu et al. (2016). Operating conditions of the simulation are given in Table 4-6.

Table 4-6. Operating conditions of the olefin synthesis.

Unit	*Parameter*
Reactor	Adiabatic
	T = 465 °C
	P = 1 bar
Compressor	Isentropic
	P = 30 bar
Heat exchangers	HEX - 9 = 460 °C; Q = 47641 kW
	HEX - 10 = 178 °C; Q = 1344 kW
	HEX - 11 = 80 °C; Q = 2262 kW
	HEX - 12 = 40 °C; Q = 688 kW

After use, the catalyst is sent to a regenerator unit where deposited coke is burned, and the catalyst is regenerated. The cost of the regenerator unit is included in the purchased equipment cost of the synthesis reactor. Similarly, regarding the environmental performance, the emissions generated by the catalyst regenerator, are considered negligible compared to the total plant emissions. Additionally, the energy recovered from coke burning is minimal compared to the overall energy needs of the plant, therefore, it was excluded from the energy integration.

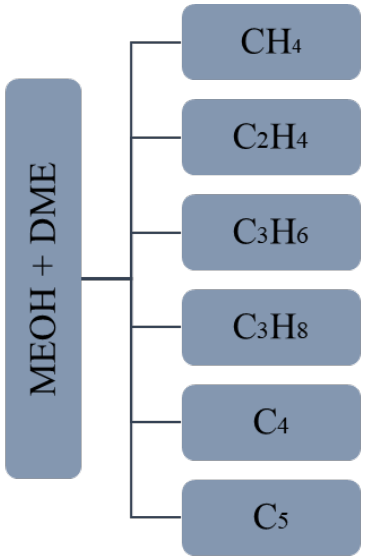

Figure 4-7. MTO reactions schematic taken from [171].

The kinetic reaction rate of each component is a function of the methanol concentration and the coke deactivation function. The kinetic model has been applied in MATLAB and solved using the non-linear system solver *fsolve* and the results were transferred to Aspen Plus by employing a user model unit operation using as intermediate Microsoft Excel [172]. Thus, the user model in Aspen Plus was used as a black box and the flowrates of the outputs were specified in the MATLAB module.

The model is based on the work of Lu et al. [171] who simulated the reaction to produce dimethyl ether and the further dehydration into the hydro-compounds in a continuous stirred tank reactor (CSTR) using SAPO-34 catalyst. The equations and parameters used in MATLAB for each compound are presented in Table 4-7 where M_i represents the molecular weight of each component i, C_i denotes concentration in mol/L, k_i and a_i are the reaction rate constants and ϕ_i is the deactivation function.

Table 4-7. Kinetic model of the MTO process [171].

	Compound	*Rate equation*	*k*	*a*
1	CH_4	$R_{CH4} = \frac{1}{2} k1\varphi 1 C_{MEOH} M_{CH4}$	0.00501	0.043
2	C_2H_4	$R_{CH4} = \frac{1}{3} k2\varphi 2 C_{MEOH} M_{C2H4}$	0.15413	0.0982
3	C_3H_6	$R_{CH4} = \frac{1}{4} k3\varphi 3 C_{MEOH} M_{C3H6}$	0.19234	0.2017
4	C_3H_8	$R_{CH4} = \frac{1}{5} k4\varphi 4 C_{MEOH} M_{C3H8}$	0.04252	0.4099
5	C_4	$R_{CH4} = \frac{1}{6} k5\varphi 5 C_{MEOH} M_{C4}$	0.09094	0.2929
6	C_5	$R_{CH4} = \frac{1}{7} k6\varphi 6 C_{MEOH} M_{C5}$	0.04895	0.3336
7	COKE	$R_{CH4} = \frac{1}{8} k7\varphi 7 C_{MEOH} M_{COKE}$	0.07432	0.3793
8	MEOH	$-\left(\sum_{1}^{6} k_i \varphi_i\right) C_{MEOH} M_{MEOH}$	-	-
9	H_2O	$\left(\sum_{1}^{6} k_i \varphi_i\right) C_{MEOH} M_{H2O}$	-	-
	φ_i	$\frac{A}{1 + Bexp(D \times (w_c - E))} \exp(-a_i w_c)$	-	-
		A = 1; B = 9; D = 2; E = 7.8 W_c = coke content (g/100gcat) Molecular weight coke = 84 g/mol	-	-
	Parameter	*Description/units*	*Value*	-
	I_s	Catalyst inventory (g)	8,500,000	-
	w_c	Initial coke content (g/100g cat)	2	-
	G_s	Catalyst flowrate (g/s)	7782	-
	MEOH in*	Initial methanol flowrate (mol/s)	0.369	-
	H_2O in*	Initial water flowrate (mol/s)	0.375	-

The output of the MATLAB solver in Table 4-8 is given in mol/L, in addition to the total volume flow (Q) in L/s and the final coke content (Wc) in g/100 g catalyst. To show the mass fraction of each compound without considering methanol and water, appropriate conversions were done. This mass fraction was exported to Aspen Plus to calculate the respective flowrates.

Table 4-8. Mass fraction results from MATLAB equation solving.

Compound	*mol/L*	*g/L*	*g/s*	*Mass fraction*
MEOH	0.00023	0.00746	-	-
CH_4	0.00017	0.00271	118.9	0.02341
C_2H_4	0.00194	0.05437	2386.9	0.46982
C_3H_6	0.00093	0.03913	1717.9	0.33814
C_3H_8	0.00007	0.00318	139.8	0.02751
C_4	0.00020	0.01139	500.1	0.09844
C_5	0.00007	0.00494	216.8	0.04268
WATER	0.01680	0.30245	-	-
W_C	5.31745	g/100g	-	-
Q	43897.7	L/s	-	-

Figure 4-8 depicts the flowsheet diagram for the olefins production and purification. After methanol production, the MEOH/water mixture (S17) is flashed to eliminate the remaining gases (S22). Then, it is heated up by the products stream in the HEX-9 that leave the reactor at temperature of 465 °C (S25). A flash is implemented to remove water (S27), and gaseous products (S28) are compressed and further cooled through heat exchangers (HEX-10, HEX-11 and HEX-12) where low pressure steam is generated and employed in the purification section.

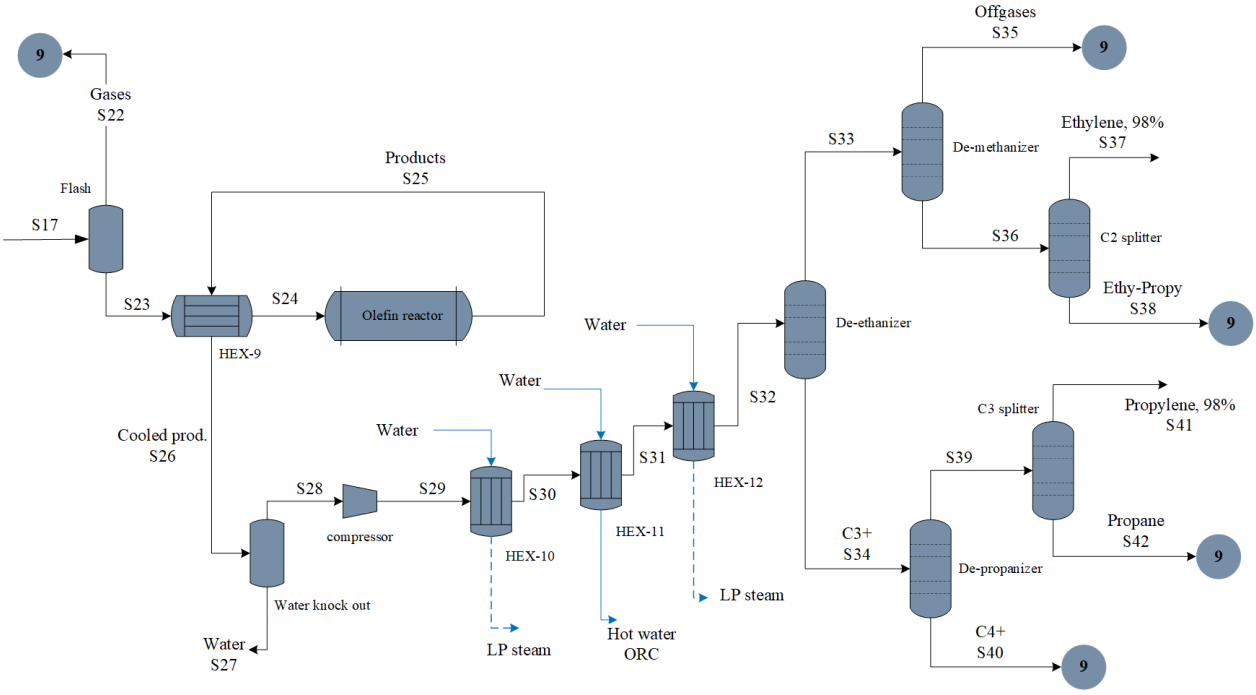

Figure 4-8. Flowsheet diagram of the methanol to olefin synthesis.

After synthesis, the olefins need to be purified through a sequence of distillation columns in order to increase their purity to a chemical grade (>95%). The purification section uses the conditions of Salkuyeh and Adams [173] and Yang and You [174]. The unreacted methanol, water, and the olefins leaving the reactor are cooled to 60 °C and flashed to separate liquid water and methanol from gaseous olefins. The gaseous stream is compressed to 35 bar, cooled up to 40 °C and flashed to remove the remaining water and methanol before entering the columns sequence. For the compressors and gas turbines, the mechanical and isentropic efficiencies are set to be 95% and 90%, respectively. During the cooling, heat is recovered to generate low pressure steam that supplies heat for the columns reboiler.

In Table 4-9 operating parameters of the distillation sequence are provided as well as the purity and recovery of the main products. After cooling, product stream (S32) is sent to the column separation section. From the de-ethanizer, S33 flows to the upper section, where de-methanizer separates off gases (S35) from the ethylene and propylene (S36). C_2 splitter recovers ethylene 98% at the top of the column and a mixture of remaining ethylene and propylene are recovered in the bottoms (S38). Stream S34 from the de-etanizer column passes through the de-propanizer, here, S40 contains C_{4+} olefins and S39 include propylene and propane that are separated in C_3 splitter where the propylene reaches a purity of 98%. The off gases (S22), (S35), ethylene-propylene mix (S38), propane (S42) and C_{4+} (S40) are mixed and sent to the DAC system for fuel recovery. Methane and propylene had recoveries above 99% whereas ethylene achieves a recovery of 95%. This is because part of the ethylene was lost in the de-methanizer, and an increasing recovery of ethylene would imply higher energy requirement.

Table 4-9. Operating conditions of distillation sequence for olefins purification.

Column	*Operating parameters*	*Recovery*	*Reference*
De - ethanizer	Stages = 35 Reflux ratio = 3.5 Boilup ratio = 4 Pressure = 35 bar	-	[173]
De - propanizer	Stages = 30 Reflux ratio = 6 Boilup ratio = 19 Pressure = 25 bar	-	[173]
De - methanizer	Stages = 35 Reflux ratio = 6 Boilup ratio = 1.03 Pressure = 34 bar	Methane recovery 99.8%	[173]
C_2 - splitter	Stages = 30 Reflux ratio = 0.1 Boilup ratio = 5 Pressure = 10 bar	Ethylene recovery 95.6% Purity 98.7%	[173]
C_3 - splitter	Stages = 150 Reflux ratio = 12.88 Boilup ratio = 0.92 Pressure = 17 bar	Propylene recovery 99.5% Purity 98.2%	Adapted from [174]

4.2.4. Heat integration and Refrigerant cycles

A heat integration is implemented in the whole PtO process. The maximum temperature difference between the hot and cold streams is fixed in 10 °C. Cooling duty for the electrolyser and the MTO is provided by using cooling water (CW) that after being used, is sent to an Organic Rankine cycle (ORC) for electricity generation (Figure 4-9). In the ORC, R245Fa is pumped at 3 bar towards the evaporator and absorbs heat from the water that enters at 79 °C and leaves at 41 °C. A turbine unit recovers the energy as electricity due to the expansion of the vapour. After that, the saturated fluid vapour is condensed to return at the initial conditions. The system is modelled in a closed loop and 5% of the cooling water lost because of evaporation is counted [100].

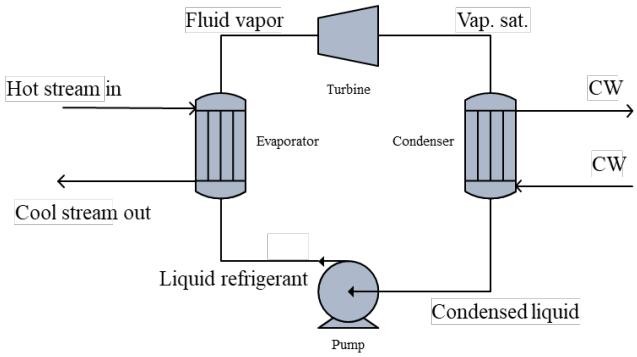

Figure 4-9. Organic Rankine Cycle in the PtO.

According to Yang and You [174], propylene and ethylene can be used in the refrigerant cycle. Hence, propylene is used in the C_2 splitter to supply part of the cooling duty at -52 °C; similarly, propane is employed in the de - ethanizer condenser at -17 °C, both modelled as open refrigerant cycles. In addition to this, the external refrigerant utility is used to supplement the cooling requirements in all the columns. The requirements and temperatures of each column are summarized in Table 4-10.

Table 4-10. Energy requirements and coverings for the column sequence.

Column	*Q_C required (kW)*	*Temperature (°C)*	*Cold utility*	*Q_C recovered (kW)*
De-ethanizer	-2,971	-17	Propylene	266
			Propane	118
			Methane	37
			Refrigerant	2,550
De-methanizer	-1,477	-62	Refrigerant	1,477
C_2 splitter	-833	-52	Propylene	212
			Refrigerant	621
De-propanizer	-3,234	60	Cooling Water	-
C_3 splitter	-7,176	40	Cooling Water	-

Propylene, propane, and methane were used as part of the cold utilities in the de - ethanizer condenser. Condensates were expanded to reach low temperature before passing through the column condenser. After heat exchanging, gases were compressed and condensed, using cooling water to return at the initial conditions. Similarly, in the C_2 splitter part of the cold utility was supply by the propylene stream, reducing the amount of refrigerant requirement in the purification stage. In total, this heat integration approach was able to provide 12% of cold utility.

4.3. Key performance indicators

In the following sections the technical, economic and environmental indicators have been described. Moreover, the main assumptions are listed for the modelling of the power-to-olefins process.

4.3.1. Technical performance indicators

The performance of the PtO process is assessed in technical, economic, and environmental perspectives. Carbon efficiency (C_e), specific energy consumption (*SEC*) and additional indicators such as overall CO_2 conversion and CO_2 to olefin ratio are included in the technical performance. Economic and environmental performance indicators are described in the subsequent sections.

The carbon efficiency determines the fraction of the original carbon source that is found in the products as part of the conversion. The equation 4-6 correlates the moles of carbon in the olefin products (ethylene and propylene) and the moles of carbon present in the CO_2 feedstock [175].

$$C_e = \frac{\dot{n}c_{ethylene} + \dot{n}c_{propylene}}{\dot{n}c_{CO2}} \qquad 4\text{-}6$$

The specific energy consumption (*SEC*) is defined as the energy requirement per unit mass of the product, equation 4-7.

$$SEC = \frac{Energy\ consumption\ [MW]}{Mass\ flow\ products\ [kg/s]} \qquad 4\text{-}7$$

Similarly, complementary indicators include the amount of CO_2 required per tonne of olefins output (kg/kg) and the overall CO_2 to the olefin conversion denoted in equation 4-8:

$$Overall_{CO2\ conv} = \frac{\dot{n}_{CO2-in} - \dot{n}_{CO2-out}}{\dot{n}_{CO2-in}} \qquad 4\text{-}8$$

Where $n_{CO2\text{-}in}$ is the moles of CO_2 that enters the system, and. $n_{CO2\text{-}out}$ is the moles of CO_2 that are released to the atmosphere during the capture and synthesis.

4.3.2. Economic analysis

The CAPEX has been calculated with the methodology described in Chapter III, section 3.4. Table 4-11 lists the equipment costs of the PtO plant. The equipment cost data for the DAC system were taken from Keith et al. [89]. Costs reported at a different year were adjusted to the year of study (i.e., 2021) using CEPCI. Currency was also adjusted using the exchange rate of the reference year before the year update. Capacities, size, or flowrates of each equipment were obtained from Aspen Plus simulations.

Table 4-11. Equipment cost data of PtO.

Equipment	*Variable of design*	*Ref. year*	*Ref. cost GBP*	*Ref. size*	*Scaling factor*	*References*
Air contactor	$MtCO_2/y$	2016	84,463,398	0.98	1	[89]
Pellet reactor	$MtCO_2/y$	2016	56,975,748	0.98	1	[89]
Calciner-slaker	$MtCO_2/y$	2016	32,451,727	0.98	0.7	[89,176,177]
Steam turbine	kW	2014	3,579,173	4100	0.8	[178]
Electrolyser (installed)	MW	2016	1,229,225	1	0.65	[178]
Heat exchangers	m^2	2017	394,506	1000	0.7	[168]
Compressors	kW	2002	364,720	1007	0.67	[179]
Compressors (Refrigerant cycle)	kW	2016	14,644	100	0.9	[168]
Distillation columns	m^3	2017	3,550,550	92.3	0.8	[168]
Evaporator/ Condenser	m^2	2014	201,530	1000	1	[178]
Gas turbine	kW	2012	17,012,074	16100	0.8	[178]
Pump	m^3/s	2001	62,182	10	0.36	[178]
MEOH reactor	ton/day	2016	4,493,041	1190	0.6	[180]
Olefins reactor	MEOH/s	2014	125,541	62.5	0.6	[163]

The OPEX include variable and fixed operating costs. The variable costs, comprising raw materials, process water, catalyst, and disposals are calculated based on their market prices and simulation results. The catalysts are accounted for a renewal of two years and the levelized cost of electricity (LCOE) has been calculated by the SAM software. Fixed operating costs, supervision, maintenance, insurance, and general plant overhead are computed using default factors as specific percentages of the PEC. In addition, variable and fixed costs are summarized in Table 4-12.

Table 4-12. Fixed and variable costs[181].

Fixed operating and maintenance costs (FOM)	*Basis*	*Factor*	
Operating Labour (OL)	Equation 3-5	-	-
Operating Supervision (OS)	OL	0.25	-
Direct overhead (DO)	OL + OS	0.5	-
General overhead	OL + OS + DO	0.5	-
Maintenance labour	FCI	0.015	-
Maintenance materials	FCI	0.015	-
Insurance and tax	FCI	0.01	-
Financing working capital	WC	0.1	-
Variable costs	*Unit*	*Value*	*Reference*
Catalyst price (MeOH)	£/kg	93.2	[182]
Catalyst price (MTO)	£/kg	81.8	[183]
Electricity wind	£/kWh	0.051	SAM software
Electricity grid*	£/kwh	0.025	[184]
Wastewater treatment	£/tonne	0.42	[161]
Cooling water	£/tonne	0.03	[161]
Process water	£/m^3	0.08	[89]
Ca disposal and make up	£/tonne CO_2	0.16	[89]

*Only the cost for the use of the network is computed

4.3.3. Sensitivity analysis

Further, a sensitivity analysis is conducted to analyse the effects of the key parameters over the olefin MSP applying a change of ± 25% to the original values. The parameters of interest are the LCOE, the PEM investment cost, the IRR, the O_2 price, and the CO_2 capture cost expressed as the levelized cost of CO_2 ($LCCO_2$). The $LCCO_2$ is the sum of the levelized capital cost (LCC) of the DAC, the DAC operation and maintenance (FOM) cost and the energy cost required for the CO_2 capture. The $LCCO_2$ and LCC of the capture system are estimated using the equation 4-9 and equation 4-10 as described in Keith et al. [89].

$$LCCO_2 = LCC + DAC\ O\&M + energy\ cost \quad 4\text{-}9$$

$$LCC = C_i \times \frac{CRF}{U} \quad 4\text{-}10$$

Where: C_i is the capital cost intensity per unit capacity (U), calculated by applying a Lang factor of 3.2 to the DAC equipment cost, and CRF is the capital recovery factor detailed in equation 4-11.

$$CRF = \frac{i \times (1+i)^n}{(1+i)^n - 1} \quad 4\text{-}11$$

Where i is the discount rate and n is the number of years for the project. Finally, DAC $O\&M$ are taken as \$42/tonne-CO_2 [89]. The energy cost was neglected since the energy input in the CO_2 capture is supplied by internal resources.

4.3.4. Environmental assessment

The environmental assessment has been performed according to the guidance of ISO 14044 which describes the stages included in a proper life cycle assessment. These stages are described below.

Goal and scope

The goal of the current LCA is to quantify the global warming potential (GWP) of the olefin production using carbon capture utilisation and the Power to X approach. Other categories such as abiotic depletion, eutrophication, and ozone depletion are also considered and reported.

System boundaries

Figure 4-10 illustrates the system boundaries that include the relevant process steps from *cradle to gate*. The LCA includes all material and energy inputs as well as the emissions to the water, soil, and air involved in the processing. The life cycle steps of CO_2 capture, H_2 production through water electrolysis, olefin synthesis and separation in addition to the wind electricity supply are considered. The CO_2 captured (uptake) is not accounted for as negative emissions since at the product end of life, it is released as positive emissions adding up to zero in a carbon neutrality cycle [113]. Infrastructure for the DAC, olefin synthesis and electrolyser are not considered due to their low contribution to the environmental impacts [150]. However, infrastructure emissions of the offshore wind farm were considered.

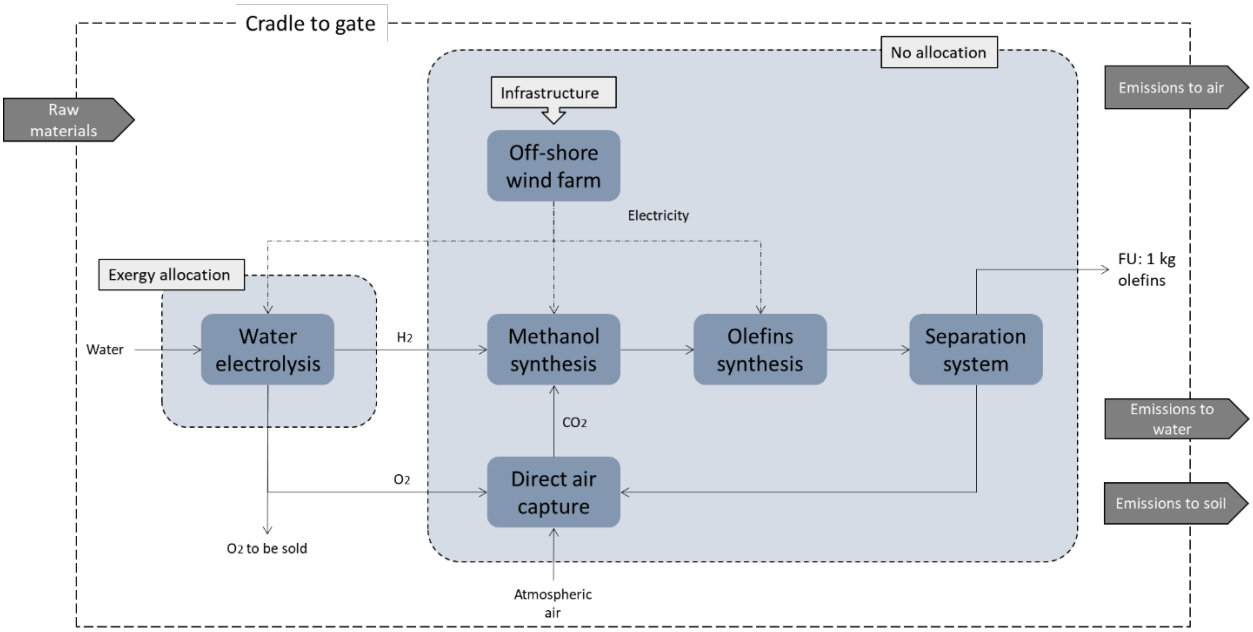

Figure 4-10. System boundary for the PtO process.

Functional unit and allocation method

The functional unit is defined as 1 kg of olefin (in our case summation of ethylene and propylene), since butene and pentene are on-site utilised to run the DAC calciner, and therefore no outputs are reported for them. Despite O_2 is considered as unintended product, it is considered in the emissions counting. According to the ISO-14044 guidance, the first step is to avoid or minimise allocation wherever it is possible by subdividing the system into two or more sub processes [185]. Olefin and commercial O_2 are the products of the PtO. The strategy to avoid an allocation between these two different products, is the subdivision of the water electrolysis from the rest of the plant as depicted in Figure 4-10. Thus, an exergy analysis is applied to allocate water electrolysis emissions between H_2 and O_2 and then, the resulting allocated emissions to H_2 are used to calculate the overall process impacts.

Data collection and impact assessment

The life cycle inventory (LCI) for the DAC, electrolysis and MTO synthesis and separation is constructed from the mass and energy balances obtained from the process modelling results, relevant literature, and using the datasets available in the *Ecoinvent* database v3.1 [113,186,187]. The catalyst LCA impact is typically neglected [188] and this approach has been followed herein. The complete LCI is found in the results section. The impact categories studied are the Global Warming Potential (GWP), abiotic depletion potential (ADP), eutrophication (EP) and ozone layer depletion (ODP) [186].

4.4. Results and discussion

In the next sections, the results of the PtO modelling are presented. Technical efficiency, conversion rates and mass and energy balances are reported and discussed. Additionally, the economic and environmental indicators are presented and discussed in detail.

4.4.1. Process modelling results

The process flow diagram for the proposed power to olefins process, is illustrated in Figure 4-11. The designed plant has a production rate of 103.4 ktonne/y of olefins. For that purpose, around 876,600 ktonne/y of air at 400 ppm CO_2 concentration (stream 1) was injected to the DAC producing 505.2 ktonne/y of captured CO_2 (stream 3) and releasing depleted air to the atmosphere at 100 ppm CO_2 concentration (stream 2).

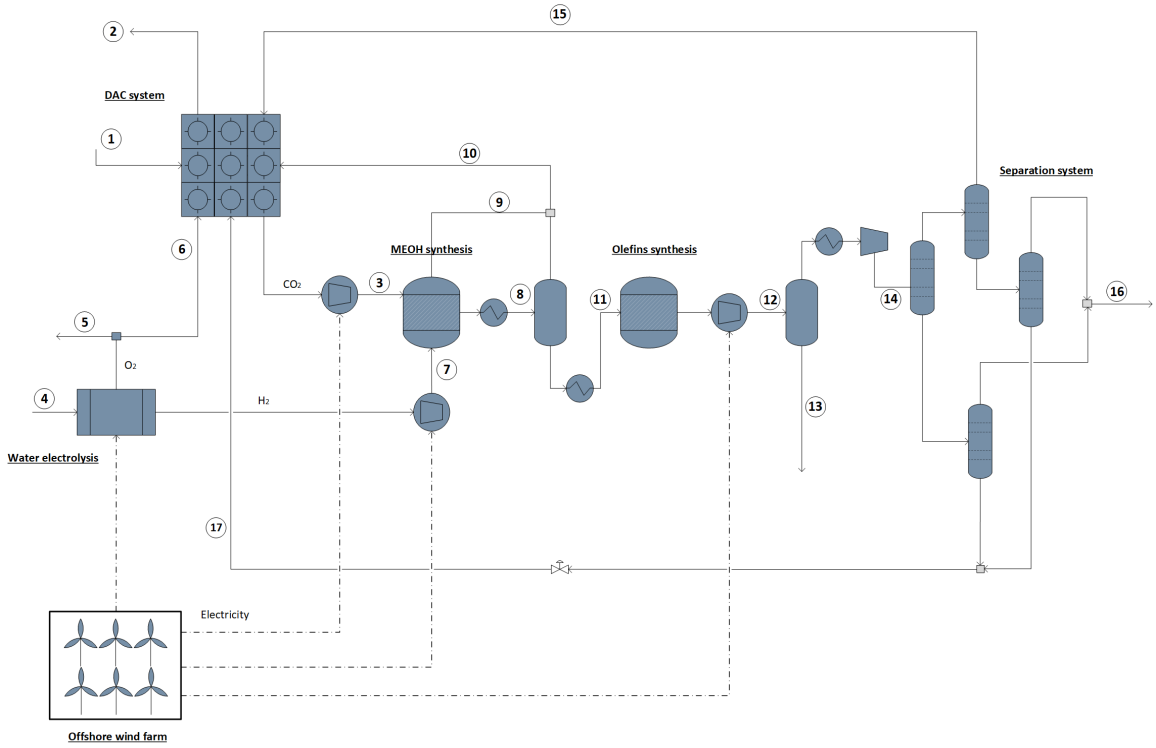

Figure 4-11. Process flow diagram and the main streams of the olefins production.

Additionally, 708 ktonne/y of water (stream 4) were required to produce 76 ktonne/y of H_2 (stream 7) and 598 ktonne/y of O_2. In the latter, around 67% of the stream was liquefied to be sold as a co-product (stream 5) while the remaining was sent to the DAC for oxy-combustion (stream 6). The H_2 along with the captured CO_2 were sent to the methanol synthesis. After the reaction, the outlet stream (stream 8) was cooled down and flashed to separate gases from the MeOH/H_2O liquid mixture. The cooled gases are recycled to the reactor (stream 9) and a purge with most of the unreacted H_2 was sent to the DAC for combustion (stream 10). The MEOH/H_2O mixture (stream 11) is converted into olefins in the olefin synthesis reactor. The stream containing the products was cooled down (stream 12) before the water removal (stream 13). Dehydrated olefins were compressed and further cooled (stream 14) before the column sequence. Heat was recovered and used to generate low pressure steam for the reboiler. Once in the separation section, light gases (stream 15) and the heavier C_4 and C_5 products (stream 17) are sent to the DAC oxy-fired combustion. Finally, ethylene and propylene are recovered as the main product (stream 16). Both achieved purities that are considered to be chemical grade (>95%) [189], about 98.7% and 98.2%, respectively. The CO_2 and H_2 to methanol per pass conversion in the methanol synthesis were 97.96% and 99.97%, respectively whereas an overall CO_2 conversion of 95.4% was achieved. A summary of the main inputs and outputs is shown in Table 4-13.

Table 4-13. Mass and energy inputs and outputs of the PtO.

Electrolyser		
Input	*Amount*	*Unit*
Electricity	526	MW
Deionised water	708	ktonne/y
Output		
H_2	76	ktonne/y
O_2	598	ktonne/y
Direct Air Capture		
Input		
Electricity	11.7	MW
Heat	67.2	MW
Output		
CO_2	554	ktonne/y
MTO plant		
Input		
CO_2	554	ktonne/y
H_2	76	ktonne/y
Electricity	19.3	MW
Output		
Olefins	103	ktonne/y
Light gases (CO, CH_4)	11.7	ktonne/y
C_{4+}	22.5	ktonne/y

Further, Figure 4-12 presents the exit mass fraction (dry basis) outputs of the olefins reactor and compares with experimental data derived from Lu et al. (2016). Clearly, the model obtained in this study is in good agreement with the experimental data with a slightly increment on the ethylene production. Also, the Coke content was compared to the results in the 5.31 g/100 g catalyst provided by the model against 5.64 g/100 g cat. reached in the experimental work.

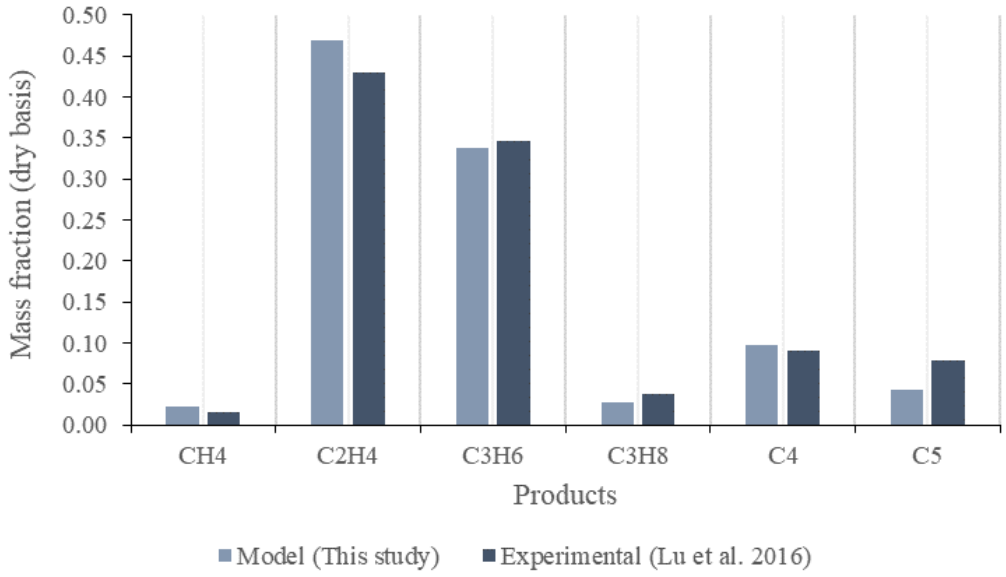

Figure 4-12. Exit mass fraction composition (model) of the olefin reactor against experimental data from Lu et al.[171].

4.4.2. Carbon balance

Figure 4-13 displays the carbon flow through the PtO process. Initially, 1,283 kmol/h of carbon enters the DAC and due to the capture efficiency part of the carbon is vented to the air (321 kmol/h). An additional carbon flow (449 kmol/h) is added to the system in the form of light gases coming from the MTO that are used in the calciner for energy recovery. Thus, the carbon exiting the DAC system is 1,411 kmol/h and this is sent to the MTO and it is distributed into CH_3OH (methanol), CO_2, ethylene, propylene, butene (C_4), pentene (C_5), methane, propane and CO. A small amount of carbon is wasted in the methanol wastewater while the remaining carbon is partitioned between ethylene and propylene that leave the system as main products and the other olefin products that are used internally.

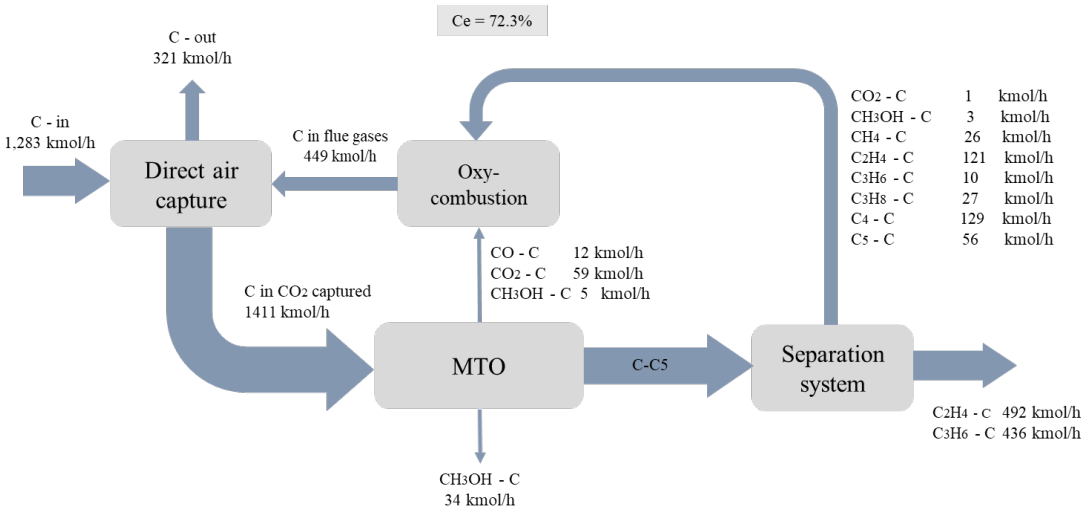

Figure 4-13. Carbon flow in the proposed PtO process.

The result of this carbon flow was an overall carbon efficiency of 72.3%, the major losses of carbon were in DAC due to the low capture efficiency (75%). Do and Kim [109], found a carbon efficiency of 99.2% of a CO_2 to C_2-C_4 process, which is higher than reported here. That is because our study includes the CO_2 capture, where most of the carbon is lost. The CO_2 capture is a crucial step of the infrastructure and must be included. Hence, the carbon efficiency can be improved by increasing the efficiency of the carbon capture technology. For example, CO_2 can be derived from biogenic sources (e.g., biomass or waste) or unavoidable point sources (e.g., cement plants) at capture rates greater than 90% by using typical amine-based post combustion processes. Further research on this aspect is highly recommended.

Based on the simulation, 4.88 tonne of CO_2 are required to produce 1 tonne of olefins. This lines up with Zhao et al. [107] who estimated 4.3 tonne CO_2 per tonne of olefin. Do and Kim [109] found that 1 tonne of $C_2 – C_4$ hydrocarbons requires 3.89 tonne CO_2. Alternatively, since methanol production has been studied more than olefins, a comparison of the CO_2 to methanol ratio is also provided. From the present simulations, to produce 1 tonne of methanol, around 1.39 tonne of CO_2 is required. This has been compared to several studies [175,190–192] in which the CO_2/MEOH ratio ranges between 1.56 and 1.69 tonne CO_2/tonne.

4.4.3. Energy balance

The electricity and heat requirements are the core of the PtO process. Table 4-14 shows the energy balance of the plant. The heat requirement in the DAC was around 67.2 MW (3.8 GJ/tonne CO_2) due to the thermal decomposition of carbonates in the calciner that requires high temperatures (900 °C). To supply this, three different streams were used to generate heat; the vented gases including H_2, CO and methanol in the MTO system, the off gases (CH_4, CO, CO_2, C_2H_4) and the heavier olefins C_{4+} recovered in the olefins purification section (stream 10, 15 and 17, Figure 4-11). Approximately 73.3 MW of heat was recovered by the oxy-combustion of these streams. The electricity consumption in the DAC was around 12 MW which was supplied by the steam turbine in the slaker. In the electrolyser, 526 MW of electricity was required due to the stack energy plus the auxiliary equipment. Also, the cooling energy was used to generate electricity in the ORC. The MTO process had different energy requirements, heating was almost 107 MW while the cooling demand was 209 MW. Hot and cold streams in the MTO were integrated using a maximum temperature difference of 10 °C, resulting in a 100% and 47% covering, respectively for heating and cooling. Also, cooling remnant (110 MW) was used in the ORC, where 6.4 MW of electricity was generated. This amount was subtracted from the final PtO electricity demand resulted in 13 MW which was supplied by the offshore wind turbines.

Table 4-14. Energy balance of the PtO process.

Unit/Process	*Heat (kW)*	*Cooling (kW)*	*Electricity (kW)*
DAC	67,281[a]	-	11,746[b]
Electrolyser	-	131,545[c]	526,299[d]
MTO	106,899[e]	208,979[e]	19,369[d]
Heat generation	77,344	-	-
Power generation (ORC)	-	-	6,452

[a] Covered by heat generation
[b] Covered by Steam turbine
[c] Used in ORC power generation
[d] Electricity covered by wind turbines
[e] Heat Integrated

The specific energy consumption reflects the energy consumption and the integration of the heat and cooling through the whole process per unit of product. It was found that PtO has an overall *SEC* of 150 MJ/kg olefin (41 kWh/kg). This includes the H_2 production through water electrolysis and CO_2 capture in addition to the olefin synthesis. The SEC is higher compared to the energy intensity of ethylene produced using different fossil - based feedstock such as ethane, naphtha and gas oil; these processes have a SEC that ranges between 19.4 and 31.9 MJ/kg [193] and hence the PtO uses 5-fold more energy. Compared with other PtX studies, Keller et al. [112] reported a power demand of olefin from the CO_2 flue gases of about 96.9 MJ/kg olefins and this accounts for the electrolysis, flue gas scrubbing and olefin production. Further,

the energy consumption in the PtX routes is intensive due to the high electricity consumption in the electrolyser. All of the electricity of the plant was supplied by the offshore wind farm. The wind farm had an arrangement of 176 *Senvion* turbines with a height of 87 m. They were able to provide around 540 MW of electricity with a capacity factor of 45.4% that indicates the average power output over the maximum power capability provided by the software. The power generated by the system clearly, is not constant, therefore, the fluctuations were covered by taking energy from grid, while the surplus energy was sent back to the grid to compensate for that consumption. Thus, the energy was in balance between the consumption and generation.

4.4.4. Economic analysis results

In this study, the economic feasibility of the PtO process was assessed by estimating the olefins MSP. Table 4-15 presents the overall financial results. CAPEX included the PEC for the DAC, electrolyser, methanol, and olefins synthesis and separation. Around 825 million GBP are needed for the capital investment and 258 million GBP for the operational cost of the whole plant.

Table 4-15. Economic CAPEX and OPEX results and the olefins MSP.

Parameter	*Value*	*Units*
CAPEX	£ 825	MMGBP
CAPEX/Unit	£ 7.98	£/kg
PEC	£ 277	MMGBP
FCI	£ 570	MMGBP
OPEX	£ 258	MMGBP
OPEX/unit	£ 2.49	£/kg

The breakdown of PEC is displayed in Figure 4-14. As can be seen, the DAC contributes about 55% of the total purchased equipment cost, followed by the electrolyser with 37% and the olefin synthesis in 8%. As expected, the DAC implies a greater cost because the relative lack of technological development. The air contactor and the pellet reactor were the leading costs since they treat a large volume due to the low CO_2 concentration in the air (400 ppm). Within the water electrolysis, the costs include the stack, auxiliary equipment, and the additional compressors for the O_2 liquefaction. Lastly, MTO despite to list more equipment, it has a low contribution in the overall PEC.

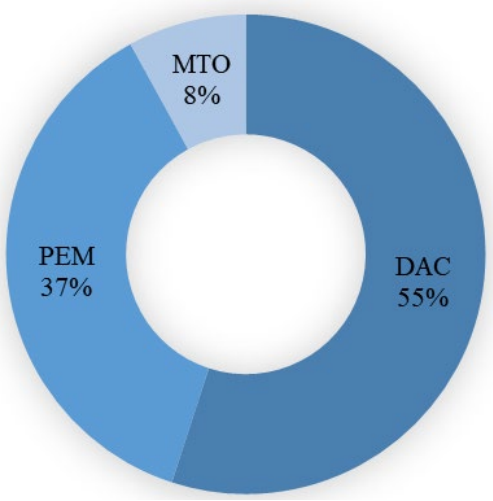

Figure 4-14. Purchased equipment cost breakdown of the olefins plant.

Bos et al. [190], evaluated the production of methanol through CO_2 hydrogenation using DAC and an alkaline electrolysis. They found that the cost of the CO_2 capture and the electrolysis dominate the PEC, that accounts for 50% and 45%, respectively. As observed in Figure 4-14, the DAC and H_2 production are the primary constraints in the fixed costs. It is expected that the costs of the capture decrease in the following years as the interest of its application at large scales increases, and more advanced technology is proved.

The operational cost distribution can be seen in Figure 4-15. Clearly, the cost of the electricity is the dominant factor. It represents 85% of the total cost due to the large amount of electricity that is needed for the electrolyser in addition to the cost of the grid network usage that represents 17% within the cost. This finding is prevalent in the literature since it has been cited as being crucial in the economic viability in numerous research papers [66,102,103,192,194]. The maintenance materials and labour, both composed, accounted for 9% of the total while insurances and tax contribute 3%. The catalysts, labour, and the rest of the expenses represented only about of 2% of the total.

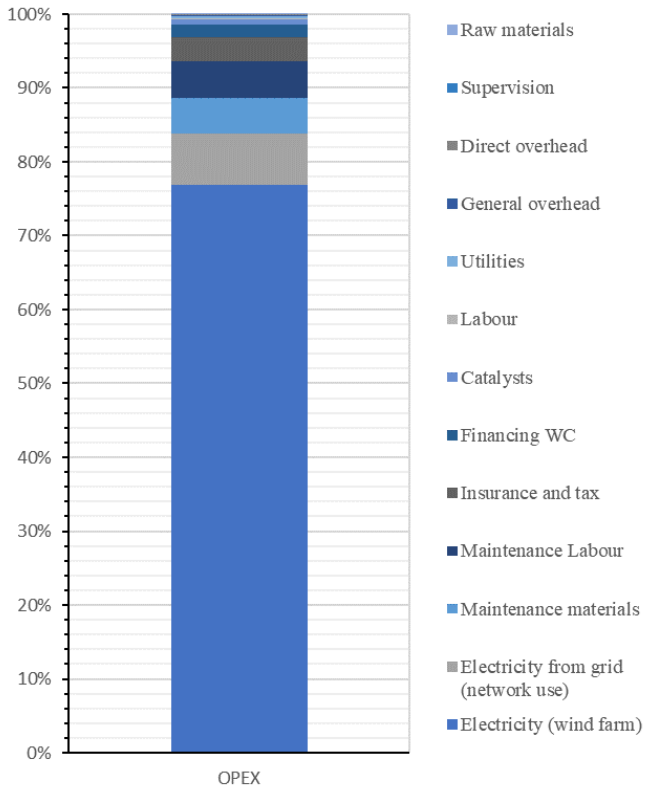

Figure 4-15. Operational expenditures breakdown.

The olefins MSP has been calculated through a break-even analysis. An estimated MSP of £3.67 per kg of olefin had resulted. The price is higher than the current market price for fossil - based ethylene and propylene production, which is around £1.05 – £1.4 per kg [194]. Other studies have been evaluated olefins production in a Power to X approach with price ranging from £1.95 – £3.03 per kg olefins as listed in Table 4-16.

Table 4-16. Power to olefins economic results comparison

Study	*Main product*	*MSP*, £/kg*	*Comments*
Do and Kim, [109]	C_2-C_4 hydrocarbon	2.79	Onshore wind and electrolyser, CO_2 capture from MEA process.
Goud et al., [195]	Ethylene	2.8	Purchased Methanol from renewables, MEA CO_2 captured
Goud et al., [195]	Ethylene	2.1	H_2 from PEM using wind energy
Pappijn et al., [111]	Ethylene	1.95	Electrochemical CO_2 conversion and wind energy
Savaete, [110]	Ethylene	3.03	Purchased renewable methanol
Nyhus et al., [194]	Ethylene	2.92	Wind, DAC, AEL
Conventional olefin	Ethylene	1.05-104	Naphtha, fossil-based energy
This study	Ethylene/Propylene	3.67	Offshore wind, PEM, DAC

*Prices in the original sources have been converted to GBP by using exchanges rates of the year.

The range of prices primarily relies on the type of technology employed such as solar, wind, photovoltaic and nuclear renewable energy, and fossil-based options. Wind energy is one of the most profitable renewable electricity sources, however, the low electrolyser efficiency causes the effective energy utilisable is lower and more electricity must be supplied to meet the final request. Savaete [110] estimated a price of £3.03/kg (€3.7/kg) olefin accounting for renewable methanol and stated by using fossil - based methanol feedstock, price drops to 0.93 €/kg. Do and Kim [109] reported a price of £2.79/kg C_2-C_4 product (USD 3.58/kg). They concluded that the use of fossil-fuel options for H_2 production result in relative low production cost but relative high emissions, in contrast, using renewable H_2 alternatives results in unfavourable economics for H_2 production highlighting the importance of a high efficiency electrolysis system.

Sensitivity analysis

The sensitivity analysis was performed to assess the influence of the parameters of interest over the olefins MSP. The LCOE, $LCCO_2$, electrolyser investment cost per MW, IRR and O_2 price were the considerations. The $LCCO_2$ was estimated as £150/tonne CO_2, which is in line with Keith et al., [89], i.e. 94 to 232 USD/tonne CO_2; more details about the economic assumpions can be found in the same reference. The sensitivity analysis result is represented Figure 4-16. As seen, the cost of the electricity leads to a notable effect on the olefins MSP. When the cost of electricity increases 25%, the MSP increases of about 12% over the original price (from £3.67 to £4.16). Conversely, if the LCOE decreases by 25%, the MSP reaches a value of £3.25, 12.6% less than the original price. Moreover, the CO_2 capture cost and the electrolyser investment cost had a moderate impact over the MSP, their variation was about half of the LCOE impact, about ±6% of the initial value. The IRR and the O_2 price showed minor impacts over the final price with changes below ±3% of the original price. Notably, improvements on the supply chain along with an effective utilisation of electricity should be further investigated to provide a better economic scenario for the PtX projects.

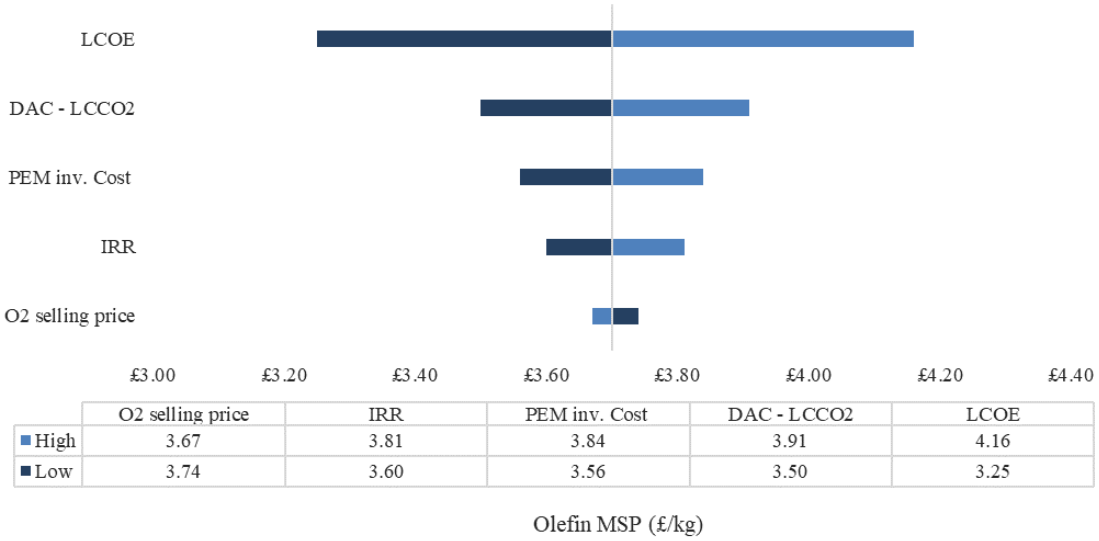

	O2 selling price	IRR	PEM inv. Cost	DAC - LCCO2	LCOE
High	3.67	3.81	3.84	3.91	4.16
Low	3.74	3.60	3.56	3.50	3.25

Figure 4-16. Sensitivity analysis for the olefins MSP.

4.4.5. Life cycle assessment results

The GWP emissions are expressed per FU, and only the process emissions were reported. The uptake of CO_2 entering the system during the capture and the end of life were excluded to preserve carbon neutrality. This assumption was made in accordance with the study of Rosental et al. [113]. As a result of the adopted allocation in the electrolysis stage, all emissions were assigned to the H_2 because its exergy value was much higher than for O_2.

The main inputs and outputs for the PtO process are provided in Table 4-17. Data was generated by Aspen Plus simulations and adapted by Harrison et al. [152] and Keith et al. [89].

Table 4-17. Life cycle inventory of PTO process (FU: 1 kg olefin).

Electrolyser			
Stage	*Amount*	*Unit*	*Source*
Input			
Electricity	40.7	kWh	[152]
Deionised water	6.69	kg	[152]
output			
Hydrogen	0.67	kg	Aspen Plus
Oxygen1	1.71	kg	Aspen Plus
Oxygen2	3.57	kg	Aspen Plus
Direct Air Capture			
Input			
Water	20.6	kg	Aspen Plus
Electricity	0.90	kWh	Aspen Plus; [89]
Heat	5.20	kWh	Aspen, covered by internal fuel
KOH	0.001	kg	Aspen Plus
$CaCO_3$ make up	0.20	kg	Aspen Plus
output			
CO_2	4.88	kg	Aspen Plus
$CaCO_3$ disposal	0.20	kg	Aspen Plus, [89]
CaO disposal	0.70	kg	Aspen Plus; [89]
MTO plant			
Input			
CO_2	4.88	kg	Input from DAC
H_2	0.67	kg	Input from electrolyser
Electricity	1.00	kWh	Aspen Plus
MEOH	3.50	kg	Aspen Plus
Output			
Olefins	1.00	kg	Aspen Plus
Methane	0.03		Aspen Plus
Propane	0.03	kg	Aspen Plus
C_4	0.14	kg	Aspen Plus
C_5	0.06	kg	Aspen Plus

Table 4-18 shows the GWP impact breakdown of the PtO. About 0.74 kg CO_2e are emitted per kg olefin produced. In addition, the electrolysis stage is responsible for around 85% of the total emissions, with the remaining 15% being split between the DAC and the MTO stages.

Table 4-18. Global warming potential impact of 1 kg of olefins.

		Stage		
Impact category	*Total*	*DAC*	*Electrolysis*	*MTO*
GWP (kg CO_2e/kg olefin)	0.74	0.08	0.64	0.02

The GWP of the electrolysis and the MTO systems are dominated by the electricity consumption; despite the fact that wind electricity is employed, due to the high electricity consumption, predominantly in the electrolyser (a typical feature of Power-to-X systems), and the embedded emissions associated with the supply chains of the construction of the turbines the impact of electricity on the GWP is significant. Regarding the DAC, the necessary heat and electricity to run the system are covered internally; the H_2-rich stream and the C_{4+} olefins stream from the MTO synthesis supplied heat while the electricity has been supplied by the steam turbine in the slaker. As a result, energy consumption has no contribution to the carbon emissions in the DAC system. Instead, emissions are caused by calcium and potassium additions, the water usage and waste disposal.

To compare the PtO with the fossil - based process, a theoretical module of ethylene/propylene in the same proportions as in this study (47% and 53% respectively) from steam cracking of naphtha production, available in the *Ecoinvent* database v3.1 has been simulated in the SimaPro software. The impact of this equivalent fossil - based olefin was 1.40 kg CO_2e per kg which is shown in Figure 4-17.

The GWP resulted for the olefins production in the present study is 0.75 kg CO_2e/kg olefin. This indicates that there is a 47% reduction in GWP by using PtO compared to fossil-based. The fossil - based process is based on the use of fossil resources, such as the electricity from the grid which has a higher carbon intensity than the wind electricity.

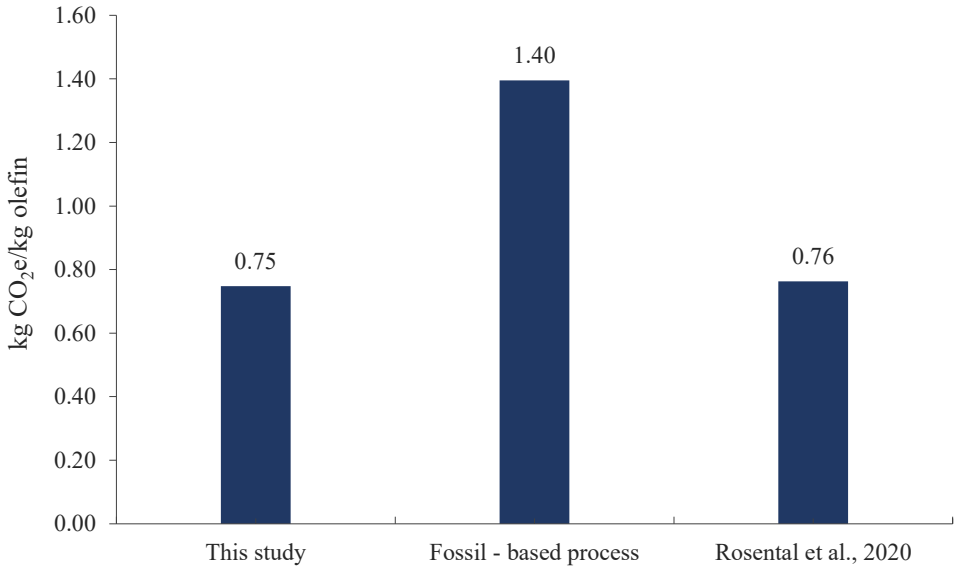

Figure 4-17. Comparison of cradle to gate global warming potential of PtO with Rosental et al. (2020) and fossil - based process

The result of this study is similar to Rosental et al. [113], who investigated the production of olefins through CO_2 that is captured using the *Climeworks* technology and an alkaline electrolytic H_2 in a cradle to grave life cycle assessment including offshore wind electricity. The similarity of the GWP at cradle to gate system boundaries can be attributed to the use of same source of energy with similar carbon intensity, such as offshore wind. The main difference is that Rosental et al. employs an alkaline electrolysis and amine capture for H_2 and CO_2, respectively. In addition, they assume an electric-driven DAC while in the present study a complete energy integration has been applied. The heat requirement of the DAC has been covered internally by using the H_2-rich stream and C_{4+} olefins from the MTO process. A steam turbine is employed in the DAC system to supply electrical need. Additionally, olefins have been used as refrigerants in an open loop in order to decrease the cooling need of the separation stage. Our design approach aims to efficiently integrate the different components of a Power-to-X system aiming at reducing costs and environmental impacts. This confirms that the low emissions in the PtX approaches are achievable and beneficial if renewable resources are combined with a total energy integration approach.

Based on a literature review, it was found that the GWP of olefins produced with CCU and electrolytic H_2, ranges between 0.37 – 2.6 kg CO_2e/kg olefin [108,113,196] as illustrated in Table 4-19 depending on the technology applied, such as CO_2 capture from the biomass gasification, post combustion capture, or electrolytic CO_2 conversion in addition to the different technologies of H_2 production.

Table 4-19. Global warming potential results comparison.

Study	*FU (1 kg)*	*GWP, kg CO_2/kg FU*	*Comments*
Rosental et al., [113]	Ethylene	0.76	Wind, AEL, electrical DAC, accounting only processing emissions
Hoppe et al., [196]	Polypropylene	2.3	DAC and wind energy for H_2 production, grid mix energy used in synthesis
Hoppe et al., [196]	Polyethylene	2.5	DAC and wind energy for H_2 production, grid mix energy used in synthesis
Kuusela et al., [108]	Polypropylene	2.6	CO_2 capture, electrolysis, methanol and propylene synthesis included.
Pappijn et al., [111]	Ethylene	0.37	Wind, excluding CO_2 production and separation & purification stages
Keller et al., [112]	Ethylene/propylene	2.2	Flue gas, AEL electrolysis, wind energy
Conventional olefin	Ethylene	1.4	Naphtha and fossil resources
This study	Ethylene/propylene	0.74	DAC, wind energy for H_2 and synthesis, energy integration

Another study performed by Keller et al. [112] shows a carbon footprint of 14.01 kg CO_2e/kg olefin produced from secondary feedstock, such as flue gases CO_2 extracted with amine-based scrubbing along with electrolytic H_2 powered by the grid and natural gas. They presented substitution electricity scenarios using wind turbines in which the GWP impact reached -1.77 kg CO_2e/kg olefin due to the inclusion of the CO_2 mitigation because of the uptake. When grid was substituted by wind the GWP drops to 2.2 kg CO_2e/kg olefin without accounting the uptake. They concluded that the electricity supply is essential to use CO_2 feedstock and have positive environmental effects. The use of renewable resources, along with heat integration, improves the environmental performance of the PtX process and this has served as the motivation behind this research.

The electricity carbon intensity (CI) is a parameter of paramount importance in the environmental performance of PtX projects. The major drivers of the electricity CI are the construction materials of the fixed and moving parts of the turbines, which represent 48.9% and 49.8% of the total emissions, respectively (derived from SimaPro). The CI of the wind electricity used in the PtO process was taken from the available module in the SimaPro software for an offshore wind turbine in the United Kingdom. This module exhibits an emission factor of 0.0043 kg CO_2e/MJ of electricity (base case), however, according to the literature, it can vary between 0.002 to 0.123 kg CO_2e/MJ depending on the size, model and location of the turbines [197]. Thus, a sensitivity analysis of the CI electricity on the GWP of the investigated process has been carried out. Figure 4-18 displays the olefin GWP for a different wind electricity carbon intensity and the range of carbon intensity presented here varies from 0.002 to 0.01 kg CO_2e/MJ.

If the wind electricity CI reduces to 0.002 kg CO_2e/MJ, the GWP decreases by 42% and reaches a value 0.43 kg CO_2e/kg olefin. In contrast, when the base case CI is increased by 50% (from 0.0043 to 0.0086) the GWP increases by 44% up to 1.08 kg CO_2e/kg olefin.

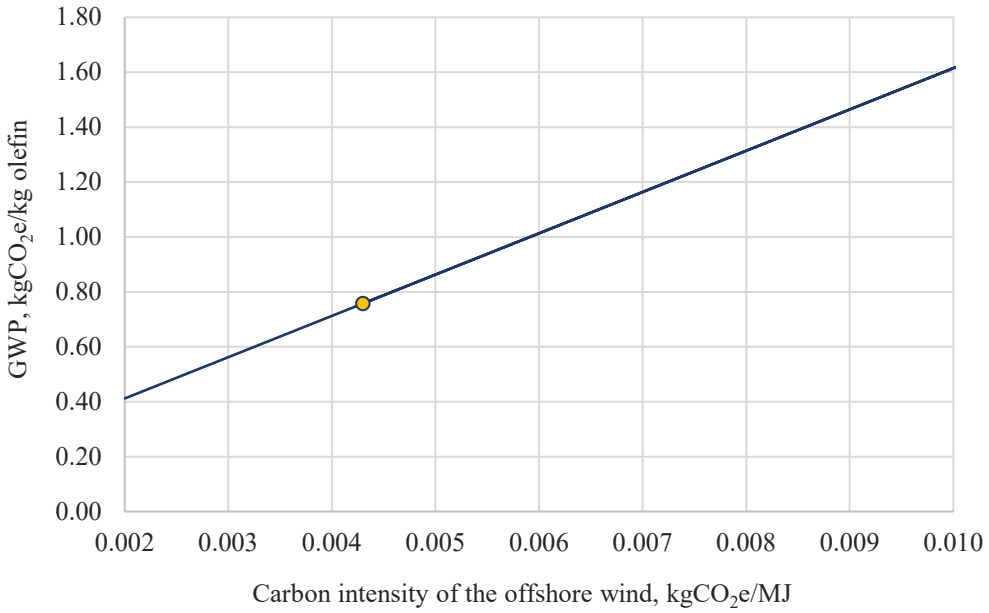

Figure 4-18. Effect of the offshore wind electricity carbon intensity on the olefin GWP (yellow dot indicates base case olefin GWP).

The electricity from the current UK grid has a CI of 0.085 kg CO_2e/MJ. This means that the use of grid electricity is prohibitive for the investigated PtO process as the GWP will rise to 12.96 kg CO_2e/kg olefin. This value is even much higher than the conventional ethylene/propylene production, thus demonstrating the importance of using renewable energies with low carbon intensities in PtX projects.

4.4.6. Other environmental impacts

The environmental impacts for the PtO process are given in Figure 4-19. Abiotic depletion (ADP) category refers to the depletion of natural resources employed for the processing. Eutrophication potential (EP) is related to the nitrogen oxides emissions of the construction materials production in the wind turbines. Photochemical oxidation (POP) involves secondary air pollution and it is formed by the reaction of volatile organic compounds and nitrogen oxides in the presence of heat and sunlight [198]. From the Figure 4-19 it can be seen; the electrolysis stage is the major driver of emissions in all categories. This is due to the fact the whole energy for the plant comes from the wind farm and materials and fixed parts of the turbines are responsible for most emissions. Correspondingly, the DAC system contributes an average of ~20% over the total emissions in all categories and less than 5% is attributed to the olefin synthesis.

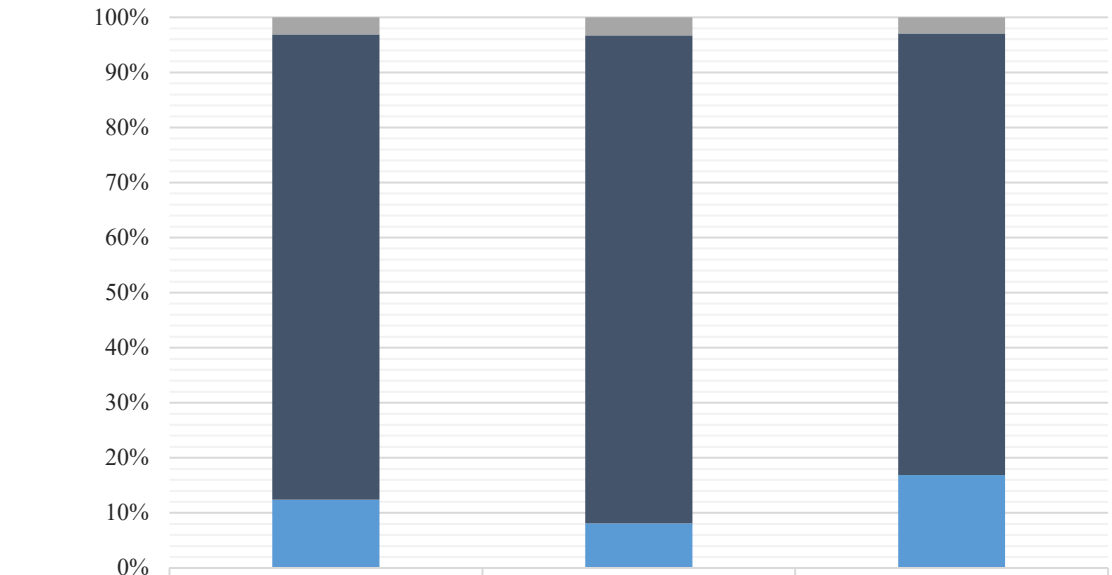

	ADP (kg Sb eq/kg)	EP (kg PO4- eq/kg)	POP (kg C2H4 eq/kg)
3-MTO	1.54E-04	4.64E-05	8.02E-06
2-Electrolysis	4.22E-03	1.27E-03	2.19E-04
1-DAC	6.18E-04	1.16E-04	4.62E-05

Figure 4-19. Emissions contribution by stage for abiotic depletion, eutrophication, and photochemical oxidation categories.

PtO impacts can be compared against fossil - based ethylene production. Figure 4-20 shows the comparison of the ADP, EP, GWP and POP impacts of the PtO and the fossil-based ethylene production which is fixed as baseline 100%. It can be observed that the EP impact is worse for the PtO and four times higher than the fossil-based ethylene. This can be attributed to the construction materials employed in the wind farm, since larger infrastructures are needed to supply the required amount of electricity.

On the other hand, abiotic depletion of the PtO impact is 83% lower than the conventional ethylene. The GWP impact is lower by 46% compared to the fossil-based production emissions whereas the POP is greater by 16%.

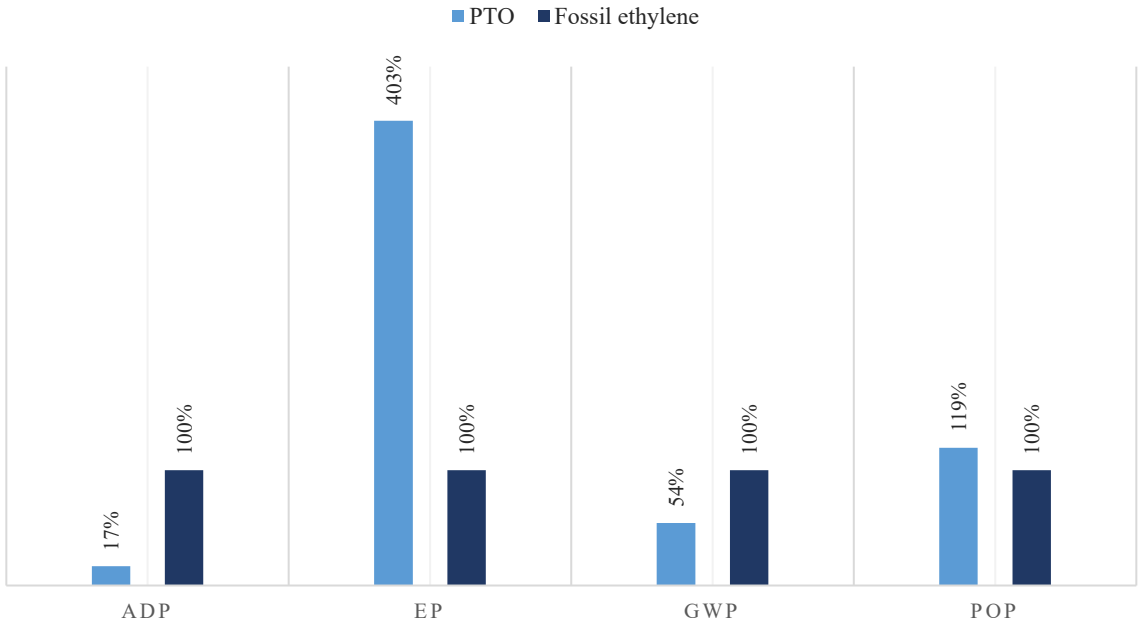

Figure 4-20. Environmental impacts comparison of PtO vs fossil ethylene production (100%)

4.5. Conclusions of PtO

The chapter focuses on a new and important detailed model for the power to olefin process employing direct air capture and electrolytic hydrogen from an offshore wind farm. Data on the economic and environmental performance of the power to olefins pathway are currently scarce. Current Power to olefins studies use system boundaries that typically exclude the CO_2 capture and/or the H_2 production, focusing on the olefins synthesis. In this paper a new and more comprehensive study of a cradle to gate power to olefins process considering also heat integration opportunities has been critically assessed to holistically assess the economic and environmental performance.

The PtO process has an overall carbon efficiency of 72.3%. Most of the carbon losses are in the DAC unit due to the CO_2 capture efficiency (i.e., 75%). Further, it is found that 4.64 kg of CO_2 is required to produce 1 kg olefin. The DAC heat requirement, i.e., 3.8 GJ/tonne CO_2, was covered internally after heat integration and hence no external source such as fossil fuel is required. Nevertheless, the specific energy consumption of the whole PtO assembly was higher than the respective fossil - based production due to the high electricity demand of the electrolyser, i.e. 150 MJ/kg vs 19.4-31.9 MJ/kg, respectively.

Based on a typical discounted cash flow analysis, the MSP of the PtO is more than three times higher than the market price of the conventional ethylene, i.e. 3.67 £/kg vs 1.05 £/kg, respectively. In addition, the sensitivity analysis exposed that the cost of electricity and the cost of CO_2 capture are the main cost drivers.

A cradle-to-gate LCA estimated that the PtO process results in CO_2 emission reduction. The GWP drops by 47% compared to the fossil-based production. The dominant carbon emitter was the electrolysis, and it contributes around 85% of the process GWP. Further reductions of up to 69% can be achieved if the supply chains of wind energy further decarbonised.

Overall, the study assessed an integrated design for a low carbon olefins synthesis route contributing to the research of decarbonising the chemicals industry and the results can inform policy and engineering decision making.

Chapter V

5. A comprehensive process modelling, techno-economic and life cycle assessment of a Power to Ammonia process

Ammonia is the second most produced chemical globally and has the potential for multiple applications. Currently, ammonia is produced through H_2 derived from fossil sources and hereby alternative low carbon ammonia routes are of paramount importance for net-zero. To this effect, the present study investigates the techno-economic analysis (TEA) and life cycle assessment (LCA) of a power-to-ammonia (PtA) process. The study provides a comprehensive economic and environmental assessment of a power to ammonia production system. The research is holistic and assesses the whole supply chain of the PtA assembly and this includes offshore electricity generation, hydrogen produced through water electrolysis, nitrogen production through cryogenic air separation, and the Haber – Bosch (H-B) ammonia synthesis loop. The Aspen Plus software has been utilised to establish the mass and energy balances and the offshore wind farm has been modelled in the System Model Advisor (SAM) software. The hydrogen conversion efficiency, the energy efficiency and the specific energy consumption (SEC) are calculated and included as technical key indicators. A full TEA and a cradle to gate LCA are performed for the whole assembly. Moreover, a sensitivity analysis is carried out to assess the influence of the main parameters on the economic and environmental performances. The results show an overall hydrogen conversion and ammonia energy efficiency of 95% and 49%, respectively which is in line with the literature. Energy integration resulted in a power generation of 14.3 MW, which covered 46% of the Haber-Bosch loop energy requirement. The *SEC* of the total PtA process is 10.53 MWh/tonne NH_3, which is 18% higher than the fossil-based production method due to the electricity consumption of the electrolyser. The economic analysis revealed a levelized cost of ammonia (LCOA) of £687/tonne NH_3 which is higher than the current fossil based ammonia of $200-600/tonne. However, the economic sensitivity analysis shows that a 50% reduction in the levelized cost of electricity (LCOE) can decrease the LCOA by 49%. Based on the environmental LCA, the global warming potential (GWP) of the PtA is reduced by approximately 94% compared to the conventional fossil-based ammonia (151 vs 2445 kg CO_{2e}/tonne NH_3). Further, around 940 m^3 of water is consumed per tonne of ammonia produced. Overall, the investigated PtA assembly offers great environmental gains, but subsidies and/or technical improvements are required to improve its market competitiveness.

5.1. Introduction

The chemical industry is undergoing a major transformation to reduce its carbon footprint and align with global sustainability goals [199]. Within this context, the Power-to-Ammonia (PtA) process, where renewable energy is harnessed to produce ammonia, a critical chemical used in fertilizers, industrial processes, and as a potential energy carrier emerges as a promising approach.

Conventional fossil-based ammonia production relies heavily on the Haber-Bosch process, which uses natural gas and other fossil fuels as feedstock [116]. This method is energy-intensive, with significant carbon dioxide emissions primarily from the steam methane reforming (SMR) stage [121]. In contrast, the PtA process seeks to produce green ammonia by combining electrolytic hydrogen production with nitrogen from air separation, powered by renewable electricity sources such as wind. This approach significantly reduces greenhouse gas emissions and the overall environmental impact of ammonia production [35,129].

The PtA process offers an alternative for chemicals substitutes, energy storage and transport because of its high energy density and established distribution infrastructure. Green ammonia plays an essential role in decarbonizing sectors such as agriculture, chemicals, and transportation. However, several challenges need to be addressed to make this commercially feasible, including the high electricity consumption of the electrolyser, the integration of renewable energy sources, and the overall process economics.

The present chapter aims to provide a comprehensive TEA/LCA assessments based on exhaustive process modelling that include the energy integration of the entire assembly. The investigated energy system includes offshore wind power supply, hydrogen production through a low temperature PEM electrolyser, and nitrogen production through cryogenic distillation.

5.2. Methodology

Figure 5-1 displays the main steps involved in the investigated PtA process chain including electricity supply from an offshore wind farm, H_2 production through electrolysis including O_2 liquefaction, N_2 production via cryogenic air separation and the Haber-Bosch loop which includes a compression system, ammonia synthesis and condensation/recovery. Purge stream is used for energy recovery before being released. The plant is located in the region of Teesside, United Kingdom. The annual production rate of the liquid ammonia at plant gate is 408 ktonne. Mass and energy balances have been computed using the software Aspen Plus V12.2 and Microsoft Excel as well as the SAM software. Detailed conditions of the whole simulation model, economic and environmental analysis are listed in the following sections.

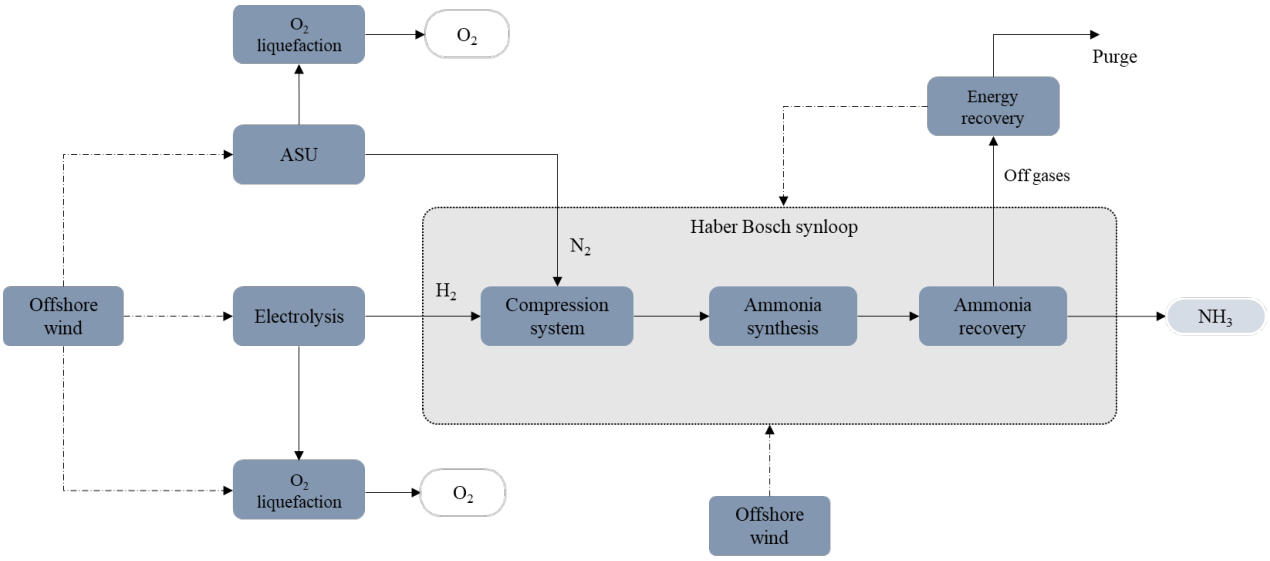

Figure 5-1. Block flow diagram of the PtA process.

5.2.1. Nitrogen production (ASU)

Cryogenic air separation is the preferred method because of the high-volume capacity and high nitrogen purity greater than 99% [128]. The process was simulated in Aspen Plus V12.2 using conditions stated in [31]. The air separation unit (ASU) consists of a double column system in which high purity N_2 is produced.

Figure 5-2 displays the N_2 production through a double column air separator following the conditions of Cheng et al.[200]. Initially, the atmospheric air is compressed and injected into the system at 5 bar and then the air is divided into two streams in SPL 1 to feed each of the two columns (low and high pressure) at different conditions. Both the low-pressure (LPC) and high-pressure columns (HPC) are designed as packed columns that are simulated using the available RadFrac model.

In the HPC, nitrogen and oxygen are separated at 5 bar and -179°C. The nitrogen is released at the top of the column and condensates at -180 °C through HEX-3. The condensate is split into two liquid streams in SPL 3; one of the streams is recycled to the HPC for further purification while the other stream is sent to the LPC. Similarly, oxygen is obtained at the bottoms of the HPC column as liquid, it is also heated in HEX-5 and sent to the LPC. In the LPC, pure nitrogen is obtained at the top of the column while the oxygen is recovered at the bottoms at 1 bar. The stream of nitrogen gas passes through heat exchangers (HEX 4, HEX 5 and HEX 2) where temperature is increased to 207 °C before the compression system. In turn, oxygen is partially condensed in the HEX-3 and flashed to liquid form before leaving the system at 209 °C.

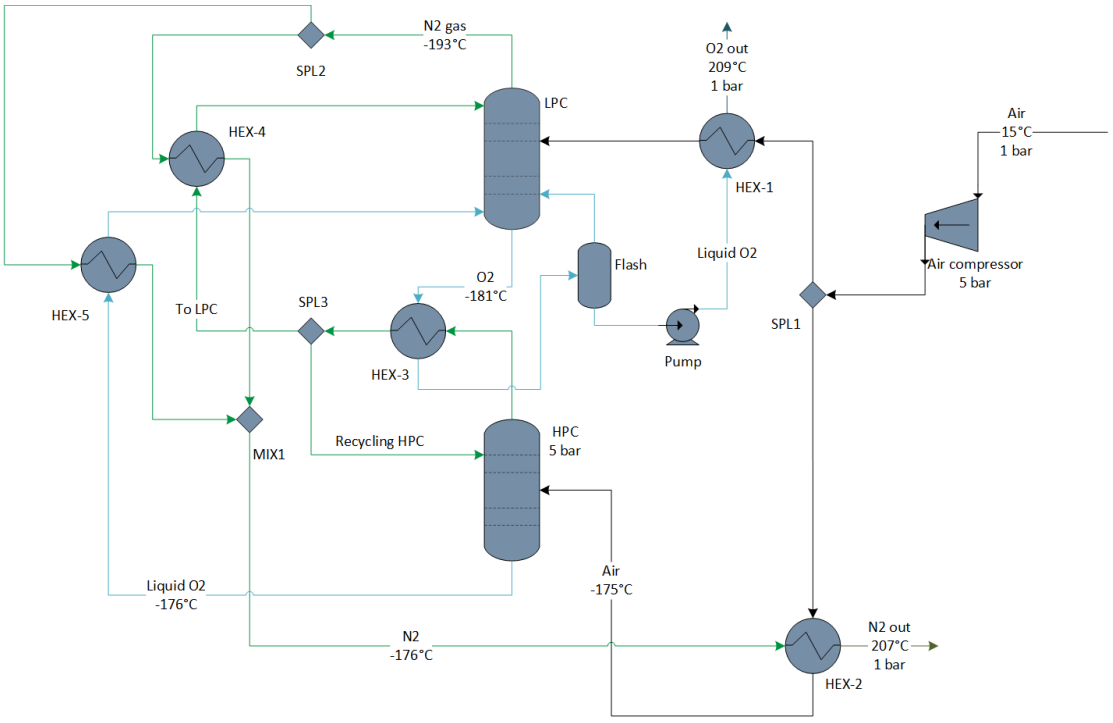

Figure 5-2. Process flow diagram of the double column ASU

To simulate the heat transfer between the two columns, such that only one integrated heat exchanger is required, the exchanger HEX-3 is externally modelled as the reboiler of the LPC and the condenser of the HPC column. Additionally, a full heat integration is applied to the system, including the use of the liquid oxygen to cool down the inlet gas in the low-pressure column. The oxygen in the gas form is mixed with oxygen produced in the electrolyser followed by liquefaction. The nitrogen at 99% purity heads to the compression system to reach the required conditions for ammonia synthesis, i.e. 100 bar. The detailed conditions of the ASU model are summarized in Table 5-1.

Table 5-1. Design parameters used in the ASU simulation model [200].

Equipment	*Design parameters*
Air compressor	P = 5 bar
	Isentropic 85%, Mechanical 95%
Low pressure column	Stages = 29
	P = 1.35 bar
High pressure column	Stages = 20
	P = 5 bar
HEX-1	Type = counter-current
	Vapour fraction = 0.732
HEX-2	Type = counter-current
	Hot stream outlet temperature = -190.3 °C
HEX-3	Type = counter-current
	Hot stream outlet temperature = -180.7 °C
HEX-4	Type = counter-current
	Hot stream outlet temperature = -174.6 °C
HEX-5	Type = counter-current
	Hot stream outlet temperature = -179.3 °C
Flash	Pressure = 1.35 bar
	Vapour fraction = 0.732

5.2.2. Ammonia synthesis

The ammonia synthesis loop in Figure 5-3 has been modelled with conditions of Tripodi et al. [201]. High purity N_2 and high purity H_2 are compressed in a multi compressor system. H_2 comes from the PEM electrolyser at 35 bar and it is further compressed in COMP-1 to 100 bar before being mixed with the N_2, which is compressed from 1 to 100 bar in an intercooling compression system (ICS). The compressors and turbines units have been defined at 95% mechanical efficiency as stated in [202].

The pressurised gases are mixed and heated up to 430 °C passing through HEX-3 to be fed into the first bed reactor (R1) in a molar ratio H_2/N_2 of 3. The reaction section consists of a series if three Rplug flow reactors (R1-R3). Each reactor has been modelled as a bed packed reactor utilizing a Fe-based catalyst which is commonly used to accelerate and promote the exothermic reaction [203–205]. A single pass yield between 10 to 30 vol% NH_3 has been reported [201,206] and due to this low conversion, three reactors in series have been considered and modelled with intercooling with the purpose of increasing the loop efficiency and then the ammonia conversion[205,207].

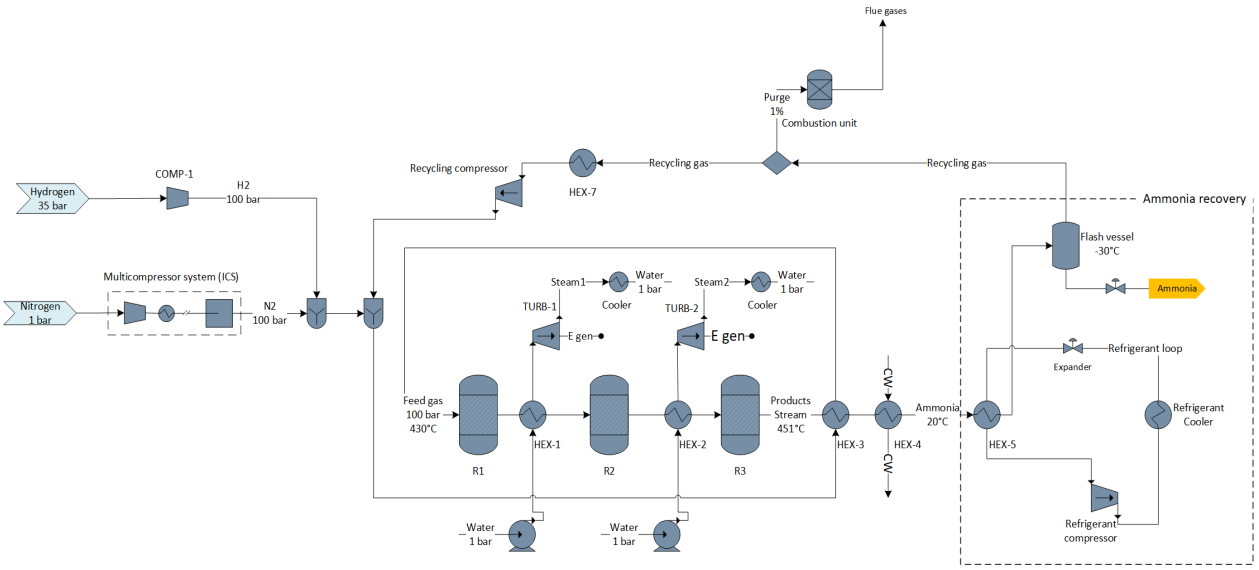

Figure 5-3. Schematic of the H-B synthesis loop and recovery in the PtA process

The synthesis uses the kinetic factors and driving force coefficients needed in a typical Langmuir Hinshelwood Hougen Watson (LHHW) model, which are listed in Table 5-2. It is important to mention that each reactor was defined with the same conditions for consistency as indicated in Tripodi et al. [201]

Table 5-2. Kinetic parameters for the ammonia reaction.

Rate expression	N_2	H_2	NH_3
Stoichiometry	-0.5	-1.5	1
Kinetic constant			
Ea (kcal/mol)	45		
k_0 (kmol/s· kg_{cat})	7.47×10^{8}		
Exponents	N_2	H_2	NH_3
Forward term	1	2.25	-1.5
Reverse term	0	-0.75	0.5
Coefficients	*A*	*B*	*C*	*D*
Term 1	-7.8	9218	-5.42	7.8×10^{-4}
Term 2	2.88	0	0	0

The temperature of the system is increased to 529 °C at the outlet of R1, therefore, in order to keep the adiabatic condition of the system, an intercooler (HEX-1) is added between R1 and R2 to return the temperature at the initial condition (430 °C). This is also applied for the second reactor outlet (HEX -2) where the temperature was also increased. During the reactors intercooling, the heated gases were passed through the heat exchangers where pressurized water (PUMP-1 and PUMP-2) is converted into high-pressure steam. The steam is expanded by the action of the turbines TURB-1and TURB-2 followed by coolers until condensation at 1 bar. The electricity generated in the turbines is used in the compression system to minimize the external consumption.

The performance of the synthesis is affected by the pressure, temperature, composition, ammonia recycled and the amount of inert gases [206]. For that reason, the accumulation of inert gases is controlled by a withdrawal stream after the ammonia removal and before the fresh gas input. This purge fraction was set to 1% to avoid convergence issues in the software by setting a *Broyden* algorithm as suggested in Tripodi et al. [201]. The design specifications of the ammonia synthesis loop is listed in Table 5-3.

Table 5-3. Process design specifications of the ammonia synthesis and recovery.

Equipment	*Design parameters*	*Source*
H_2 compressor	P = 100 bar Isentropic 85%, Mechanical 95%	Aspen model
N_2 compressors and intercooling	C1 Type = Isentropic P = 10 bar HEX1 = hot temperature outlet, 90 °C C2 Type = Isentropic P = 30 bar HEX1 = hot temperature outlet, 90 °C C3 Type = Isentropic P = 100 bar Outlet temperature = 264 °C	Aspen model
Recycling compressor	P = 100 bar	Aspen model
Pumps	Pump1 = 39 bar Pump2 = 39 bar	Aspen model
Reactors R1-R3	Type = Rplug Adiabatic reactor Bed voidage = 0.46 Particle density = 2850 kg/m^3	[201]
Turbines	Turb-1 Type = Isentropic P = 1 bar Turb-2 Type = Isentropic P = 1 bar	Aspen model
Refrigerant compressor	Type = Isentropic P = 10 bar	Aspen model
Refrigerant expander	P = 1 bar	Aspen model
HEX-1	Type = counter-current Hot stream outlet temperature = 430 °C	Aspen model
HEX-2	Type = counter-current Hot stream outlet temperature = 430 °C	Aspen model
HEX-3	Type = counter-current Cold stream outlet temperature = 430 °C	Aspen model
HEX-4	Type = counter-current Hot stream outlet temperature = 20 °C	Aspen model
HEX-5	Type = counter-current Hot stream outlet temperature = - 30 °C	Aspen model
HEX-6 (refrigerant cooler)	Type = counter-current Hot stream outlet vapour fraction = 0	Aspen model
HEX-7	Type = counter-current Hot stream outlet temperature = -15 °C	Aspen model
Flash	Pressure = 100 bar Temperature = -30 °C	Aspen model
Combustion unit	RGibbs P = 1 bar T = 1000 °C	Aspen model
Gas turbine	Type = Isentropic P = 1 bar	Aspen model

5.2.3. Ammonia recovery

After the reaction, the ammonia and unreacted gases were cooled down to 45 °C in a heat exchanger (HEX-3) which provides the heat to the feed stream. After that, the products stream is cooled further to 20 °C using cooling water (HEX-4). This approach aims to reduce the amount of refrigerant that is required in the next step of the ammonia condensation [127]. In the condensation system, ammonia and the gases pass through a heat exchanger (HEX-5) where the temperature decreases to –30 °C by using commercial refrigerant. The refrigerant is compressed and cooled until condensation for its recovering. The ammonia is recovered as a liquid in a flash vessel followed by an expander. Because of the low single pass conversion, the flashed gases are recycled to the system for a new reaction pass while the purge is sent to a combustion unit for power generation before being released. An Organic Rankine Cycle (ORC) uses the cooling water from the system to produce power since the system needs more cooling rather than heating. Using the ORC and steam turbines in the HB synthesis loop, the process is fully integrated. Furthermore, a combustor unit uses the purge gasses, which contains hydrogen, to produce high-pressure steam that powers a second steam turbine. The specifications of the ammonia synthesis and recovery are listed in Table 5-3.

5.3. Technical key indicators

The PtA performance is evaluated using several key parameters, which include ammonia energy efficiency, hydrogen conversion, and specific energy consumption (SEC). Energy efficiency measures the proportion of input energy that is effectively utilized in the process, providing insight into the overall effectiveness and sustainability of the plant operations. Hydrogen conversion assesses the extent to which hydrogen is transformed into the desired ammonia product, offering a clear indication of the process chemical efficiency. Specific energy consumption evaluates the amount of energy required to produce a specific quantity of product, helping as a critical metric for determining the process cost-effectiveness and environmental impact. These parameters collectively provide a comprehensive understanding of the PtA operational performance and its potential for scalability and integration into broader industrial applications.

5.3.1. Energy efficiency

The ammonia energy efficiency has been estimated according to the equation 5-1 that indicates the ratio of the total energy output from the ammonia product calculated with the lower heating value (LHV) and the total energy input [125]:

$$\eta = \frac{\dot{m}_{NH3} \cdot LHV_{NH3}}{\dot{W}_{PEM} + \dot{W}_{H-B}} x100\% \qquad 5\text{-}1$$

Where $\dot{m}_{NH3}$ is the output of ammonia in kg/h, $\dot{W}_{PEM}$ is the electricity consumption in the H_2 production by the PEM electrolyser and $\dot{W}_{H-B}$ is the additional energy consumption by the Haber-Bosch synthesis loop.

5.3.2. H_2 conversion efficiency

This indicates the H_2 is transformed into the final ammonia product at reactor (R) in equation 5-2 or whole process (P), equation 5-3.

$$\eta_{H2-R} = \frac{H_{2-in} - H_{2-out}}{H_{2in}} x100\% \qquad 5\text{-}2$$

$$\eta_{H2-P} = \frac{H_{2-in} - H_{2-out}}{H_{2-in}} x100\% \qquad 5\text{-}3$$

Where $H_{2\text{-}in}$ indicates the moles of H_2 that is fed to the reactor or in the system and $H_{2\text{-}out}$ denotes the moles of the gas that leaves the reactor (R) or the whole process (P).

5.3.3. Specific energy consumption (SEC)

As presented in the previous chapter, the SEC represents the energy required, in the form of heat or electricity, to produce a unit mass of the final product. In the context of the PtA process, the overall energy demand is primarily driven by the power consumption in the PEM electrolyser for hydrogen production and in the Haber-Bosch (H-B) synthesis loop for ammonia production and recovery. Due to the unique energy requirements of these processes, the SEC formula presented in the previous chapter (equation 4-7) has been slightly adjusted to better reflect the specific energy inputs and outputs in the PtA system, as described in equation 5-4.

$$SEC = \frac{Power\ consumption\ (PEM + HB)\ [MW]}{Mass\ flowrate\ of\ ammonia\ \left[\frac{tonne}{s}\right]} \qquad 5\text{-}4$$

5.3.4. Economic analysis

The economic evaluation of the PtA plant utilizes a standard discounted cash flow analysis to determine the levelized cost of ammonia (LCOA), expressed in £/tonne NH_3. The LCOA, as outlined in equation 5-5, represents the total investment necessary to produce one tonne of ammonia. [40,43,45].

$$LCOA = \frac{TCI + \sum_{n=1}^{20} \frac{COM}{(1+i)^n}}{\sum_{n=1}^{20} \frac{Pt}{(1+i)^n}} \qquad 5\text{-}5$$

Where *TCI* is the total capital investment of the plant, *COM* indicates the operation and maintenance cost computed at every year *n* and *Pt* is the total annual production of ammonia in tonne/year [119,202].

The plant, similar to the previous scenario, is located in the United Kingdom, with 2022 serving as the baseline year. The project is planned to have a lifespan of 20 years, operating for 8,000 hours annually. A discount rate of 10% has been applied, consistent with various references [207–209]. The primary economic assumptions are detailed in Table 5-4

Table 5-4. Main assumptions for the economic evaluation [210]

Parameter	*Units*	*Value*
Plant location	-	United Kingdom
Base year	-	2022
Annual production	ktonne/y	408
Lifetime of the project	years	20
Discount rate	%	10
Depreciation method	-	straight line
Operating hours	h/y	8,000

The PtA capital expenditures are determined by calculating the purchased equipment cost (PEC), as outlined in Section 4.3.2. The cost of the synthesis reactors has been estimated using the Aspen Process Economic Analyser, while the costs for other equipment have been sourced from relevant literature. These costs have been adjusted to reflect the current scale and year using the scaling factor method.

Table 5-5 presents the primary equipment costs associated with the PtA plant. Costs reported in different years have been adjusted to reflect the year of study (2022) using the respective CEPCI. Additionally, the currency has been adjusted to align with the exchange rate of the reference year before updating to the study year. The capacities, sizes, and flow rates of each piece of equipment have been derived from simulations conducted in Aspen Plus.

Table 5-5. PtA equipment cost data

Unit	Reference unit	Ref. cost (Euro)	Ref. size	sf	Source
Electrolyser	kW	1500	1	0.9	[211]
ASU	tonne O_2/day	48,000,000	1000	0.9	[212]
H-B reactor 1	-	1,359,200*	-	-	Aspen economic analyser
H-B reactor 2	-	1,358,400*	-	-	Aspen economic analyser
H-B reactor 3	-	668,900*	-	-	Aspen economic analyser
Heat exchangers	m^2	450,000	1000	0.7	[213]
Compressors	kWh	580,000	1070	0.67	[179]
Pumps	m^3/s	1,000,000	10	0.36	[178]
Turbines	MW	4,440,000	4	0.8	[178]
Evaporator	m^2	450,000	1000	0.7	[213]
Condenser	m^2	450,000	1000	0.7	[213]
Furnace	MWth	1,000,000	6.88	0.7	[178]

*Cost of reactors in USD

The operational expenditures (OPEX) have been estimated as the summation of the fixed and variable cost. Fixed operating costs, supervision, maintenance, insurance, general plant overhead are computed using default factors as specific percentages of the PEC presented in section 4.3.2. The labour cost is estimated using the equation 3-5.

The variable costs are determined based on the market prices of the main product (ammonia), commercial catalyst, oxygen (as by-product) and electricity cost (offshore wind). It is assumed that the catalyst is replaced every ten years as recommended in reference [214]. The levelized cost of electricity (LCOE) has been calculated using SAM software as described in Section 3.2. Table 5-6 shows the variable cost of the main inputs in the PtA plant.

Table 5-6. Variable cost of the main inputs in the PtA plant.

Variable costs	*Unit*	*Value*	*Reference*
Catalyst price	£/kg	23	[31]
Electricity wind	£/kWh	0.048	SAM software
Electricity grid*	£/kwh	0.018	[184]
Wastewater treatment	£/tonne	0.42	[161]
Cooling water	£/tonne	0.03	[161]
Oxygen price	£/tonne	0.04	[36]
Process water	£/tonne	0.37	[31]

*Only the cost for the use of the network is computed

5.3.5. Sensitivity analysis

Additionally, a comprehensive sensitivity analysis is carried out to assess the impact of key economic parameters on the LCOA. This analysis provides insights into how variations in critical factors can influence the overall economic feasibility of the PtA process. Specifically, the analysis involves adjusting

electrolyser efficiency by ±15%, as well as applying a ±25% change to several crucial variables, including the LCOE, the CAPEX associated with the PEM electrolyser, the discount rate, the CAPEX of the Haber-Bosch process, and the price of oxygen. By systematically varying these parameters, the analysis identifies the extent to which each factor affects the LCOA, helping to identify the most significant cost drivers and areas where improvements could lead to greater economic viability.

5.4. Life cycle assessment

In this section, as for the previous chapter, the framework of the life cycle assessment is presented. Goal and scope, System boundaries, functional unit, data collection and impact categories are listed.

5.4.1. Goal and scope

The goal of the current LCA is to quantify the environmental impacts of the ammonia production using power-to-ammonia approach. The function unit is 1 tonne of ammonia in a *cradle to gate system boundary* (Figure 5-4) covering all stages from raw material extraction to the ammonia production at the factory gate *and* hence the storage, distribution, use and final disposal are not taken into account. This approach is adopted, as products properties, utilisation and disposal are identical for the PtA and fossil-based ammonia [28,121]. To manage the multifunctionality in the PEM electrolyser and in the ASU, the same considerations as in Chapter IV has been applied to the oxygen (by-product). Therefore, the exergy allocation has been applied to the electrolyser while a mass allocation has been considered the most appropriate method in the ASU between the nitrogen and oxygen [126]. The resulting allocated emissions to H_2 and N_2 have been included in the process impacts of the ammonia product.

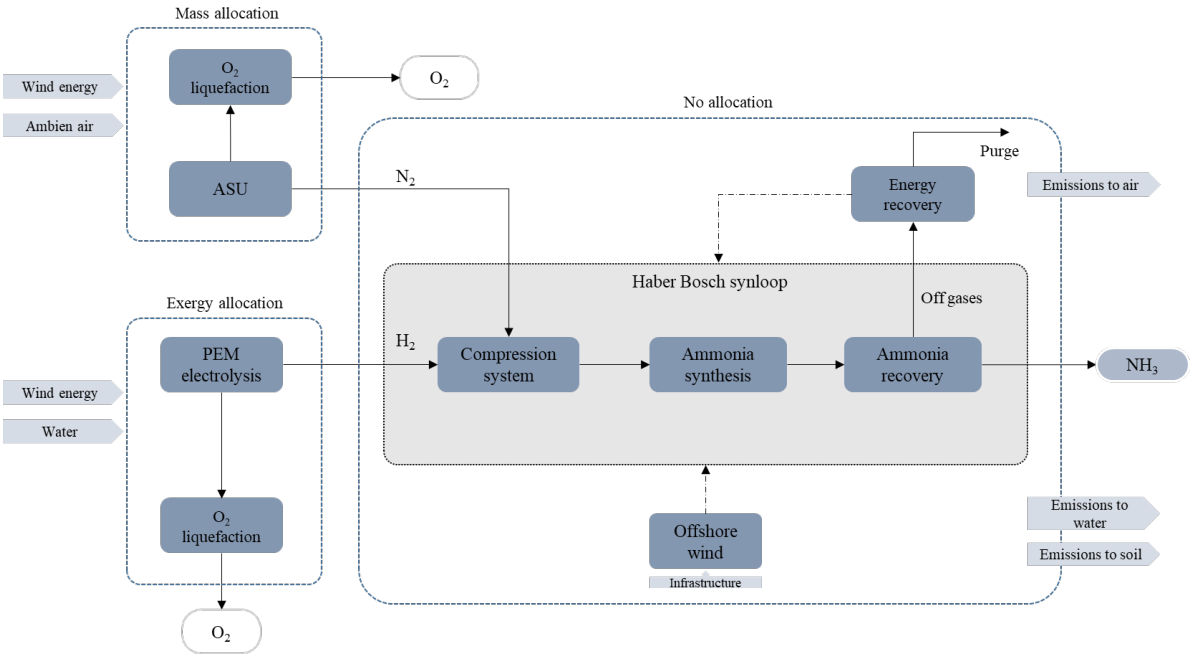

Figure 5-4. System boundaries of the power-to-ammonia plant.

5.4.2. Life cycle inventory

Data collection for the study involves quantifying the quantities of raw materials, such as water and ambient air, and tracking energy consumption, including the offshore wind energy used in the PEM electrolyser, Air Separation Unit (ASU), and Haber-Bosch (H-B) synthesis loop. Additionally, process emissions are measured for the entire system, considering emissions to air, water, and soil. The plant infrastructure has not been included in the analysis due to its minimal contribution to the overall environmental footprint. The inputs and outputs of the PtA plant are accounted for using the mass and energy values derived from Aspen Plus simulation results. Emissions to the air from the Haber-Bosch synthesis loop include minor ammonia releases during processing, which occur due to its high volatility [124].

5.4.3. Impact assessment

The model was developed in SimaPro v9.4.0.2, utilizing the CML 2001 impact assessment method. The impact categories include global warming potential (GWP), abiotic depletion potential (ADP), eutrophication potential (EP), photochemical oxidation potential (POP) and ozone layer depletion (ODP) as well as the water consumption (WC) reported per functional unit.

5.4.4. Interpretation

The environmental performance of the Power-to-Ammonia process, including GWP and water consumption, has been analysed in detail and benchmarked against the conventional ammonia production process in order to highlight the significant environmental benefits of the PtA. For this comparison, data for the traditional ammonia production method was sourced from the *Ecoinvent v3.6* database, specifically using the module titled "Ammonia, anhydrous, liquid {RER w/o RU}| ammonia production, steam reforming, liquid | Cut-off, U." This module represents a standard industrial process for ammonia synthesis, primarily based on steam reforming of natural gas, which is widely used in conventional practices.

Moreover, a sensitivity analysis has been conducted to examine the impact of electricity carbon intensity on the global warming potential of the process. This analysis is crucial due to the process heavy reliance on electricity consumption, making the carbon intensity of the electricity source a significant factor in determining the overall environmental footprint.

5.5. Results and discussion

In this section, the main results of the PtA scenario are discussed. Process modelling results including mass and energy balances are reported. The economic and environmental indicators are discussed in detail and compared to conventional production system.

5.5.1. Process modelling results

The main mass balances of the PtA process are listed in Table 5-7. The designed plant has a production rate of 408 ktonne/y of liquid ammonia at 99.4% purity. Overall, 467 ktonne/y of atmospheric air (for nitrogen production at 352.3 ktonne/y) and 708 ktonne/y of deionised water (for hydrogen production at 75.3 ktonne/y) are required for this ammonia production scale. The PtA process exhibits a low per-pass conversion in the ammonia synthesis stage (11.7%), primarily due to the inherent limitations of the Haber-Bosch (H-B) process such as thermodynamics, operating conditions, kinetics and economic considerations. Therefore, the recycling loop of unreacted gases is essential for improving overall conversion efficiency over multiple passes. Overall, almost all the H_2 supplied was converted to ammonia products, resulting in a high process hydrogen-to-ammonia conversion efficiency of 96%. The remaining 4% was sent to the combustion unit for energy recovery.

Table 5-7. Main mass balances of the PtA plant by stage.

	ASU		*Electrolysis*		*H-B synthesis*	
Parameter	*Input*	*Output*	*Input*	*Output*	*Input*	*Output*
			Mass flowrate ktonne/y			
Ambient air	467	0	0	0	0	0
Nitrogen	0	352.3	0	0	352.3	117.1[c]
Oxygen	0	105.8		703.8	0	6.72[cd]
Water	0	0	708.7	34.9	0	28.2[cd]
Hydrogen	0	0	0	75.3	75.3	2.90[e]
Ammonia	0	0	0	0	0	408

[a]Nitrogen stream/oxygen stream
[b]Oxygen coming from the ASU to be liquefied
[c]In the purge gas stream
[d]Formed by the combustion of purge gases
[e]H_2 in the purge that is further burnt in combustion unit

The overall NH_3 energy conversion efficiency on a low heating value basis was 49.43%. This means that 49% of the energy supplied to the process (in the form of electricity, heat, or other energy sources) is successfully utilized to produce ammonia. The remaining 52% of the energy is lost in various forms, such as waste heat or inefficiencies in the PEM, compressors, etc. Other studies have reported ammonia energy efficiencies between 50 – 83% using the PtA approach [215–217], while the conventional SMR-based ammonia reports an efficiency of 78% [202]. The low energy conversion efficiency obtained in this study is mostly attributed to the inefficiencies of the PEM electrolyser. A more efficient hydrogen production, e.g. solid oxide electrolyser (SOE), can lead to energy conversion up to 72% [115] compared to 40%-50% of the PEM, but the SOE come with higher costs. On the other hand, significant improvements in the energy efficiency of electrolysis are thermodynamically limited. Any further enhancements would require breakthroughs in materials science or new technologies that could reduce energy losses at a fundamental level. Despite ongoing research into advanced catalysts and novel electrolyser designs, achieving substantial gains in efficiency remains challenging due to these inherent limitations. As a result, efforts to improve the overall energy efficiency of ammonia production must also focus on optimizing other parts of the process, such as heat integration and system-wide energy management.

The energy breakdown in the PtA is provided in Figure 5-5. The overall energy consumption of the plant has been estimated at around 505 MWe. The electrolyser unit consumes 92.7% of the total energy followed by the refrigerant compressor in the ammonia condensation and the feed compressors which accounted for 3.2% and 3.0%, respectively. The ASU, O_2 liquefaction system along with pumps and recycling compressor denote a small contribution with a total of 1.1%.

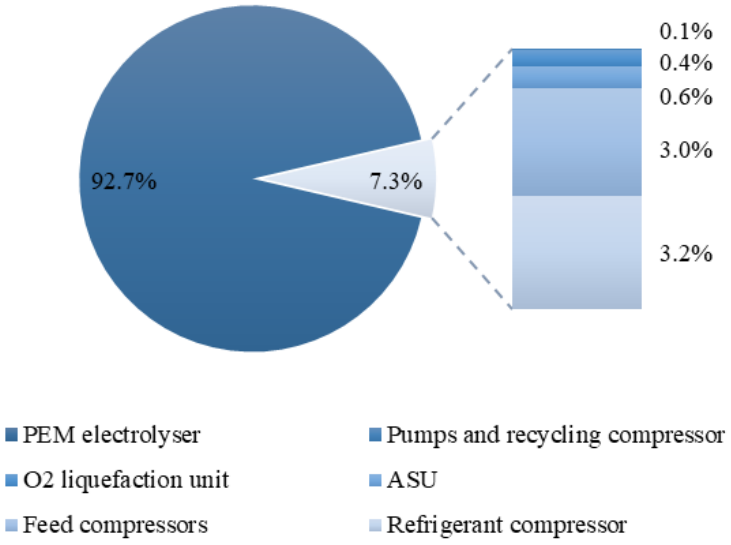

Figure 5-5. Energy consumption breakdown of the PtA

The total SEC of the PtA process is provided in Table 5-8. The electrolyser is responsible for 93.2% of the total energy consumption in the PtA, accounting for 10.11 MWh/tonne NH_3 while the air separation unit consumes 0.068 MWh/tonne NH_3 (78.7 kWh/tonne N_2) which is 0.6% of the total. Finally, the H-B synthesis loop utilises 0.673 MWh per tonne, making up 6.2% of overall energy consumption.

Table 5-8. Specific energy consumption of the PtA.

Stage	*Value (MWh/tonne NH_3)*	*%*
PEM electrolyser	10.11	93.2%
ASU	0.068	0.6%
HB process	0.673	6.2%
SEC (w/o integration)	10.85	-
Energy recovery	0.307	-
SEC (incl. energy integration)	10.54	-

The total specific energy consumption before any energy recovery or integration measures stands at 10.85 MWh per tonne of ammonia. The total energy recovered by the ORC and the steam turbines in the H-B synthesis loop was around 0.307 MWh/tonne NH_3. After accounting for this energy integration and recovery, the final specific energy consumption of the process is reduced to 10.54 MWh per tonne of ammonia (2.8% reduction). This value is higher compared with conventional process that reports a net energy intensity of 7.5 MWh/tonne NH_3 [218]. These results illustrate the critical role of energy recovery and integration in reducing the overall energy consumption of the PtA process.

5.5.2. Economic results

In this section, the results of the PtA economic analysis is presented. The breakdown of the CAPEX is displayed in Figure 5-6. The H_2 production accounts for about 54% of the total equipment cost with £130.8M. This PEM cost dominance suggests that advancements in electrolyser technology, cost reductions, and efficiency improvements could significantly impact the overall feasibility and competitiveness of PtA processes. The second-largest contributor is the H-B synthesis loop which accounts for 25% of the equipment cost and it is made up of the turbines, compressors, heat exchangers, and refrigerant cycle and reactors. The ORC contributed 13% to the total CAPEX, due to the costs of the turbine and condenser units. Finally, the ASU is responsible for 7% of total CAPEX. The cost of this section was considered as a single unit; therefore, no breakdown of the system is available. However, the most expensive equipment includes the air compressors, low- and high-pressure columns and heat exchangers. Its relative smaller cost share suggest that it is not capital intensive as the electrolyser and H-B synthesis stages.

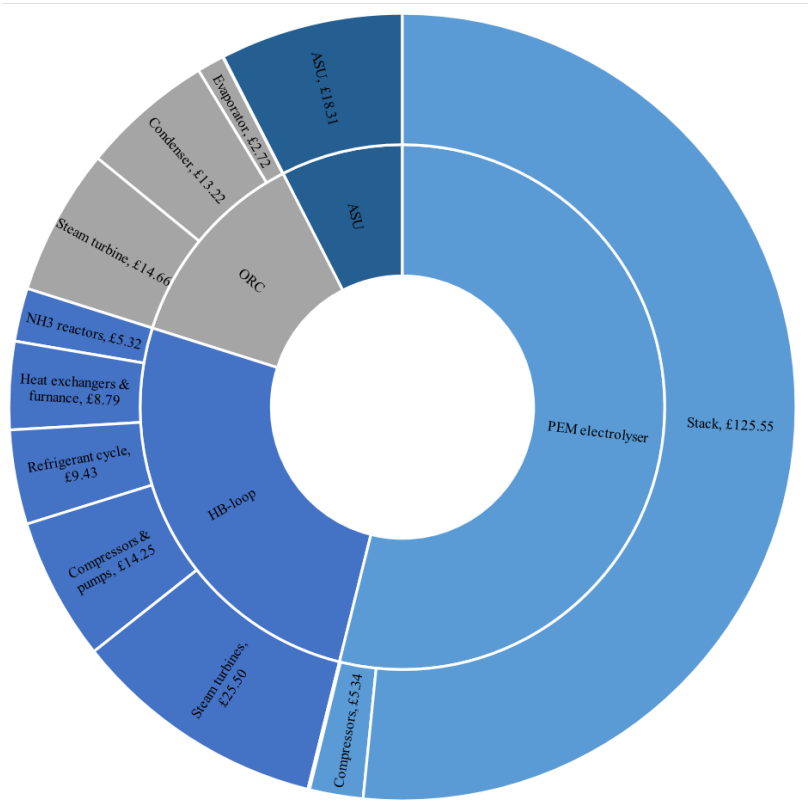

Figure 5-6. The equipment cost breakdown by process area. Costs are reported in millions GBP.

This cost breakdown provides valuable insights for future research and development in the PtA sector. Reducing the cost and improving the efficiency of electrolyser is of prime importance. In addition, despite

large cost of the steam turbines in the H-B loop, their inclusion underlines the importance of improving the energy efficiency which can lead to reducing operating costs and the sustainability of the process.

The OPEX for the PtA plant are estimated at £238 Million GBP. The majority of these costs, approximately 92%, are attributed to the hydrogen production. This significant share underscores the energy intensive nature of hydrogen production through PEM electrolyser where the electricity is the most critical cost driver in the PtA process. The remaining 8% of the OPEX is distributed across various operational costs such as the maintenance labour, maintenance materials, insurance taxes, raw materials, finance working capital, labour, general and indirect overheads, supervision and catalyst costs. The high percentage of OPEX attributed to electricity consumption is a critical factor when considering the levelized cost of ammonia (LCOA). The LCOA reflects the average cost per unit of ammonia produced over its lifetime, considering capital costs, operational costs, and expected production volume. Given that electricity constitutes the majority of OPEX, fluctuations in energy prices can significantly influence the LCOA, making energy efficiency and cost management essential for the plant's economic viability.

The LCOA calculated in this study is approximately £687/tonne NH_3; this result is aligned with the range reported in other studies [120,209,216,219], where the cost of producing ammonia using renewable energy sources varies between £400 and £1200/tonne NH_3. The variability of results recognizes the significant influence of different process parameters and regional factors on the overall cost.

Figure 5-7 details the breakdown of the components contributing to the LCOA. The analysis reveals that the cost of electricity used in hydrogen production is the most significant factor, accounting for £514 per tonne of ammonia. This dominance of electricity cost points out the heavy reliance of the PtA process on renewable energy, particularly in the electrolytic production of hydrogen via PEM electrolyser. The capital investment is the next largest contributor, adding £101 per tonne of ammonia to the total cost. This includes expenses related to the construction, installation, and commissioning of the necessary infrastructure, such as the electrolyser, air separation unit (ASU), and the Haber-Bosch (H-B) synthesis loop.

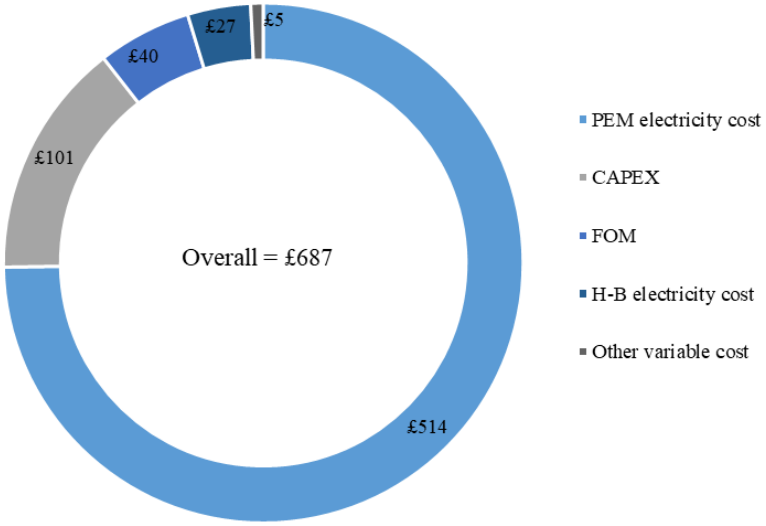

Figure 5-7. Levelized cost breakdown of ammonia.

The findings clearly indicate that operational costs, particularly electricity, are the primary drivers of the overall LCOA. Consequently, the price of electricity has a critical impact on the economic feasibility of the PtA process. Given that electricity costs dominate the LCOA, any fluctuations in electricity prices directly affect the cost of ammonia production.

The estimated LCOA of £687 per tonne for PtA-produced ammonia is substantially higher than the average market price of conventional ammonia, which stands at approximately in a range from US$200 to 600 per tonne (£170 - £500 per tonne) [218,220]. Achieving cost parity with conventional ammonia production methods requires a significant reduction in electricity prices. One of the most effective options to reduce the LCOA would be through government subsidies or incentives that lower the cost of renewable electricity. This could involve direct subsidies for green electricity generation or the introduction of carbon pricing that would make fossil-based ammonia more expensive relative to green alternatives.

5.5.3. LCOA Sensitivity analysis

A sensitivity analysis was conducted to evaluate the impact of key parameters on the LCOA and the results are summarized in Figure 5-8. This analysis is crucial for understanding how different factors influence the economic viability of the PtA and identifying areas where improvements could make the process more cost competitive.

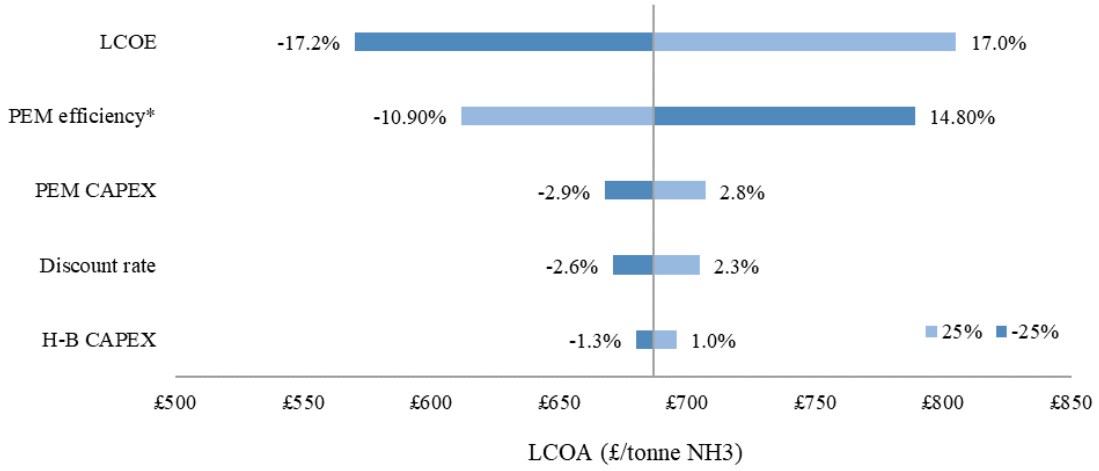

*Figure 5-8. Economic sensitivity analysis of the LCOA (*PEM efficiency has been evaluated at ±15% change).*

The LCOE is the most influential factor in sensitivity analysis. A 25% increase in the LCOE leads to a 17.2% rise in the LCOA, pushing it from £687 to £805 per tonne of ammonia. This significant increase underscores the critical role of electricity costs in determining the overall economic feasibility of the PtA process as mentioned previously. Conversely, a 25% reduction in the LCOE results in a 17.0% decrease in the LCOA, lowering it to £570 per tonne.

The efficiency of the PEM electrolyser also plays a significant role in the LCOA. A 15% increase in PEM efficiency results in a 10.9% reduction in the ammonia cost, bringing it down to £612 per tonne. On the other hand, a 15% decrease in PEM efficiency causes a 14.8% increase in the LCOA, raising it above the nominal value. Although the efficiency of PEM electrolysis is thermodynamically constrained, ongoing technological advancements could enhance this efficiency, thereby lowering production costs and improving the overall economic viability of the PtA process.

Other parameters, such as the capital expenditures (CAPEX) associated with the PEM electrolyser and the Haber-Bosch (H-B) process, as well as the discount rate, were found to have a relatively minor impact on the LCOA. Changes in these parameters resulted in variations of less than ±3% from the nominal LCOA value, indicating that they are less critical compared to the LCOE and PEM efficiency. The price of oxygen, a by-product of the electrolysis process, was also considered in the sensitivity analysis. However, its variation had a negligible impact on the LCOA compared to the other factors examined. As a result, the impact of oxygen pricing was not noticeable emphasized in Figure 5.8. This indicates that fluctuations in the O_2 market price are unlikely to significantly affect the overall economics of the PtA process.

The sensitivity analysis evidences the critical importance of low-cost renewable electricity and high PEM efficiency in making the PtA process economically viable. While other factors such as CAPEX and

discount rate have a lesser impact, optimizing electricity costs and improving PEM efficiency are key strategies for reducing the LCOA and enhancing the competitiveness of green ammonia against conventional fossil-fuel-based production methods. Moreover, the LCOE is the most significant factor influencing the economic viability of the PtA process. Given its crucial role, a more detailed analysis of the LCOE is included to understand its impact on the Levelized Cost of Ammonia (LCOA).

Figure 5-9 illustrates how the LCOA varies as a function of the LCOE, with the electricity cost range set between £20 and £100 per MWh, based on values reported in the literature [36,118]. The current study employs a LCOE of £66.6/MWh, which is derived from a wind farm model developed using the SAM (System Advisor Model) software for an offshore wind farm in the Teesside region. This LCOE includes the cost associated with using the grid network when intermittency.

At this current electricity cost, the LCOA aligns with the costs seen in other green ammonia projects (see Figure 5-9) [36,115,125,209,216]. To make green ammonia more competitive with fossil-based production, the LCOE must decrease significantly. The analysis shows that a LCOE within the range of £20 to £47 per MWh is necessary to achieve a competitive LCOA between £235 and £498. For example, a 50% reduction in the LCOE from £66.6/MWh to £33/MWh results in a LCOA of approximately £361 per tonne which represents a reduction of 49% from the current cost. This lower ammonia cost would make renewable ammonia much more competitive in the market.

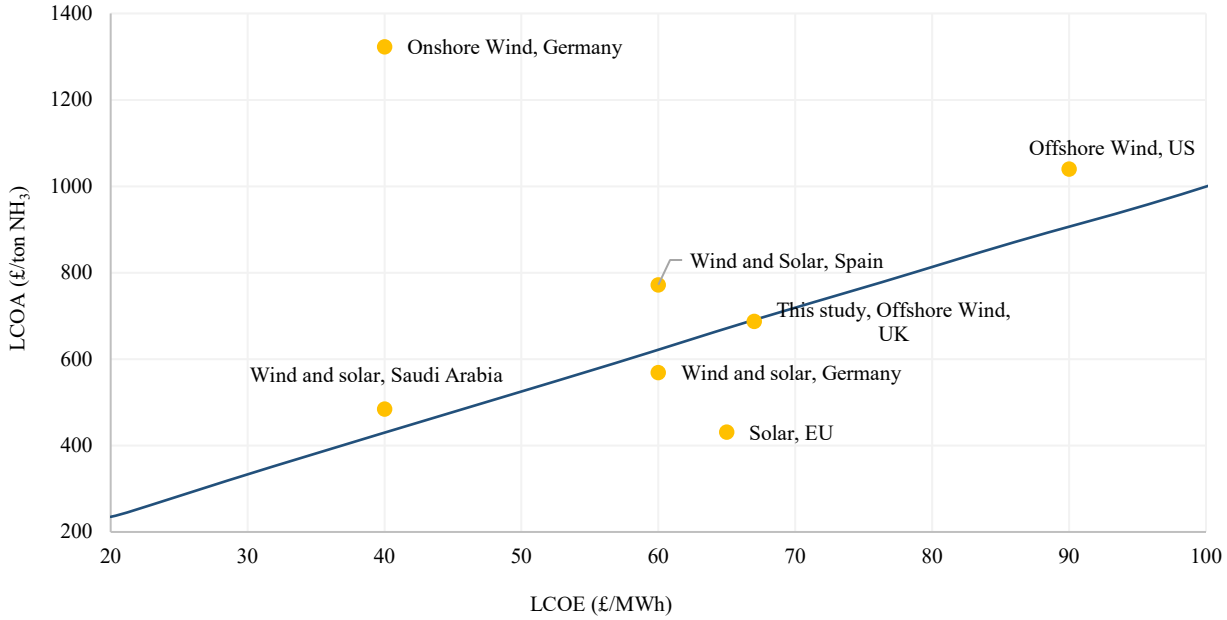

Figure 5-9. The LCOA sensitivity to the LCOE. Results from previous studies are presented for the sake of comparison.

Achieving such low electricity costs, however, is challenging and would likely require substantial subsidies, particularly in regions with abundant renewable energy resources. High-efficiency renewable technologies, such as a combination of solar, nuclear, and wind energy, are commonly suggested as viable options to achieve these lower costs. These technologies could play a fundamental role in lowering the LCOE and, consequently, the LCOA, making green ammonia a more economically feasible alternative to its fossil-based counterpart. Conversely, if the LCOE were to increase to £95/MWh, the LCOA of the PtA process would rise significantly by 39% from the current cost, reaching £958 per tonne of ammonia. This scenario underlines the sensitivity of the ammonia cost to electricity prices and the critical need for affordable renewable energy sources.

To bring the cost of renewable ammonia to a more competitive levels, significant reductions in electricity costs are necessary. This could be achieved through technological advancements, efficient integration of renewable energy sources, and supportive policy measures, such as subsidies, to reduce the financial burden of electricity production.

5.5.4. Environmental impact assessment

In this study, a cradle to gate life cycle assessment of PtA process has been conducted to evaluate its environmental impact. The Life cycle inventory of the system, which details the inputs and outputs associated with each stage of the process, is provided in Table 5-9. Data have been retrieved from aspen simulation results which provide detailed insights into mass and energy usage. Additionally, relevant literature has been consulted to ensure all emissions are considered.

Table 5-9. Main inputs and outputs of the PtA process per 1 tonne NH_3.

Stage	*Input/Output*	*Value*	*Unit*	*Reference*
PEM electrolyser	Water	1.85	tonne	Aspen Plus
	Electricity	10.05	MWh	Aspen Plus
	Hydrogen	0.18	tonne	Aspen Plus
	Oxygen	1.46	tonne	Aspen Plus
Air separation unit	Air	1.14	tonne	Aspen Plus
	Electricity	0.068	MWh	Aspen Plus
	Nitrogen	0.87	tonne	Aspen Plus
	Oxygen	0.27	tonne	Aspen Plus
HB loop	Nitrogen	0.87	tonne	Aspen Plus
	Hydrogen	0.18	tonne	Aspen Plus
	Catalyst	0.20	tonne	[221]
	Electricity	0.36*	MWh	Aspen Plus
	Ammonia	1	tonne	Aspen Plus
	Purge gases	0.05	tonne	Aspen Plus
	NH_3 emissions	0.07	kg	[124]

*After energy integration

The Life Cycle Assessment results for the Power-to-Ammonia process, as illustrated in Figure 5-10, provide insights into the environmental impact of producing ammonia through renewable energy sources. The Global Warming Potential (GWP) for the PtA process is calculated to be 152.2 kg CO_{2e} per tonne of ammonia produced.

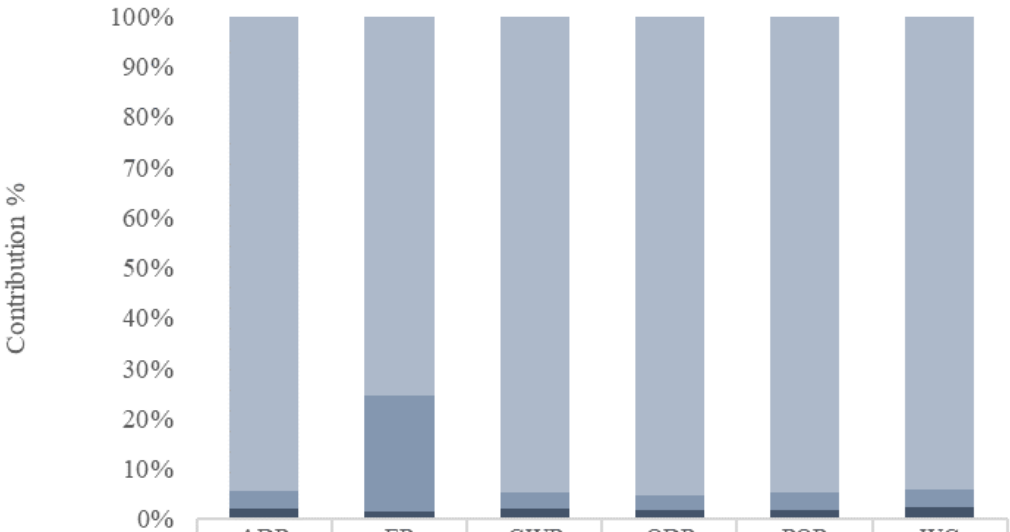

	ADP	EP	GWP	ODP	POP	WC
P2A - Electrolysis	0.95	0.084	143.96	7.5E-06	0.049	884.50
P2A - H-B process	0.03	0.025	5.19	2.5E-07	0.002	31.8
P2A - ASU	0.02	0.002	3.07	1.4E-07	0.001	23.9
Total	1.01	0.111	152.2	7.8E-06	0.052	940.3

Figure 5-10. Environmental impact results of the PtA process, breakdown by stage.

The electrolysis stage, which is critical for generating hydrogen from water using electricity, is identified as the most significant contributor to all environmental impacts. Particularly, in the GWP, it accounts for a 95% of the total emissions. This high percentage reflects the energy-intensive nature of water electrolysis and emphasises the challenge of decarbonizing hydrogen production, even when using renewable electricity sources. The carbon footprint of the electricity generation process, even when using renewables, includes upstream emissions associated with the manufacturing, installation, and maintenance of renewable energy infrastructure, such as wind turbines. In contrast, the other stages of the PtA process contribute minimally to the overall GWP. The Air Separation Unit responsible for providing the nitrogen needed for ammonia synthesis, contributes 1.6% to the total emissions. The Haber-Bosch synthesis process, where hydrogen and nitrogen are combined under high pressure and temperature to produce ammonia, accounts for 3.4% of the total emissions. These lower contributions are due to the relatively smaller energy requirements of these processes compared to electrolysis. The GWP result of this study is in good agreement with other relevant studies of renewable ammonia. For example, Chisalita et al. [28] calculated a GWP of

149 kg CO_{2e}/tonne NH_3 where the electrolyser contributes 94.4% and Boero et al. [124] reported a GWP of 240 kg CO_{2e}/tonne NH_3 for medium scale plants powered by wind in the UK. The dependence of the hydrogen production within the P2X projects in the environmental performance has been evidenced, efforts should be focused on the technology improvements and clean energy sources of the current systems in order to attain net zero emissions.

The PtA process requires a significant amount of water, with a consumption rate of 940 m^3 per tonne ammonia produced. This high-water usage is attributed to the electrolysis stage, where water is utilised as the feedstock, but additionally the production of 1 MWh of offshore wind electricity consumes around 70 m^3 of fresh water. The water consumption impact underlines the importance of considering water resource availability, especially in regions where water scarcity is a concern.

Additionally, the Global Warming Potential was computed for conventional fossil-based ammonia production in Europe and compared to PtA. The analysis evaluates the production of 1 tonne of anhydrous liquid ammonia using conventional steam methane reforming (SMR) available in the database of Ecoinvent 3.6. This process was assessed using the same environmental impact assessment method applied to the PtA process, allowing for a direct comparison of their environmental footprints in six different environmental indicators: Eutrophication Potential (EP), Global Warming Potential (GWP), Abiotic Depletion Potential (ADP), Photochemical Ozone Creation Potential (POP), Water Consumption (WC), and Ozone Depletion Potential (ODP).

In Figure 5-11, it has been demonstrated the environmental advantage of the PtA process over traditional fossil-based ammonia production across all assessed categories. The GWP of fossil-based ammonia is significantly higher than that of PtA (2444 vs 152 kg CO_{2e}/tonne NH_3). This comparison clearly proves the significant environmental advantage of green ammonia, as the PtA process can achieve a 94% reduction in total emissions. Thus, PtA can play a critical role in mitigating the environmental impacts of ammonia production and aligns with global efforts to transition toward more sustainable industrial practices. Other categories such as abiotic depletion and ozone depletion potential show similar reduction compared to fossil-based above 90%. Water consumption indicates a significant reduction by using PtA with around 54% less water consumption.

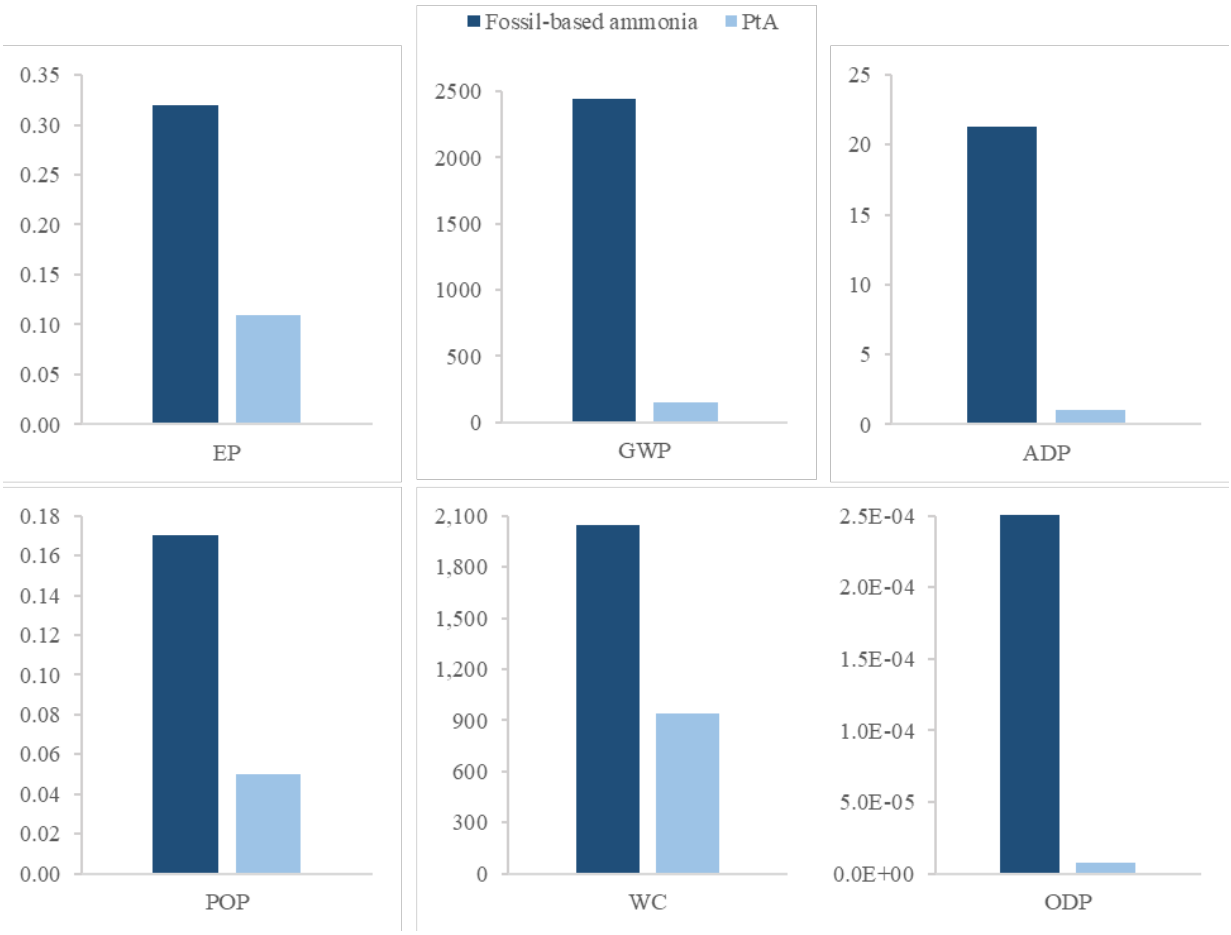

Figure 5-11. Environmental impact results comparison of the PtA process and fossil-based ammonia

The use of green ammonia can be considered as a mitigation potential strategy because of the great reduction potential not only in the GWP impact but in other the impact categories as presented before. Studies have assessed environmental emissions beyond GWP [29], nevertheless comparisons are not easy due to the variations on the methodology, assumptions and considerations adopted.

5.5.5. GWP sensitivity analysis

As seen before, the electricity consumption is a critical factor in determining the sustainability of PtA. Despite PtA being significantly lower in GWP compared to fossil-based ammonia production, the electricity consumption in the electrolysis process still contributes substantially to the overall emissions. This is because even renewable electricity generation can have upstream emissions, depending on the technology and lifecycle considered. Although some studies [125,208] attribute zero emissions to the renewable sources, there are inherent emissions involved in the offshore wind turbines including manufacturing materials, installation and maintenance and that are important in the carbon accounting [197]. The carbon intensity (CI) measures carbon emissions associated with the whole supply chain of

generating electricity. This parameter varies depending on the location, efficiencies and assumptions made. Ensuring access to low-carbon electricity is essential to maximizing the benefits of PtA and making it a solution for sustainable ammonia production.

Therefore, a GWP sensitivity analysis to the CI of the renewable electricity source has been evaluated in Figure 5-12. According to the literature, the CI of the offshore wind ranges from 5.3 – 24 g CO_{2e}/kWh [222]. The same range is applied here to evaluate the sensitivity of the GWP in the PtA process. The current CI of the offshore wind utilised in this study has been taken from the library of the SimaPro software for an offshore wind turbine in the UK (15.6 g CO_{2e}/kWh). Moreover, a comparison of different electricity sources with low carbon intensity is also depicted in Figure 5-12. The carbon intensities of each source are taken from the library of the SimaPro software for 1MWh of electricity in the UK, with the exception of solar and hydro based which are available for the rest of the world.

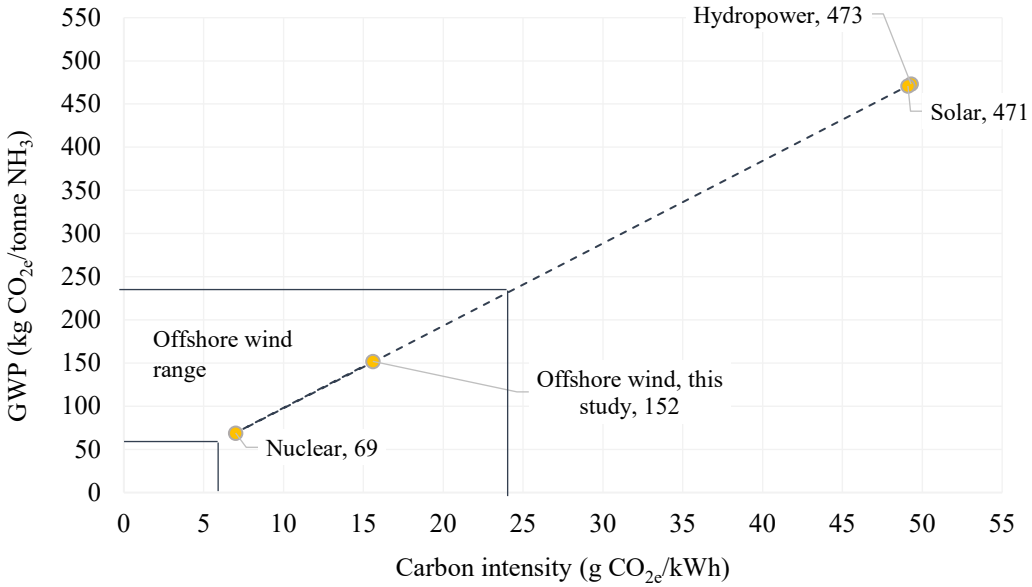

Figure 5-12. Global warming potential sensitivity to the electricity carbon intensity

The results evidenced that GWP varies linearly with the CI, for instance, at the lowest CI (5.3 g CO_{2e}/kWh), the GWP resulted in 52.9 kg CO_{2e}/tonne NH_3, which is 65% less than the baseline GWP. Alternatively, at the highest offshore wind carbon intensity (24 g CO_{2e}/kWh), the ammonia GWP increases by 53% to a value of 231 kg CO_{2e}/tonne NH_3. This exhibits the important of choosing electricity supply chains with low carbon impact to optimise the environmental impact of the PtA. Low CIs for offshore wind are associated with the economies of scale, since installations of offshore farms are larger than the onshore farms, the intensities tend to be underestimated as the information about the GHG emissions for the turbine

construction and material transportation are limited [222]. Hence, a more comprehensive analysis of the electricity supply chain is suggested.

The study also suggests that using nuclear energy instead of offshore wind could further reduce the GWP of PtA by 54%, showcasing the potential of nuclear power as a low-carbon alternative. However, not all renewable sources offer the same benefits. Hydropower, particularly when based on reservoir plants, can result in a higher GWP than offshore wind due to the environmental impacts associated with dam construction and land use changes. Similarly, solar power, while renewable, may also contribute to a higher GWP depending on the specifics of its distribution and lifecycle emissions.

While PtA offers significant potential for reducing the carbon footprint of ammonia production, its overall environmental performance is highly dependent on the carbon intensity of the electricity used. The study highlights the need for a strategic approach in choosing and optimizing the electricity supply chain to achieve the best environmental outcomes. This includes considering not just the type of renewable energy but also the full lifecycle emissions associated with each energy source.

5.6. Conclusions of PtA

The present study undertakes a comprehensive cradle-to-gate techno-economic analysis (TEA) and life cycle assessment (LCA) of a Power-to-Ammonia (PtA) system. This integrated analysis aims to identify the key factors influencing both the economic and environmental performance of the PtA process, providing a holistic understanding of its viability and sustainability. The study incorporates detailed process modelling, economic evaluation, and environmental impact assessment, focusing on a PtA system powered by an offshore wind farm. The system includes hydrogen production through Proton Exchange Membrane (PEM) electrolysis, nitrogen production via cryogenic air separation, and ammonia synthesis using the Haber-Bosch (H-B) process.

The process modelling results indicate an overall hydrogen conversion efficiency of 96%, implying that nearly all the hydrogen produced is effectively converted into ammonia. This high conversion spots PtA as a promising candidate for large-scale energy storage, particularly in scenarios involving renewable energy integration. However, the analysis reveals a significant Specific Energy Consumption (SEC) of the PtA process in approximately 18% higher than that of conventional Steam Methane Reforming (SMR). This increased energy demand is predominantly attributed to the electrolysis stage, which constitutes 95% of the total energy consumption. The system incorporates full heat integration, enabling the recovery of approximately 2.4% overall and 46% of the Haber-Bosch electricity demand.

The economic evaluation estimates a Levelized Cost of Ammonia (LCOA) at £687 per tonne, which exceeds the current market price of ammonia. Nevertheless, the analysis identifies potential for substantial cost reduction. Specifically, the LCOA could be reduced by 49% to £351 per tonne if the electricity cost decreases to £32 per MWh, compared to the current rate of £66 per MWh. Achieving such a low electricity cost would require specific conditions, including the development of advanced renewable energy infrastructure and the implementation of supportive government policies that incentivize low-cost power supply.

The life cycle assessment provides critical insights into the environmental performance of the PtA process. The cradle-to-gate LCA results demonstrate the potential of PtA to significantly reduce the Global Warming Potential (GWP) associated with ammonia production. When powered by offshore wind energy, the PtA process can achieve a 93% reduction in GWP compared to conventional fossil-based production methods. However, the study emphasizes the substantial influence of the carbon intensity (CI) of electricity on the GWP. For instance, utilizing a low-carbon intensity energy source such as nuclear power could further reduce ammonia emissions to as low as 69 kg CO_2e per tonne of ammonia. In contrast, using solar power, which has a higher carbon intensity relative to the current offshore wind power plants, could increase the GWP to 471 kg CO_2e per tonne of ammonia.

This chapter provides a thorough evaluation of the PtA process, generating critical insights into both its economic and environmental performance. While the PtA process exhibits considerable potential in terms of reducing greenhouse gas emissions and facilitating efficient energy storage, its economic viability is highly contingent on electricity costs. The results suggest that, with strategic investments in low-carbon energy infrastructure and the implementation of supportive policies, PtA could emerge as a key technology in the transition towards a sustainable, low-carbon economy.

Chapter VI

6. Techno-economic and Life Cycle Assessment of Power-to-Formic Acid production using Direct Air Capture and Green Hydrogen

The chemical industry is responsible for producing a wide array of valuable products. Defossilising the chemical industry is crucial for achieving climate change targets. Carbon capture and utilisation (CCU) has emerged as a promising alternative for chemicals production. Formic acid is increasingly important in the global economy as a versatile chemical used in agriculture, food preservation, and as a potential hydrogen storage.

To this direction, this study evaluates the environmental and economic performance of producing formic acid (FA) through a Power-to-Formic Acid (PtFA) process, focusing on the utilisation of green hydrogen and carbon dioxide captured from direct air capture (DAC). A cradle-to-gate life cycle assessment (LCA) was conducted, focusing on the climate change, fossil depletion and water consumption, using the ReCiPe Midpoint (H) while the minimum selling price (MSP) has been used as the main economic indicator.

The economic assessment identified the DAC and the electrolyser as the major contributors to CAPEX, while catalyst and electricity cost are the main OPEX contributors. The MSP of the PtFA resulted twice that of the conventional FA, at £1,290 per tonne compared to £560 (€650) per tonne. Additionally, LCA revealed that the PtFA process emits 92% less CO_2 than the conventional production process (0.173 vs. 2.19 tonnes CO_2eq./tonne FA), uses 94% less water, and consumes 92% fewer fossil resources. The primary drivers of carbon emissions are the chemicals consumed in FA synthesis, and electricity generation. This study is the first attempt to holistically assess from a technical, economic and environmental perspective of a PtFA process that contributes to the defossilisation efforts of the chemicals sector.

6.1. Introduction

Among the various chemicals that can be synthesized using captured CO_2, formic acid (FA) stands out as promising material due to its versatility and the broad range of industrial applications. FA is considered a good candidate for Power-to-X (PtX) processes aimed at decarbonisation, as it offers potential as both a renewable fuel and a feedstock for other high value chemicals [223]. As presented before, the chemical industry, is one of the major contributors to global CO_2 emissions. It accounts for a significant portion of the global greenhouse gas emissions, largely due to energy-intensive processes such as ammonia

production, petrochemical manufacturing, and cement production [47]. As such, finding sustainable pathways for chemical production is essential for reducing the industry carbon footprint. Formic acid, produced from captured CO_2, could provide a pathway to decarbonise parts of the chemical sector, contributing to mitigate emissions while simultaneously educing reliance on fossil fuels [61,132].

However, for FA production to be scaled up and integrated into PtX systems, a comprehensive understanding of the techno-economic aspects and environmental impact is necessary. Life cycle assessment (LCA) and techno-economic analysis (TEA) are important tools for evaluating the feasibility and sustainability of formic acid production pathways. These analyses can help identify the most promising routes, as well as determine key hotspots in the process, such as energy consumption, CO_2 utilization efficiency, and cost factors.

While much of the research on FA production has focused on the electrochemical reduction of CO_2, the thermochemical route remains relatively underexplored [18,44,56]. This presents a significant opportunity for further investigation, particularly in the context of CO_2 hydrogenation to formic acid (PtFA). Thermochemical methods offer advantages, such as higher reaction rates and the ability to operate at higher scales. Furthermore, integrating PtFA into existing industrial infrastructure could facilitate more rapid adoption and lower the capital expenditure compared to electrochemical systems [44,53].

In summary, while electrolytic methods for FA production have been the primary focus in recent studies, there is a clear gap in research on thermochemical processes, especially CO2 hydrogenation. Exploring this route could provide valuable insights into optimizing PtFA systems, improving process efficiencies, and advancing CO_2 utilization technologies for a sustainable future.

This study aims to fill existing research gaps by comprehensively evaluating the environmental and economic performance of the entire PtFA process. This study investigates all unit operations involved including green H_2 and CO_2 captured from the air, powered by renewable offshore wind energy as the primary electricity source and FA synthesis and purification as well as integration of system components to minimise energy requirements. This approach provides valuable insights of the potential of carbon capture utilisation, CCU-based, formic acid in reducing greenhouse gas emissions, water consumption, and fossil resource use compared to traditional production methods.

6.2. Methodology

The present study focuses on the techno-economic and environmental assessment of a Power to Formic Acid (PtFA) assembly. The PtFA facility is located in North Yorkshire, United Kingdom where the Teesside offshore wind farm supplies around 7 MW electricity to produce around 15 ktonne FA /y. The plant size

has been determined by referencing similar CCU-based formic acid production studies [48,53] and is designed to cover 5% of the installed capacity of Europe's leading formic acid producer, BASF, which currently has an installed capacity of 305 ktonne/year. The methods applied for the technical, economic and environmental assessment of the system are described in this section.

6.2.1. Description of the model

The model consists of an offshore wind farm that supplies electricity to the plant, an electrolysis unit where hydrogen is obtained at high purity and a DAC module that captures CO_2 from ambient air at purity >95%. The process is divided into 4 sections: Direct air capture module, hydrogen production, formic acid synthesis and formic acid purification. The plant produces 15 ktonne of FA per year. A simulation model of the PtFA plant has been developed using the process simulator Aspen Plus V12.2 to establish the mass and energy balances. A block flow diagram of the PtFA is shown in Figure 6-1.

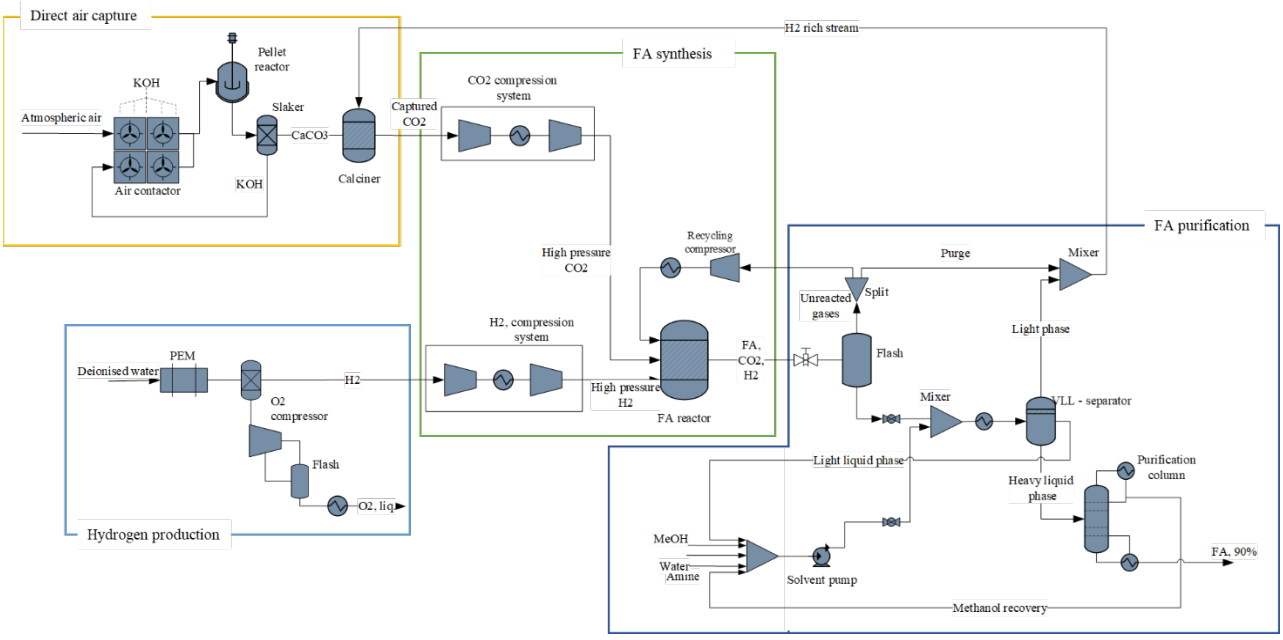

Figure 6-1. The block flow diagram of the investigated PtFA assembly.

The DAC system has been modelled based on the technology developed by Carbon Engineering [89]. H_2 production is achieved using a PEM electrolyser system. The DAC and the PEM electrolyser provide the raw materials, i.e. CO_2 and H_2, for the synthesis of FA that is achieved through homogenous catalysis and modelled using a rigorous kinetic model. The last step incorporates the purification of FA.

6.2.2. Direct air capture model

The CO_2 capture system has been modelled according to the carbon engineering air-liquid technology. The simulations have been conducted based on data provided by Keith et al., [89] and Bianchi. [147]. The system comprises four major unit operations: air contactor, pellet reactor, slaker and calciner. The ionic reaction has been defined in the properties section of chemistry in Aspen plus as described in methodology Chapter III, Section 3.1.1. The four stages comprising DAC model are described below. For this scenario, the simulation has been slightly modified due to the energy integration approach.

Air contactor and pellet reactor

The air contactor and pellet reactor have been simulated similarly as for Chapter VI, Section 4.2.1 but adjusting the amount of air required to deliver the amount of captured CO_2 required by the PtFA plant.

Slaker

The next step is the slaking, a flowsheet of the slaker reactor is presented in Figure 6-2. The calcium pellets from the previous reaction (S1), are washed to remove residues of hydroxide liquid. Then, they are dried up to 300 °C (S2 by passing through D-HTX1 and D-HTX2 to remove the remaining water in dryer before being sent to the calciner (3). The water removed in form of vapour is injected to the steam slaker.

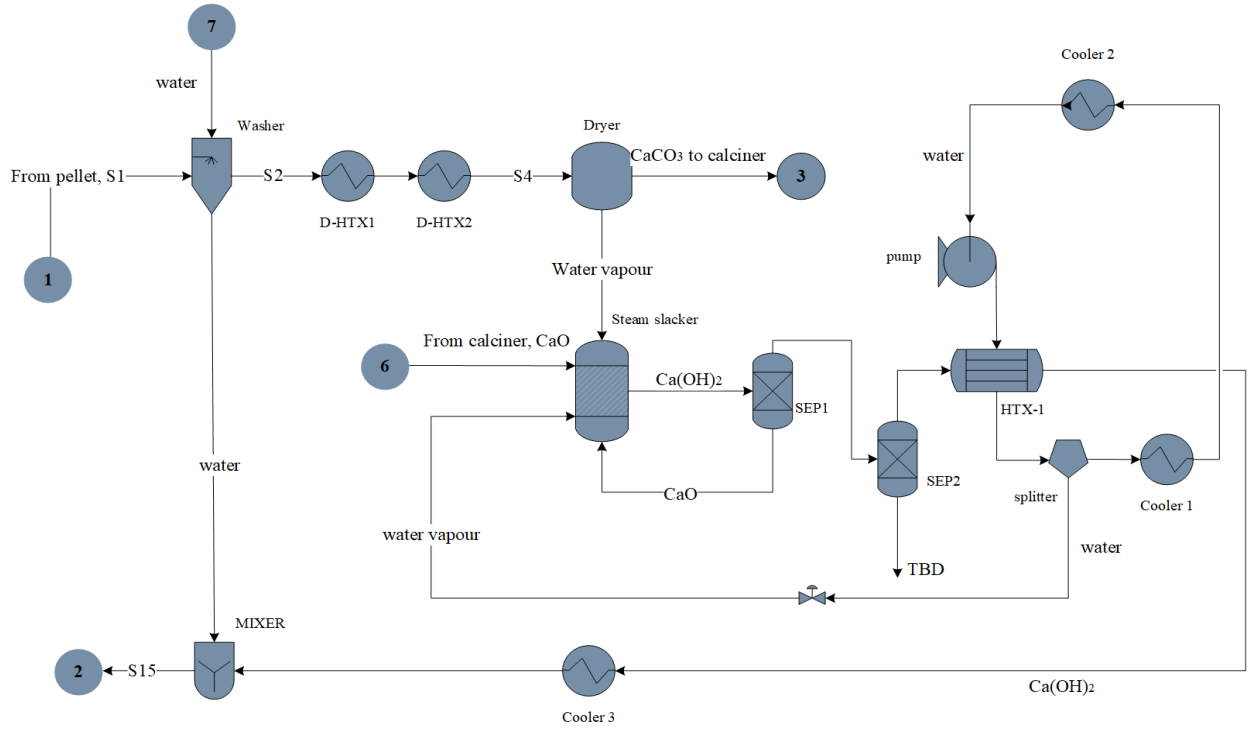

Figure 6-2. Process flow diagram of the slaker section.

In the steam slaker, calcium oxide (CaO) at 674 °C from the calciner section (S6) is hydrated to form $Ca(OH)_2$ through equation 4-3. The hydrated lime, $Ca(OH)_2$, product stream (S8) is cleaned from small CaO particles by passing through a series of cyclones (simulated as SEP1 and SEP2). CaO particles are recirculated to the slacker (S9) while $Ca(OH)_2$ at 300 °C is cooled down using a water loop (HTX-1) and cooler 3 (S15) for mixing with the water coming from the washing section in the mixer. The liquid $Ca(OH)_2$ (S16) is sent to the pellet reactor for crystallization.

In the water loop, pressurized water (S19) is used as the cooler agent, then a minimal portion of the vapour formed is used in the slacker to keep the slaking reaction (S13 & S14). The stream S17 is cooled down (cooler 1&2) and returned to the initial conditions. Operating conditions of the slaker section are shown in Table 6-1.

Table 6-1. Operating conditions of slaker subsystem.

Parameter/equipment	*Value*
Slaker reactor	RSTOIC; Conversion = 0.85
	$CaO + H_2O \rightarrow Ca(OH)_2$
	T = 300 °C; P = 1 bar
Dryer	HTX - D1
	vapour fraction = 1, P = 1 bar
	HTX - D2
	Temperature = 300 °C
	Pressure drop correlation parameter = 0
Washer	Liquid to solid ratio = 0.8
	T = 57 °C
	P = 1 bar
Pump	Discharge pressure = 42 bar
HTX-1	Hot/cold outlet temperature approach = 5 K
Cooler 1	T = 99.6 °C
	P = 1000 mbar
Cooler 2	T = 50 °C
	Pressure drop correlation parameter = 0
Cooler 3	T = 85 °C
	P = 1 bar

Calciner

A flowsheet diagram of the calcination section is presented in Figure 6-3. The design of the calciner has been modelled according to the design of Keith et al [89]. The dry $CaCO_3$ pellets coming from slaker (3) are heated up to the reaction temperature (i.e., 900 °C) using the heat exchanger HEX-3.

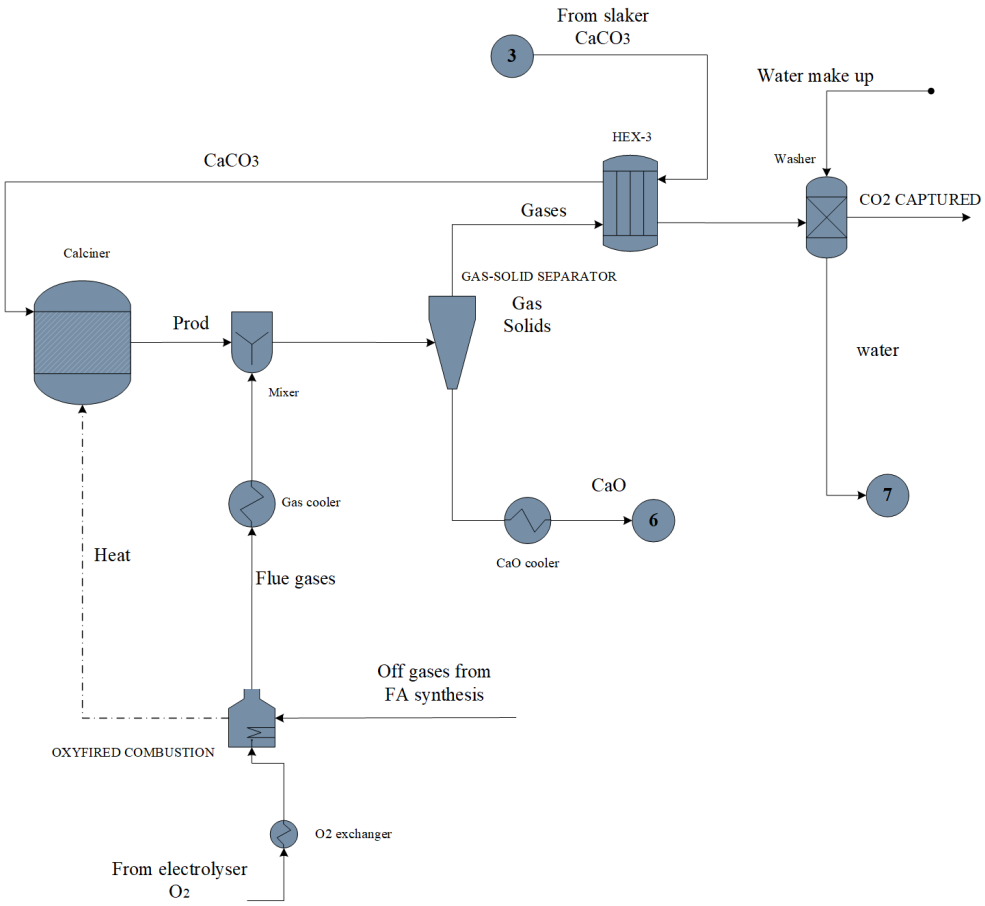

Figure 6-3. Process flow diagram of the calciner section.

Dry pellets are fed to the calciner section where CO_2 is recovered as product of the calcination reaction in equation 4-4. Carbon Engineering has designed the calciner reactor fitted with an oxy-combustion unit. For modelling purposes, these two operations have been modelled as separate units, however, in the real design both represent a single unit operation as stated in [147]. Initially, $CaCO_3$ pellets at 300°C from the slaker are passed through a heat recover system to recover heat from the exhaust gas stream. The model differs from Keith et al., [89] since in the original model, a second heat exchanger has been used to recover heat from the outgoing stream and produce steam for power generation. In this model, the second heat exchanger for power generation has been omitted. Instead, the power requirements of the whole DAC plant is supplied by the wind farm, and the heat from the products stream is used to increase the temperature of the feed from 300 °C to 770 °C before the calciner that operates at 900 °C. The energy for calcination in the original design is provided by an oxy-fired combustion of natural gas, which is injected into the calciner releasing CO_2 and water as flue gases [89]. In our proposed model, a H_2 rich stream derived from the successive formic acid synthesis section has been used as a fuel. Consequently, in this study the utilisation of external fossil resources is avoided.

After calcination, the outcome stream containing mainly CO_2 and water is sent to the CO_2 cleaning unit where water is knocked out and CO_2 reaches purity of 98%. CaO that leaves the reactor at 900 °C is cooled by exchanging heat with the oxygen from the electrolyser, which is used in the oxy-fired combustor. Finally, CaO returns to the slaker section. Table 6-2 indicates the operating conditions of the calciner reactor and the oxy-fired combustion units.

Table 6-2. Operating conditions of calciner reactor and the oxy-fired combustion.

Equipment	*Parameters*
Calciner (RSTOIC)	T = 900 °C; P = 1 bar
	$CaCO_3 \rightarrow CaO + CO_2$
	Conversion = 0.98
	Q = 1584 kW
Oxy-fired (RGibbs)	P = 1 bar, Duty = -1650 kW
	O2 exchanger
	P = 35 bar
	T = 80 °C
	Calculate phase equilibrium and chemical equilibrium
	Considers all components as products
HEX-3	Hot stream outlet temperature = 370 °C
Gas cooler	T = 900 °C
	P = 1 bar
CaO cooler	T = 674 °C
	P = 1 bar

6.2.3. Green hydrogen production

The Green hydrogen production has been simulated using the same model as for the previous scenarios through water electrolysis described in Chapter III, Section 3.3 but adjusting the amount of hydrogen that is required in the PtFA plant. Additionally, the amount of oxygen that is sold and sent to the DAC unit have been modified due to the energy integration applied in the DAC unit for the formic acid production.

6.2.4. FA synthesis

In this study, a conceptual design of the catalytic conversion to produce high purity formic acid (90%) from CO_2 is presented. The model has been developed using Aspen Plus simulator V12.2 and using the conditions described in Mantoan et al. [224]. Figure 6-4 displays the simulation flowsheet of CCU-based FA synthesis. This section involves the CO_2 and hydrogen compression, FA reaction synthesis, solvent recovery, and FA purification.

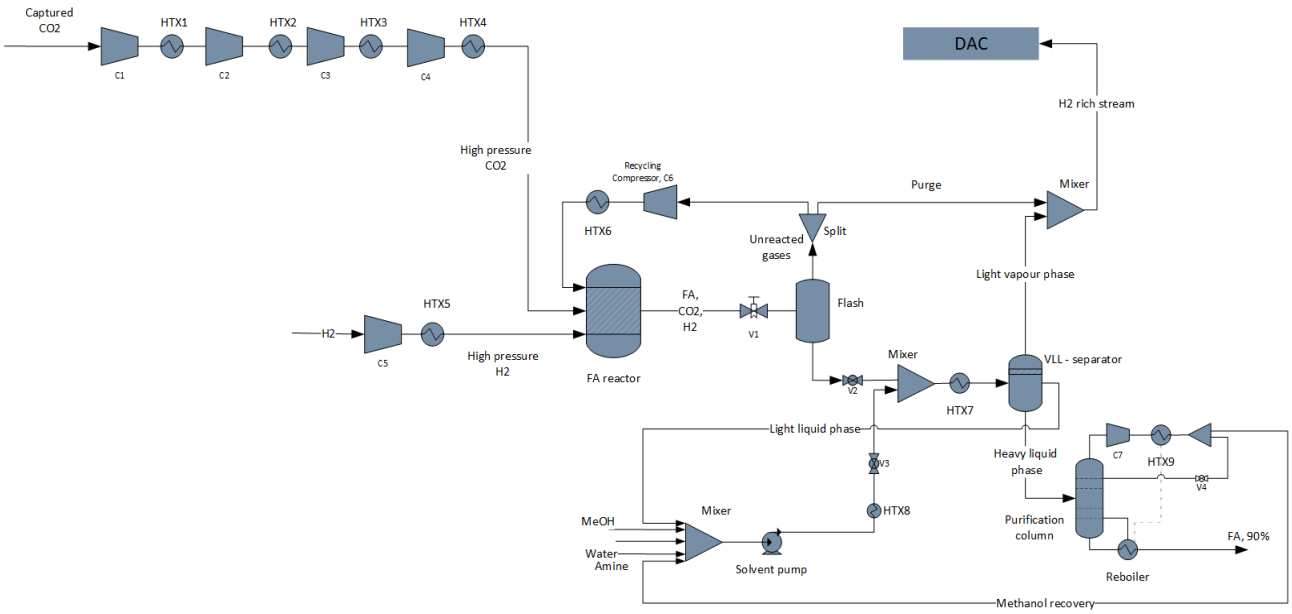

Figure 6-4. Process flow diagram of the FA synthesis and purification section

Compression system

The CO_2 coming from the DAC module at 60 °C and 1 bar is compressed to reactor conditions (105 bar and 50 °C) through a series of four compressors (C1-C5) with intermediate cooling (HTX1-HTX-5) to control the temperature before entering the reactor. The isentropic efficiency has been set at the default Aspen Plus value of 92%. Similarly, the H_2 stream from the electrolysis unit at 25 °C and 35 bar is compressed to 105 bar using a compressor unit and it is cooled down to the reactor temperature through a heat exchanger.

Reaction synthesis

The formic acid synthesis is based on the studies of Barbera et al. [146], Mantoan [224] and Perez-Fortes et al. [48] which attempted to reproduce the commercial BASF patent [225] for CO_2 hydrogenation into formic acid. The process comprises a catalytic reaction of CO_2 and H_2 in presence of a tertiary amine and a polar solvent. The reaction 6-1 takes place at high pressure of 105 bar and 50 °C as reported in [146,226].

$$CO_2 + H_2 + C_{15}H_{33}N \leftrightarrow C_{15}H_{33}N - HCOOH \qquad 6\text{-}1$$

The triamylamine ($C_{15}H_{33}N$) is used to stabilize the formic acid product as a 2:1 adduct; a water/methanol mixture has been used as a polar solvent additive which is known to accelerate the reaction [227]. The catalyst chosen is the complex Ru/Ph as indicated in [46,225,228]. The reactor has been

simulated as an isothermal continuous stirred tank reactor (CSTR) using the kinetic parameters presented in the supplementary information. MATLAB has been used to solve the kinetic equations while Excel serves as the intermediary to transfer data from and to Aspen Plus [146,224]. The FA reactor simulation was implemented as a user model in Aspen Plus, linking an Excel file to a MATLAB code. The MATLAB function *fsolve* was employed to solve the non-linear system of reaction rate equations in order to obtain molar concentration of products. Table 6-3 summarises the main process design specification for FA synthesis.

The VVAP parameter in the kinetics listed in Table 6-3 denotes the volume occupied by vapour phase in reactor and it has been estimated through an iterative process to achieve a target per pass CO_2 conversion of 40% as reported in [224].

Table 6-3. Main process design specifications of formic acid synthesis.

Equipment	*Parameters*	*Reference*
Compressor & turbine efficiencies	Isentropic = 0.92 Mechanical = 1.0	Aspen Plus
C1	Isentropic P = 4 bar	Aspen Plus
C2	Isentropic P = 15 bar	Aspen Plus
C3	Isentropic P = 50 bar	Aspen Plus
C4	Isentropic P = 105 bar	Aspen Plus
C5	Isentropic P = 105 bar	Aspen Plus
C6	Isentropic P = 105 bar	Aspen Plus
C7	Isentropic P = 2.5 bar	Aspen Plus
HTX1	Hot outlet temperature = 45 °C	Aspen Plus
HTX2	Hot outlet temperature = 45 °C	Aspen Plus
HTX3	Hot outlet temperature = 45 °C	Aspen Plus
HTX4	Hot outlet temperature = 50 °C	Aspen Plus
HTX5	Hot outlet temperature = 50 °C	Aspen Plus
HTX6	Hot outlet temperature = 50 °C	Aspen Plus
HTX7	Hot outlet temperature = 25 °C	Aspen Plus
HTX8	Hot outlet temperature = 50 °C	Aspen Plus
HTX9	Pressure = 2.5 bar Duty = -3032 kW	Aspen Plus
Solvent pump	Centrifugal P = 105	[146]
V1	Outlet pressure = 90 bar	[224]
V2	Outlet pressure = 1 bar	[224]
V3	Outlet pressure = 1 bar	[224]
V4	Outlet pressure = 1 bar	Aspen Plus
FA reactor	Model = CSTR (model user 3) T = 50 °C P = 105 bar	[224]
Kinetics	$CO_2 + H_2 \rightarrow CH_3OH + H_2O$	[224]
	$r_{HCOOH} = \frac{k_4 k_2 [P_{CO2}][P_{H2}]}{1 + \frac{k_2 [P_{CO2}][corr * P_{H2}]}{3600}} * cat$ k_2 = 0.00001376208 (1/h/bar) k_4 = 0.01942411111 (1/h/bar)	[224]
Correlation constant (corr.)	0.0145095 (1/bar)	[224]
Catalyst molar concentration (cat.)	9.677E-5 (kmol/m^3)	[224]
Reaction rates	R1 = -1*R_{HCOOH}*VVAP R2 = -1* R_{HCOOH} *VVAP R3 = 1* R_{HCOOH} *VVAP Where 1,2 and 3 indicates components H_2, CO_2 and FA, VVAP = 0.029 (from iterative process)	[224]
Catalyst	Ru = 38.1 kg/y Ph = 19.1 kg/y	Calculated from [48], [225]

Table 6 3. Main process design specifications of formic acid synthesis (Cont.)

Equipment	*Parameters*	*Reference*
Flash	T = 90 °C Duty = 0	[224]
Split	Purge (H_2 rich stream) = 5%	[146]
VLL flash	Type = Pressure & duty P = 1 bar Duty = 0	[146,224]
Separation column	Calculation type = Equilibrium Stages = 20 Distillate rate = 3.5 ton/h Reflux ratio = 1.5 P = 1 bar	[146]

Solvent recovery and FA purification

After the reaction, the product stream is throttled through a valve (V1) to 90 bar before entering the flash separator, where formic acid liquid is recovered at the bottom and unreacted gases such as CO_2 and H_2 are collected at the top. A portion of these gases is recirculated to the reactor using a compressor (C6) and heat exchanger (HTX6) for reconditioning, while a purge of 5% is considered to avoid accumulation of components. This purge is a H_2-rich stream, and it is sent to the DAC-calciner system to provide heat. Further, the solvent mixture of methanol/water and amine is pumped from 1 to 105 bar. In the real process, the mixture is fed to the reactor for enhancing FA formation. However, due to lack of information about thermodynamic equilibrium in the reactor, the solvent mixture is simulated separately from the reactor and conditioned to the same temperature and pressure only to account for the energy requirements of the separation and purification system as suggested in [146,224]. The stream is cooled down to 50 °C and laminated at 1 bar before being mixed with FA product. The amine, methanol, and water mixture is pumped to 105 bar and cooled from 52 °C to 25 °C (HTX8) to account for the energy and heat consumption during conditioning. Subsequently, the mixture is throttled to 1 bar in V3 and combined with the FA product stream from the reactor. The resulting mix of amine, solvent, and FA are sent to a vapour liquid-liquid (VLL) separator. Here, the remaining gases are separated and sent them to the purge stream while the liquid phase forms two immiscible liquid phases [224]. The light liquid phase, comprising mostly the triamylamine, is recovered and sent back to the reactor.

The heavy liquid phase is directed to a purification column where formic acid is recovered as the main product with a purity of 90.5%. The purification column has been designed as an equilibrium Radfrac unit with 20 stages and operating at 1 bar [146]. The reflux ratio has been set at 1.5. Methanol and water are recovered in the distillate and recycled while purified formic acid is recovered at the bottom. The top of the column was simulated as a vapour recompression column (VRC) where the condenser (HTX9) is preceded by a compressor (C7) and the vapour is compressed in order to increase its temperature and maximize the

heat recovery that can be used in the reboiler. Finally, the mixture of methanol and water, is recirculated back into the system for the next cycle. This recirculation helps to optimize the use of resources, contributing to the overall efficiency and sustainability of the process.

The amount of solvent required for the separation of FA has been determined by a design specification tool in Aspen Plus based on the amount that is recirculated from the VLL streams and the column, and preserve the ratio 2:1 between solvents and FA according to Table 6-4.

Table 6-4. Design specification for the amine and polar solvent inputs

Specification	*Value*	*Units*
Triamylamine		
Variable	NETFLOW	
Specification	13738	kg/h
Vary	NET-INPUT	kg/h
Methanol		
Variable	METFLOW	
Specification	4392	kg/h
Vary	MET-INPUT	kg/h
Water		
Variable	WATFLOW	
Specification	187	kg/h
Vary	WAT-INPUT	kg/h

It has been assumed that methanol solvent is renewed once every ten years while catalyst is renewed once per year. It is also assumed that catalyst is completely recovered as stated in Perez-Fortes et al. [48] and Dattarao et al. [226]. The simulation of the catalyst recovery is not considered in this study, but the equipment cost data has been taken into account in the economic analysis.

6.3. Key performance indicators (KPIs)

The key performance indicators have been defined as technical indicators retrieved from the process modelling. Carbon efficiency, CO_2 conversion efficiency, and energy efficiency and specific energy consumption are described as follows.

6.3.1. Carbon efficiency

The carbon efficiency is defined as the fraction of the initial carbon source that is found in the final product, i.e. formic acid. The equation 6-2 indicates the moles of carbon present in the FA product per unit of carbon in the feedstock.

$$C_e = \frac{\dot{n}_{C_{FA}}}{\dot{n}_{C_{CO_2}} + \dot{n}_{C_{met+amine}}} x100\% \qquad 6\text{-}2$$

6.3.2. CO_2 conversion efficiency

In this study, both per pass, equation 6-3, and the overall CO_2 conversion, equation 6-4 have been calculated as technical indicators.

$$\eta_{CO2-R} = \frac{CO_{2-in} - CO_{2-out}}{CO_{2in}} x100\% \quad 6\text{-}3$$

$$\eta_{CO2-P} = \frac{CO_{2-in} - CO_{2-out}}{CO_{2-in}} x100\% \quad 6\text{-}4$$

Where $CO_{2\text{-in}}$ indicates the moles of CO_2 that is fed to the reactor or in the system, and $CO_{2\text{-out}}$ denotes the moles of CO_2 that leaves the reactor (R) or the whole process (P).

6.3.3. Energy efficiency

The energy efficiency corresponds to the total output energy to the total input energy [144]. Equation 6-5:

$$\eta = \frac{E_{FA}}{E_{H2} + E_{amine} + E_{sol.} + E_{heat} + E_{elect}} x100\% \quad 6\text{-}5$$

Where E_{FA} is the heating value of formic acid, E_{H2}, E_{amine} and E_{sol} are the heating values of the H_2, amine and solvent fed to the system, and E_{heat}, E_{elect} are heating values from required energy streams such as heat and electricity.

6.3.4. Specific energy consumption (SEC)

The specific energy consumption indicates the amount of energy requirement in form of heat or electricity that is required for the manufacture per unit of mass of final product. It is determined by equation 6-6:

$$SEC = \frac{Energy\ consumption\ [MW]}{Mass\ flowrate\ of\ products\ [tonne/s]} \quad 6\text{-}6$$

6.4. Economic analysis

A typical discounted cash flow analysis has been carried out to appraise the financial performance of the system. This includes the estimation of the total capital and operational expenditures (CAPEX and OPEX). The calculation of the total capital expenditures (CAPEX) has been estimated using data from the simulations and literature data. The main assumptions for the economic analysis are presented in Table 6-5.

Table 6-5. Main assumptions for the PtFA economic evaluation.

Parameter	*Units*	*Value*
Plant location	-	United Kingdom
Base year	-	2023
Production rate	ktonne/y	15.3 ktonne/y
Lifetime of the project	years	20
Discount rate	%	10
Depreciation method	-	straight line
Operating time	h/y	8,000

The purchased equipment cost has been calculated using relevant literature and adjusted to the current year and size using the scaling factor in equation 3-4. Equipment cost data for the rest of the plant are detailed in Table 6-6.

Table 6-6. Equipment cost data.

Equipment	*Variable of design*	*Ref. year*	*Ref. cost GBP*	*Ref. size*	*Scaling factor*	*References*
Air contactor	$MtCO_2/y$	2016	84,463,398	0.98	1	[89]
Pellet reactor	$MtCO_2/y$	2016	56,975,748	0.98	1	[89]
Calciner-slaker	$MtCO_2/y$	2016	32,451,727	0.98	0.8	[86,89,157]
Electrolyser (installed)	MW	2016	1,229,225	1	0.95	[229]
Heat exchangers	m^2	2017	394,506	1000	0.7	[168]
Compressors	kW	2002	364,720	1007	0.67	[179]
Distillation column	m^3	2017	3,550,550	92.3	0.8	[168]
Pump	m^3/s	2001	62,182	10	0.36	[178]
FA separation process	tonne FA/y	2016	160,650	12kt	0.7	[48]
FA reactor	tonne FA/y	2016	98,016	12kt	0.7	[48]

The Chemical Engineering Plant Cost Index (CEPCI) was utilised to update the cost plant equipment to the base year of the study (i.e., 2023) using value of 798.2. When the cost of the equipment is reported in a different currency than GBP (£), the value is first converted to GBP by using the exchange rate of the reference year and then updated to the actual year. As depicted in Table 6-7, the Lang factor methodology is applied to estimate the CAPEX**.**

Table 6-7. CAPEX estimation methodology [48], [230].

Component	*Lang factor*
Purchased Equipment Cost (PEC)	1
Installed direct costs (IDC)	PEC + (1) + (2) + (3) + (4) + (5)
(1) Purchased equipment installation	0.47×PEC
(2) Instrumentation and controls	0.36×PEC
(3) Piping	0.68×PEC
(4) Electrical systems	0.11×PEC
(5) Service facilities	0.70×PEC
Non-installed direct costs (NIDC)	(6) + (7)
(6) Buildings	0.18×PEC
(7) Yard improvements	0.10×PEC
Total direct costs (TDC)	(ICD) + (NIDC)
Indirect costs (IDC)	(8) + (9) + (10) + (11) + (12)
(8) Engineering and supervision	0.33×PEC
(9) Construction expenses	0.41×PEC
(10) Legal expenses	0.04×PEC
(11) Contractor's fee	0.22×PEC
(12) Contingency	0.44×PEC
Fixed Capital Investment (FCI)	TDC + IDC
Working Capital (WC)	0.05×FCI
CAPEX	FCI + WC

The OPEX include variable and fixed operating costs. The variable costs, comprising raw materials, process water, catalyst, and disposals and are calculated based on their market prices and flowrates derived from simulation results. The catalysts are accounted for a renewal once per year while methanol solvent and amine are renewed every ten years. The levelized cost of electricity (LCOE) of the offshore wind has been calculated by the SAM software which is defined as the total life cycle cost of energy generation system over the total electricity generated [231]. Fixed operating costs, supervision, maintenance, insurance, and general plant overhead are computed using default factors as specific percentages of the PEC. In addition, variable and fixed costs are summarized in Table 6-8.

Table 6-8. Fixed and variable costs.

Fixed operating and maintenance costs (O&M)	*Basis*	*Factor*	Reference
Operating Labour (OL)	Equation 3-5	-	-
Operating Supervision (OS)	OL	0.25	[48]
Direct overhead (DO)	OL + OS	0.5	[48]
General overhead	OL + OS + DO	0.45	[48]
Maintenance labour	FCI	0.015	[145]
Maintenance materials	FCI	0.015	[48]
Insurance and tax	FCI	0.01	[181]
Financing working capital	WC	0.1	[181]

*Only the cost for the use of the network is computed

Table 6-8. Fixed and variable cost (cont.)

Variable costs	*Unit*	*Value*	*Reference*
Catalyst price (Ru)	£/kg	120,000	Sigma Aldrich
Catalyst price (Ph)	£/kg	81,180	Sigma Aldrich
Solvent Methanol	£/kg	0.44	[232]
Amine	£/kg	0.212	[48]
Oxygen price	£/kg	0.044	[36]
Electricity wind	£/kWh	0.051	SAM software
Electricity grid*	£/kwh	0.025	[184]
Wastewater treatment	£/tonne	0.42	[161]
Cooling water	£/tonne	0.03	[161]
Process water	£/m^3	0.08	[89]
Ca disposal and make up	£/tonne CO_2	0.16	[89]

*Only the cost for the use of the network is computed

6.4.1. Sensitivity analysis

Further, a sensitivity analysis is conducted to analyse the effects of the key parameters over the formic acid MSP by applying a change of ± 25% and ± 50% to the original values. The parameters of interest are the LCOE, the PEM installed cost, the discount rate, the O_2 price, and the CAPEX of the DAC that are listed in Table 6-9.

Table 6-9. Main assumptions for PtFA sensitivity analysis.

	Base value	*Units*	*Reference*
LCOE	0.040	£/kWh	SAM software
PEM Installed cost	750	£/kW	[229,233]
Discount rate	10	%	-
O_2 price	0.044	£/kg	[36]
CO_2 CAPEX	294	£/tonne-CO_2	[89]
Catalyst price:			
Ruthenium	120	£/tonne	[234]
Phosphine	81	£/tonne	[235]

6.5. Life cycle assessment (LCA)

A life cycle assessment approach has been applied evaluate the environmental performance of the PtFA system. The ISO-14040 standard is employed as the framework of the assessment. The four stages considered are: goal and scope definition, inventory analysis, impact assessment, and interpretation [58].

6.5.1. Goal and scope

The goal of this LCA is to quantify the environmental impacts of formic acid production through CO_2 hydrogenation and green H_2 including climate change, and fossil depletion (FD) and water consumption to identify the main system contributors. Further, a comparison of the climate change impact with conventional fossil-based formic acid production process is also discussed.

Functional unit and allocation procedure

In this paper, the functional unit (FU) is 1 tonne of formic acid produced through PtX. All inputs and environmental impacts results are normalized to the FU. The O_2 produced in the water electrolysis is considered as by-product and this necessitates the utilisation of an allocation procedure. According to ISO-14044 guidelines, the initial step is to avoid or minimize allocation whenever possible by subdividing the system into two or more sub processes [185]. Therefore, the approach followed herein is the subdivision of the water electrolysis system and the rest of the plant (Figure 6-5) into two subsystems. The exergy allocation is applied to H_2 and O_2. Exergy analysis can be found in Chapter III, Section 3.5.

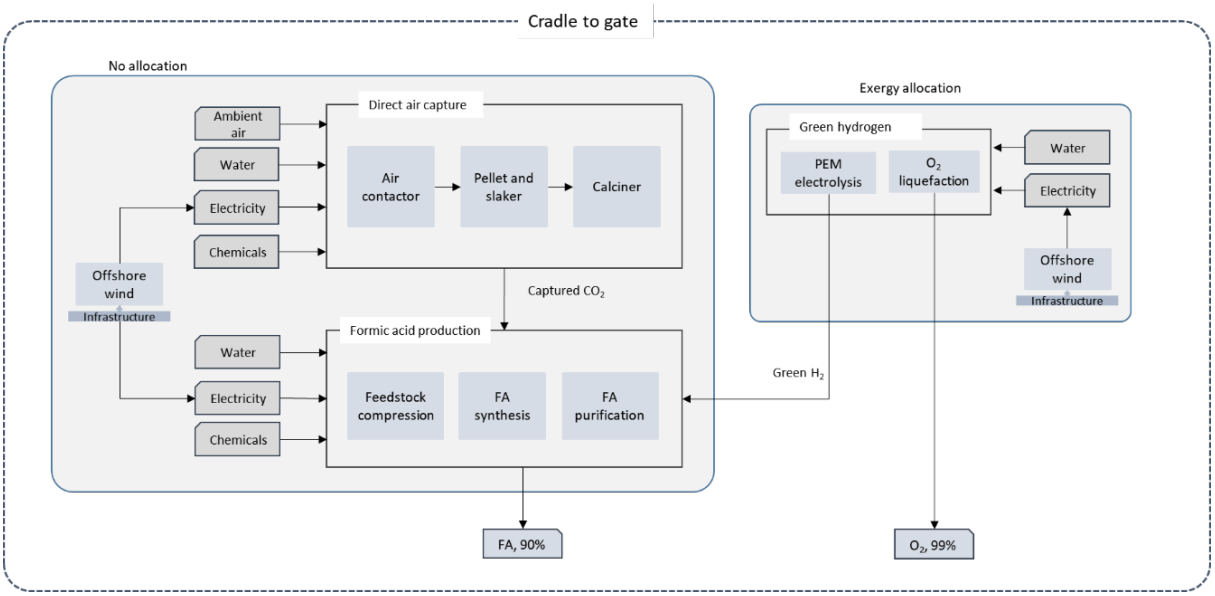

Figure 6-5. The system boundaries for the LCA of the investigated PtFA process.

System boundaries

A cradle to gate approach has been considered in Figure 6-5, thus, the distribution, use and final disposal are not included. The reason behind this is because the formic acid produced through PtFA has the same physical properties as conventional fossil-based FA and therefore they have similar end use phase

[236,237]. The LCA includes all materials and energy inputs in addition to the outputs including emissions to soil, water and air during the processing stage. The CO_2 captured is not accounted for negative emissions since at the product end-of-life, it is released as positive emissions adding up to zero in a carbon neutrality cycle [113], since it is recaptured in the DAC. The infrastructure for the DAC, FA synthesis, and PEM electrolyser are not included due to their low contribution to environmental impacts [150]. However, infrastructure emissions of the offshore wind farm were taken into account.

6.5.2. Life cycle inventory

The life cycle inventory for the PtFA steps has been constructed from the mass and energy balances from the CO_2 and H_2 production, as well as the FA synthesis and purification. These have been obtained from simulation modelling results, relevant literature and using the datasets available in the Ecoinvent database v3.6. [238]. Process emissions have been taken into account through the entire system. Emissions to the air have been retrieved from simulation of the combustion process while wastewater treatment has been assumed for emissions to water. The catalyst LCA impact is usually neglected (REF) within chemical processes, therefore, the same approach if considered here. The plant infrastructure has not been included in the analysis due to its minimal contribution to the overall carbon footprint.

6.5.3. Impact assessment

The environmental impacts of the CCU-based formic acid process were evaluated using the ReCiPe Midpoint (H) level methodology available in SimaPro v9.4.0.2. This method includes 18 impact categories: Climate change (CC) abiotic depletion (ADP), Ozone depletion (ODP), Terrestrial acidification (TAP), Freshwater eutrophication (FEP), Marine eutrophication (MEP), Human toxicity (HTP), Photochemical oxidant formation (POP), Particulate matter formation (PM), Terrestrial ecotoxicity (TEP), Freshwater ecotoxicity (FWEP), Marine ecotoxicity (MEP), Ionising radiation (IR), Agricultural land occupation (ALO), Urban land occupation (ULO), Natural land transformation (NLT), metal depletion (MD) and fossil depletion (FD). Water consumption is calculated from accounting the water needed in the production or raw materials as well as cooling water loss and water used in the electrolyser unit.

6.5.4. Interpretation

The environmental impact, water consumption and fossil depletion impact of the power-to-formic acid process has been included and compared with fossil-based formic acid production coming from natural gas in order to raise the benefits of PtFA. The model for conventional FA has been retrieved from Ecoinvent database v3.6 running the same impact method and the specific *module "Formic acid {RER}| production, methyl formate route | Cut-off, U"*. The module represents the standard industrial process of FA production.

Additionally, a sensitivity analysis of the electricity carbon intensity on the climate impact of the PtFA process has been conducted to understand its significance. The analysis is prime of importance due to the reliability of the process in the electricity consumption. The sensitivity includes various electricity sources such as offshore wind, hydropower, nuclear, and solar power. Each of these energy sources has a distinct carbon intensity and, consequently, a different impact on the overall greenhouse gas emissions associated with the PtFA process.

6.6. Results and discussion

This section provides the main outcomes of the technical, economic and environmental assessments of the PtFA production process. The results are compared and discussed against the conventional FA production system.

6.6.1. Key performance indicators results

As described in the methodology section, compressed CO_2 and H_2 are synthetized into formic acid through thermocatalytic route. The mass and energy balance of the main inputs and outputs of the PtFA process are summarized in Table 6-10.

Table 6-10. Annual inputs and outputs of PtFA plant.

Mass balance	*Value*	*Units*
Inputs		
Air	25,149	ktonne/y
CO_2 available	14.2	ktonne/y
Water	9.37	ktonne/y
H_2 produced	868	tonne/y
Methanol	861	tonne/y
Amine	130	tonne/y
Outputs		
FA	14.01	ktonne/y
O_2	7.22	ktonne/y
CO_{2-R}	45.4%	
CO_{2-P}	99.9%	
Carbon efficiency	73.4%	
Energy balance		
Electricity	4.49	MWh/tonne
Heating	3.6*	MWh/tonne
Cooling	3.9*	MWh/tonne
Total SEC (w/o integration)	12.01	MWh/tonne
Total SEC (w/integration*)	4.49	MWh/tonne
Energy efficiency	22	%

The process involves handling approximately 25,149 ktonne of atmospheric air to capture 10.98 ktonne of CO_2 annually. This captured CO_2, combined with an additional 2.96 ktonne of CO_2 recovered from the combustion of off-gases during formic acid synthesis, results in a total of 14.2 ktonne of CO_2 available per

year. Additionally, 868 tonne/year of hydrogen is produced from 9.37 ktonne of deionized water through electrolysis. The process also generates 7.22 ktonne of oxygen, which is partially utilized in the combustion process within the calciner unit (57%), with the remaining 43% being considered a by-product available for sale. The small quantities of amine and methanol listed in Table 6 represent the renewal of the solvent that compensates for any losses incurred during the recycling process. While most of the methanol and amine solvent are recovered and recycled within the plant, a minor fraction is inevitably lost due to factors such as evaporation, degradation, or addition in product streams. These losses require the addition of fresh solvent to maintain the desired operational levels and ensure the efficiency and stability of the process. The reported amounts thus reflect the make-up quantities required to sustain the continuous operation of the plant.

6.6.2. CO_2 conversion efficiency

The process achieves complete CO_2 conversion into formic acid (99.9%), primarily due to the continuous recycling of unreacted materials throughout the entire system. This approach significantly enhances the overall efficiency of the CO_2 utilization, making the process highly effective in converting the greenhouse gas into valuable products. However, it is important to note that the reactor itself, does not achieve full conversion in a single pass. According to the process model, the CO_2 conversion rate within the reactor is fixed at approximately 45%, as reported by Mantoan et al. [224]. This lower conversion rate in the reactor highlights the challenges in achieving high efficiency in a single stage of the process. Despite this, the overall system compensates for the reactor limitations through the recycling strategy, which ensures that unreacted CO_2 is reprocessed until it is completely converted into formic acid.

6.6.3. Carbon balance

The carbon balance of the PtFA process, illustrated in Figure 6-6 reveals a carbon efficiency of 73.43%. The process begins with the injection of approximately 514 kg/h of carbon into the DAC unit, sourced from atmospheric CO_2. Due to the DAC capture efficiency of 74.6%, a portion of this carbon (131 kg/h) is not captured and then released as exhaust gas back to the atmosphere.

In addition to the DAC-sourced carbon, an extra carbon stream of 49 kg/h is introduced in the system from the methanol and amine solvent make-up stream in the FA synthesis and purification stage. This accounts for the solvent volumes that are not recovered during recycling and must be replaced to sustain the reaction cycle. As part of the energy integration strategy, the fraction of solvents not recovered along with the unreacted gases from the FA synthesis and purification unit, are subjected to an oxy-combustion

with the purpose of recover energy for the process and supply additional carbon to the DAC unit, thus enhancing the overall carbon input (102 kg/h).

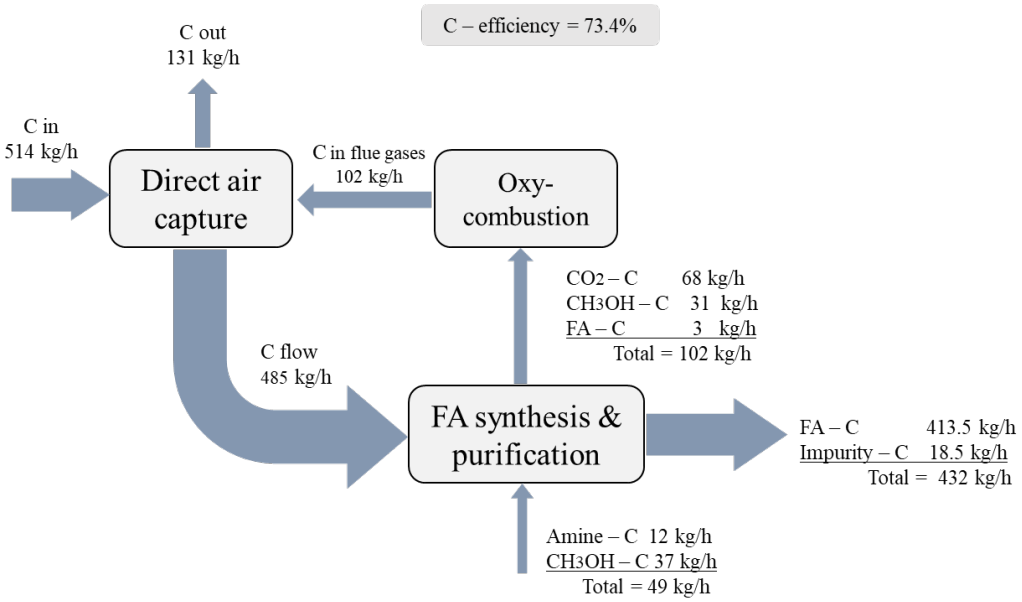

Figure 6-6. The carbon balance of the PtFA system.

As a result, the total carbon exiting the DAC system is 485.6 kg/h, which is directed to the synthesis and purification unit. In this stage, carbon is distributed between the unreacted compounds (CO_2, methanol, FA), and the main product stream. The final product stream consists of 413.5 kg/h of formic acid at a purity of 96%, and 18.5 kg/h of impurities derive from the solvent mixture (4%). This efficient management of carbon flows within the PtFA process emphasizes the potential of integrated carbon capture, solvent recycling, and energy recovery to optimize the production of formic acid while maximizing carbon utilisation.

6.6.4. Energy balance

The energy consumption per tonne of FA is also summarized in Table 6-10 as well as the energy efficiency and the specific energy consumption. The electricity consumption is responsible for around 37% of the total energy consumption, followed by heating requirements which constitute about 30% and cooling demands which make up the remaining 33% of the total. As detailed in Table 6-10, the total energy consumption of the PtFA process without any heat integration was found to be 12.01 MWh per tonne of formic acid produced. This high energy requirement is primarily driven by the electricity needs of the electrolyser, and the DAC modules. However, by implementing heat integration strategies, the SEC can be significantly reduced by 62.5%, bringing it down to 4.49 MWh/tonne FA. This reduction is achieved mainly by recovering and reusing the available heat from various process streams, thereby minimizing the external

energy input required for heating and cooling. The reduction in SEC through heat integration not only lowers operational costs but also enhances the sustainability of the process by reducing its overall energy footprint. Also, this heat recovery strategy helps in optimizing energy flows within the plant, reducing dependency on external energy sources, and improving the overall energy efficiency of the PtFA system. Other studies such as the one conducted by Kim and Han [144] have reported a SEC of 5.3 MWh/tonne FA which is in line with this study. This comparison remarks the importance of incorporating heat integration strategies in PtX processes.

Compared to the conventional formic acid production process, the PtFA approach demonstrates a different energy profile. The total electricity consumption in conventional methods ranges between 3.5 and 11.79 MWh per tonne of FA, along with a significant steam consumption of 4.13 to 93.8 MWh per tonne of FA produced [48,133]. This evidence the substantial energy requirements of traditional FA production, where both electricity and steam are critical inputs. In contrast, the PtFA process focuses on optimizing electricity consumption by renewable energy sources and implementing heat integration techniques to reduce overall energy demand. The reduction in steam consumption, achieved through these strategies, makes PtFA a more energy-efficient and environmentally friendly alternative to conventional processes.

Figure 6-7 displays the breakdown of the electricity consumption within the PtFA process. The most significant portion of the electricity consumption, approximately 89% is attributed to hydrogen production in the PEM electrolyser unit. The remaining 11% of electricity use is distributed among the other components. Specifically, 4.2% is consumed by compressors used by conditioning H_2 and CO_2 feed while the compressor in the FA purification column accounts for 3.7%. Additionally, the DAC unit requires 1.7% of the total electricity, and the solvent pump used in the FA synthesis contributes 1.6%.

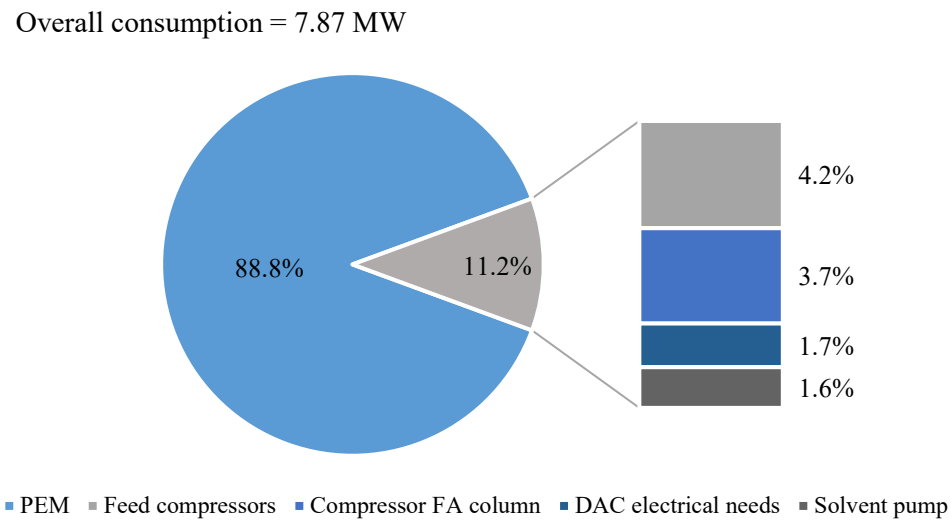

Figure 6-7. The electricity consumption breakdown of PtFA.

The energy efficiency of the PtFA process reflects the ratio of the total energy output in the form of produced formic acid to the total energy input required for its production. This efficiency has been calculated by considering the heating values of FA, H_2, and methanol, as reported in prior studies [57,239]. The heating value of the amine solvent is excluded from the calculation due to its minimal energy value contribution to the overall. The PtFA process has an energy efficiency of 22%, indicating that significantly more energy is consumed than what is recovered in the final product. This low efficiency is expected, given the substantial energy demands of the electrolysis stage and the high energy content of the hydrogen used. The obtained energy efficiency is consistent with findings by Kim and Han, who reported an efficiency of 23% for a formic acid production process via CO_2 hydrogenation. In contrast, Gokberk and Wiebren. [145] reported a higher energy efficiency of around 31%. The discrepancy in efficiency between the current study and that of Gokberk and Wiebren can be attributed to the greater electricity consumption per tonne of formic acid observed in this study compared to the values reported by these authors (0.29 MWh/tonne FA excluding CO_2 and H_2).

Heat integration

The integration of the DAC and Formic Acid synthesis processes has been achieved through strategic heat integration between the available hot and cold streams within the system. This approach aims to maximize energy efficiency by utilizing residual heat from one part of the process to meet the thermal demands of another. The primary energy-intensive component was identified as the calciner, which operates at a high temperature of 900 °C. To meet this significant thermal requirement, the system utilizes the oxy-combustion of off-gases generated during the FA synthesis. These off-gases, consisting of unreacted

compounds such as H_2, methanol, and FA, are combusted with oxygen, providing the necessary heat for the calciner.

Another critical thermal integration occurs within the slaker dryer, which is responsible for drying the carbonate pellets by removing most of the water content. The heat needed for the slaker dryer is supplied by integrating it with hot streams from the calcium hydroxide production and the water-cooling system. By spending these hot streams, the process reduces the need for external heat sources, thus enhancing overall energy efficiency.

The FA purification process requires a significant amount of energy, specifically 3.03 MW of heat for the reboiler. To meet this demand, a heat pump system has been integrated within the purification column. This approach leverages the heat released in the condenser to provide the necessary heat for the reboiler [240]. The system employs a Vapour Recompression Column (VRC) configuration, where a compressor is installed before the condenser. This compressor increases the temperature and pressure of the vapour exiting the column. By elevating these parameters, the vapour thermal energy is enhanced, enabling the recovery of heat through a dedicated heat exchanger. This recovered heat is then redirected to the reboiler, supporting the evaporation process while simultaneously condensing the vapour. The specifications of the VRC system are presented in Figure 6-8. This comprehensive heat integration contributes to reducing operational costs and minimizing the environmental impact by efficiently utilizing available energy resources within the system.

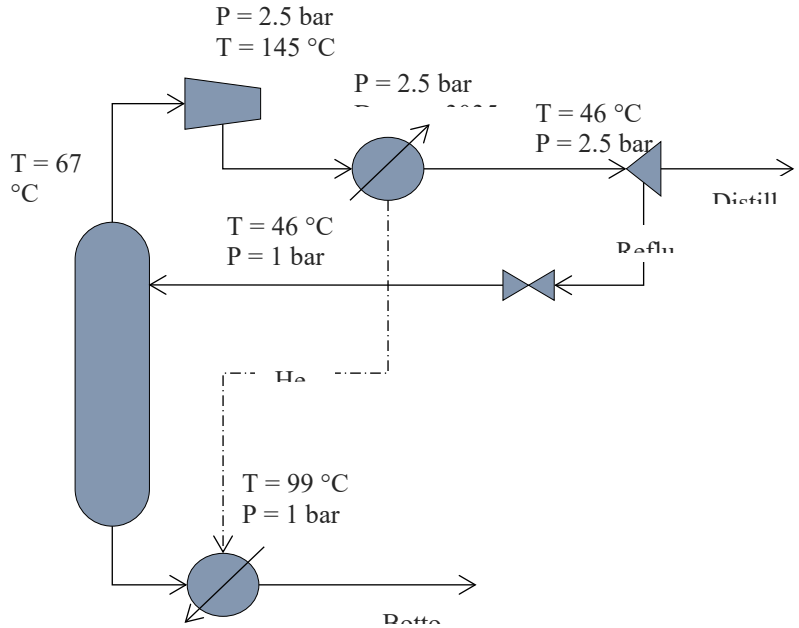

Figure 6-8. The design of the FA purification column using a VCR configuration.

6.7. Economic analysis

The results of the capital and operational expenditures are provided in the following sections. The minimum selling price has been considered as one of the main indicators of the economic feasibility, therefore is also discussed and compared with conventional FA production. Finally, a sensitivity analysis is also included to evaluate the effect of main parameters over the FA cost.

6.7.1. Capital expenditures

The main economic results are presented in Table 6-11. The total CAPEX of the PtFA process is estimated at £33.6 Million GBP. The major components include equipment cost including installation (53%), while non-installed direct costs such as buildings, and yard improvements accounted for 6%. Indirect costs such as engineering, supervision, construction and legal expenses, contractor's fee and contingency represent 33%. Finally, working capital contributes with 8% of the total CAPEX.

Table 6-11. Economic results.

Component	*Cost, Million GBP*	*Share*
Installed equipment cost	19.8	53%
Non-direct cost	2.4	6%
Indirect cost	12.3	33%
Working capital	3.2	8%
CAPEX	37.61	

The equipment cost is the most significant portion of the CAPEX due to the specialized machinery needed. Figure 6-9 provides the major equipment cost breakdown by stage and equipment type.

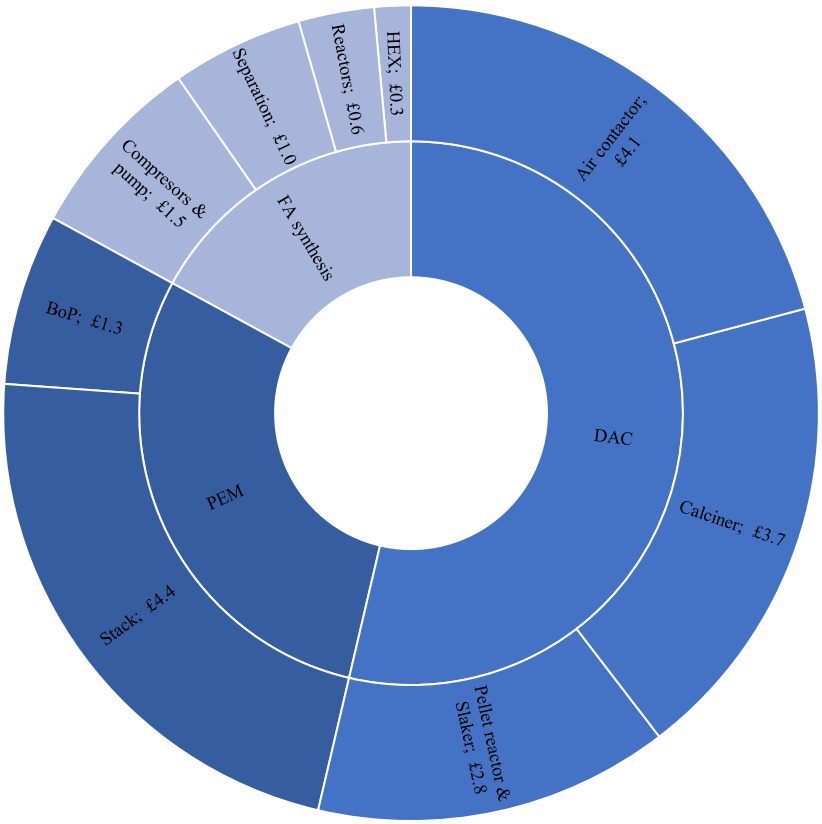

Figure 6-9. Breakdown of the installed equipment cost, data in million GBP.

The DAC process is a significant contributor to the overall equipment cost, accounting for 54% of the total cost, with the air contactor and calciner units being the primary cost drivers. The PEM equipment cost constitutes 29% of the total, comprising stack cost and balance of plant (BoP), indicating that advancements in PEM technology could enhance the economic feasibility of the process. The FA synthesis has a relatively smaller contribution to the overall cost (17%), with compressors and pumps being the most expensive components. The

Figure 6-9 indicates the critical areas where cost reductions can be most impactful. The prominence of electrolyser and DAC costs suggests that innovations in these technologies could not only reduce costs but also improve environmental performance by increasing efficiency and reducing energy consumption.

6.7.2. Operational expenses

The total OPEX for the PtFA plant is estimated at £11.2M annually. Figure 6-10 illustrates the breakdown of operational expenditures for the plant. Each bar represents the percentage contribution of various cost components to the total OPEX.

The catalyst cost is the primary factor influencing OPEX contributing around 50% of the total OPEX. This is due to the use of expensive ruthenium and phosphine catalysts, this contribution has been previously reported by Perez-Fortes et al., [48]. This indicates that catalyst costs are the most significant factor in the overall cost of the PtFA process. The high contribution suggests a need for innovations in catalyst technology or alternative catalyst to reduce this cost significantly. The next largest cost contributor is electricity sourced from the wind farm, accounting for 22% of the total OPEX. This result is expected given that electricity is a major energy input, particularly for powering the PEM electrolyser unit in the PtFA process.

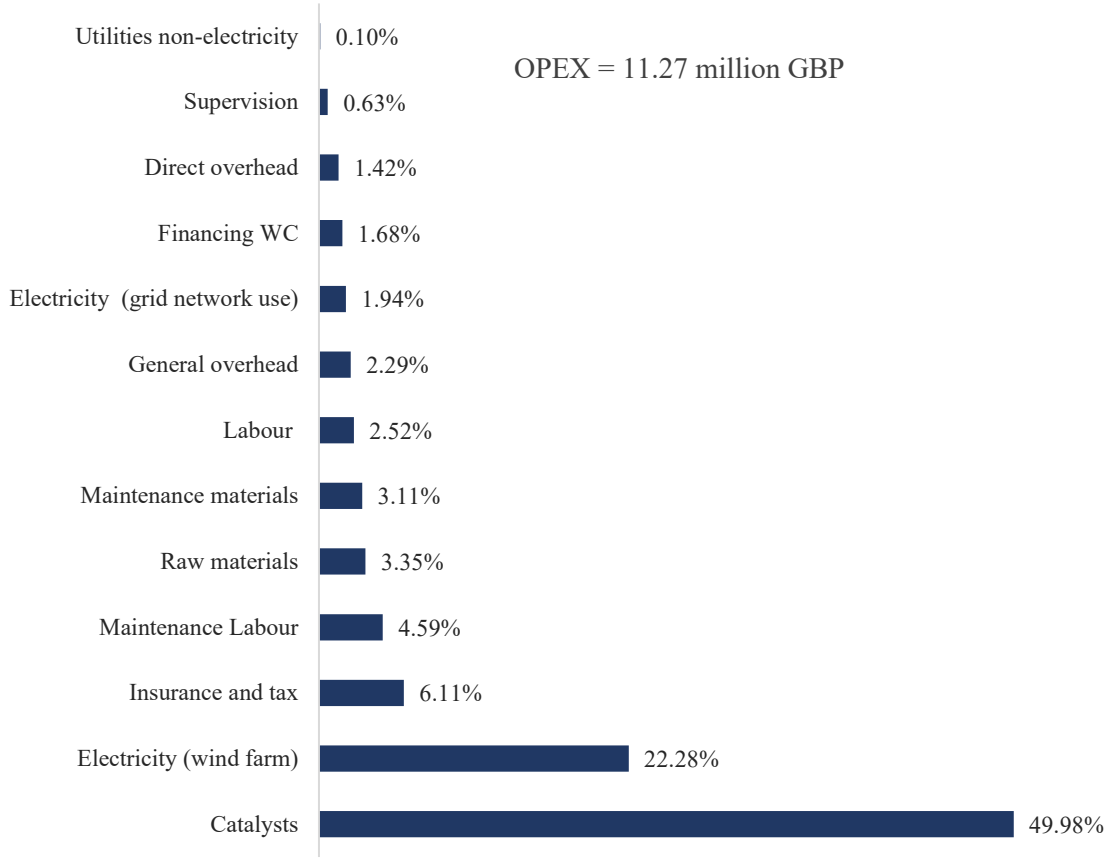

Figure 6-10. The breakdown of the OPEX.

The remaining 27.7% is distributed among various other costs. The cost of insurance and taxes, maintenance labour and materials, other raw materials such as methanol and the amine solvent, overhead, grid network use, supervision and other utilities such as processing water while not as substantial as electricity or catalysts, still represents a notable portion of the overall costs.

The prominent role of catalyst costs suggests that efforts should focus on exploring cost-effective catalyst alternatives. Various studies [142,227,228,241] are actively developing novel catalysts to optimize FA production and improve its economic performance, though the research is still in its early stages. The OPEX analysis presented here highlights critical areas where cost reductions can have a substantial impact, indicating that innovations in energy efficiency and catalyst technology could yield significant economic benefits.

6.7.3. Minimum selling price

The minimum selling price has been calculated through a break-even analysis. The minimum selling price of formic acid (MSP) has been estimated in £1,290 per tonne FA. This is 2.3 times higher than the market price in Europe of £560 (€650) per tonne [134]. This result indicates the production cost needs to be reduced to achieve a more competitive price. Formic acid production cost through PtX have been reported in a range of £802 - £1872 per tonne [48,134,144,145], where electricity, catalyst and the amine cost denote as the main contributors.

6.7.4. Sensitivity analysis

Figure 6-11 depicts the sensitivity results of the main parameters used in the economic analysis to the formic acid MSP. The parameters used for the base economic analysis are direct air capture capital expenditures (DAC-CAPEX), internal return rate, levelised cost of electricity (LCOE), PEM cost (installed) and oxygen selling price. Parameters have been varied in ±25% (grey bars) and ±50% (blue bars) of base value.

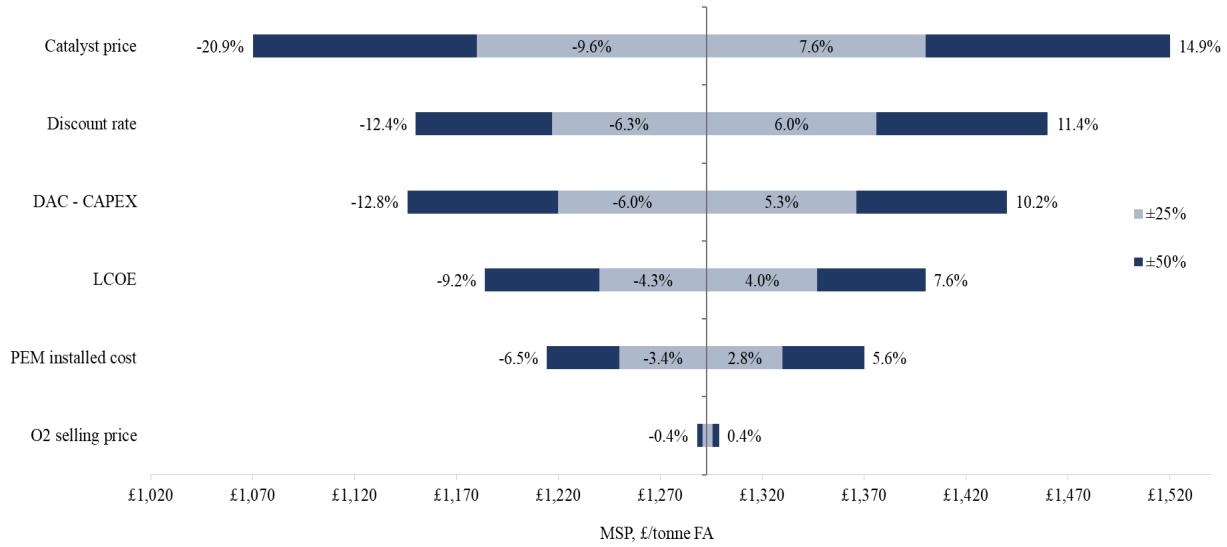

Figure 6-11. Economic sensitivity analysis on the MSP.

The catalyst price is the parameter with the most substantial impact on the MSP. Variations in the catalyst price cause the MSP to fluctuate between £1,070 and £1,520 per tonne when adjusted by ±50%. A change of ±25% in catalyst price affects the MSP in a range of £1180 - £1400 per tonne. These results evidenced the catalyst price as the most critical parameter among those evaluated. Additionally, both the discount rate and the DAC-CAPEX have comparable impacts on the MSP. When these parameters are adjusted by ±50% from the baseline, the MSP of formic acid ranges from £1,146 to £1,460 per tonne and from £1216 to £1376 per tonne when variation of ±25%. This highlights their substantial role in determining the overall production cost.

The LCOE has a moderate effect on the MSP, with the cost of formic acid ranging between £1,184 and £1,400 per tonne when the electricity price and network cost are varied by ±50%. For a ±25%, the MSP fluctuates between £1240 and £1347 per tonne. The variation in the installed cost of the PEM electrolyser shows a relatively low impact on the MSP, with the price of formic acid shifting from £1,214 to £1,288 per tonne when the baseline cost of £1,290 per tonne is modified ±50%. A change of ±25%, leads to the MSP ranging from £1250 to £1330 per tonne.

Lastly, the selling price of oxygen has the least impact on the MSP, with a change of only around ±0.4% from the baseline MSP of £1,290 per tonne. Even with a ±50% adjustment, the MSP remains virtually unchanged, reflecting the minor contribution of oxygen sales to the overall economics of the process.

6.7.5. Economies of scale

The individual scaling factors have been used to estimate the CAPEX to measure the effect of scale to the MSP of the FA. The OPEX has been calculated using the equation 3-5 for labour, while catalyst, raw materials and utilities are assumed to increase linearly to the different plant capacities. The capacities have been defined from 1 tonne/h to 200 tonne/h. Each capacity has been run in the system and the formic acid MSP was recalculated. Figure 6-12 illustrates the effect of economies of scale to the formic acid MSP.

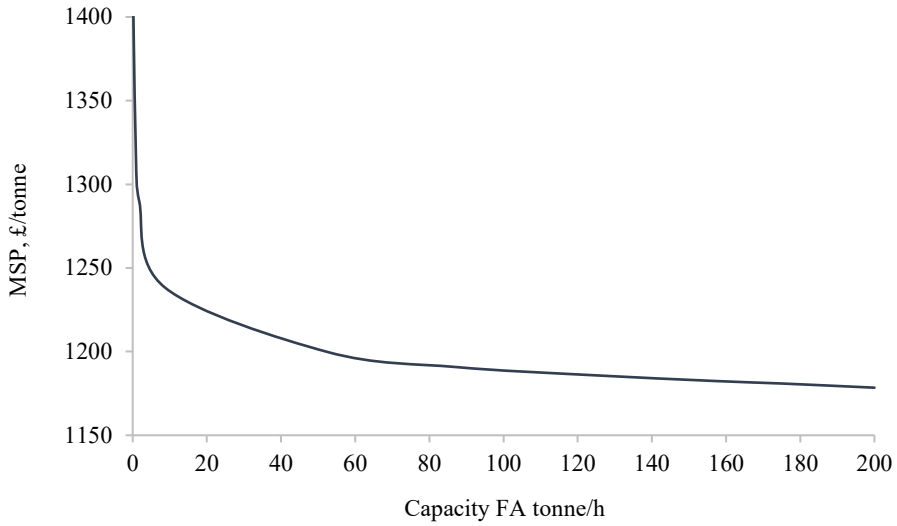

Figure 6-12. The economies of scale effect on the PtFA process.

At highest capacity (200 tonne/h) an 8.6% reduction in the MSP can be achieved. However, the MSP of formic acid stabilizes at price of 1180 £/tonne. As plant capacity increases, the anticipated cost reductions from scaling up become negligible. This is primarily because, beyond 80 tonne/h, the operating expenses (OPEX) dominate the overall costs, and their linear relationship with scale negates the advantages typically associated with larger operations. Consequently, the cost savings expected from economies of scale are not realized in these larger plants.

6.8. Life cycle assessment

In this section, the environmental impact of CCU-based formic acid is analysed and compared to fossil-based FA. The ReCiPe Midpoint (H) V1.13 impact calculation method was applied and estimated for the functional unit of 1 tonne of formic acid.

6.8.1. Life cycle inventory (LCI)

Table 6-12 presents the main inputs and outputs converted to the functional unit. It includes material and utility sources.

Table 6-12. Life cycle inventory of PtFA system.

Input/output	*Value*	*units*	*Source*
Electrolyser			
Deionised water	0.66	tonne	[152]
Electricity	3.99	MWh	[152]
Output			
Hydrogen	0.07	tonne	Aspen Plus
Oxygen	0.52	tonne	Aspen Plus
DAC system			
Electricity	0.08	MWh	Aspen Plus; [89]
Process water	4.79	tonne	Aspen Plus
$CaCO_3$ make-up	0.07	tonne	Aspen Plus
KOH make up	2.04E-4	tonne	Aspen Plus
Output			
CO_2	0.99	tonne	Aspen Plus
$CaCO_3$ disposal	0.07	tonne	Aspen Plus, [89]
KOH disposal	2.04E-4	tonne	Aspen Plus
FA synthesis			
CO_2	0.99	tonne	Input from DAC
H_2	0.07	tonne	Input from PEM
Methanol	0.06	tonne	Aspen Plus, [48]
Amine	0.01	tonne	Aspen Plus, [48]
Water	0.08	tonne	Aspen Plus, [48]
Electricity	0.43	MWh	Aspen Plus
Output			
FA	1	tonne	

6.8.2. Environmental impact results

The environmental impacts of FA production through green H_2 and DAC relative to 1 tonne of product are shown in Table 6-13.

The PtFA production process has a climate change of approximately 190 kg CO_{2e} per tonne of FA, a water use of 8.17 m^3 per tonne of FA, and a fossil depletion of 89.77 kg oil-equivalent per tonne of FA. When these impacts are compared to the conventional methyl formate route (as shown in Figure 6-13), CCU-based formic acid evidence to be more environmentally beneficial.

Table 6-13. Environmental impacts of formic acid through PtFA (FU: 1 tonne FA).

Impact category	*Unit*	*Total*
Climate change	kg CO_2 eq	173.6
Ozone depletion	kg CFC-11 eq	2.02E-05
Terrestrial acidification	kg SO2 eq	0.68
Freshwater eutrophication	kg P eq	0.01
Marine eutrophication	kg N eq	0.08
Human toxicity	kg 1,4-DB eq	43.0
Photochemical oxidant formation	kg NMVOC	0.60
Particulate matter formation	kg PM10 eq	0.35
Terrestrial ecotoxicity	kg 1,4-DB eq	0.02
Freshwater ecotoxicity	kg 1,4-DB eq	0.51
Marine ecotoxicity	kg 1,4-DB eq	0.53
Ionising radiation	kBq U235 eq	3.56
Agricultural land occupation	m^2a	3.87
Urban land occupation	m^2a	2.52
Natural land transformation	m^2	0.03
Water consumption	m^3	7.45
Metal depletion	kg Fe eq	60.5
Fossil depletion	kg oil eq	81.9

In Figure 6-13, the impact values for conventional fossil-based FA are set to 100%, and the CCU-based FA impacts are presented as relative emissions.

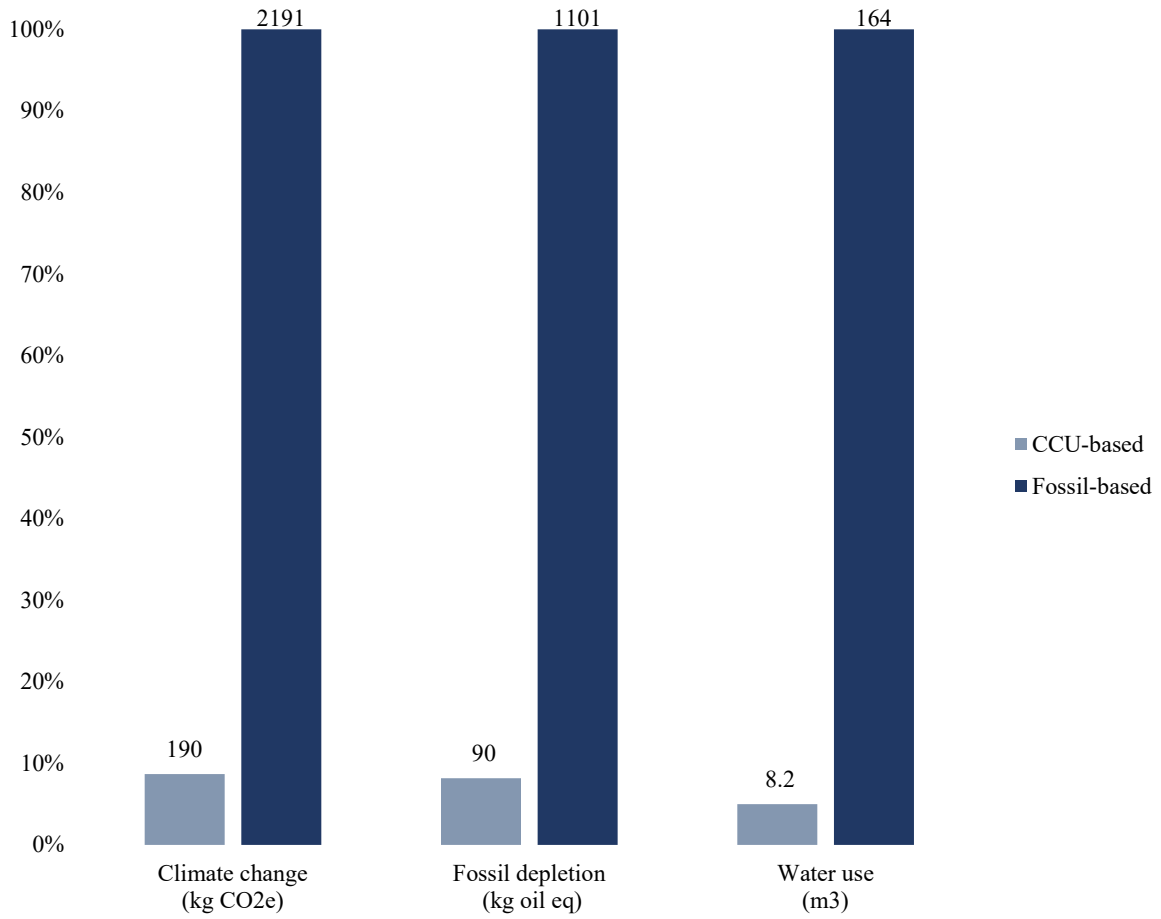

Figure 6-13. Climate change, fossil depletion and water consumption of CCU-based and fossil-based formic acid.

A reduction of more than 90% of the impacts is achieved by producing CCU-based formic acid compared to the conventional methyl formate route using fossil resources.

6.8.3. Climate change (CC)

The climate change impact as illustrated in Figure 6-13 results in 190 kg CO_{2e} per tonne of FA. A 92% less than conventional formic acid through methyl formate production process which exhibits a carbon emission of 2,191 kg CO_{2e} per tonne FA [238].

Figure 6-14 breaks down carbon emissions by stage and type. As shown, the climate change is primarily driven by fossil-derived chemical inputs in the DAC and FA synthesis stages, such as methanol, calcium carbonate, and tertiary amine that together contribute to nearly 60% of the total FA emissions. Although the quantities of these chemicals are relatively small, their contribution to the overall carbon emissions is significant because of the fossil consumption involved in their production. Additionally,

electricity consumption, which is dominant in the electrolyser stage, accounts for 36% of the total FA climate change, this is attributed to the materials employed in the offshore wind infrastructure.

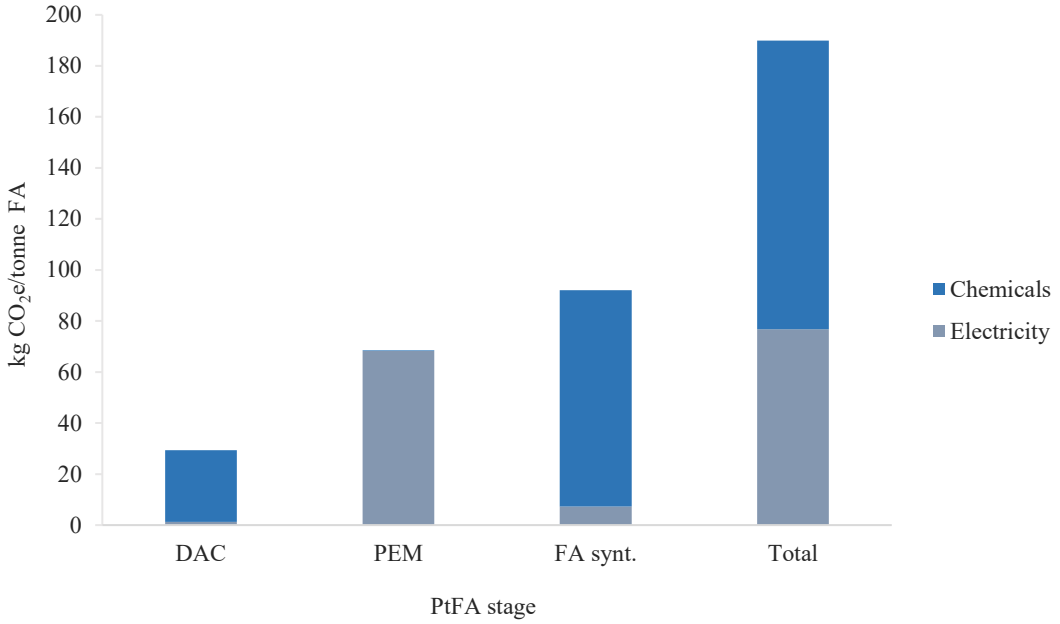

Figure 6-14. The climate change breakdown by stage and component.

One alternative to reduce chemical emissions in the PtFA is the utilisation of renewable methanol from the PtM (Power-to-Methanol) approach. For example, carbon emissions for green methanol have been reported to range from 19.1to 280 kg CO_{2e} per tonne methanol, for systems employing DAC and green hydrogen [113,242]. Incorporating this renewable methanol in the PtFA production process can further decrease the climate change impact of PtFA by 23% to 36%, respectively i.e., 154 and 139 kg CO_{2e}/tonne FA. However, due to variations in the technologies of methanol production and differences in the stages included or excluded, it is recommended to include a comprehensive simulation and LCA models when combining with PtFA, as their implications on other environmental and economic performances must be considered.

The GHG intensity of the electricity source is of prime importance due to its significant contribution to overall PtFA emissions. Consequently, a comparison of different electricity generation technology GHG intensities is shown in Figure 6-15. The assessed technologies include solar photovoltaics, hydro from reservoirs, offshore wind, and nuclear from pressurized water reactors. The carbon intensities of each source have been taken from the library of the SimaPro software for 1MWh of electricity in the UK, with the exception of solar and hydro based which are available for the rest of the world [238]. The bars in Figure

12 represent the GHG per tonne of formic acid, while the dots indicate the electricity carbon intensity (CI) of each energy source in kg CO_{2e} per kWh.

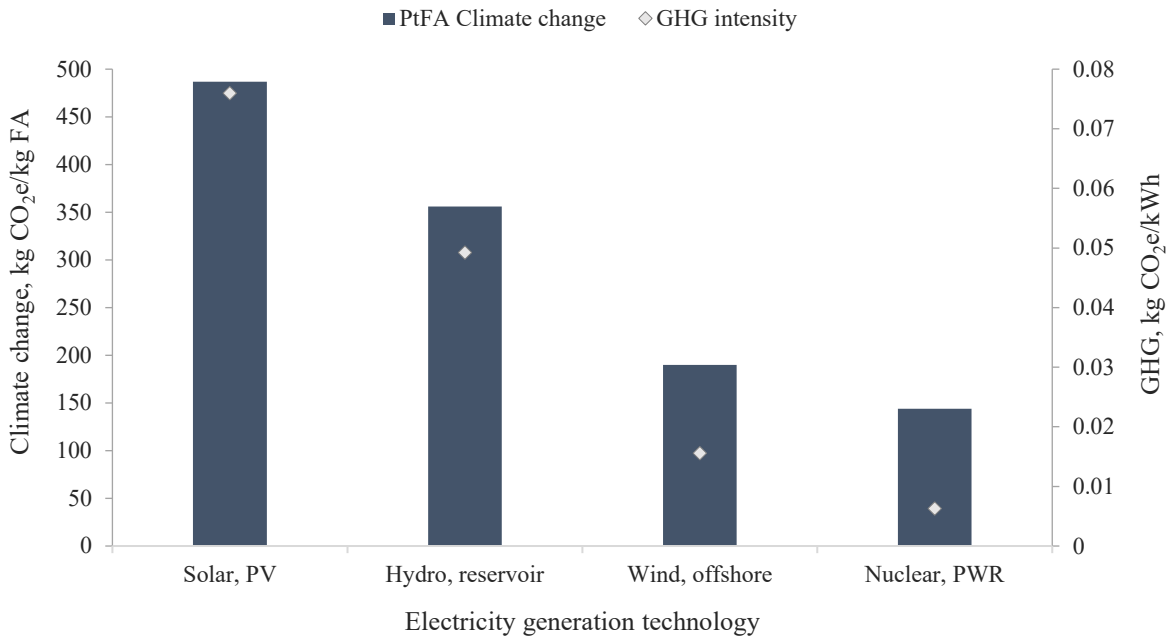

Figure 6-15. Effect of the energy carbon intensity on the global warming potential of PtFA.

Electricity generation technology with low GHG intensity, such as nuclear power, reduces the climate change of PtFA from 190 to 112 kg CO_{2e} per tonne of FA, a 41% reduction compared to offshore wind. Conversely, if solar energy is used, emissions increase by approximately 124%, reaching 425 kg CO_{2e} per tonne of FA. The choice of electricity source is highly location dependent. Therefore, countries with developed nuclear energy infrastructure benefit from significantly lower carbon emissions.

6.8.4. Fossil depletion (FD)

The PtFA process has a fossil depletion of approximately 90 kg oil-e per tonne of FA, with around 71% attributed to FA synthesis. This is primarily due to the methanol and amine chemicals, sourced from non-renewable resources, which, despite their small quantities, significantly impact the system's environmental performance. One way to reduce the use of fossil resources in the PtFA process is by incorporating green methanol. Conversely, the conventional fossil methyl formate route involves higher fossil depletion due to the primary use of methanol and CO as feedstock, which are derived from fossil sources. This leads to significant consumption of oil resources, as shown in Figure 6-13. Other studies have reported similar results, for instance, Ahn et al., [243] evaluated a CCU formic acid production pathway

against conventional. The results showed fossil depletion of CCU around 28% compared to conventional due to the feedstock. The difference is caused by the use of non-renewable energy in the CCU model. Kang, et al., [54] reported catalytic method strategy had lower FD compared to conventional strategy (0.23 vs 0.83 kg oil-e/kg FA).

6.8.5. Water consumption

Water use is an important indicator of the environmental performance in a sustainable project. The investigated CCU-based formic acid consumes around 8.2 m^3 water per tonne FA. The main contributor of this is the DAC with 68% of total. The use of non-renewable chemicals such as methanol, the tertiary amine led to a higher consumption in water that comes primary from fossil chemicals. Compared to the conventional production method, CCU-based formic acid consumes 95.4% less water, this is because in the conventional method, the water accounts for the feedstock coming from non-renewables including electricity.

6.8.6. Other environmental impact categories

Figure 6-16 compares the environmental impact categories of CCU and fossil - based FA production method across various categories. The axis represents a different category, the fossil-based FA has been set as 100% while the CCU-based FA is calculated as relative emissions.

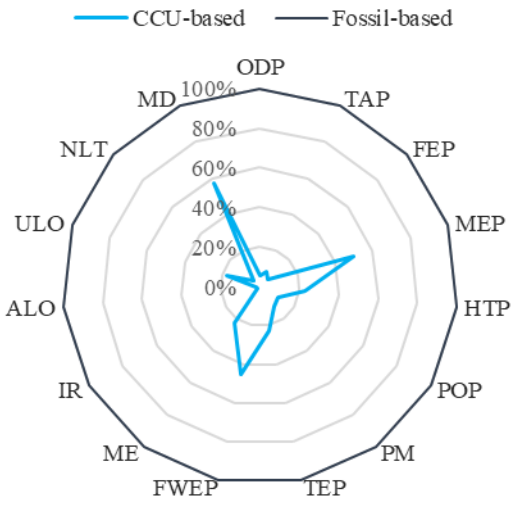

Figure 6-16. Relative comparison of the environmental impacts of CCU-based (blue line) with the fossil-based formic acid (black line).

The CCU-based formic acid under the PtFA production process is more environmentally friendly compared to the conventional fossil-based method, including TAP, FEP, HTP, POP, PM, TEP, ME, IR,

ALO, ULO, and NLT. The categories that do not show a substantial reduction are MD, FWEP, and MEP which are likely influenced by specific materials like chromium utilised in the electricity production. Overall, the CCU-based formic acid through PtFA performs better environmentally, highlighting the benefits of using renewable sources and complete heat integration in the production process.

In addition to mitigating climate change, these results underscore the potential of the PtFA process to reduce water consumption, fossil depletion and other environmental impacts compared to fossil-based FA production.

6.9. Conclusions of PtFA

The study is the first attempt to holistically assess the economic and environmental feasibility of a PtFA assembly that includes a DAC unit, a PEM electrolyser and catalytic synthesis of FA through CO_2 hydrogenation. It includes exhaustive process modelling and heat integration, techno-economic assessment and a cradle to gate LCA. The PtFA process achieves an overall carbon efficiency of 73.4%. Most carbon losses occur in the DAC unit, due to the CO_2 capture efficiency of 75% [89]. Additionally, it requires 1.01 tonne of CO_2 to produce 1 tonne of formic acid. The DAC heat requirement, 1.87 MWh per tonne of CO_2, was met internally through heat integration, eliminating the need for external fossil fuels. The specific energy consumption of the entire PtFA system is lower than that of fossil-based production, because only electricity is used whereas a large amount of steam is employed in the fossil-based system.

A standard discounted cash flow analysis indicates that the minimum selling price (MSP) of the PtFA is twice as the conventional FA, at £1,290 per tonne compared to £560 (€650) per tonne. The sensitivity analysis revealed that catalyst costs and electricity costs are the primary cost drivers. Thus, efforts should be focused on cost-effective catalyst alternatives. A cradle-to-gate life cycle assessment (LCA) estimated that the PtFA process significantly reduces carbon emissions, lowering the climate change by 95% compared to fossil-based production. The primary sources of carbon emissions were formic acid synthesis due to the non-renewable methanol employed and the electricity in the electrolysis, which together accounted for around 85% of the carbon emissions. Additionally, the CCU-based formic acid process has the potential to reduce water and fossil resource depletion by more than 90% compared to fossil-based formic acid production.

The study proposed and evaluated an innovative, integrated design for a low-carbon formic acid synthesis route, aiding the research on defossilising the chemical industry. The results can guide policy formulation and engineering decisions

Chapter VII

7. Conclusion and recommendations

This study presents a critical assessment of three innovative, integrated power-to-chemical processes specifically power-to-olefins (PtO), power-to-ammonia (PtA), and power-to-formic acid (PtFA) that aim to be a more sustainable option for defossilising the chemical industry. Every PtX scenario offers significant environmental benefits, particularly in terms of reducing greenhouse gas emissions and improving carbon efficiency. The integration of direct air capture (DAC), electrolytic hydrogen from offshore wind, and heat recovery highlights the potential of these processes to contribute to a low-carbon future. However, the economic feasibility of these pathways remains a key challenge, with electricity costs, CO_2 capture efficiency, and catalyst expenses emerging as the primary economic drivers. Achieving competitive market prices will require significant reductions in energy costs, advancements in renewable infrastructure, and supportive policies.

The first case study presents a comprehensive and detailed model for the power-to-olefins (PtO) process, integrating direct air capture (DAC) and electrolytic hydrogen production powered by offshore wind farms. The PtO pathway represents a promising approach to decarbonizing the chemical industry, however, data on its economic and environmental performance remain limited. Most existing studies on power-to-olefins typically exclude critical components such as CO_2 capture and hydrogen production, focusing only on the olefin synthesis. This study, in contrast, provides a more holistic "cradle-to-gate" assessment, evaluating the entire process, from CO_2 capture and hydrogen generation to olefin synthesis, while also considering full heat integration opportunities between DAC and olefins synthesis by utilising co-products such as C4+ olefins as a source of energy in the most intensive unit. In addition, the ethylene and propylene have been utilised in the refrigerant cycle, reducing costs and emissions by the use of these components.

The power-to-olefins (PtO) process is effective in reducing carbon emissions, with a carbon efficiency of 72.3%. Most carbon losses occur during CO_2 capture, because of the low efficiency of the DAC system. Thus, the efficiency of the DAC system is one of the most important parameters that can offer the major benefits for the CCU. On the other hand, the process eliminates the need for external energy sources like fossil fuels, thanks to its internal heat recovery system. However, one significant challenge is the high energy demand, particularly from the electrolyser, which consumes much more electricity compared to traditional methods of producing olefins. This is because of the efficiency of the PEM unit. Similar to the DAC efficiency, the PEM efficiency is considered low (75%). Despite the energy lost in the form of heat

is recovered in the organic Rankine cycle, the amount of energy required is massive. One recommendation is to analyse the emissions of the PTO using different electrolyser systems with higher efficiency such as a solid oxide or the alkaline electrolyser.

Economically, the cost of producing olefins using the PtO process is significantly higher than conventional methods, and this is mainly due to the high electricity and CO_2 capture costs. The minimum selling price for PtO-derived olefins is more than triple that of traditional ethylene. On the other hand, the process shows significant environmental benefits, reducing greenhouse gas emissions by 47%. With improvements in the decarbonisation of the energy supply, especially in wind power, emission reductions could increase to 69%.

A second study on Power-to-Ammonia presents an integrated life cycle assessment and technoeconomic analysis for ammonia production, encompassing both nitrogen and hydrogen synthesis. The model is heavily dependent on electricity consumption, with the primary inputs derived from renewable sources, such water and air. While these renewable sources are environmentally favourable, they still require substantial electricity inputs to be transformed, which can significantly impact the overall resource demand.

The economic analysis reveals that the choice of low-cost electricity source plays a critical role in reducing ammonia production costs. However, achieving such low electricity costs would necessitate specific conditions, such as the development of advanced renewable energy infrastructure and the implementation of supportive government policies that promote low-cost, reliable power supplies. The research also highlighted the need to address the low efficiency of the electrolyser in order to improve the future performance. Despite thermodynamic limitations, enhancing the efficiency of hydrogen production could lead to a significant reduction in ammonia costs, making the process more economically competitive.

From a sustainability perspective, the Power-to-Ammonia process has emerged as a promising low-carbon emission pathway for ammonia production. By utilizing renewable energy sources, it significantly reduces the carbon footprint compared to traditional ammonia production methods, such as those relying on natural gas such as steam methane reforming. However, while the process relies on renewable electricity, it is important to recognize that embedded emissions still exist, particularly in the construction and operation of offshore wind turbines. These emissions, though smaller than those from fossil-based ammonia production, indicate that the Power-to-Ammonia process is not entirely free from environmental impact. Given that the Power-to-Ammonia process is highly reliant on electricity, future research should prioritize several key areas to improve its sustainability. First, energy integration will be critical in optimizing the overall efficiency of the system. Second, enhancing the reaction efficiency in the ammonia synthesis

process can have a significant impact. Improvements in catalytic processes, reaction conditions, and system design could reduce the energy consumption, which results in a more efficient process. Finally, the integration of low-carbon power options is essential for maximizing the sustainability of PtA. Research into alternative renewable energy sources, such as solar, geothermal, or advanced nuclear energy, could enhance environmental performance.

In the third case study, the production of formic acid via the Power-to-Formic Acid (PtFA) process is evaluated. The simulation model developed for this study incorporates both CO_2 capture and utilization, as well as the production of green hydrogen through water electrolysis. This chapter represents the first attempt to comprehensively assess the thermochemical conversion route for formic acid production, a topic that has been underexplored in the literature. Most existing studies primarily focus on electrochemical routes for formic acid production, evaluating their environmental and economic impacts using literature data. This is largely due to the limited availability of data on formic acid thermochemical synthesis.

A few studies have attempted to model formic acid production using patented data to better understand the practical challenges and opportunities of thermochemical synthesis. Our research aims to fill the gap by offering a detailed integrated analysis of both the economic and environmental implications of the thermochemical route for PtFA. The results highlight significant challenges in achieving economic feasibility, with the model indicating a minimum selling price (MSP) that exceeds the current market price for formic acid. The key factors that contribute to this issue include the technology maturity, high catalyst costs, and the lack of sufficient incentives for the adoption of renewable technologies. In particular, the high cost of catalysts in the thermochemical process indicated FA is economically unviable at present, making it clear that further innovation is required in catalyst development.

On the environmental side, the study reveals that carbon capture and utilization (CCU)-based formic acid production has significant potential for emissions mitigation. When compared to traditional fossil-based methods, the PtFA process can reduce CO2 emissions, water usage, and resource consumption by up to 90%. This demonstrates the substantial environmental benefits that can be achieved by shifting to a Power-to-X (PtX) approach for the production of chemicals such as formic acid. Furthermore, if the process is coupled with a low-carbon power source, such as nuclear energy, the reduction in carbon emissions could be even more noticeable, denoting PtFA a promising pathway for decarbonizing the chemical industry.

This study makes a meaningful contribution to the ongoing effort to decarbonize the chemical industry by proposing and evaluating an integrated, low-carbon synthesis route for olefins, ammonia and formic acid. The results provide valuable insights that can inform both policy and engineering decisions,

particularly in relation to reducing the carbon footprint of chemical production and advancing the development of sustainable industrial processes. Some recommendations for this system are as follows:

1. Reduce electricity costs: Focus on lowering the cost of renewable energy to make the PtX process more economically competitive.
2. Improve CO_2 capture efficiency: Increasing the effectiveness of CO_2 capture technology will reduce carbon losses and overall process costs. This implies more challenges around carbon capture systems design; however it is a parameter of primal importance in the reduction of the final production cost.
3. Invest in renewable infrastructure: Continued decarbonisation of energy sources, particularly wind energy, is essential to maximizing the environmental benefits of every PtX scenario.
4. Investigate a more cost-effective catalyst and enhance reactors efficiency to reduce operational expenses. Especially in formic acid production where this is the main driver of the cost.
5. Supportive policy and incentives: Government policies that support low-carbon technologies, such as subsidies or carbon pricing, could help bridge the cost gap between PtX and conventional methods.

The three scenarios presented in this thesis demonstrated the technical feasibility of the technological routes, suggesting that PtX could become a reality. However, challenges to the economic feasibility of PtX processes were also highlighted, restricting from the technical and economic limitations discussed earlier. Environmentally, these scenarios emphasized the potential of PtX technologies as key strategies for carbon mitigation, indicating significant progress toward achieving net-zero sustainability goals. While further research is recommended, this study has established the basis for identifying the critical "hotspots" in each scenario and this serves as a starting point for future improvements. Additionally, it gives valuable insights into other environmental impacts that must be considered alongside carbon emissions, underscoring the broader environmental considerations needed for comprehensive sustainability analysis.

References

[1] Obrist MD, Kannan R, Schmidt TJ, Kober T. Decarbonization pathways of the Swiss cement industry towards net zero emissions. J Clean Prod 2021;288:125413. https://doi.org/10.1016/j.jclepro.2020.125413.

[2] Freire Ordóñez D, Shah N, Guillén-Gosálbez G. Economic and full environmental assessment of electrofuels via electrolysis and co-electrolysis considering externalities. Appl Energy 2021;286:116488. https://doi.org/10.1016/j.apenergy.2021.116488.

[3] Kolosz BW, Luo Y, Xu B, Maroto-Valer MM, Andresen JM. Life cycle environmental analysis of "drop in" alternative aviation fuels: A review. Sustain Energy Fuels 2020;4:3229–63. https://doi.org/10.1039/c9se00788a.

[4] IEA. Transforming Industry through CCUS M a y 2 0 1 9. Int Energy Agency 2019;https://ww:1–58.

[5] IEA. Direct CO2 emissions from primary chemical production in the Net Zero Scenario, 2010-2030 2023. https://www.iea.org/data-and-statistics/charts/direct-co2-emissions-from-primary-chemical-production-in-the-net-zero-scenario-2010-2030-2.

[6] Finkbeiner M, Bach V. Life cycle assessment of decarbonization options-towards scientifically robust carbon neutrality. Int J Life Cycle Assess 2021;26:635–9. https://doi.org/10.1007/s11367-021-01902-4.

[7] Ostadi M, Paso KG, Rodriguez-Fabia S, Øi LE, Manenti F, Hillestad M. Process integration of green hydrogen: Decarbonization of chemical industries. Energies 2020;13:4859. https://doi.org/10.3390/en13184859.

[8] Wulf C, Linßen J, Zapp P. Review of power-to-gas projects in Europe. Energy Procedia, vol. 155, Elsevier Ltd; 2018, p. 367–78. https://doi.org/10.1016/j.egypro.2018.11.041.

[9] de Vasconcelos BR, Lavoie JM. Recent advances in power-to-X technology for the production of fuels and chemicals. Front Chem 2019;7:1–24. https://doi.org/10.3389/fchem.2019.00392.

[10] Ince AC, Colpan CO, Hagen A, Serincan MF. Modeling and simulation of Power-to-X systems: A review. Fuel 2021;304:121354. https://doi.org/10.1016/j.fuel.2021.121354.

[11] Daiyan R, Macgill I, Amal R. Opportunities and Challenges for Renewable Power-to-X. ACS Energy Lett 2020;5:3843–7. https://doi.org/10.1021/acsenergylett.0c02249.

[12] Wulf C, Zapp P, Schreiber A. Review of Power-to-X Demonstration Projects in Europe. Front Energy Res 2020;8:191. https://doi.org/10.3389/fenrg.2020.00191.

[13] Dahiru AR, Vuokila A, Huuhtanen M. Recent development in Power-to-X: Part I - A review on techno-economic analysis. J Energy Storage 2022;56:105861. https://doi.org/10.1016/j.est.2022.105861.

[14] Pérez-Fortes M, Bocin-Dumitriu A, Tzimas E. CO2 utilization pathways: Techno-economic assessment and market opportunities. Energy Procedia 2014;63:7968–75. https://doi.org/10.1016/j.egypro.2014.11.834.

[15] Dimitriou I, García-Gutiérrez P, Elder RH, Cuéllar-Franca RM, Azapagic A, Allen RWK. Carbon dioxide utilisation for production of transport fuels: Process and economic analysis. Energy Environ Sci 2015;8:1775–89. https://doi.org/10.1039/c4ee04117h.

[16] Okesola AA, Oyedeji AA, Abdulhamid AF, Olowo J, Ayodele BE, Alabi TW. Direct Air Capture: A Review of Carbon Dioxide Capture from the Air. IOP Conf Ser Mater Sci Eng 2018;413:012077. https://doi.org/10.1088/1757-899X/413/1/012077.

[17] Pérez-Fortes M, Bocin-Dumitriu A, Tzimas E. CO2 utilization pathways: Techno-economic assessment and market opportunities. Energy Procedia 2014;63:7968–75. https://doi.org/10.1016/j.egypro.2014.11.834.

[18] Aldaco R, Butnar I, Margallo M, Laso J, Rumayor M, Dominguez-Ramos A, et al. Bringing value to the chemical industry from capture, storage and use of CO 2 : A dynamic LCA of formic acid production. Sci Total Environ 2019;663:738–53. https://doi.org/10.1016/j.scitotenv.2019.01.395.

[19] IEA. Putting CO 2 to Use Creating value from emissions. Int Energy Agency 2019;https://ww.

[20] Saad DM, Bilbeisi RA, Alnouri SY. Optimizing network pathways of CO2conversion processes. J CO2 Util 2021;45:101433. https://doi.org/10.1016/j.jcou.2020.101433.

[21] Ganesh I. Conversion of carbon dioxide into methanol - A potential liquid fuel: Fundamental challenges and opportunities (a review). Renew Sustain Energy Rev 2014;31:221–57. https://doi.org/10.1016/j.rser.2013.11.045.

[22] Zhang C, Jun KW, Gao R, Kwak G, Park HG. Carbon dioxide utilization in a gas-to-methanol process combined with CO2/Steam-mixed reforming: Techno-economic analysis. Fuel 2017;190:303–11. https://doi.org/10.1016/j.fuel.2016.11.008.

[23] Dutta A, Karimi IA, Farooq S. Technoeconomic Perspective on Natural Gas Liquids and Methanol as Potential Feedstocks for Producing Olefins. Ind Eng Chem Res 2019;58:963–72. https://doi.org/10.1021/acs.iecr.8b05277.

[24] IEA. The future of petrochemicals. Int Energy Agency 2018. https://doi.org/10.1787/9789264307414-en.

[25] GPCA. Ethylene: a litmus test for the chemical industry. Gulf Petrochemicals Chem Assoc 2019:8.

[26] Chung C, Kim J, Sovacool BK, Bazilian M, Griffiths S, Yang M. Decarbonizing chemical industry: A systematic review of sociotechnical systems, technological innovations, and policy options. Energy Res Soc Sci 2023;89:102955. https://doi.org/10.1016/j.erss.2022.102565.

[27] Reyniers PA, Vandewalle LA, Saerens S, de Smedt P, Marin GB, Van Geem KM. Techno-economic analysis of an absorption based methanol to olefins recovery section. Appl Therm Eng 2017;115:477–90. https://doi.org/10.1016/j.applthermaleng.2016.12.124.

[28] Chisalita DA, Petrescu L, Cormos CC. Environmental evaluation of european ammonia production considering various hydrogen supply chains. Renew Sustain Energy Rev 2020;130:109964. https://doi.org/10.1016/j.rser.2020.109964.

[29] Pfromm PH. Towards sustainable agriculture: Fossil-free ammonia. J Renew Sustain Energy 2017;9:034702. https://doi.org/10.1063/1.4985090.

[30] Chehade G, Dincer I. Progress in green ammonia production as potential carbon-free fuel. Fuel 2021;299:120845. https://doi.org/10.1016/j.fuel.2021.120845.

[31] Zhang H, Wang L, Van herle J, Maréchal F, Desideri U. Techno-economic comparison of green ammonia production processes. Appl Energy 2020;259:114135. https://doi.org/10.1016/j.apenergy.2019.114135.

[32] Kurien C, Mittal M. Review on the production and utilization of green ammonia as an alternate fuel in dual-fuel compression ignition engines. Energy Convers Manag 2022;251:114990. https://doi.org/10.1016/j.enconman.2021.114990.

[33] Sadeek S, Lee Chan T, Ramdath R, Rajkumar A, Guo M, Ward K. The influence of raw material availability and utility power consumption on the sustainability of the ammonia process. Chem Eng Res Des 2020;158:177–92. https://doi.org/10.1016/j.cherd.2020.03.020.

[34] Egerer J, Grimm V, Niazmand K, Runge P. The economics of global green ammonia trade – "Shipping Australian wind and sunshine to Germany." Appl Energy 2023;334:120662. https://doi.org/10.1016/j.apenergy.2023.120662.

[35] Liu X, Elgowainy A. Life-Cycle Analysis of Green Ammonia and its Application as Fertilizer Building Block. Ammon Energy Conf 2019 2019;1.

[36] Bellotti D, Rivarolo M, Magistri L. A comparative techno-economic and sensitivity analysis of Power-to-X processes from different energy sources. Energy Convers Manag 2022;260:115565. https://doi.org/10.1016/j.enconman.2022.115565.

[37] Olabi AG, Abdelkareem MA, Al-Murisi M, Shehata N, Alami AH, Radwan A, et al. Recent progress in Green Ammonia: Production, applications, assessment; barriers, and its role in achieving the sustainable development goals. Energy Convers Manag 2023;277:116594. https://doi.org/10.1016/j.enconman.2022.116594.

[38] Fothergill K, Greenwood S, Makepeace J, Wilkinson I, Jackson C, Davenne T, et al. Ammonia to green hydrogen project. Feasibility Study 2020;33:1–70.

[39] Zhang H, Wang L, Van herle J, Maréchal F, Desideri U. Techno-economic comparison of green ammonia production processes. Appl Energy 2020;259:114135. https://doi.org/10.1016/j.apenergy.2019.114135.

[40] Valera-Medina A, Xiao H, Owen-Jones M, David WIF, Bowen PJ. Ammonia for power. Prog Energy Combust Sci 2018;69:63–102. https://doi.org/10.1016/j.pecs.2018.07.001.

[41] Liu X, Li S, Liu Y, Cao Y. Formic acid: A versatile renewable reagent for green and sustainable chemical synthesis. Cuihua Xuebao/Chinese J Catal 2015;36:1461–75. https://doi.org/10.1016/S1872-2067(15)60861-0.

[42] Supronowicz W, Ignatyev IA, Lolli G, Wolf A, Zhao L, Mleczko L. Formic acid: A future bridge between the power and chemical industries. Green Chem 2015;17:2904–11. https://doi.org/10.1039/c5gc00249d.

[43] Dutta I, Chatterjee S, Cheng H, Parsapur RK, Liu Z, Li Z, et al. Formic Acid to Power towards Low-Carbon Economy. Adv Energy Mater 2022;12:1–17. https://doi.org/10.1002/aenm.202103799.

[44] Kim C, Lee Y, Kim K, Lee U. Implementation of Formic Acid as a Liquid Organic Hydrogen Carrier (LOHC): Techno-Economic Analysis and Life Cycle Assessment of Formic Acid

Produced via CO2 Utilization. Catalysts 2022;12:1–7. https://doi.org/10.3390/catal12101113.

[45] Solakidou M, Gemenetzi A, Koutsikou G, Theodorakopoulos M, Deligiannakis Y, Louloudi M. Cost Efficiency Analysis of H2 Production from Formic Acid by Molecular Catalysts. Energies 2023;16:1723. https://doi.org/10.3390/en16041723.

[46] Singh AK, Singh S, Kumar A. Hydrogen energy future with formic acid: A renewable chemical hydrogen storage system. Catal Sci Technol 2016;6:12–40. https://doi.org/10.1039/c5cy01276g.

[47] ChemAnalyst. Formic Acid Price Trend Forecast 2022. https://www.chemanalyst.com/Pricing-data/formic-acid-1242 (accessed May 4, 2024).

[48] Pérez-Fortes M, Schöneberger JC, Boulamanti A, Harrison G, Tzimas E. Formic acid synthesis using CO2 as raw material: Techno-economic and environmental evaluation and market potential. Int J Hydrogen Energy 2016;41:16444–62. https://doi.org/10.1016/j.ijhydene.2016.05.199.

[49] Chauvy R, De Weireld G. CO2 Utilization Technologies in Europe: A Short Review. Energy Technol 2020;8:1–17. https://doi.org/10.1002/ente.202000627.

[50] Artz J, Müller TE, Thenert K, Kleinekorte J, Meys R, Sternberg A, et al. Sustainable Conversion of Carbon Dioxide: An Integrated Review of Catalysis and Life Cycle Assessment. Chem Rev 2018;118:434–504. https://doi.org/10.1021/acs.chemrev.7b00435.

[51] Rumayor M, Dominguez-Ramos A, Irabien A. Formic Acid manufacture: Carbon dioxide utilization alternatives. Appl Sci 2018;8:1–12. https://doi.org/10.3390/app8060914.

[52] Chatterjee S, Dutta I, Lum Y, Lai Z, Huang KW. Enabling storage and utilization of low-carbon electricity: Power to formic acid. Energy Environ Sci 2021;14:1194–246. https://doi.org/10.1039/d0ee03011b.

[53] Rumayor M, Dominguez-Ramos A, Perez P, Irabien A. A techno-economic evaluation approach to the electrochemical reduction of CO2 for formic acid manufacture. J CO2 Util 2019;34:490–9. https://doi.org/10.1016/j.jcou.2019.07.024.

[54] Kang D, Byun J, Han J. Evaluating the environmental impacts of formic acid production from acid production from CO2: Catalytic hydrogenation: Vs. electrocatalytic reduction. Green Chem 2021;23:9470–8. https://doi.org/10.1039/d1gc02997e.

[55] Thonemann N, Schulte A. From Laboratory to Industrial Scale: A Prospective LCA for Electrochemical Reduction of CO2 to Formic Acid. Environ Sci Technol 2019;53:12320–9.

https://doi.org/10.1021/acs.est.9b02944.

[56] Banu A, Mir N, Ewis D, El-Naas MH, Amhamed AI, Bicer Y. Formic acid production through electrochemical reduction of CO2: A life cycle assessment. Energy Convers Manag X 2023;20:100441. https://doi.org/10.1016/j.ecmx.2023.100441.

[57] Gao T, Xia B, Yang K, Li D, Shao T, Chen S, et al. Techno-economic Analysis and Carbon Footprint Accounting for Industrial CO2 Electrolysis Systems. Energy and Fuels 2023;37:17997–8008. https://doi.org/10.1021/acs.energyfuels.3c01581.

[58] Von Der Assen N, Jung J, Bardow A. Life-cycle assessment of carbon dioxide capture and utilization: Avoiding the pitfalls. Energy Environ Sci 2013;6:2721–34. https://doi.org/10.1039/c3ee41151f.

[59] Müller LJ, Kätelhön A, Bringezu S, McCoy S, Suh S, Edwards R, et al. The carbon footprint of the carbon feedstock CO2. Energy Environ Sci 2020;13:2979–92. https://doi.org/10.1039/d0ee01530j.

[60] Von Der Assen N, Voll P, Peters M, Bardow A. Life cycle assessment of CO2 capture and utilization: A tutorial review. Chem Soc Rev 2014;43:7982–94. https://doi.org/10.1039/c3cs60373c.

[61] Pérez-Fortes M, Bocin-Dumitriu A, Tzimas E. CO2 utilization pathways: Techno-economic assessment and market opportunities. Energy Procedia, vol. 63, Elsevier Ltd; 2014, p. 7968–75. https://doi.org/10.1016/j.egypro.2014.11.834.

[62] Neuling U, Kaltschmitt M. Techno-economic and environmental analysis of aviation biofuels. Fuel Process Technol 2018;171:54–69. https://doi.org/10.1016/j.fuproc.2017.09.022.

[63] Vázquez FV, Koponen J, Ruuskanen V, Bajamundi C, Kosonen A, Simell P, et al. Power-to-X technology using renewable electricity and carbon dioxide from ambient air: SOLETAIR proof-of-concept and improved process concept. J CO2 Util 2018;28:235–46. https://doi.org/10.1016/j.jcou.2018.09.026.

[64] Antonini C, Treyer K, Streb A, van der Spek M, Bauer C, Mazzotti M. Hydrogen production from natural gas and biomethane with carbon capture and storage - A techno-environmental analysis. Sustain Energy Fuels 2020;4:2967–86. https://doi.org/10.1039/d0se00222d.

[65] Sunny N, Mac Dowell N, Shah N. What is needed to deliver carbon-neutral heat using hydrogen and CCS? Energy Environ Sci 2020;13:4204–24. https://doi.org/10.1039/d0ee02016h.

[66] Shiva Kumar S, Himabindu V. Hydrogen production by PEM water electrolysis – A review. Mater Sci Energy Technol 2019;2:442–54. https://doi.org/10.1016/j.mset.2019.03.002.

[67] Millet P. Fundamentals of Water Electrolysis. Hydrog Prod By Electrolysis 2015;2:33–62. https://doi.org/10.1002/9783527676507.ch2.

[68] Li W, Tian H, Ma L, Wang Y, Liu X, Gao X. Low-temperature water electrolysis: fundamentals, progress, and new strategies. Mater Adv 2022;3:5598–644. https://doi.org/10.1039/d2ma00185c.

[69] Gahleitner G. Hydrogen from renewable electricity: An international review of power-to-gas pilot plants for stationary applications. Int J Hydrogen Energy 2013;38:2039–61. https://doi.org/10.1016/j.ijhydene.2012.12.010.

[70] Götz M, Lefebvre J, Mörs F, McDaniel Koch A, Graf F, Bajohr S, et al. Renewable Power-to-Gas: A technological and economic review. Renew Energy 2016;85:1371–90. https://doi.org/10.1016/j.renene.2015.07.066.

[71] Zeng K, Zhang D. Recent progress in alkaline water electrolysis for hydrogen production and applications. Prog Energy Combust Sci 2010;36:307–26. https://doi.org/10.1016/j.pecs.2009.11.002.

[72] Carmo M, Fritz DL, Mergel J, Stolten D. A comprehensive review on PEM water electrolysis. Int J Hydrogen Energy 2013;38:4901–34. https://doi.org/10.1016/j.ijhydene.2013.01.151.

[73] Deka DJ, Gunduz S, Kim J, Fitzgerald T, Shi Y, Co AC, et al. Hydrogen Production from Water in a Solid Oxide Electrolysis Cell: Effect of Ni Doping on Lanthanum Strontium Ferrite Perovskite Cathodes. Ind Eng Chem Res 2019;58:22497–22505. https://doi.org/10.1021/acs.iecr.9b03731.

[74] Galadima A, Muraza O. Catalytic thermal conversion of CO2 into fuels: Perspective and challenges. Renew Sustain Energy Rev 2019;115:109333. https://doi.org/10.1016/j.rser.2019.109333.

[75] Toro-Molina C, Bouallou C. Comparison of post-combustion CO2 capture by solutions of ammonia and organic amines: Assessment using direct and indirect contactors. Energy Procedia 2014;63:550–8. https://doi.org/10.1016/j.egypro.2014.11.060.

[76] Figueroa JD, Fout T, Plasynski S, McIlvried H, Srivastava RD. Advances in CO2 capture technology-The U.S. Department of Energy's Carbon Sequestration Program. Int J Greenh Gas Control 2008;2:9–20. https://doi.org/10.1016/S1750-5836(07)00094-1.

[77] Wilberforce T, Olabi AG, Sayed ET, Elsaid K, Abdelkareem MA. Progress in carbon capture technologies. Sci Total Environ 2021;761:143203. https://doi.org/10.1016/j.scitotenv.2020.143203.

[78] Al-Hamed KHM, Dincer I. A comparative review of potential ammonia-based carbon capture systems. J Environ Manage 2021;287:112357. https://doi.org/10.1016/j.jenvman.2021.112357.

[79] Rao AB, Rubin ES. A technical, economic, and environmental assessment of amine-based CO2 capture technology for power plant greenhouse gas control. Environ Sci Technol 2002;36:4467–75. https://doi.org/10.1021/es0158861.

[80] Fazeli H, Panahi M, Rafiee A. Investigating the potential of carbon dioxide utilization in a gas-to-liquids process with iron-based Fischer-Tropsch catalyst. J Nat Gas Sci Eng 2018;52:549–58. https://doi.org/10.1016/j.jngse.2018.02.005.

[81] Basile A, Gugliuzza A, Iulianelli A, Morrone P. Membrane technology for carbon dioxide (CO2) capture in power plants. In: Woodhead Publishing, editor. Adv. Membr. Sci. Technol. Sustain. Energy Environ. Appl., Elsevier; 2011, p. 113–59. https://doi.org/10.1533/9780857093790.2.113.

[82] Hua W, Sha Y, Zhang X, Cao H. Research progress of carbon capture and storage (CCS) technology based on the shipping industry. Ocean Eng 2023;281:114929. https://doi.org/10.1016/j.oceaneng.2023.114929.

[83] Sanz-Pérez ES, Murdock CR, Didas SA, Jones CW. Direct Capture of CO2 from Ambient Air. Chem Rev 2016;116:11840–76. https://doi.org/10.1021/acs.chemrev.6b00173.

[84] Breyer C, Fasihi M, Bajamundi C, Creutzig F. Direct Air Capture of CO2: A Key Technology for Ambitious Climate Change Mitigation. Joule 2019;3:2053–7. https://doi.org/10.1016/j.joule.2019.08.010.

[85] IEA. Direct Air Capture: A key technology for net zero. IEA Publ 2022:1–76.

[86] Sabatino F, Grimm A, Gallucci F, van Sint Annaland M, Kramer GJ, Gazzani M. A comparative energy and costs assessment and optimization for direct air capture technologies. Joule 2021;5:2047–76. https://doi.org/10.1016/j.joule.2021.05.023.

[87] Viebahn P, Scholz A, Zelt O. The potential role of direct air capture in the German energy research program—results of a multi-dimensional analysis. Energies 2019;12:3443. https://doi.org/10.3390/en12183443.

[88] Broehm M, Strefler J, Bauer N. Techno-Economic Review of Direct Air Capture Systems for Large Scale Mitigation of Atmospheric CO2. Potsdam Inst Clim Impact Res 2015.

[89] Keith DW, Holmes G, St. Angelo D, Heidel K. A Process for Capturing CO2 from the Atmosphere. Joule 2018;2:1573–94. https://doi.org/10.1016/j.joule.2018.05.006.

[90] McQueen N, Gomes KV, McCormick C, Blumanthal K, Pisciotta M, Wilcox J. A review of direct air capture (DAC): Scaling up commercial technologies and innovating for the future. Prog Energy 2021;3:032001. https://doi.org/10.1088/2516-1083/abf1ce.

[91] Deutz S, Bardow A. Life-cycle assessment of an industrial direct air capture process based on temperature–vacuum swing adsorption. Nat Energy 2021;6:203–213. https://doi.org/10.1038/s41560-020-00771-9.

[92] Fasihi M, Efimova O, Breyer C. Techno-economic assessment of CO 2 direct air capture plants. J Clean Prod 2019;224:957–80. https://doi.org/10.1016/j.jclepro.2019.03.086.

[93] Beuttler C, Charles L, Wurzbacher J. The Role of Direct Air Capture in Mitigation of Anthropogenic Greenhouse Gas Emissions. Front Clim 2019;1:469555. https://doi.org/10.3389/fclim.2019.00010.

[94] Jayarathna C, Mathisen A, Øii LE, Tokheim L-A. Process Simulation of Calcium Looping With Indirect Calciner Heat Transfer. Proc 56th Conf Simul Model (SIMS 56), October, 7-9, 2015, Linköping Univ Sweden 2015;119:71–80. https://doi.org/10.3384/ecp1511971.

[95] Breyer C, Fasihi M, Bajamundi C, Creutzig F. Direct Air Capture of CO 2 : A Key Technology for Ambitious Climate Change Mitigation. Joule 2019;3:2053–7.

[96] Gogate MR. Methanol-to-olefins process technology: current status and future prospects. Pet Sci Technol 2019;37:559–65. https://doi.org/10.1080/10916466.2018.1555589.

[97] Bansode A, Urakawa A. Towards full one-pass conversion of carbon dioxide to methanol and methanol-derived products. J Catal 2014;309:66–70. https://doi.org/10.1016/j.jcat.2013.09.005.

[98] Zhang C, Jun KW, Gao R, Kwak G, Park HG. Carbon dioxide utilization in a gas-to-methanol process combined with CO2/Steam-mixed reforming: Techno-economic analysis. Fuel 2017;190:303–11. https://doi.org/10.1016/j.fuel.2016.11.008.

[99] Goeppert A, Czaun M, Jones JP, Surya Prakash GK, Olah GA. Recycling of carbon dioxide to methanol and derived products-closing the loop. Chem Soc Rev 2014;43:7995–8048.

https://doi.org/10.1039/c4cs00122b.

[100] Van-Dal ÉS, Bouallou C. Design and simulation of a methanol production plant from CO2 hydrogenation. J Clean Prod 2013;57:38–45. https://doi.org/10.1016/j.jclepro.2013.06.008.

[101] Zang G, Sun P, Elgowainy AA, Bafana A, Wang M. Performance and cost analysis of liquid fuel production from H2and CO2based on the Fischer-Tropsch process. J CO2 Util 2021;46:101459. https://doi.org/10.1016/j.jcou.2021.101459.

[102] Nyári J. Techno-economic feasibility study of a methanol plant using carbon dioxide and hydrogen. KTH School of Industrial Engineering and Management, 2018.

[103] Jasper S, El-Halwagi MM. A techno-economic comparison between two methanol-to-propylene processes. Processes 2015;3:684–98. https://doi.org/10.3390/pr3030684.

[104] Irena/Iea-Etsap. Production of Bio-ethylene: Technology Brief. IEA-ETSAP Int Renew Energy Agency I 2013:1–20.

[105] Mohsenzadeh A, Zamani A, Taherzadeh M. Bioethylene Production from Ethanol A Review and Techno-economical Evaluation. ChemBioEng 2017;4:3. https://doi.org/10.1002/cben.201600025.

[106] Alonso-Fariñas B, Gallego-Schmid A, Haro P, Azapagic A. Environmental assessment of thermo-chemical processes for bio-ethylene production in comparison with bio-chemical and fossil-based ethylene. J Clean Prod 2018;202:817–29. https://doi.org/10.1016/j.jclepro.2018.08.147.

[107] Zhao Z, Jiang J, Wang F. An economic analysis of twenty light olefin production pathways. J Energy Chem 2021;56:193–202. https://doi.org/10.1016/j.jechem.2020.04.021.

[108] Kuusela K, Uusitalo V, Ahola J. The transformation of plastics production from net positive greenhouse gas emissions to net negative : An environmental sustainability assessment of CO 2 - based polypropylene. J CO2 Util 2021;52:101672. https://doi.org/10.1016/j.jcou.2021.101672.

[109] Do TN, Kim J. Green C2-C4 hydrocarbon production through direct CO2 hydrogenation with renewable hydrogen: Process development and techno-economic analysis. Energy Convers Manag 2020;214:112866. https://doi.org/10.1016/j.enconman.2020.112866.

[110] Savaete T. Catalytic CO 2 conversion : a techno-economic analysis and theoretical study. Universiy off Gent, 2016.

[111] Pappijn CAR, Ruitenbeek M, Reyniers MF, Van Geem KM. Challenges and Opportunities of Carbon Capture and Utilization: Electrochemical Conversion of CO2 to Ethylene. Front Earth Sci

2020;8:1–12. https://doi.org/10.3389/fenrg.2020.557466.

[112] Keller F, Lee RP, Meyer B. Life cycle assessment of global warming potential, resource depletion and acidification potential of fossil, renewable and secondary feedstock for olefin production in Germany. J Clean Prod 2020;250:119484. https://doi.org/10.1016/j.jclepro.2019.119484.

[113] Rosental M, Fröhlich T, Liebich A. Life Cycle Assessment of Carbon Capture and Utilization for the Production of Large Volume Organic Chemicals. Front Clim 2020;2:1–14. https://doi.org/10.3389/fclim.2020.586199.

[114] Bicer Y, Dincer I, Vezina G, Raso F. Impact Assessment and Environmental Evaluation of Various Ammonia Production Processes. Environ Manage 2017;59:842–55. https://doi.org/10.1007/s00267-017-0831-6.

[115] IRENA and AEA. Innovation Outlook: Renewable Ammonia. Innov Outlook Renew Ammon 2022.

[116] Ghavam S, Vahdati M, Wilson IAG, Styring P. Sustainable Ammonia Production Processes. Front Energy Res 2021;9:1–19. https://doi.org/10.3389/fenrg.2021.580808.

[117] Ikäheimo J, Kiviluoma J, Weiss R, Holttinen H. Power-to-ammonia in future North European 100 % renewable power and heat system. Int J Hydrogen Energy 2018;43:17295–308. https://doi.org/10.1016/j.ijhydene.2018.06.121.

[118] Nayak-Luke R, Bañares-Alcántara R, Wilkinson I. “green” Ammonia: Impact of Renewable Energy Intermittency on Plant Sizing and Levelized Cost of Ammonia. Ind Eng Chem Res 2018;57:14607–16. https://doi.org/10.1021/acs.iecr.8b02447.

[119] Cesaro Z, Ives M, Nayak-Luke R, Mason M, Bañares-Alcántara R. Ammonia to power: Forecasting the levelized cost of electricity from green ammonia in large-scale power plants. Appl Energy 2021;282:116009. https://doi.org/10.1016/j.apenergy.2020.116009.

[120] Osman O, Sgouridis S, Sleptchenko A. Scaling the production of renewable ammonia: A techno-economic optimization applied in regions with high insolation. J Clean Prod 2020;271:121627. https://doi.org/10.1016/J.JCLEPRO.2020.121627.

[121] Liu X, Elgowainy A, Wang M. Life cycle energy use and greenhouse gas emissions of ammonia production from renewable resources and industrial by-products. Green Chem 2020;22:5751–61. https://doi.org/10.1039/d0gc02301a.

[122] Al-Breiki M, Bicer Y. Comparative life cycle assessment of sustainable energy carriers including production, storage, overseas transport and utilization. J Clean Prod 2021;279:123481. https://doi.org/10.1016/j.jclepro.2020.123481.

[123] Bicer Y, Dincer I. Life cycle assessment of ammonia utilization in city transportation and power generation. J Clean Prod 2018;170:1594–601. https://doi.org/10.1016/j.jclepro.2017.09.243.

[124] Boero AJ, Kardux K, Kovaleva M, Salas DA, Mooijer J, Mashruk S, et al. Environmental Life Cycle Assessment of Ammonia-Based Electricity. Energies 2021;13:4859.

[125] Arnaiz del Pozo C, Cloete S. Techno-economic assessment of blue and green ammonia as energy carriers in a low-carbon future. Energy Convers Manag 2022;255:115312. https://doi.org/10.1016/j.enconman.2022.115312.

[126] Lee K, Liu X, Vyawahare P, Sun P, Elgowainy A, Wang M. Techno-economic performances and life cycle greenhouse gas emissions of various ammonia production pathways including conventional, carbon-capturing, nuclear-powered, and renewable production. Green Chem 2022;24:4830–44. https://doi.org/10.1039/d2gc00843b.

[127] Kakavand A, Sayadi S, Tsatsaronis G, Behbahaninia A. Techno-economic assessment of green hydrogen and ammonia production from wind and solar energy in Iran. Int J Hydrogen Energy 2023;48:14170–91. https://doi.org/10.1016/j.ijhydene.2022.12.285.

[128] Gomez JR, Baca J, Garzon F. Techno-economic analysis and life cycle assessment for electrochemical ammonia production using proton conducting membrane. Int J Hydrogen Energy 2020;45:721–37. https://doi.org/10.1016/j.ijhydene.2019.10.174.

[129] Mayer P, Ramirez A, Pezzella G, Winter B, Sarathy SM, Gascon J, et al. Blue and green ammonia production: A techno-economic and life cycle assessment perspective. IScience 2023;26:107389. https://doi.org/10.1016/j.isci.2023.107389.

[130] Palina Nicolas. Technical, environmental and economic analysis of green ammonia as an energy vector in Spain 2022.

[131] Decourt B. Weaknesses and drivers for power-to-X diffusion in Europe. Insights from technological innovation system analysis. Int J Hydrogen Energy 2019;44:17411–30. https://doi.org/10.1016/j.ijhydene.2019.05.149.

[132] Thonemann MAN. Environmental impacts of CO2-based chemical production: A systematic literature review and meta-analysis. Appl Energy 2020;263:114599.

https://doi.org/10.1016/j.apenergy.2020.114599.

[133] Sternberg A, Jens CM, Bardow A. Formic acid, methane, and methanol 2017:1–14.

[134] Kim C, Park K, Lee H, Im J, Usosky D, Tak K, et al. Accelerating the net-zero economy with CO2-hydrogenated formic acid production: Process development and pilot plant demonstration. Joule 2024;8:693–713. https://doi.org/10.1016/j.joule.2024.01.003.

[135] Chiang CL, Lin KS, Chuang HW. Direct synthesis of formic acid via CO2 hydrogenation over Cu/ZnO/Al2O3 catalyst. J Clean Prod 2018;172:1957–77. https://doi.org/10.1016/j.jclepro.2017.11.229.

[136] Mura MG, De Luca L, Giacomelli G, Porcheddu A. Formic acid: A promising bio-renewable feedstock for fine chemicals. Adv Synth Catal 2012;354:3180–6. https://doi.org/10.1002/adsc.201200748.

[137] Mariyaselvakumar M, Kadam GG, Mani M, Srinivasan K, Konwar LJ. Direct hydrogenation of CO2-rich scrubbing solvents to formate/formic acid over heterogeneous Ru catalysts: A sustainable approach towards continuous integrated CCU. J CO2 Util 2023;67:102326. https://doi.org/10.1016/j.jcou.2022.102326.

[138] Liu M, Xu Y, Meng Y, Wang L, Wang H, Huang Y, et al. Heterogeneous Catalysis for Carbon Dioxide Mediated Hydrogen Storage Technology Based on Formic Acid. Adv Energy Mater 2022;12:1–41. https://doi.org/10.1002/aenm.202200817.

[139] Nie R, Tao Y, Nie Y, Lu T, Wang J, Zhang Y, et al. Recent Advances in Catalytic Transfer Hydrogenation with Formic Acid over Heterogeneous Transition Metal Catalysts. ACS Catal 2021;11:1071–95. https://doi.org/10.1021/acscatal.0c04939.

[140] Reymond H, Corral-Pérez JJ, Urakawa A, Rudolf Von Rohr P. Towards a continuous formic acid synthesis: A two-step carbon dioxide hydrogenation in flow. React Chem Eng 2018;3:912–9. https://doi.org/10.1039/c8re00142a.

[141] Bulushev DA, Ross JRH. Heterogeneous catalysts for hydrogenation of CO2 and bicarbonates to formic acid and formates. Catal Rev - Sci Eng 2018;60:566–93. https://doi.org/10.1080/01614940.2018.1476806.

[142] Zhang W, Wang S, Zhao Y, Ma X. Hydrogenation of CO2 to formic acid catalyzed by heterogeneous Ru-PPh3/Al2O3 catalysts. Fuel Process Technol 2018;178:98–103. https://doi.org/10.1016/j.fuproc.2018.05.024.

[143] Park K, Gunasekar GH, Kim S, Park H, Kim S, Park K, et al. CO2 hydrogenation to formic acid over heterogenized ruthenium catalysts using a fixed bed reactor with separation units. Green Chem 2020;22:1639–49.

[144] Kim D, Han J. Comprehensive analysis of two catalytic processes to produce formic acid from carbon dioxide. Appl Energy 2020;264:114711. https://doi.org/10.1016/j.apenergy.2020.114711.

[145] Gokberk Ö, Wiebren de J. Process System Modeling of Large-Scale Energy Storage , CO 2 and Biomass Based Formic Acid Production Systems. Delft University of Technology, 2020.

[146] Barbera E, Mantoan F, Bertucco A, Bezzo F. Hydrogenation to convert CO2 to C1 chemicals: Technical comparison of different alternatives by process simulation. Can J Chem Eng 2020;98:1893–906. https://doi.org/10.1002/cjce.23755.

[147] Bianchi S. Process modelling of a Direct Air Capture (DAC) system based on the Kraft process. POLITECNICO DI TORINO, 2020.

[148] Manwell, J. F., McGowan, J. G., & Rogers AL. Wind energy explained: theory, design and application. John Wiley & Sons, Inc; 2010.

[149] Hank C, Gelpke S, Schnabl A, White RJ, Full J, Wiebe N, et al. Economics & carbon dioxide avoidance cost of methanol production based on renewable hydrogen and recycled carbon dioxide-power-to-methanol. Sustain Energy Fuels 2018;2:1244–61. https://doi.org/10.1039/c8se00032h.

[150] Lundberg S. Comparative LCA of Electrolyzers for Hydrogen Gas Production. KTH ROYAL INSTITUTE OF TECHNOLOGY, 2019.

[151] Johnson WL, Hauser DM, Plachta DW, Wang XYJ, Banker BF, Desai PS, et al. Comparison of oxygen liquefaction methods for use on the Martian surface. Cryogenics (Guildf) 2018;90:60–9. https://doi.org/10.1016/j.cryogenics.2017.12.008.

[152] Harrison KW, Remick R, Martin GD. Hydrogen Production: Fundamentals and Case Study Summaries. Natl Renew Energy Lab 2014;2:6–11.

[153] Terlouw T, Bauer C, McKenna R, Mazzotti M. Large-scale hydrogen production via water electrolysis: a techno-economic and environmental assessment. Energy Environ Sci 2022;15:3583–602. https://doi.org/10.1039/d2ee01023b.

[154] McQueen N, Psarras P, Pilorgé H, Liguori S, He J, Yuan M, et al. Cost Analysis of Direct Air Capture and Sequestration Coupled to Low-Carbon Thermal Energy in the United States. Environ

Sci Technol 2020;54:7542–51. https://doi.org/10.1021/acs.est.0c00476.

[155] Mostafa M, Antonicelli C, Varela C, Barletta D, Zondervan E. Capturing CO2 from the atmosphere: Design and analysis of a large-scale DAC facility. Carbon Capture Sci Technol 2022;4:100060. https://doi.org/10.1016/j.ccst.2022.100060.

[156] Peters R, Baltruweit M, Grube T, Samsun RC, Stolten D. A techno economic analysis of the power to gas route. J CO2 Util 2019;34:616–34. https://doi.org/10.1016/j.jcou.2019.07.009.

[157] Prats-Salvado E, Monnerie N, Sattler C. Techno-Economic Assessment of the Integration of Direct Air Capture and the Production of Solar Fuels. Energies 2022;15:5017. https://doi.org/10.3390/en15145017.

[158] Buttler A, Spliethoff H. Current status of water electrolysis for energy storage, grid balancing and sector coupling via power-to-gas and power-to-liquids: A review. Renew Sustain Energy Rev 2018;82:2440–54. https://doi.org/10.1016/j.rser.2017.09.003.

[159] Fernanda Rojas Michaga M, Michailos S, Akram M, Cardozo E, Hughes KJ, Ingham D, et al. Bioenergy with carbon capture and storage (BECCS) potential in jet fuel production from forestry residues: A combined Techno-Economic and Life Cycle Assessment approach. Energy Convers Manag 2022;255:115346. https://doi.org/10.1016/j.enconman.2022.115346.

[160] G. Towler and R. Sinnott. Chemical Engineering Design: Principles, Practice and Economics of Plant and Process Design. Butterworth-Heinemann; 2021.

[161] Peters MS, Timmerhaus KD. Plant Design and Economics for Chemical Engineers. 5th ed. Estados Unidos: McGraw-Hill; 2002.

[162] Office for National Statistics. A01: Summary of labour market statistics. Off Natl Stat 2020. https://www.ons.gov.uk/employmentandlabourmarke%0At/peopleinwork/employmentandemployeetypes/datasets/summaryoflabourmar%0Aketstatistics.

[163] Jiang P, Parvez AM, Meng Y, Xu M xia, Shui T chi, Sun C gong, et al. Exergetic, economic and carbon emission studies of bio-olefin production via indirect steam gasification process. Energy 2019;187:115933. https://doi.org/10.1016/j.energy.2019.115933.

[164] Xiang D, Yang S, Li X, Qian Y. Life cycle assessment of energy consumption and GHG emissions of olefins production from alternative resources in China. Energy Convers Manag 2015;90:12–20. https://doi.org/10.1016/j.enconman.2014.11.007.

[165] Dincer I, Rosen MA. Chemical Exergy. Exergy 2013:31–49. https://doi.org/10.1016/B978-0-08-097089-9.00003-6.

[166] Tian P, Wei Y, Ye M, Liu Z. Methanol to olefins (MTO): From fundamentals to commercialization. ACS Catal 2015;5:1922–38. https://doi.org/10.1021/acscatal.5b00007.

[167] Zhao Z, Chong K, Jiang J, Wilson K, Zhang X, Wang F. Low-carbon roadmap of chemical production: A case study of ethylene in China. Renew Sustain Energy Rev 2018;97:580–91. https://doi.org/10.1016/j.rser.2018.08.008.

[168] Spallina V, Velarde IC, Antonio J, Jimenez M, Godini HR, Gallucci F, et al. Techno-economic assessment of different routes for olefins production through the oxidative coupling of methane (OCM). Energy Convers Manag 2017;154:244–61. https://doi.org/10.1016/j.enconman.2017.10.061.

[169] Vanden Bussche KM, Froment GF. A steady-state kinetic model for methanol synthesis and the water gas shift reaction on a commercial Cu/ZnO/Al2O3 catalyst. J Catal 1996;161:1–10. https://doi.org/10.1006/jcat.1996.0156.

[170] Mignard D, Pritchard C. On the use of electrolytic hydrogen from variable renewable energies for the enhanced conversion of biomass to fuels. Chem Eng Res Des 2008;86:473–87. https://doi.org/10.1016/j.cherd.2007.12.008.

[171] Lu B, Luo H, Li H, Wang W, Ye M, Liu Z, et al. Speeding up CFD simulation of fluidized bed reactor for MTO by coupling CRE model. Chem Eng Sci 2016;143:341–50. https://doi.org/10.1016/j.ces.2016.01.010.

[172] Fontalvo J. Usando modelos de usuario en Matlab en la interfaz de Aspen plus con Excel como puente. Ing e Investig 2014;34:39–43.

[173] Salkuyeh YK, Adams TA. Co-production of olefins, fuels, and electricity from conventional pipeline gas and shale gas with near-zero CO2 emissions. Part I: Process development and technical performance. Energies 2015;8:3739–61. https://doi.org/10.3390/en8053739.

[174] Yang M, You F. Comparative Techno-Economic and Environmental Analysis of Ethylene and Propylene Manufacturing from Wet Shale Gas and Naphtha. Ind Eng Chem Res 2017;56:4038–51. https://doi.org/10.1021/acs.iecr.7b00354.

[175] Arnaiz del Pozo C, Cloete S, Jiménez Álvaro Á. Techno-economic assessment of long-term methanol production from natural gas and renewables. Energy Convers Manag 2022;266:115785.

https://doi.org/10.1016/j.enconman.2022.115785.

[176] Sabatino F, Mehta M, Grimm A, Gazzani M, Gallucci F, Kramer GJ, et al. Evaluation of a Direct Air Capture Process Combining Wet Scrubbing and Bipolar Membrane Electrodialysis. Ind Eng Chem Res 2020;59:7007–20. https://doi.org/10.1021/acs.iecr.9b05641.

[177] Sabatino F, Grimm A, Gallucci F, van Sint Annaland M, Kramer GJ, Gazzani M. A comparative energy and costs assessment and optimization for direct air capture technologies. Joule 2021;5:2047–76. https://doi.org/10.1016/j.joule.2021.05.023.

[178] Michailos S, McCord S, Sick V, Stokes G, Styring P. Dimethyl ether synthesis via captured CO2 hydrogenation within the power to liquids concept: A techno-economic assessment. Energy Convers Manag 2019;184:262–76. https://doi.org/10.1016/j.enconman.2019.01.046.

[179] Kourkoumpas DS, Papadimou E, Atsonios K, Karellas S, Grammelis P, Kakaras E. Implementation of the Power to Methanol concept by using CO2 from lignite power plants: Techno-economic investigation. Int J Hydrogen Energy 2016;41:16674–87. https://doi.org/10.1016/j.ijhydene.2016.07.100.

[180] Zang G, Sun P, Elgowainy A, Wang M. Technoeconomic and Life Cycle Analysis of Synthetic Methanol Production from Hydrogen and Industrial Byproduct CO2. Environ Sci Technol 2021;55:5248–57. https://doi.org/10.1021/acs.est.0c08237.

[181] Herz G, Rix C, Jacobasch E, Müller N, Reichelt E, Jahn M, et al. Economic assessment of Power-to-Liquid processes – Influence of electrolysis technology and operating conditions. Appl Energy 2021;292:116655. https://doi.org/10.1016/j.apenergy.2021.116655.

[182] Pérez-Fortes M, Schöneberger JC, Boulamanti A, Tzimas E. Methanol synthesis using captured CO2 as raw material: Techno-economic and environmental assessment. Appl Energy 2016;161:718–32. https://doi.org/10.1016/j.apenergy.2015.07.067.

[183] Knighton LT, Snowden-Swan L, Wendt DS, Jenks J, Askander J, Li S. Techno-Economic Analysis of Synthetic Fuels Pathways Integrated with Light Water Reactors. US Dep Energy INL/EXT-20-59775 2020:85.

[184] Eurostat. Eurostat database 2021.

[185] Ekvall T, Tillman AM. Open-loop recycling: Criteria for allocation procedures. Int J Life Cycle Assess 1997;2:155–62. https://doi.org/10.1007/BF02978810.

[186] Garcia-Garcia G, Fernandez MC, Armstrong K, Woolas S, Styring P. Analytical Review of Life-Cycle Environmental Impacts of Carbon Capture and Utilization Technologies. Chem Sustain Energy Mater 2021;14:995–1015.

[187] Kibria Nabil S, McCoy S, Kibria MG. Comparative life cycle assessment of electrochemical upgrading of CO2to fuels and feedstocks. Green Chem 2021;23:867–80. https://doi.org/10.1039/d0gc02831b.

[188] Althaus H, Chudacoff M, Hischier R, Jungbluth N, Osses M, Primas A, et al. Life cycle inventories of chemicals. ecoinvent report No.8, v2.0. Final Rep Ecoinvent Data … 2007:1–957.

[189] Dow. Ethylene 2022.

[190] Bos MJ, Kersten SRA, Brilman DWF. Wind power to methanol: Renewable methanol production using electricity, electrolysis of water and CO2 air capture. Appl Energy 2020;264:114672. https://doi.org/10.1016/j.apenergy.2020.114672.

[191] Nguyen TBH, Zondervan E. Methanol production from captured CO2 using hydrogenation and reforming technologies- environmental and economic evaluation. J CO2 Util 2019;34:1–11. https://doi.org/10.1016/j.jcou.2019.05.033.

[192] Sharma I, Shah V, Shah M. A comprehensive study on production of methanol from wind energy. Environ Technol Innov 2022;28:102589. https://doi.org/10.1016/j.eti.2022.102589.

[193] Worrell E, Ernst Worrell, Phylipsen D, Einstein D, Martin N. DE-AC03-76SF00098 . Energy Use and Energy Intensity of the U . S . Chemical. 2000. https://doi.org/10.2172/773773.

[194] Nyhus AH, Yliruka M, Shah N, Chachuat B. Green ethylene production in the UK by 2035: a techno-economic assessment. Energy Environ Sci 2024;17:1931–49. https://doi.org/10.1039/d3ee03064d.

[195] Goud D, Gupta R, Maligal-ganesh R, Peter SC. Review of Catalyst Design and Mechanistic Studies for the Production of Ole fi ns from Anthropogenic CO 2. ACS Catal 2020;10:14258–14282. https://doi.org/10.1021/acscatal.0c03799.

[196] Hoppe W, Thonemann N, Bringezu S. Life Cycle Assessment of Carbon Dioxide–Based Production of Methane and Methanol and Derived Polymers. J Ind Ecol 2018;22:327–40. https://doi.org/10.1111/jiec.12583.

[197] Wang S, Wang S, Liu J. Life-cycle green-house gas emissions of onshore and offshore wind

turbines. J Clean Prod 2019;210:804–10. https://doi.org/10.1016/j.jclepro.2018.11.031.

[198] Klöpffer W. The Hitch Hiker´s Guide to LCA - An orientation in LCA methodology and application. Int J Life Cycle Assess 2006;11:142–142. https://doi.org/10.1065/lca2006.02.008.

[199] El-Shafie M, Kambara S. Recent advances in ammonia synthesis technologies: Toward future zero carbon emissions. Int J Hydrogen Energy 2023;48:11237–73. https://doi.org/10.1016/j.ijhydene.2022.09.061.

[200] Cheng M, Verma P, Yang Z, Axelbaum RL. Flexible cryogenic air separation unit—An application for low-carbon fossil-fuel plants. Sep Purif Technol 2022;302:122086. https://doi.org/10.1016/j.seppur.2022.122086.

[201] Tripodi A, Compagnoni M, Bahadori E, Rossetti I. Process simulation of ammonia synthesis over optimized Ru/C catalyst and multibed Fe + Ru configurations. J Ind Eng Chem 2018;66:176–86. https://doi.org/10.1016/j.jiec.2018.05.027.

[202] Lin B, Wiesner T, Malmali M. Performance of a Small-Scale Haber Process: A Techno-Economic Analysis. ACS Sustain Chem Eng 2020;8:15517–31. https://doi.org/10.1021/acssuschemeng.0c04313.

[203] Rouwenhorst KHR, Krzywda PM, Benes NE, Mul G, Lefferts L. Ammonia Production Technologies. Techno-Economic Challenges Green Ammon. as an Energy Vector, 2021. https://doi.org/10.1016/b978-0-12-820560-0.00004-7.

[204] Demirel Y. Technoeconomics and Sustainability of Renewable Methanol and Ammonia Productions Using Wind Power-based Hydrogen. J Adv Chem Eng 2015;5. https://doi.org/10.4172/2090-4568.1000128.

[205] Grodzinskiy A. Techno-economic assessment of low-carbon ammonia production. 2021.

[206] Flórez-Orrego D, de Oliveira Junior S. Modeling and optimization of an industrial ammonia synthesis unit: An exergy approach. Energy 2017;137:234–50. https://doi.org/10.1016/j.energy.2017.06.157.

[207] Tuna P, Hulteberg C, Ahlgren S. Techno-economic assessment of nonfossil ammonia production. Environ Prog Sustain Energy 2014;33:1290–7. https://doi.org/10.1002/EP.11886.

[208] Maia M. Techno-Economic Analysis of Green Ammonia Production using Offshore Wind Farms. REYKJAVIK UNIVERSITY, 2021.

[209] Morgan ER, Manwell JF, McGowan JG. Sustainable Ammonia Production from U.S. Offshore Wind Farms: A Techno-Economic Review. ACS Sustain Chem Eng 2017;5:9554–67. https://doi.org/10.1021/acssuschemeng.7b02070.

[210] Rojas-Michaga MF, Michailos S, Cardozo E, Akram M, Hughes KJ, Ingham D, et al. Sustainable aviation fuel (SAF) production through power-to-liquid (PtL): A combined techno-economic and life cycle assessment. Energy Convers Manag 2023;292:117427. https://doi.org/10.1016/j.enconman.2023.117427.

[211] Skordoulias N, Koytsoumpa EI, Karellas S. Techno-economic evaluation of medium scale power to hydrogen to combined heat and power generation systems. Int J Hydrogen Energy 2022;47:26871–90. https://doi.org/10.1016/j.ijhydene.2022.06.057.

[212] Andersson J, Lundgren J. Techno-economic analysis of ammonia production via integrated biomass gasification. Appl Energy 2014;130:484–90. https://doi.org/10.1016/j.apenergy.2014.02.029.

[213] Spallina V, Velarde IC, Jimenez JAM, Godini HR, Gallucci F, Van Sint Annaland M. Techno-economic assessment of different routes for olefins production through the oxidative coupling of methane (OCM): Advances in benchmark technologies. Energy Conversion Management 2017;154:244–61. https://doi.org/10.1016/j.enconman.2017.10.061.

[214] Fúnez Guerra C, Reyes-Bozo L, Vyhmeister E, Jaén Caparrós M, Salazar JL, Clemente-Jul C. Technical-economic analysis for a green ammonia production plant in Chile and its subsequent transport to Japan. Renew Energy 2020;157:404–14. https://doi.org/10.1016/j.renene.2020.05.041.

[215] Campion N, Nami H, Swisher PR, Vang Hendriksen P, Münster M. Techno-economic assessment of green ammonia production with different wind and solar potentials. Renewavble Sustainable Energy Reviews 2023;173:113057. https://doi.org/10.1016/j.rser.2022.113057.

[216] Nosherwani SA, Neto RC. Techno-economic assessment of commercial ammonia synthesis methods in coastal areas of Germany. J Energy Storage 2021;34:102201. https://doi.org/10.1016/J.EST.2020.102201.

[217] Saygin D, Blanco H, Boshell F, Cordonnier J, Rouwenhorst K, Lathwal P. Ammonia Production from Clean Hydrogen and the Implications for Global Natural Gas Demand. Sustainability 2023;15:1623. https://doi.org/10.3390/su15021623.

[218] H2 Europe, Bonnet-Cantalloube B, Espitalier-Noël M, Ferrari De Carvalho P, Fonseca J, Pawelec

G. Clean Ammonia in the future energy system. 2023.

[219] Ikäheimo J, Kiviluoma J, Weiss R, Holttinen H. Power-to-ammonia in future North European 100 % renewable power and heat system. Int J Hydrogen Energy 2018;43:17295–308. https://doi.org/10.1016/j.ijhydene.2018.06.121.

[220] CHEMANALYST. Ammonia Price Trend and Forecast 2023. https://www.chemanalyst.com/Pricing-data/ammonia-37#:~:text=The prices of Ammonia in,USD 710%2FMT in September. (accessed October 15, 2023).

[221] Chisalita DA, Petrescu L, Cormos CC. Environmental evaluation of european ammonia production considering various hydrogen supply chains. Renew Sustain Energy Rev 2020;130:109964. https://doi.org/10.1016/j.rser.2020.109964.

[222] Amponsah NY, Troldborg M, Kington B, Aalders I, Hough RL. Greenhouse gas emissions from renewable energy sources: A review of lifecycle considerations. Renew Sustain Energy Rev 2014;39:461–75. https://doi.org/10.1016/j.rser.2014.07.087.

[223] Jarvis SM, Samsatli S. Technologies and infrastructures underpinning future CO2 value chains: A comprehensive review and comparative analysis. Renew Sustain Energy Rev 2018;85:46–68. https://doi.org/10.1016/j.rser.2018.01.007.

[224] Mantoan F, Bezzo F, Barbera E. Design and Simulation of Hydrogenation Processes for Co 2 Conversion To C-1 Chemicals. UNIVERSITÀ DEGLI STUDI DI PADOVA, 2019.

[225] Schaub T, Fries DM, Paciello R, Mohl K-D, Schäfer M, Rittinger S. Process for preparing formic acid by reaction of carbon dioxide with hydrogen. US2011319658 (A1), 2014.

[226] Surywanshi GD, Pillai BBK, Patnaikuni VS, Vooradi R, Anne SB. Formic acid synthesis–a case study of CO2 utilization from coal direct chemical looping combustion power plant. Energy Sources, Part A Recover Util Environ Eff 2022;44:2220–35. https://doi.org/10.1080/15567036.2019.1649325.

[227] Thomas CA, Bonilla RJ, Huang Y, Jessop PG. Hydrogenation of carbon dioxide catalyzed by ruthenium trimethylphosphine complexes - Effect of gas pressure and additives on rate in the liquid phase. Can J Chem 2001;79:719–24. https://doi.org/10.1139/cjc-79-5-6-719.

[228] Wang A, He P, Wu J, Chen N, Pan C, Shi E, et al. Reviews on Homogeneous and Heterogeneous Catalysts for Dehydrogenation and Recycling of Formic Acid: Progress and Perspectives. Energy and Fuels 2023;37:17075-93. https://doi.org/10.1021/acs.energyfuels.3c02595.

[229] Element Energy. BEIS - Hydrogen (H2) supply chain evidence base 2018.

[230] Zhang C, Jun KW, Gao R, Lee YJ, Kang SC. Efficient utilization of carbon dioxide in gas-to-liquids process: Process simulation and techno-economic analysis. Fuel 2015;157:285–91. https://doi.org/10.1016/j.fuel.2015.04.051.

[231] Sadiq M, Alshehhi RJ, Urs RR, Mayyas AT. Techno-economic analysis of Green-H2@Scale production. Renew Energy 2023;219:119362. https://doi.org/10.1016/j.renene.2023.119362.

[232] Methanex. Methanex posts regional contract methanol prices for North America, Europe and Asia 2016. http://www.methanex.com/our-business/pricing#sthash.3E7vxKd8.dpu.

[233] María Villarreal Vives A, Wang R, Roy S, Smallbone A. Techno-economic analysis of large-scale green hydrogen production and storage. Appl Energy 2023;346:121333. https://doi.org/10.1016/j.apenergy.2023.121333.

[234] Sigma Aldrich. Bis(cyclopentadienyl)ruthenium(II) 2023. https://www.sigmaaldrich.com/GB/en/substance/biscyclopentadienylrutheniumii23126.

[235] Thermo Scientific Chemicals. 1,2-Bis(dicyclohexylphosphino)ethane 2023. https://www.thermofisher.com/order/catalog/product/363850010.

[236] Sternberg A, Jens CM, Bardow A. Life cycle assessment of CO2-based C1-chemicals. Green Chem 2017;19:2244–59. https://doi.org/10.1039/c6gc02852g.

[237] Robledo-Díez A. Life cycle assessment on the conversion of CO2 to formic acid. Norwegian University of Science and Technology, 2012.

[238] Ecoinvent. Ecoinvent database. Https://EcoinventOrg/the-Ecoinvent-Database/ 2021.

[239] Kibria Nabil S, McCoy S, Kibria MG. Comparative life cycle assessment of electrochemical upgrading of CO2to fuels and feedstocks. Green Chem 2021;23:867–80. https://doi.org/10.1039/d0gc02831b.

[240] Bruinsma S. Heat Pumps in Distillation. Chem Eng Prog 2010;72:58–64.

[241] Maru MS, Ram S, Shukla RS, Khan N ul H. Ruthenium-hydrotalcite (Ru-HT) as an effective heterogeneous catalyst for the selective hydrogenation of CO2 to formic acid. Mol Catal 2018;446:23–30. https://doi.org/10.1016/j.mcat.2017.12.005.

[242] Arnaiz del Pozo C, Cloete S, Jiménez Álvaro Á. Techno-economic assessment of long-term methanol production from natural gas and renewables. Energy Convers Manag 2022;266:115785.

https://doi.org/10.1016/j.enconman.2022.115785.

[243] Ahn Y, Byun J, Kim D, Kim BS, Lee CS, Han J. System-level analysis and life cycle assessment of CO2 and fossil-based formic acid strategies. Green Chem 2019;21:3442–55. https://doi.org/10.1039/c9gc01280j.